KDUiRC
INTERNATIONAL RESEARCH CONFERENCE

14TH INTERNATIONAL RESEARCH CONFERENCE

" Security, Stability and National Development in the New Normal "

09TH - 10TH SEPTEMBER 2021

ENGINEERING

PROCEEDINGS

GENERAL SIR JOHN KOTELAWALA DEFENCE UNIVERSITY

14TH INTERNATIONAL RESEARCH CONFERENCE

SECURITY, STABILITY AND NATIONAL DEVELOPMENT IN THE NEW NORMAL

Engineering

PROCEEDINGS

General Sir John Kotelawala Defence University

Ratmalana, Sri Lanka

©General Sir John Kotelawala Defence University
All rights reserved

This book contains the Conference Proceedings of the Egineering Sessions of the 14th International Research Conference of General Sir John Kotelawala Defence University, Ratmalana, Sri Lanka held on 9th and 10th of September 2021. No part of this publication may be reproduced, stored in a retrieval system or transmitted in any form, without prior permission of General Sir John Kotelawala Defence University, Ratmalana, Sri Lanka.

Published by

General Sir John Kotelawala Defence University, Ratmalana, Sri Lanka

Tel: +94-11-263-5268
e-Mail: irc2021@kdu.ac.lk
Website: http://library.kdu.ac.lk/irc2021/

ISBN 978-624-5574-51-3

Other Proceedings of the Conference:

Defence and Strategic Studies: ISBN 978-624-5574-49-0

Medicine: ISBN 978-624-5574-50-6

Built Environment and Spatial Sciences: ISBN 978-624-5574-47-6

Management, Social Sciences and Humanities: ISBN 978-624-5574-44-5

Law: ISBN ISBN 978-624-5574-43-8

Allied Health Sciences: ISBN 978-624-5574-46-9

Computing: ISBN 978-624-5574-45-2

Basic and Applied Sciences: ISBN 978-624-5574-48-3

November 2021

Conference Chair

Dr Harinda Vidanage

Conference Secretary

Ms Lihini M De Silva

Co-secretaries

Maj BMR Ferdinandesz psc IG

Ms GAI Uwanthika

Capt SAAAK Athukorala

Steering Committee

Brig W Chandrasiri RSP USP psc – President

Brig RGU Rajapakshe RSP psc

Col HMGE Herath RSP USP psc

Lt Col AMDB Adhikari RWP RSP psc

Prof KAS Dhammika

Prof CL Goonasekara

Snr Prof ALS Mendis

Snr Prof SR De Senevirathne

Mr VD Kithsiri

Dr LS Liyanage

Dr NK Gunasekara

Mrs RMNP Rajapakse

Dr LP Kalansooriya

Dr KSC de Silva

Ms SDKC Sandanayake

Editorial Committee

Mr WAAK Amaratunga – President

Dr FMMT Marikkar – Assistant Editor

Cmde (E) MCP Dissanayaka

Maj JPWK Abaywickrama

Sqn Ldr IKJP Kumara

Capt (E) SU Dampage (Retd)

Snr Prof RN Pathirana

Dr JMKB Jayasekara

Ms BKM Jayasekera

Dr PBV Navaratne

Dr YJSN Fernando

Dr UG Rajapakse

Mrs CJ Kothalawala

Dr HRWP Gunathilake

Dr R Vijitha

Dr MMPT Jayasekara

Dr AR Arooz

Dr KGKG Kottegoda

Mr WLPK Wijesinghe

Mr HR Tharanga

Ms BDK Anandawansa

Ms Lakshani Willarachchi

Ms WS Sudusinghe

Ms UWMUSK Walisundara

Ms TD Kothalawala

Ms WMMMTJ Weerarathne

Session Coordinators

Defence and Strategic Studies	Brig RGU Rajapaksha RSP psc Col HMGE Herath RSP USP psc Lt Col PP Serasinghe RSP USP LCdr JPPC de Silva Ms SUW Jayaratne
Medicine	Air Cdre (Prof) RANK Wijesinghe Lt Col (Dr) PH Premaratne Dr SL Malaviarachchi Dr SAC Dalpatadu Dr AU Gamage
Engineering	Capt (E) SU Dampage (Retd) Dr PPCR Karunasekara Mr WSP Fernando
Management, Social Sciences and Humanities	Mr WAAK Amaratunga Ms VU Jayasinghe Mr AHMS Sharic
Law	Mr WS Wijesinghe Maj HSD Mendis Dr YP Wijerathne
Allied Health Sciences	Dr DU Kottahachchi Dr WM Ediriarachchi Dr HMAJ Halahakoon
Built Environment and Spatial Sciences	Dr AH Lakmal Lt Col TC Kathriarachchi (Retd) Archt HT Rupasinghe Mr KT Withanage Mr KAM Chathuranga
Computing	Dr ADAI Gunasekara Dr GACN Priyadarshani Ms TGI Udayangi
Basic and Applied Sciences	Prof CL Goonasekara Dr AWMKK Bandara Dr KW Samarakoon

KDUIRC
INTERNATIONAL RESEARCH CONFERENCE 2021

Table of Contents

Welcome Address

Major General Milinda Peiris RWP RSP USP ndc psc

Vice Chancellor, General Sir John Kotelawala Defence University

Keynote Speaker, Mr. Lalith Weeratunga Principal Advisor to H.E. President Gotabaya Rajapaksa, Secretary to the Ministry of Defence, General (Retd.) Kamal Gunaratne, DVC Administration and Defense, Brigadier Wipula Chandrasiri, DVC Academic, Prof Sanath Dhammika, Deans of the respective faculties, Centre Directors, Academics, Senior Military Officers, Administrative Staff, Students and all distinguished guests who are connected with us in the cyber space.
Good Morning to you all!

It is indeed with a great sense of responsibility that I deliver the welcome address at this 14th consecutive international research conference of General Sir John Kotelawala Defence University held on the timely theme, 'Security, Stability and National Development in the New Normal", at one of the most crucial times of our history.

To begin with, let me very warmly welcome our chief guest and keynote speaker, Mr. Lalith Weeratunga, the principal advisor to HE the President Gotabhaya Rajapakse. Of course, Mr. Lalith Weeratunga is not at all a stranger to KDU. He is one of the great personalities who clearly understands the role played by KDU for the betterment of the nation and who has long been assisting us in numerous ways to develop this institution to what it is today. As I remember Mr. Lalith Weeratunga was the keynote speaker of our 6th research conference in 2013. Sir, your keynote on our theme, "Sri Lanka as a Hub in Asia: the Way Foreword" still reverberate in our minds even after 8 long years.

And it is a remarkable coincidence that I welcome you once again to deliver the keynote address on our current theme, 'Security, Stability and National Development in the New Normal", which highlights the importance of stability created by the development and security nexus in the context of emerging new threats to national, human, and global security. Sir, we are looking forward to listening to your words of wisdom today as well.

Mr Weeratunga, it is also remarkable that eight years ago, you were accompanied by the Secretary Defence during that time, who has been destined to be President of our country today, H.E. Gotabaya Rajapaksa, and today you are accompanied by the present Secretary Defence and the Chairman of our Board of Management, General (Retd.) Kamal Gunarathne, and I am indeed honoured to welcome General Kamal to this conference as the Guest of Honour because he has been a tower of strength for KDU at this crucial time of its history.

Let me also welcome all distinguished invitees including the Tri-Service Commanders and other BOM members including the Chairman of the UGC, distinguished members of the diplomatic corps, Vice Chancellors and academics from other universities, senior tri-service and police officers, and national and international participants joining this event on line.

Ladies and gentlemen, this year's conference is significant to us at KDU on several accounts. First, 2021 is the year in which we mark the 40th year of KDU's existence in the higher education landscape of Sri Lanka, and we are proud of the role we have been playing therein, whilst continuously growing in its stature as a national university doing its call of

duty towards the nation with fullest commitment and dedication.

Secondly, this year's conference is the one that we hold under the most trying circumstances in our history. Last year too, we conducted our research conference in a hybrid mode due to the first wave of the COVID 19 pandemic that took us all by surprise.

But we hoped that we would be able to conduct the 2021 conference freely and in the usual glamour. But this year, it turned out to be even a worse scenario with the third wave of the pandemic hitting us harder. So we consider that this is a more challenging test of our resilience as the nation's defence university.

Ladies and gentlemen, we always believe in the dictum that a quitter never wins and a winner never quits. So we were determined to challenge the challenges, how hard they may be. And we ensure the continuity of the conference adjusting and amending the circumstances, while taking the highest precautions against the pandemic scenario. We were able to slowly but steadily accept the prevailing danger, assess the situation realistically, and to see the best options for the best interest of our University. Therefore, we finally decided that this year's conference will a hybrid one with a major virtual orientation.

Ladies and gentlemen, the reason why we conduct this conference somehow or the other is because of our belief that we need to set an example for the nation to stand on its feet at times of crises. We as a nation cannot afford to continue to play the waiting game for ever. As our theme highlights, we need to find ways to ensure security and national development in the new normal adjusting ourselves to the new normal conditions sooner than later.

And thirdly, we believe that this is the time in which a nation's intellectual community must come forward to engage in serious and meaningful research to help overcome innumerable issues and problems that crop up in diverse fields such as defence and security, economics, science, technology and engineering, medicine and health services, management, social sciences and humanities, law and so on and so forth. It is the responsibility of a university to create the necessary environment and enabling grounds for important research outcomes, which the nation yearns for.

Ladies and gentlemen, we are glad that the intellectual community of the country has very positively responded to our initiative. Despite some adverse comments and criticisms of KDU and its role in higher education in Sri Lanka from certain quarters in recent times, the large majority of fair thinking academics, professionals and ordinary people are with us fully, and that is evident from the large number of research papers submitted by researchers from all over the country representing various higher educational institutions.

Despite the difficulties in adjusting to the online mode, the organizers of the KDU international research conference have done their best to maintain the quality of the conference in the highest level. They intend to set the tone to initiate more collaborative research to face new global challenges. As I always point out these types of research conferences are ideal platforms to make connections nationally and internationally for mutual benefit.

I hope that authors of KDU and various other local and international universities will take the opportunity to interact and develop friendly relationships, establish networks, and explore opportunities to embark on productive research collaborations.

While assuring our commitment to providing best opportunities for research collaborations, I wish all the very best for the presenters and hope you will enjoy every moment of this academic fusion. Thank you.

Keynote Address

Mr Lalith Weeratunga

Principal Advisor to His Excellency the President of Sri Lanka

Secretary, Ministry of Defence, Chief of Defence Staff and Commander of the Army, Commander of the Air Force, Vice Chancellor of the KDU, Distinguished academics, Honoured guests, Friends, *Ayubowan!*

Once again, I am delighted to be with you this morning at this research conference. It gives me much pleasure to be at the KDU because it is one of the best universities we have in Sri Lanka. Since of late, there have been much attack on and criticism of the KDU. That's because the KDU is doing well and has brooked no nonsense. With a village background, my mind goes back to a famous Sinhala saying, which means "only those mango trees that have sweet fruits are attacked."

The entire world is undergoing a massive reorganization with the COVID-19 pandemic, and the traditional themes and arguments in security seems rather irrelevant in the present context. "Security, Stability, National Development in the New Normal" is a timely theme, giving us much food for thought in terms of the advancement of a country like Sri Lanka. If you take the first component, security, the bottom line of security is survival. *Survival,* is based on a number of factors. Barry Buzan, the veteran in international security rejected the practice of restricting security to just one sector and defined it as "a particular type of politics applicable to a wide range of issues."

As eminent representatives of the security sector, you are aware that the concept of security can somewhat vary from one country to another. When Mexico's major national security threat has remained to be organized crime for quite some time, Afghanistan's has been religious extremism. For a country like Somalia, it is the inbuilt corruption into their governance. For some countries, it might change abruptly. A few days ago, we all saw corruption and mismanagement which was the major security threat of the African nation Guinea, getting substituted by another – an armed unrest. In spite of these differences, almost all countries in the world have developed a commonality during the past year, where the health insecurity assumed a major role over and above all others.

The COVID-19 pandemic has caused the entire world to assume a 'new normal' to fight this common insecurity that is caused by a tiny, microscopic virus. Even during the new normal, however, certain fundamental features of the modern-day security have not changed. Security in the 21st Century was, to a great extent, focused on internal factors of a country, rather than external ones. The organization of the threat factor has changed from state militaries to terrorist organizations to even pirates. The underlying motivation for creating insecurities has shifted from being political to one that is economic.

Targets have shifted from soldiers to civilians. The distinction between 'high profiles' of national security and 'low profiles' of economic and social interactions have softened. This has given rise to new sources of global insecurity in the 21st Century which are essentially 'soft' in nature.

The 21st Century has continued to witness these new sources throughout its first two decades. Donald Rumsfeld, the onetime Defence Secretary of the United States said at a key decision-making point in the history of his country, "there are known knowns; the things we know we know, we also know there are known unknowns; that is to say we know there are some things we do not know. But there are also unknown unknowns—the ones we don't know we don't know." Although stated in relation to a completely different scenario, when recalling this statement, I see that it resonates with the pandemic that we are facing now. In 'security

terms', COVID-19 is a 'wild card', an 'unknown unknown'. It is a security threat without a passport. It caused the 'health security' to assume the prime position in the security landscape of the modern day, surpassing the food security, water security and all other soft securities.

When we view the modern-day threats, we see that none of these is of a purely military nature, as those perhaps were, during the cold-war period. As a result, they also cannot be tackled by purely military means. There is another factor that contributes to the restriction of military means as a response to insecurities. In today's security landscape, States do not have the monopoly that they used to enjoy. Human beings have assumed that role. When the individual is considered as the central point in security rather than the 'State' as before, it gives a new insight into all our security related concerns. This helps us to understand the present-day global vulnerabilities with a new eye.

When the centre of focus in security becomes the individual, it changes the state-centric understanding of national, regional as well as global security. When a pandemic, which cannot be controlled by military means is plaguing the world, the human-centric understanding of security becomes vital to address it in order to ensure development of any country. This is why the 'soft component' of security, or the 'human security' gains more prominence over the 'hard component' of security during this new normal, created by the worst health pandemic in the recent history of the world.

The pandemic has given rise to a number of human security threats. To mention a few, the threat to economic security through unemployment, to health security through the deadly infectious virus and to environmental security through the mass accumulation of the waste generated in the health sector. It has also given a signal on food security as well, which is precisely when the Government declared essential services and appointed an authority to manage the situation in Sri Lanka. So you see, security in the new normal is connected with the stability of a country, but in a different way from how it did with conventional security under the normal conditions.

National development, as we all know, is an all-encompassing term. It includes both the individual and the nation. Therefore, national development can be considered as the process of development and reconstruction of all dimensions of the nation, along with the development of the individual. This concept is essentially linked with both the growth and the change where *change* can be socio-cultural or economic, tangible or intangible. National development involves activities through a planned national economy, application of modern technology in agriculture to enhance production, application of science and technology in the production sector, improving the human resource and providing education for all among many others.

During a disaster such as the COVID pandemic, it also includes providing facilities and assistance to the poorest segments of the society. In theory, addressing the security needs, especially those of soft security and implementing broad array of the previously mentioned key activities in national development ensures the stability of the country during the new normal. This theory is in practice in Sri Lanka today, in different sectors to different degrees.

Let us consider the vaccination drive for example. Two months ago, Sri Lanka was struggling with the inadequate human resource in the civilian component of the health sector to conduct the vaccination programme at its full length. Health sector employees were getting exhausted with the enhancing demand for services. At this point, the Government employed its military health professionals to assist their civilian component. That accelerated our vaccination drive to such an extent that Sri Lanka became the first country in the world to have the fastest vaccination drive to its population.

H.E. the President had first-hand supervision of this process, at times acting as a 'vaccination planner', which contributed to the success of the

whole programme. This measure addresses our health security, and at the same time contributes to our national development by making the workforce resistant to the pandemic. Together, the two outcomes contribute to enhancing the stability of the country during this new normal.

Now let us consider a few of the numerous initiatives that the Government has introduced to ensure food security. The Government recently decided to take a transition from inorganic agriculture to organic agriculture, in keeping with pledge given to our people by the President, H.E Gotabaya Rajapaksa, in his policy document, 'Vistas of Prosperity and Splendour." The primary aim was to safeguard the public, and especially the future generations from non-communicable diseases including renal diseases, again ensuring the health security. This also gave an added advantage where the imports of chemical fertilizers became minimal and that saved a considerable amount of money to our Treasury. This also resulted in enhancing organic and bio fertilizer production within the country, opening up new employment opportunities.

Linked with these two activities, the Government also launched 'Wari Saubhagya', a programme to rehabilitate 1000 small tanks across the country. This was to provide water for both irrigation and drinking purposes. These projects ensured irrigation water to a greater area of paddy and other field crop cultivations and also created additional employment opportunities within the country. Overall, those made a noteworthy contribution to the national development as well as to the soft security of the country during the new normal.

National development not only involves the infrastructure development, but also the human development. A developed human resource is a shield against certain soft threats. The programme 'connect Sri Lanka' was launched during the new normal, initially providing four remote areas with 4G connectivity. We are planning to expand it into all 9 provinces.

The pandemic period where schools had to be closed was also used to plan education reforms aiming at producing future generations that are better equipped with battling their way through the ever-changing global order. These enhance opportunities for the public, especially the children to gain access to knowledge that is amply available to children and citizens of many developed countries, and also to equip themselves better to assist with development initiatives of the Government.

Fruits of this labour will be reaped only in the future, where our country will continue to have a learned, open minded younger generations, and through them, smarter work forces. The activities that the Government has started today contribute to national development in the future on the one hand, security on the other, and to stability of the country, overall.

The last example that I wish to draw has a direct connection with all institutions in the public as well as the private sector, electricity. The Government spent over US$ 2.3 Bln for oil imports in 2020. We all know that a considerable amount of this is spent for generating electricity. This is an unbearable amount for a developing country like Sri Lanka, to be spent notwithstanding the prevailing health pandemic. It is also a waste of funds considering the vast and untapped potential that Sri Lanka has for renewable energy.

The Government gave due consideration to both these when establishing 'Thambapawani' the first wind power station owned by the Government of Sri Lanka. Another similar plant has been launched in Pooneryn. Use of solar power has been introduced to households. A waste-to-power plant was also declared open at Kerawalapitiya. It is not an easy task for a developing country like Sri Lanka to manage this shift while battling with a pandemic, but amidst all, the Government plans to increase the renewable energy component to 70% of the total consumption of the country by 2030. It Is an ambitious target, but it helps the country to reach a higher status in self-sufficiency and also prepares the country to face worse calamities than the present one that might arise in the future. The 'failure to prepare' as the old saying

goes, is 'preparation for failure'. We intend to avoid it.

Moving back to the concept of security with these examples, with special emphasis on human security, it is evident that the national development and security are inter-linked. These cannot be achieved separately. This is probably what caused the formerly known definition of security, 'freedom from fear', to be redefined as 'freedom from want', indicating the link between security and development. Human security, as we all know, is an integral part of State security, which in turn, has an equally strong connection with national development. This is why if you have a closer look at Sustainable Development Goals, you will see that all 17 goals are connected to human security.

In this context, I believe there is something vital that we all need to understand about security, development and the stability that those bring about. The new normal caused by the COVID-19 pandemic is calling us to re-think our actions, plans and concepts on security and development both.

Is it not high time for us to re-think our national security and national development?

Is this not the best time for us to redefine our development-security nexus?

Let me conclude by bringing back to your memory, extracts from a famous speech delivered by Robert F. Kennedy during his run for the Democratic nomination for the Presidency of the United States. Over 50 years later, his remarks about the measurements of development resonate with something that we need to re-discover with experience we had during this new normal. He said, and I quote,

"… the gross national product does not allow for the health of our children, the quality of their education or the joy of their play. It does not include the beauty of our poetry or the strength of our marriages, the intelligence of our public debate or the integrity of our public officials. It measures neither our wit nor our courage, neither our wisdom nor our learning, neither our compassion nor our devotion to our country, it measures everything in short, except that which makes life worthwhile."

Distinguished scholars, ladies and gentlemen, let us try to fathom the lesson that this global pandemic and the new normal is trying to teach us. Let us acknowledge the all-encompassing nature of national development and pay attention to the vital fact that has evaded our comprehension thus far – the fact that the individual, the human has assumed the central focus in security as well as in national development. Let us use that understanding to re-define our development-security nexus and bring a lasting stability to our country during the new normal.

Stay safe and take care of yourselves.

Thank you.

Address by Secretary, Ministry of Defence, Sri Lanka

General Kamal Gunaratne (Retd) WWV RWP RSP USP ndc psc MPhil

Secretary, Ministry of Defence, Sri Lanka

Chief Guest and Keynote Speaker of the 14th International Research Conference of KDU, Principal Advisor to the President Mr. Lalith Weerathunga, Ambassadors and High Commissioners, Foreign Secretary Professor Jayanath Kolombage, Chancellor of KDU General Jerry De Silva (Retd), Chief of Defence Staff and Commander of Army General Shavendra Silva, Commander of the Navy Vice Admiral Nishantha Ulugetenne, Chairman of University Grants Commison Professor Sampath Amarathunga, Vice Chancellors of other Universities, Vice Chancellor of KDU, Chief of Staff of Air Force, Director General at Institute of National Security Studies Professor Rohan Gunarathna, Deputy Vice chancellors, All Deans and Directors, former Chancellors and Commanders at KDU, Eminent Scholars, Senior Officers of the Armed forces and Police, distinguished guests joining us virtually from Sri Lanka and Overseas, Ladies and Gentlemen;

I consider it as a great pleasure and a privilege to be present here today at the inauguration ceremony of General Sir John Kotelawala Defense University's International Research Conference which is taking place for the 14th consecutive year and I would like to thank the Vice Chancellor and the conference organizers for the invitation extended for me to be present here to participate in this event. The International Research Conference of KDU is providing the opportunity for academics, professional researchers and practitioners to share their research findings and expertise addressing the mutual challenges in their fields. Therefore, this event has gained tremendous recognition among all interested parties around the world. Further, the provision of a wider interaction and networking with national and international scholars in respective fields would be absolutely beneficial for all the participants to broaden their horizons of knowledge through intellectual discussions. However, due to the global pandemic situation in effect, most participants may join the event through a virtual platform for this conference as same as the last year. Yet, I'm sure we will be able to achieve the desired objectives in a state amidst this pandemic situation.

Furthermore, I'm extremely pleased that the theme selected by the KDU for the conference this year security, stability, and the national development in the new normal is a timely theme capable of augmenting the significance and focus of the subject of strategic national importance. Further, I firmly believe that the endeavor towards warranting the national development and ensuring national security becomes further from achievement by undermining the routine activities due to the ill effects of the pandemic but becomes attainable by ensuring the adaptability to the new normal as widely accepted by all the countries in the world, today which is implied by the theme that you have selected. In fact, as comprehensively illustrated by the keynote speaker Mr. Lalith Weerathunga it is quite imperative that all of us understand and pursue the ways and means of adopting the circumstances embedded with the new normal. in order to coexist with the Covid 19 pandemic which has not shown any expiry date as of yet.

Ladies and Gentlemen in a context of globalization and further economic

integration, in recent decades the relationship between national development and national security of a country has become increasingly interlinked for Sri Lanka. These connections represent both opportunities and potential threats to the country's national security. The open and interconnected Sri Lankan economy creates vulnerabilities from potential international and external threats. Against this backdrop, national development has emerged as an important strategic priority for the Sri Lankan government with the connection between development and national security which will be orchestrated upon the vistas of prosperity and splendor, the national policy framework of our government headed by his excellency the president Gotabhaya Rajapaksha.

Ladies and gentlemen, the development generally depend on the stability of a country which should be achieved by ensuring national security. Sri Lanka being a country endangered by ruthless terrorism for almost three decades has experienced a lot of hardships during the past and was in the stage of eyeing its development in the last decade. Even though we were able to relieve the country from the menace of terrorism we have found another security threat in the form of a pandemic which has posed a greater threat to the entire world. The threat that we face today is progressing in its second continuous year without any indication of a possible termination we are yet to find a permanent solution for the same. However, we must always work towards reaching our development goals without letting our country at peril. In such a context our endeavor here as Sri Lankans should be to seek possibilities to find ways and means to steer the country towards development goals amidst said difficulties. Sri Lankan government is at the threshold of trying all possible methods to meet its economic growth and objectives yet with lots of empidements while ensuring human security. When the domestic affairs of a country are affected it is extremely difficult for a country to reach its desired end state. Sri Lanka is no exception in this, regard being a developing country Sri Lanka cannot accept any economic standstills for a protacted time frame. However, any plans to expedite the economic gains should never be at the expense of human lives. Therefore, his excellency the president himself has expressed his keenness on this aspect to see and inspire all possibilities available to ensure the maintenance of momentum in the economic sphere.

On the contrary, we should also note the other contemporary security concerns such as violent extremism, terrorism, piracy, drug, and human trafficking, smuggling, cybercrimes, and other organized crimes and natural disasters pose a grave threat to the stability of a country. Sri Lanka's geostrategic location is susceptible to such threats as it is located in the main sea routes in the Indian ocean. The same geopolitical significance has given a greater recoginition to the country, thus it has gained greater demand from the rest of the world. In such an instance, the possibility of Sri Lanka becoming susceptible to threats posed from violent extremism and organized crimes is very high and present the government has initiated several steps to curtail such illegal activities and such measures taken such as the demarcation of maximum security prisons concept and highly effective maritime domination programs launched by the Sri Lankan Navy which have become very effective in restricting such threats. However, the effects of such activities pose a moderate level threat to the stability of our country.

Ladies and gentlemen, a government alone cannot afford to force all these threats that are in concert ruining the stability of a country. Therefore, as responsible citizens, it

is our bounded duty to provide novel ideas, suggestions, and proposals to consider in regaining our country's stability and development. I hope the academic events of this nature will undoubtedly serve this national requirement. Such efforts are arranged to address emerging challenges. Promoting more research and development becomes a task of topmost priority for all of us.

Fortunately, as the Secretary of Defense, I feel tremendously proud and content to say that the Kotelawala Defence University is at the forefront of researching the development of security-related problems in the new normal. The approach adopted by the Kotelawala Defense University to understand the contempaty complex situations concerning the bigger picture rather than dwelling on the narrow passages will become far more effective in resolving the emerging complexity of future challenges. Therefore, I'm well certain that the faculties of General Sir John Kotelawela Defence University with their interest, commitment, dedication, and knowledge in diverse academic disciplines and outside rich researches inputs would contribute immensely to this year's conference theme. The knowledge that you are going to unearth and share during this conference would be of immense benefit not only to the academic community but to the entire humankind to make their lives better.

In conclusion ladies and gentlemen, I should express my most sincere appreciation to the Vice Chancellor and the organizers of the General Sir John Kotelawala Defense University's 14th International Research Conference 2021 for organizing this timely important event amidst the covid 19 pandemic concerns and I wish this event be successful in all way imaginable. Ladies and Gentlemen thank you very much for your patience, thank you.

Vote of Thanks

Dr Harinda Vidanage

Conference Chair, 14th International Research Conference, General Sir John Kotelawala Defence University

Mr Lalith Weeratunga, Principal Advisor to HE the President of Sri Lanka, Secretary to the Ministry of Defence, General Kamal Gunaratne, Vice Chancellor – Maj Gen Milind Peiris, Deputy Vice Chancellor (Defence & Administration), Deputy Vice Chancellor (Academics), Rector – Southern Campus, Senior Professors, Deans and Directors, Senior officers representing Tri Forces and Police, Distinguished guests, colleagues, Ladies & Gentlemen, Good morning!

In its 40th Anniversary since its inception the flagship academic conference of the KDU, the international research conference progresses to 14 years of continuity. I stand here to reflect and provide my gratitude to a team of individuals who despite every challenge in the form of material and the forces of nature has confronted us with, have managed to successfully bring us to where we are today.

Since 2019, the country has witnessed unprecedented upheavals from violent extremism to microbial threats that have forced a drastic rethinking of every aspect of social life. These challenges have made all of us believe in a reality that long established norms, traditions, beliefs do have their limits and if we are to survive and thrive in the new normal, we must adapt, adopt and innovate. The core fundamentals driving this year's IRC is based on this conviction and that the KDU as a leading force of defiance and a beacon of hope amidst such calamities.

On behalf of KDU, I would first and foremost like to extend a heartfelt appreciation to our Chief Guest and Keynote Speaker, Mr Lalith Weeratunga the Principal advisor to H E President Gotabaya Rajapaksa. Your presence today is a blessing to us as an institution and to the IRC as a process and your observations made at the keynote enriched us with knowledge and perspective. Your wise words of wisdom will have a bearing on the deliberations of all academic communities within and well beyond this conference. I also would like to thank Secretary to the Ministry of Defence, General Kamal Gunaratne for his presence, his insights and his towering leadership that has seen KDU through fair weather and through some rough storms.

I would like to highlight and appreciate the visionary leadership of the Vice Chancellor, Maj Gen Milinda Peiris and his belief in maintaining continuity of this apex academic event of the KDU. I must then appreciate the critical roles played by Deputy Vice Chancellor (Defence & Administration) Brigadier Wipula Chandrasiri in ensuring that the IRC will take place and in providing the administrative leadership towards the materializing of the conference. The support and blessing of the Deputy Vice Chancellor (Academic) Professor KAS Dhammika is highly appreciated, along with the support of all Deans of faculties who came together to make this event a success.

Even at a time when every institution is careful about its purse, our sponsors have stood by us, let me profoundly thank and appreciate the generosity of our Gold Sponsors, the Bank of Ceylon and the People's Bank and with Huawei Sri Lanka and National lotteries board being our silver partners. There are many more who have chipped in and do not want their names mentioned and a big thank you for all.

I must mention that this year it is the first time the faculty of Defense and Strategic Studies have been tasked with the overall IRC and holds the chair. I must with gratitude mention the hard work of my colleagues in both departments of Defense and Strategic

Studies under the leadership of Col Enoj Herath the Dean of the faculty. The FDSS represents the tip of the Spear of the KDU and bears testimony to the perfect convergence of civic-military relations.

Towards the buildup to the conference the shutdowns became lockdowns and lockdowns became enforced quarantined curfews, yet the main committee of the IRC 2021 managed to work tirelessly around the clock. We knew it was all for a greater cause and I must appreciate the gargantuan task that was handled by the secretary of the IRC committee Ms Lihini De Silva who virtually was my prime buffer and the tremendous work done by the three co secretaries, Maj Ranushka Ferdinandesz, Ms Isuri Uwanthika and Captain Abeetha Athukorala. We were all supported by the dynamic team of faculty coordinators who labored hard and were endowed with patience.

It is with sincere gratitude I appreciate the services of Mr Kithsiri Amaratunga the president of the Editorial committee and Dr Faiz Marikar the deputy editor. I also want to mention the prudent actions taken by Commander Bogahawatte, the president of the publication committee. I would like to thank all committee presidents, committee members, faculty committees, the office of Bursar, Registrar, Adjutant and C/O Admin and the staff at the Vice Chancellor's office.

New normal pushed us to the limits, yet we managed to overcome as we functioned as a collective team. Yet, finally the work would be incomplete if not for the researchers who had put faith in us and submitted papers and reviewers who filtered them. This year's IRC is the most decentralized event out of all IRCs, facilitating intellectual deliberations of this scale is no easy task. To keep this grid alive and robust the contributions made by Director IT and his team needs a special word.

We have truly embraced the new normal. We have not run away from it, instead we have transcended it. Thank you all for accepting and believing in us. We shall prevail and we shall overcome.
Thank you very much!

ENGINEERING

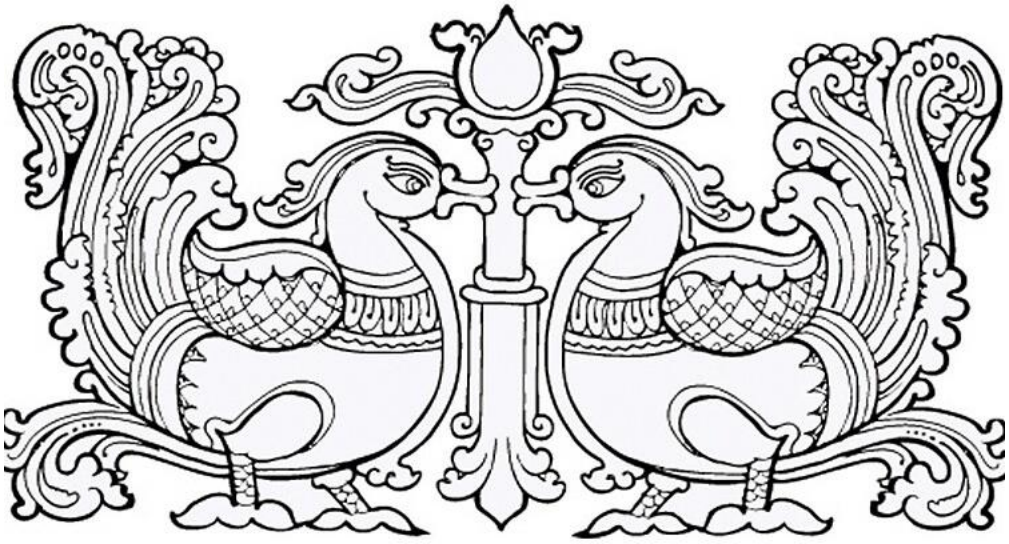

Technical Sessions

Verifying of 'Orifice Plate' Connecting Duct Lengths to Validate Performance of a 'Vent Test Rig at Australian Maritime College' by Computational Fluid Dynamics (CFD) as Part of the Oscillation Water Column Power Take Off

MCP Dissanayake

Department of Marine Engineering, Faculty of Engineering, General Sir John Kotelawala Defence University, Sri Lanka

dissanayakemcp@kdu.ac.lk

Abstract— Oscillating Water Column (OWC), ocean wave energy converter, transforms the energy of ocean waves into low pressure pneumatic power. This pneumatic power is extracted by a turbine and converted to electric energy through a generator. Australian Maritime College (AMC) has set up a vent test rig to conduct experiments on 'OWC' operation, quantify air leakage, and find differential pressures across the orifice plate as per the Australian standard of fan performances. However, the upstream and downstream of duct lengths of vent test rig did not match the given specified standards due space restriction. Therefore, the technical team of AMC chose Computational Fluid Dynamic (CFD) application as an alternative method to continue the investigation with economy of effort. Subsequently, it is understood that, CFD is a very attractive method to carry out investigations and obtain a detailed report with all tested parameters and conditions. In addition, it is revealed that the shape of the flow pattern which cannot be seen during the experimental study. The objective of this investigation was to apply CFD instead of vent test rig experiment and carry out modelling, and then compare the outcomes with experimental results. Further, CFD application was used to test differential pressure across the orifice plate with the same upstream and downstream lengths of pipe, which were utilized during the vent test rig experiment. In addition, CFD was applied again for specified lengths of pipe with the same orifice plate to measure the differential pressure across it. Finally, it was proven that specified duct lengths directly impacted the performance of the vent test rig and decreasing of the generating pressure along with the length of the pipe due to relative roughness.

Keywords: ***oscillating water column, inflow radial turbine, vent test rig, orifice plate, computational fluid dynamic.***

I. INTRODUCTION

Oscillating Water Column (OWC), ocean wave energy converter that transforms energy of ocean wave into low pressure pneumatic power. This pneumatic power is extracted by a turbine and converting to electric energy through a generator. Australian Maritime College (AMC) was set up a vent test rig to conduct experiments on 'OWC' operation, quantify the air leakage and find differential pressures across the orifice plate as per Australian standard of fan performances. However, the upstream and downstream duct lengths of the vent test rig were not matched with given specified standards due to space restriction. Therefore, the technical team of AMC was chosen Computational Fluid Dynamic (CFD) application as an alternative method to continue the investigation with the economy of effort.

Computational Fluid Dynamic (CFD) simulation is cost effective, quick out come and attractive compare to experimental investigations. Further, it is providing a detail report with all tested parameters and conditions. Moreover, it is revealed that the shape of the flow pattern, which cannot see during the experimental study. Generally, CFD permits for the modelling of extra complications, that affect the outcomes. When flow pattern is showing, high-fidelity CFD simulations will make available detailed statistics in the calculation domain. Add advantages of this CFD simulation are to repeat the same conditions and situations and obtain accurate results. Making pipe geometry was not much complex in this CFD simulation. ANSYS was applied and used lots of energy to obtain superior

pre-processing and established high fidelity turbulence models, such as the Large Eddy Simulation model and Reynolds average Naiver-Stokes model. Then, CFD was applied to resolve the turbulent problems utilizing super-grid scale and could practice empirical models for sub-grid turbulent structures (Leap CFD team, 2015).

The objective of this investigation was to apply CFD instead of vent test rig experiment and carry out modelling, then compare outcomes with experimental results. Further, CFD application was used to test differential pressure across the orifice plate with the same upstream and downstream lengths of pipe, that were utilized during the vent test rig experiment. In addition, CFD was applied again for specified lengths of pipe with the same orifice plate to measure the differential pressure across it.

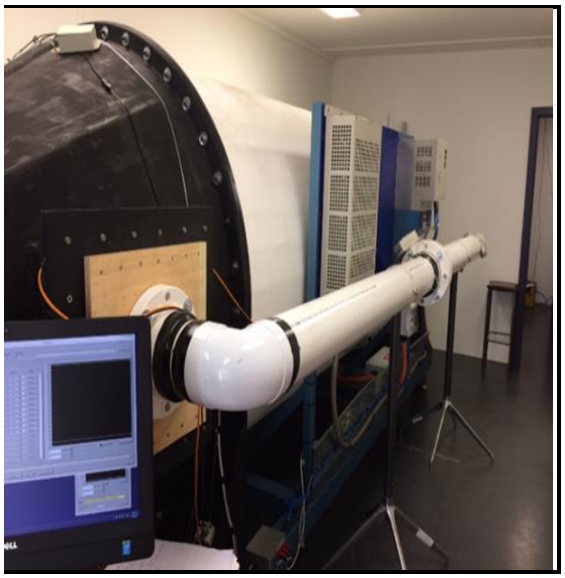

Figure 1: Vent Test Rig to Test OWC Operation (Australian Maritime College)

II. DESIGN FEATURES

In this simulation, the differential pressures, mass flow rate, and piston velocities were investigating by CFD application based on the following equation (1). The vital factors of this experiment were to maintain adiabatic condition, the effectiveness of sealing, a consistent control arrangement, coaxially fixing the orifice, installing exact duct lengths, the precise placing of pressure sensors, temperature sensors, and smooth mechanical operations to obtain accurate consequences.

$$C = \frac{q_m\sqrt{1-\beta^4}}{\frac{\pi}{4}d^2\sqrt{\Delta p \rho_1}} \quad (1)$$

$$\beta = d / D \quad (2)$$

Where, β is Diameter Ratio

d is Diameter of Orifice

D is Diameter of Duct

A. Reynold Number Effects

Exploiting the correct flow pattern was vital in the vent test rig operation to acquire the correct measurement of air flow. Reynold number based equation (2) was utilized to calculate the measurement. Required Reynold number was fluctuating as per variation of the parameters, of the equation. Though, vital to encompasses the practically viable and lucrative method to change the parameters during the experiment.

The changing kinematic viscosity (ν) was effortless, though, altering other parameters was to developed more pressure inside the vent test rig. The variation of the test facility and compressibility effects were deliberated restrictive influences to transform the kinematic viscosity during the test. The generated velocity was maintained between 0.06 m\s to 0.31 m\s to accomplish the Reynold number. The industrial fans- performance testing standards was emphasizing that the Reynold number might be ignored. Though, confirm to continue the Reynold number was keeping more than 3 x 106. Further, the diameter of the prototype needs to be at least 0.9 m or model scale 1/5th, whichever should be larger.

$$Re = \frac{\rho v l}{\mu} \quad (3)$$

Table 1: Fluctuations of Reynold number as per different pipe lengths

Velocities (m\s)	Re of Upstream (1675 mm)
0.06	6.81×10^3
0.1	1.12×10^4
0.11	1.21×10^4
0.14	1.61×10^4
0.15	1.73×10^4
0.24	2.71×10^4
0.25	2.82×10^4
0.3	3.41×10^4
0.31	$3.5\ 1 \times 10^4$

B. Coefficients of Orifice Plates

Many types of standard orifice plates can be utilized for the experiments, though all of them need to be alike, with only one explanation. More, all type of standard orifice plates is to be distinct as per positioning of pressure tapings. The detailed schematic of the standard orifice plate is shown in figure 2. The standard orifice plate is comprising of a thin circular plate of two flat faces with a 90 mm diameter of an orifice. Moreover, the orifice was positioned coaxially to the pipe center with the straight line and uphold the thickness of the plate between 0.005D to 0.02D. Usually, more attention was paid to the fabrication process of the orifice plate and ensure the sustainability of the developing pressures and avoid plastic buckling and deformation taking place during the experiment.

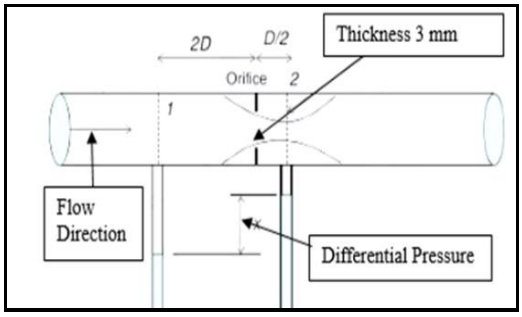

Figure 2: Schematic of Orifice Plate Application

The vent test rig was operated in different velocities in steady state conditions and selected three velocities were to make an easy comparison with CFD outcome. The flowrate and differential pressures across the orifice plate were obtained through the control system and tabulated in table 2.

Table 2: Experimental Results

Velocity (m/s)	Generated Air Flow by the Piston (m^3/s)	Inlet Pipe Pressure at Short Pipe (Pa)	Outlet Pipe Pressure at Short Pipe (Pa)
0.06	0.118	197	113
0.15	0.132	1258	923
0.25	0.54	3490	2052

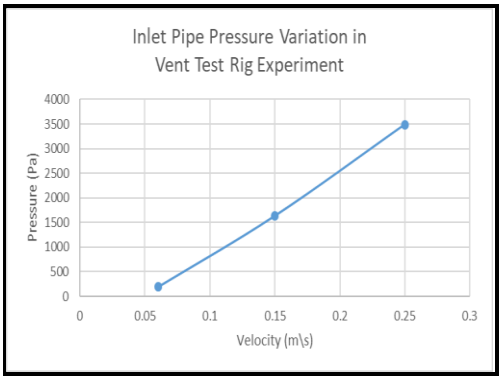

Figure 3: Inlet pressure variation at upstream of a pipe

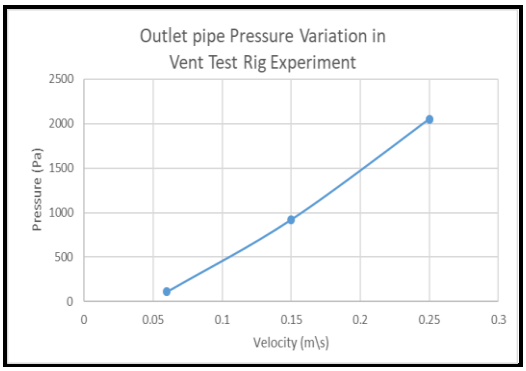

Figure 4: Outlet pressure variation at downstream of a pipe

C. Vent Test Rigs' Operation

A servo motor operated vent test rig was comprising of 3000 mm in length and piston diameter of 1500 mm chamber, and generate the basic airflow features of an OWC, ocean energy extraction. The vent test rig was right scaled and set up with a volume of 3.534 m^3. Further, the vent test rig was operated in the range of velocity from 0 to 1.25 m/s. All the measurements were carryied out in the adiabatic condition at ideal gas air velocity not as much as 1.25 m/s, chamber pressure, below 5 kPa and dry air density in 1.225 kg/m^3. The block orifice plate was fixed between upstream and downstream of the pipe to assess the leakage of air and related uncertainty occurring inside the vent test rig. A 'PVC' is chosen as a suitable material for the duct with 150 mm diameter to fulfil the ISO 5167, standards. A specified range of diameter of the duct was not less than 50 mm and not more than 1200 mm, either application of Reynold number should be more than 3150. Installed pressure sensors and temperature sensors were factory calibrated and fixed through the drilled holes of the upstream and the downstream of the duct

adjacent to the orifice plate to obtain the outcome. The upstream and downstream pipe lengths were taken as 1675 mm and 1800 mm respectively, due to the limited space in the room. The orifice diameter was 90 mm and established pressure wall with a distance 150 mm from the orifice plate to the upstream and 75 mm to the downstream. The static pressure and differential pressure (Δp) were measured through pressure sensors. According to fan performancestandards, the stated diameter ratio (β) of the orifice was selected through the given charts and fabricated the orifice plate. Subsequently, it is placed between upstream and downstream of the duct coaxially with a straight line to maintain the uniform flow of air.

D. Developing a Geometry

The 3-D geometry of two pipes and orifice was generated by Inventor software and exported to ANSYS 19.1 work bench software shown in figures 4 & 5.Subsequently, a fixed diameter orifice was made and selected x, y, and z coordinates correctly, then developed upstream duct length with 1.675 m and downstream duct length with 1.8 m as a condition one. Then simplify the geometry by introducing inlet, outlet, walls, orifice inlet and, orifice outlet to the ducts and orfice. Similarly, the upstream duct length was extended up to 3 m and downstream duct length was shortened to 1.2 m, as per given standards with the same orifice as condition two.

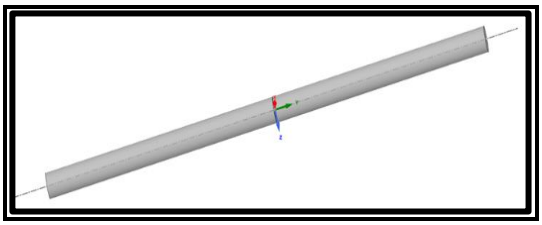

Figure 5: Geometry of the Short Pipe

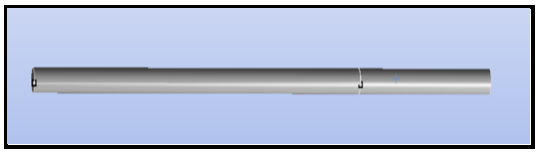

Figure 6: Geometry of the Long Pipe

E. Generate a Mesh

The mesh generation is a pre-processing phase of the computational fluid dynamic simulation and the discretization of the domain. The process of meshing is a time-consuming and complex affair to generate an accurate mesh. The mesh is essential to be in quality to give accurate answers. The movement of flow is a bit complex in this application and approach with the coarse mesh to begin the task. The meshing process is comprised of two categories such as structured and unstructured meshes. A numbering of structured mesh cells or nodes are described as (i, j, k) indices at the Cartesian coordinate structure with interior nodes and surrounded by the constant number of elements Moreover, unstructured mesh cells are specified with a point to point connections between nodes and significantly affect the modelling software. The hybrid mesh is consisted of a combination of structured and unstructured meshes and providing additional provisions during the meshing. The significant controlling effect of the nods and sufficient to operate fewer memory capacities of the computers for structured meshing in process of referencing of cells. This application can be handled by even unskilled operators during the meshing process and the possibility to obtain better results with fewer nodes (Seo, J.H., Seol, D.M., Lee, J.H. and Rhee, S.H., 2010).

The mesh was generated using ANSYS Meshing 19.1, with physics and solver preferences set to CFD and CFX respectively. The constraint was imposed up to 512,000 nodes and completed the fine mesh, as per table 2 and shown in figures 6 & 7.

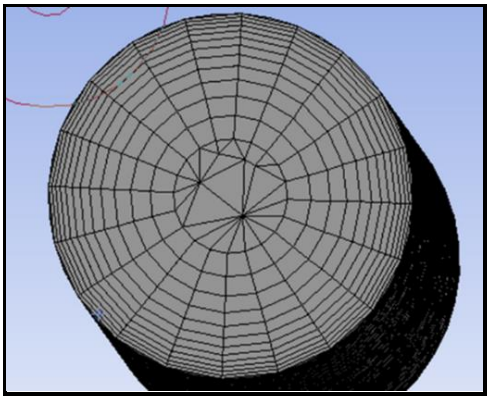

Figure 7: Fine Mesh of Short Pipe, Inlet Face

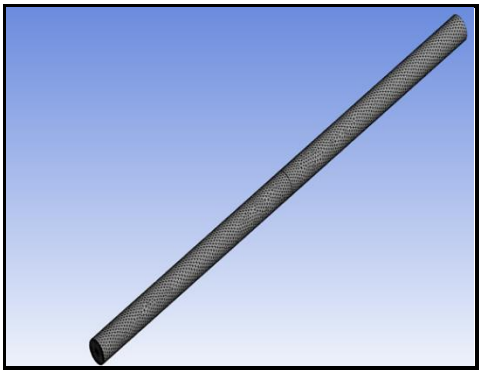

Figure 8: Application of Fine Mesh of Short Pipe

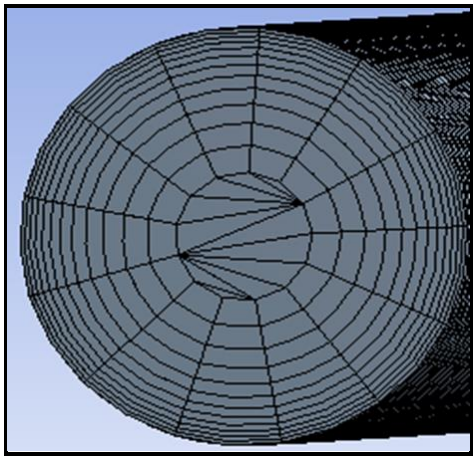

Figure 9: Application of Fine Mesh of Long Pipe, Inlet Face

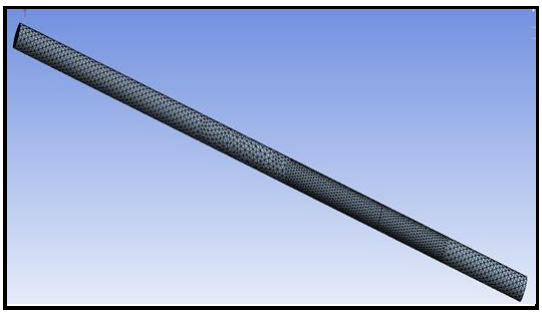

Figure 10: Aplication of Fine Mesh of Long Pipe

F. Calculation of Inflation Layer

The inflation layer was established based on boundary layer modelling theory and ensure to develop the inflation layer thickness fully exceeded the boundary layer thickness. The calculation was carried out as per the following equation at (3).

$$Y_{BL} = 0.16.\, x/\, (Re_x)^{1/7} \qquad (3)$$

where, x is critical length

Y_{BL} is turbulance boundary layer height

The boundary layer was modelled by low Reynold number wall treatment consisted with a y+ value of 1 and growth rate of 120% laminar sublayer that made the path way to capture the outcome of frictional resistance and seperation.

Table 3: Application of Low Reynold Treatment and Wall Function.

	Low Reynold wall treatment	Wall function
	y+1	y+30
L[m] (chord length)	1	1
Viscosity	1.512×10^{-5}	1.512×10^{-5}
Density	1.225	1.225
Speed [m/s]	0.25	1
Re	1,000,000	1,000,000
Y BL [m]	0.04446	0.04
y+	1	30
Delta Y 1st layer	0.00	0.000719843
Growth rate	1.2	1.2
Tol. Inflation (maximum thickness in analysis)	0.049091633	0.051853955
No. Layers		27

G. CFX Pre Solver

The mesh files were imported into CFX Pre Solver, and conducted analytical study. Then defined the properties of air and boundary conditions. The two numbers of monitoring points were establised with 0.15 m distance from the orifice plate inside the upstream of the pipe as per specified standards. Similarlly, two more numbers of monitoring points were set up with 0.075 m distance from the orifice plate inside the downstream of the pipe to obtain relevant measurements of the pressures. The mass flowarte was calculated as per piston moving velocity and fed as an input to the application and obtain the related pressure by monitor points.

Table 4: Details of Input Mass Flowrate to CFD application

Velocity (m\s)	Input Mass Flowrate (kg\s)
0.25	0.54
0.15	0.32
0.06	0.129

H. Analysis Procedure

An analytical setup was recognized in steady state to avoid all time and computational source restrains. The face sizing was conducted to diminish errors and maximize separation areas. The turbulence model is selected as per the resolution and place of nodes inside the boundary layer. According to the proper selection, low Reynold wall treatment is being applied with y+ = 1 and the Shear Stress Transport (SST) turbulence model is being chosen to model free stream and boundary layer turbulence.

I. Boundary Condition

The boundary conditions were applied in ANSIS 19.1 pre and boundary regions have been decided to solve the problem in the best way. The inlet flow of the duct, pressure monitor points of either side of the orifice plate, and outlet of the duct are shown in figure 5. The inlet and outlet domains were modelled and with air in three different velocities shown in table 4. The inlet and out let pressures were monitored through monitoring points and carry out the simulation, then it ensures to get convergence in inlet pressure variations along with velocities.

Table 5: Application of Boundary Conditions

	Type of Boundary	**Situations**
Pipe Inlet	Inlet	Velocity is varying from 0.06 m\s, 0.15 m\s and 0.25 m\s.
Pipe Outlet	Outlet	
Wall	Wall	

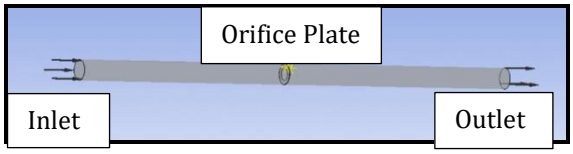

Figure 11: Boundary condition details of Short pipe

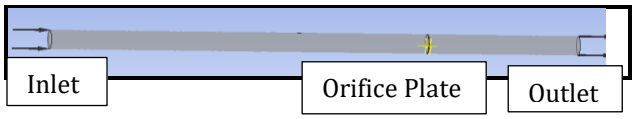

Figure 12: Boundary condition details of Long pipe

J. Solution Control

The solution control application was used to defined solver control inputs and convergence criteria, then setup the system to make use of the resources efficiently at table 4.

Table 6: Control Inputs

Solver Control Inputs	
Maximum Iterations	500
Maximum Iterations	5000
Criteria for the Convergence	
Type of Residual	RMS
Residual of the Target	0.0000001

K. CFX Solver Application

The CFX solver files were written for the different pressures all as per velocities in two different pipe lengths in separate computers using 7 cores. The studied variables and examined the convergence explanations, before exporting the solution files.

L. Verifications

A grid independence study was conducted to examine mesh reliability on different pressures across the fixed diameter orifice, during two different lengths of pipes. A Richardson Extrapolation was conducted to authenticate the three sets of mesh resolutions and specified them as 'coarse', 'medium', and 'fine'. In addition, all three mesh types were ruled by modification of, face sizing with support of inflation layers. The Richardson extrapolation method was applying to impact the mesh size and anticipate the constant expansion ratio for node count of the mesh. The Richardson Extrapolation prediction was based on the expansion ratio along with the non-dimensional coefficients and emphasized that the solution of a mesh sufficed with infinite nodes. Subsequently, results of the coarse, medium and fine meshes were assessed in line with a comparative error related to the Richardson-extrapolate clarification. The calculation of Richardson Extrapolation is sited at Appendix B.

M. Sensitivity Study of Mesh

A mesh sensitivity research was conducted to confirm the optimization of meshing to solve the problem and ensured the obtained outcome

which was totally independent of the quality of the mesh. The mesh refinement was done by changing face sizing and kept other parameters constant. All three types of meshes are specified in table 6. The mass flow rate was fed as per input to the inlet of the duct. Subsequently pressures of specified two number of monitor points were provided the measurement of pressures that located either side of the orifice plate of the pipe, and indicated by the cartesian coordinates.

N. Convergence Study for Short Length Pipe

The inlet pressure is converged with an estimated error of 0.0352, 0.021, and 0.0175 for the coarse, medium, and fine mesh respectively, at a velocity of 0.25 m\s for short length ipe. It was revealed that the fine mesh providing the minimum error compare to other meshes. Thus, the fine mesh was designated to conduct the analysis process. The plot is clearly specified that the highest inlet pressure at fine mesh, then second highest inlet pressure at medium mesh, and finally lowest inlet pressure at the coarse mesh in figure 9. Further, it is meeting the requirement of grid convergence theory. The details of the conevrgence study for short length pipe are shown in table 7.

Table 7. Number of Nodes and Sizes of Short Pipe

Type of Mesh	Number of Nodes	Number of Elements	Size	Inflation Thickness
Coarse	23904	50703	0.0352	0.1
Medium	73223	152726	0.021	0.1
Fine	113093	236585	0.0175	0.1

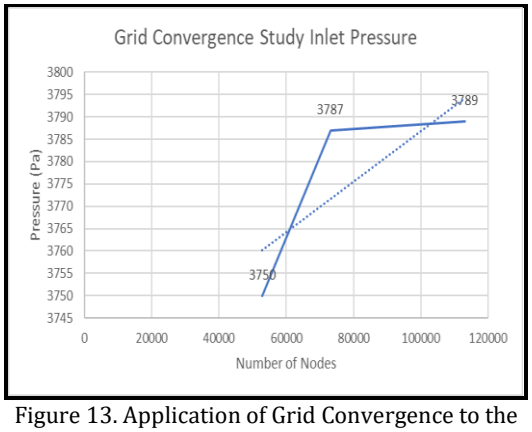

Figure 13. Application of Grid Convergence to the Short pipe

O. Convergence Study for Long Length Pipe

The inlet pressure is converged with an estimated error of 0.04, 0.0395, and 0.039 for the coarse, medium, and fine mesh respectively, at a velocity of 0.25 m\s for a long length pipe. It was revealed that the fine mesh providing the minimum error compare to other meshes. Thus, fine mesh was designated to conduct the analysis process. The plot is clearly specified that the highest inlet pressure at fine mesh, then second highest inlet pressure at medium mesh and finally lowest inlet pressure at the coarse mesh in figure 10. Further, it is meeting the requirement of grid the convergence theory. The details of conevrgence study for short length pipe are shown in table 9.

Table 8: Number of Nodes and Sizes of Long Pipe

Type of Mesh	Number of Nodes	Number of Elements	Size	Inflation Thickness
Coarse	229961	95054	0.04	0.1
Medium	232451	96318	0.0395	0.1
Fine	263527	236585	0.039	0.1

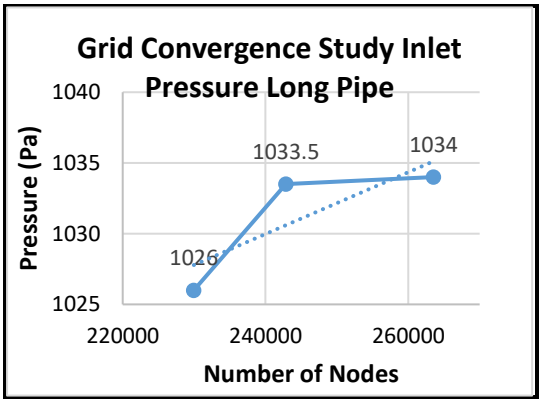

Figure 14: Application of Grid Convergence to the Long pipe

Table 9: Details of Convergence Study for Long Pipe

Mesh	Size	Nodes	Elements	Inlet CFD (Pa)
Coarse	0.04	229961	95054	1021
Medium	0.0395	242876	96318	1025
Fine	0.0175	263527	236585	1030

III RESULTS AND DISCUSSION

A. Short Pipe

According to three different piston velocities of the vent test rig, the mass flowrate was calculated and fed as input to the inlet of the boundary condition one. Subsequently, the pressures were obtained through the monitoring points that were established across either side of the orifice plate in line with specified standards shown in table 7. Both inlet pressures of experimental results and CFD outcome were increasing with advancement of velocities. The percentage difference is (-2.53) at 0.06 m\s, (-1.77) at 0.15 m\s and (-0.57) at 0.25 m\s during the comparison and shown in figure 14. Similarly, outlet pressures were growing along with the the advancement of velocities. However, the percentage difference is (-3.53) at 0.06 m\s, (-0.68) at 0.15 m\s and (-1.07) at 0.25 m\s during the comparison, and bit vary from the inlet pressure difference, due to orifice plate effect and shown in figure 15.

Table 10: Comparison of Pressures, Short Pipe

Velocity (m\s)	P1 (Inlet)			P2(Outlet)		
	CFD (Pa)	EFD (Pa)	%	CFD (pa)	EFD (pa)	%
0.06	192	197	-2.53	109	113	-3.53
0.15	1250	1258	-1.77	724	729	-0.68
0.25	3470	3490	-0.57	2030	2052	-1.07

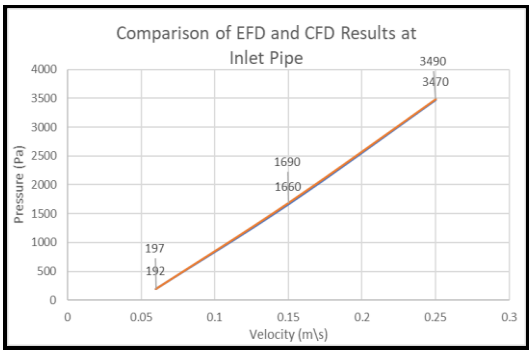

Figure 15: Assessment of Experimental Outcome and CFD Outcomes of Inlet Pipe

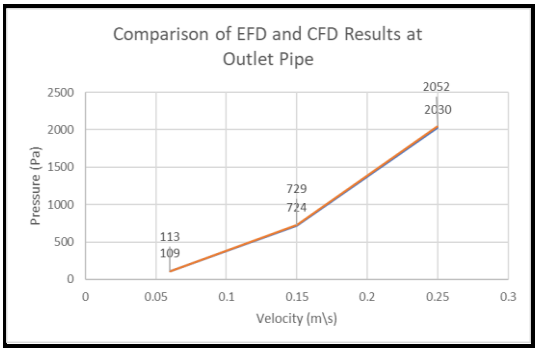

Figure 16: Assessment of Experimental Outcome and CFD Outcomes of Outlet Pipe

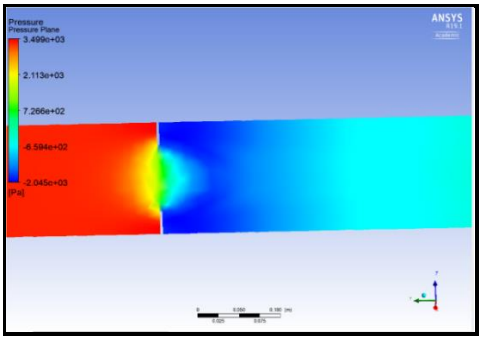

Figure 17: Results of Velocity 0.25 m\s, short pipe.

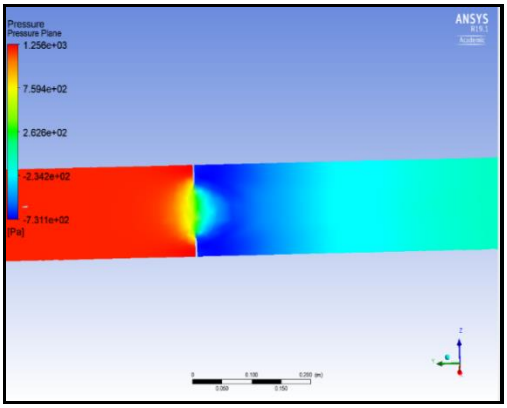

Figure 18: Results of Velocity 0.15 m\s, short pipe.

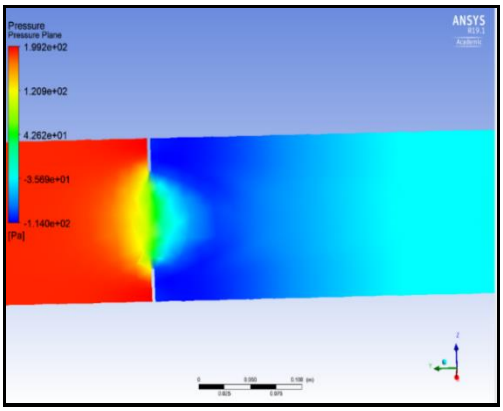

Figure 19: Results of Velocity 0.06 m\s, short pipe.

B. Long Pipe

There were no experimental results in the process and only CFD results were obtaining through monitoring points. On this occasion, the inlet pipe was 3 m and the outlet pipe was 1.2 m, the input variables were applied similar to condition one and obtained the pressures from the monitoring points and shown in table 7. Compare to short pipe, both inlet pressure, and out let pressures were low in the long pipe due to the effect of relative roughness shown in figure 19 & 20.

Table 12: Comparison of Pressures, Long Pipe

Velocity (m\s)	Inlet	Outlet
	CFD (Pa)	CFD (Pa)
0.06	1021	12.9
0.15	1025	32.8
0.25	1030	54

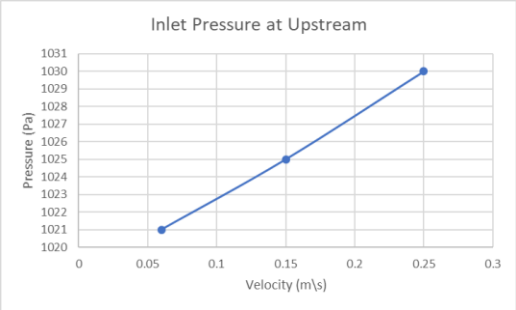

Figure 20: Results of Inlet of Long Pipe

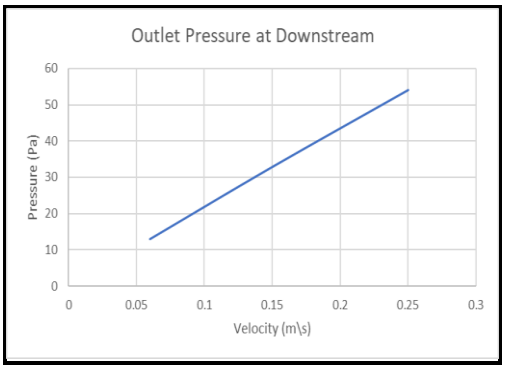

Figure 21: Results of Outlet of Long Pipe

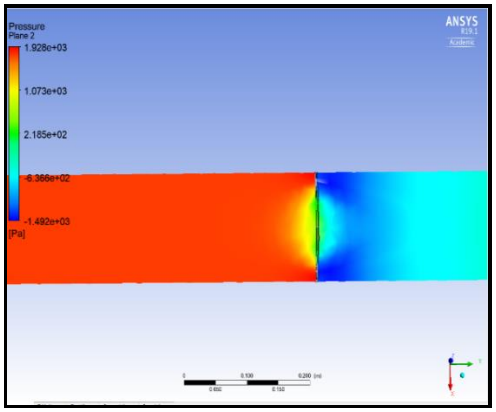

Figure 22: Results of Velocity 0.25 m\s, long pipe

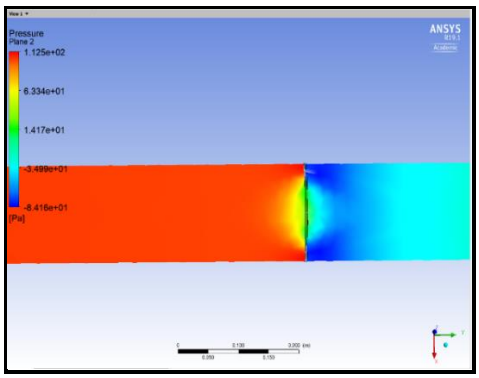

Figure 23: Results of Velocity 0.15 m\s. long pipe

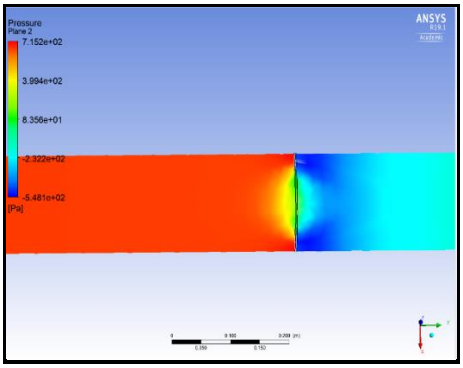

Figure 24: Results of Velocity 0.06 m\s, long pipe

According to figures 16, 17, 18 related to the short pipe and figures 21, 22, 23, of the long pipe, it is revealed that the pressure development through orifice plate was high when the upstream pipe was short and uniform flow of outcome was showing due to sufficient length of downstream of pipe. When the upstream of the pipe was lengthy, the pressure generated through the orifice plate was reduced due to relative roughness, and outlet pressure further, dropped down. The total pressure is encompassed with radial variations and circumferential variations. Radial variations are generated causing boundary layers' effect and influence for the result. Though, circumferential

variations are developed due to the tangential element and insignificant.

IV. CONCLUSION

The CFD application was proven that specified duct lengths were directly impacting to performance of the vent test rig and decreasing the generating pressure along with the length of the pipe due to relative roughness.

REFRENCES

Fleming, A., MacFarlane, G., Hunter, S., and Dennis, T., 2017. Power performance prediction for a vented oscillating water column wave energy converter with a unidirectional air turbine power take-off. *12th European Wave and Tidal Energy Conference* (pp. 1204-1). EWTEC.

Fleming, A.N., 2012. Phase-averaged analysis of an oscillating water column waves energy converter *Doctoral dissertation, University of Tasmania.*

Herring, S., 2007. Design and evaluation of turbines for use in OWC power plants.

Bauman, R.P. and Schwaneberg, R., 1994. Interpretation of Bernoulli's equation. *The Physics Teacher*, 32(8), pp.478-488.

LEAP CFD Team, 2013. How does the Reynolds Number affect my CFD model *URL: http://www. computational fluid dynamics. com*. [cited May 2015].

ACKNOWLEDGEMENT

I would like to acknowledge my supervisor Dr. Alan Fleming (Australian Maritime College) for his guidance kind assistance and cordial relationship throughout this research project. I would like to thank Mr. Liam Honeychurch for his support to set up the vent test rig. Finally, I would like to thank Mr. Michael Underhill for his contribution to establishing the orifice plate and related duct installation.

AUTHOR BIOGRAPHIES

Cmde (E) MCP Dissanayake, CEng (India) is currently performing as the Head of Department (Marine Engineering) and holds 2 patents for his research papers published so far. He is an inventor and published 06 No's publications on Brackish Water Reverse Osmosis application, Fan Boat Building and Oscillation Water Column, Ocean Wave Energ Converter. He was the Director in Research & Development at Sri Lanka Navy and has received commendations on number of occasions from the Commander of the Navy, HE the President of Sri Lanka for his innovation. Further, he was awarded with prestigious, Japanese, Sri Lanka Technical Award for his own developed low-cost Reverse Osmosis Plant, to eliminate Chronic Kidney Disease from Sri Lanka. Moreover, he has vast exposure on marine diesel engines and possesses a Master's degree in Marine Engineering from Australian Maritime College, University of Tasmania, Australia.

A Hybrid Diesel Engine Simulator as a Skill Development Tool for Marine Engineering Undergraduates

MCP Dissanayake#, KGC Pathmal and VADJV Perera

Department of Marine Engineering, Faculty of Engineering, General Sir John Kotelawala Defence University, Sri Lanka

#dissanayakemcp@kdu.ac.lk

Abstract— This paper explains a prospect of using a scenario from a marine engine room simulator as a device for educating marine engineer undergraduates. Basic technical parameters have been indicated for the entire scenario of the marine engine room simulator which is used to educate marine engineer undergraduates of the General Sir John Kotelawala Defence University (KDU), Sri Lanka. The Hybrid Diesel Engine Simulator (HDES) is primarily a training method that simulates a realistic engine room set-up, through a controlled environment for marine engineer undergraduates and engine room watch keepers training on-board ships in operational circumstances. Further, HDES can be utilized for training engine room watch keepers in both war and peace times equally. Subsequently, to comprehend the actual operational parameters of Main engines and Auxiliary engines and the smooth functioning of the vessel, the engine room watch keepers will be able to respond to any defect with efficiency, expertise, and confidence gained from training in similar situations. The authors argue that the projected tutorials in the simulator could significantly contribute to the development of alert and responsible machinery utilization of trainees during marine engine room operations.

Keywords*: *hybrid diesel engine simulator, niigata 6M26AGT marine diesel engine, thermodynamics, engine room watch keeper, machinery control room (MCR), console, simulation mode, actual mode

I. INTRODUCTION

The first-ever learning programs through simulator were made in the early 1970's and, as software based teaching, they openly had an inverse academic orientation from the traditional teaching with computer support. Generally, simulation teaching can be distinguished in majors as teaching offered by the trainer (support of the teaching subject with the aid of collaborative simulation), use of simulation and interaction with the trainer and individual or collective use by the trainees (Laskowski, R., Chybowski, L. and Gawdzińska, K., 2015).

Qualitative advancement of the learning progression at university domain, marine engineering education depends mostly on the development of hands on skill training sessions and educational software. Therefore, this Hybrid Diesel Engine Simulator (HDES) is designed and developed with Niigata marine engine and Arduino based control systems to conduct realistic engine room scenarios and performance evaluation of the current technical state of engines and devices. Further, this platform provides facility for marine engineering undergraduates to develop skills on management, operational and support activities (Tsoukalas, et.al.; 2008).

The HDES is primarily a training method that simulates a realistic engine room set-up, though a controlled environment for engine room watch keepers training in ship operation circumstances. Further, HDES can be utilized for engine room watch keepers training in both war and peace times equally. Subsequently, to comprehend the actual operational parameters of Main engines, Auxiliary engines, management issues and re-establishment of damages of engine room. In addition, engine room watch keepers are trained to respond, against any defect or damage with efficiency, knowledge and confidence to overcome realistic status quo inside the engine room (Cao, H. and Zhang, J., 2020). The realistic engine room operation scenarios and crisis generated in the HDES contributes invaluably in driving away fear among the trainees and in improving team building traits, thereby

preparing them for unforeseen hardships and emergencies at sea.

Analytical study reveals that 90 % of engine room breakdowns were occurred due to operator's negligence or errors. Therefore, HDES is designed and developed as a perfect teaching method to train modern ship crews in the following areas;

a. Asses watchkeeper's behaviour in emergencies or crucial situations.

b. Enhance practical knowledge on previously acquired theoretical aspects.

c. Improve the ability on problem solving

d. Spareparts ordering and identification for replacement.

II. DESIGN FEATURES

A. Outfit

The HMES of General Sir John Kotelawala Defence University (KDU), Sri Lanka is comprised with Niigata 6M26AGT Marine Diesel Engine and Microcontroller based work stations. The Machinery Control Room is comprised with two work stations;one is operated by the instructor and other is handled by a trainee during simulations. This is a unique simulator that can directly start the engine remotely (from the main console at the work station) and monitor realistic parameters such as starting air pressure, fresh water temperature, lubricating oil pressure, sea water temperature, fuel pressure and exhaust temperature. Further, safety alarms and automatic cutouts are incorporated with this HDES for the safety of both the Marine Diesel Engine and control system. Moreover, both workstations are availed with data storing facility to carry out the analytical study by undergraduates, on completion of exercises. In addition, the same workstations can be utilized to create simulated scenarios while the engine is on run. However, the requirement of delivering the experience on watchkeeping and engine room resource management is met by said activities.

Figure 1: HDES at Marine Engineering Laboratory

The said engine was acquired from a naval vessel which was decommissioned lately. The installation parameters of the ship and general specifications of the engine are tabulated as follows.

Table 1: Main Engine Parameters

Parameters	Value	Unit
Length Overall	60.43	m
Dead Weight	600	tones
Speed	10	Knots
Main Engine Specifications		
Type	Inline, single acting, 4 stroke, diesel engine	
Make	Niigata	
Model	6M26AGT	
Weight	12,700	kg
Cylinder Bore	260	mm
Piston Stroke	400	mm
Cylinder Number	06	
Max rpm	390	
Max continuous output	850	HP
Rotation	Clockwise	
Starting System	Compressed Air	
Governor		Hydraulic

Source: Operation manual of Niigata 6M26AGT Marine Diesel Engine

B. Operational Modes

HDES has two operation modes namely; **Actual** and **Simulation.** Starting, stopping and commissioning of the engine to be done in actual mode and all simulations to be done in simulation mode. Therefore, two consoles are available for controlling, responding and simulation of the

entire system and are named as student's console and instructor's console.

1) Machinery Control Room (MCR) for instructor – Instructor console:

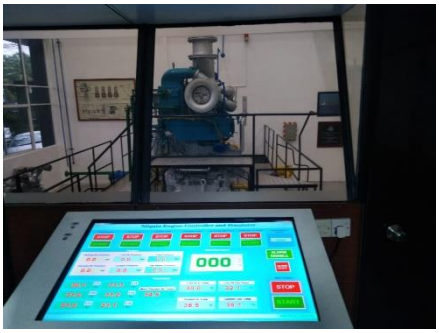

Figure 2: Instructor console

Simulation of scenarios, interchanging the modes of the control system and monitoring actual parameters shall be done from this console. Since the actual parameters are to be monitored by skilled personal while the system is on simulation, it has been enabled for the instructor to avoid actual failures to the system. However, all responses are to be done from the student's console if any alarm arises while the system is on either simulator or actual mode.
Further, trainees can practice the issues of management, supervision, and damage re-establishment in the engine system. Trainees are assessed on the aspects of the response time of identifying an amplifying situation and respond well before triggering an alarm or make necessary preventive measures with a minimum time after triggering an alarm.

2) Machinery Control Room (MCR) Workstation for undergraduate – Student's console:
All initial activities shall be done through the said console which includes, starting/ stopping of the main engine, starting/ stopping of auxiliary machinery and acceptance of remote to local controls. Further, the student shall be able to accept alarms, overrun alarms, respond for actions generated by the instructor's console and management of engine room machinery resources by having over control.

Figure 3: Student's console

C.. Engine Room
Engine room is comprised with an HP air compressor, lub oil and fresh water coolers, standby lub oil pump, fuel pump and a fuel tank along with the main engine.
All system lines are laid meeting the need of traceability and painted as per the standard colour code.

D. Control System
The control system of the HDES consists with two modes namely Remote and Local. The local control system is a Microcontroller based control system which is almost similar to a PLC based control system. Selection of modes is enabled with a Remote-Local selector switch.

1) Local Mode –
Direct end–to–end controlling is enabled when operated in local mode. The Control signal is directly forwarded from the local control panel to the input card of the microcontroller input card. According to the given algorithm, the signal is directed to the output card of the microcontroller and through relevant relays and contactors, the control signal will be transmitted.

2) Remote Mode –
Once the system is changed into the remote mode, all signals receiving from the local port will be omitted and connects with the remote module of the console and microcontroller. The remote module is interfaced with a wifi card enabling fully duplex communication within the console, sensors and machinery.

3) Consoles –
Both trainer's and students' consoles and 42" touch displays and the entire control system run on a MS Windows based software program. Data acquisition and transmission is done through aforesaid USB connected wifi module.

III. RESULTS AND OUTCOMES

Exercises are designed at the outset of thermodynamics, concept of marine diesel engines, ship's machinery, engine propulsion systems and watch keeper's role. The practical session is encompassed with Marine Diesel Engine system tracings, fueling and preparation of engine for the startup. Further, the session is limited to four hours and with 10 crew members maximum. In this exercise, real time engine operation is restricted to 30 minutes to maintain the economy of effort. Further, the major concern factor of HMES operation is to facilitate undergraduates to obtain hands on skills; performing basic operational activities such as starting up, follow operating procedures and supervising. Procedures to follow when operating the HDES are as follows.

A. Pre-Checks

i. Trace the system lines to confirm no leakage.
ii. Check main engine sump, air compressor, turbocharger and rocker arm lubricating oil levels.
iii. Check fuel level in service tank and cooling water level in the expansion tank.
iv. Check the pressure in compress air bottles (Max.15 bar).
v. Open valves of lubricating oil, fuel and compressed air bottle valves.
vi. Check power availability of the control system.
vii. Carryout visual inspection of the engine.

B. Starting Procedure

Subsequently, starting procedure should be conducted by watch keeper and start the engine accordingly.

i. Switch on the lubricating oil priming pump and rocker arm lubricating pump.
ii. Open De-compression valves and turn the engine manually.
iii. Put the engine lever stop position and crank the engine 2/3 turns with compressed air.
iv. Close De-compression valves and put the engine lever in start position.
v. Conform manual turning gear disengage.
vi. Touch the start button (If Remote)/Open the starting air valve (If locally) and start the engine.

C. After Starting the Engine

Then, after starting the engine followings are to be monitored by the watch keepers and record accordingly.

i. Check the main engine lubricating oil pressure.
ii. Check the RPM at the set point.
iii. Close the starting air valve properly.
iv. Be alert with engine sound, if any abnormal sound or vibration comes, make sure to stop the engine.

D. While Running the Engine

Finally, following are to be observed to continue the operation of the engine.

i. Check all the parameters and be alert with any abnormalities.
ii. Check Lubricating oil pressure/ temperature.
iii. Check Engine RPM.
iv. Check Cooling water pressure/ temperature.
v. Check Secondary cooling water (Sea water) pressure/ temperature.
vi. Check Exhaust temperatures.

E. Stopping Procedure

Following procedure will be followed in stopping the simulator.

i. Reduce engine RPM up to idle RPM
ii. Run the engine for 05 - 10 minutes and monitor whether the main engine parameters are normal (Lub oil pressure, Fresh Water temperature, Lub Oil Temperature)
iii. Switch mode from **Simulator** to **Actual**
iv. Check for air pressure of control air, prepare crew for manual emergency stop if control air drops.
v. Transfer **local** controls to **remote** controls (All controls to be on the student's console before shutting down the main engine)
vi. Shut down the main engine by student's console. Observe Lub Oil Stand By pump immediately kicks in after lubrication. In case of a system failure, remote or local starting to be enabled immediately after shut down.
vii. Shut down fuel pump, cooling water pump and observe for system leakages.
viii. Run the sea water cooling pump until the system temperature reaches ambient temperature and shut down.
ix. Observe for system leakages, abnormal leakage from the engine, any abnormality in head units, rocker assembly and crank case.

x. Transfer all controls to the local panel and shut down control system by the main breaker.

xi. Shut down consoles from the Machinery control room.

F. Preliminaries

The trainees are assigned to get familiar with the system initially and follow the preliminary operational procedures. Starting of the main engine will be done by the trainees as per the given procedure and closely monitored by an assigned engine room crew member. Subsequently, the instructor takes over control of the Marine Diesel Engine through his workstation and concurrently trainees to follow the instructor's commands. Ex: Increase RPM, loading the engine and etc. Accordingly instructor can change set-ups as per working conditions and state of the machinery, by creating operational turbulences such as failures, malfunctions and change of parameters through the instructor's console. Subsequently, scenario identification and reactiveness of trainees are monitored.

G. Simulation of a scenario- High Exhaust temperature

Marine Diesel Engine was started and operated at 255 rpm for 30 minutes in seven days. Mean coolant temperature (in & out of cooler), mean fresh water temperature, mean exhaust temperature in all six cylinders, mean lubricating pressure were recorded. Accordingly, same parameters for 300, 350 and 400 rpms were simulated respectively by using the system software and tabulated below.

Table 2: A template of experiment measurement table

rpm	Coolant in (°C)	Coolant out (°C)	FW_T (°C)	EXH_T (°C), Number of Cylinders						LUB $_p$ (bar)
				1	2	3	4	5	6	
255	38	28	65	74	82	54	60	79	54	5.2
300	38	30	72	79	83	59	64	80	60	5.4
350	38	33	76	80	84	68	70	81	66	5.5
400	38	35	78	82	85	74	75	84	73	5.8

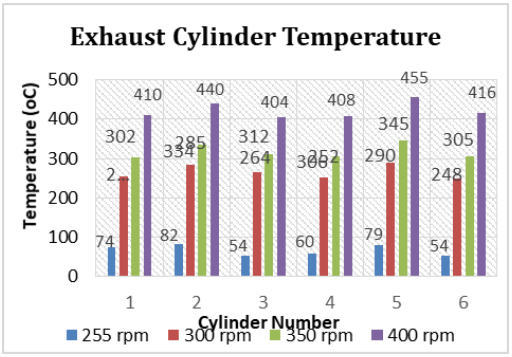

Figure 4: Individual Cylinder Exhaust Temperature as per different rpm

IV. DISCUSSION

In this experiment, the exhaust temperature of number 2 & 5 cylinders were high compared to the rest of the cylinder exhaust temperatures. Subsequently, an analytical study was carried out in this regard and matched with the theory learned during the class room lessons and understand followings in Figure 4.

i. Injection pressure may be low in both cylinders 2 & 5

ii. Injection nozzle spray pattern may be changed

iii. More Carbone deposited on cylinder head (outlet valves)

The most vital part of this investigation was the approaches of trainees on identifying the defect, rectification and repair action. Accordingly, referring to the spare parts catalogue and identifying a component which is to be replaced also observed.

V. CONCLUSION

This HDES equipped with two work stations facilitate individual training and control of the abilities of numerous watch keepers at the same time. Therefore, enlightening marine engineers employing Hybrid Marine Engine Room Simulator is the least expensive and the safest training and evaluating method in present day context. This HDES encompasses with Mictrocontroler based control system and is able to simulate 15 scenarios related to parameters and operational conditions. Subsequently, trainees can evaluate the performances of changes for selected active and economic parameters of the Niigata 6M26AGT Marine Diesel Engine operation and fuel supply system. Eventually, the acquired knowledge by undergraduates of marine engineering is tested in writing on completion of HMES exercises and is essential to prepare a report and submit it to the lecturer within a given time frame. The report should comprehend with following majors:

Purpose of the application – a short presentation of the completed exercise, methodology, conditions for the experiment (engine room operational condition; environmental conditions; set load; selecting measurement points; list of symbols with measure units);

Measurements – results e.g. in the form of a chart;

Computing – calculations of secondary (complex) values;

Presentation – plots with exercise results;

Recommendations – General evaluation of results and their values, accuracy and usefulness of methods applied for measurement and data processing, comparative analysis of experiment results and trends of parameter variation.

REFERENCES

Laskowski, R., Chybowski, L. and Gawdzińska, K., 2015. An engine room simulator as a tool for environmental education of marine engineers. *New Contributions in Information Systems and Technologies* (pp. 311-322). Springer, Cham.

Tsoukalas, V.D., Papachristos, D.A., Tsoumas, N.K. and Mattheu, E.C., 2008. Marine engineers' training: educational assessment for an engine room simulator. *WMU Journal of Maritime Affairs*, 7(2), pp.429-448.

Cao, H. and Zhang, J., 2020. Cloud Model-Based Intelligent Evaluation Method in Marine Engine Room Simulator. *IEEE Access*, 8, pp.168502-168515.

Shen, H., Zhang, J., Cao, H. and Feng, J., 2016. Development research of marine engine room simulator for offshore supply vessel based on virtual reality technology. *International Journal of Multimedia and Ubiquitous Engineering*, 11(5), pp.105-120.

ACKNOWLEDGMENT

The authors would like to acknowledge (General Sir John Kotelawala Defence University) for guidance and kind assistance throughout this research project.

AUTHOR BIOGRAPHIES

Cmde (E) MCP Dissanayake, CEng (India) is currently performing as the Head of Department (Marine Engineering) and hold 2 No's patents for his research papers published so far. He is an inventor and published 05 No's publications on reverse osmosis and membranes. He was the Director in Research & Development at Sri Lanka Navy and has received commendations on number of occasions from the Commander of the Navy, for his innovation and skills. Further, he has vast exposure on marine diesel engines and possesses a Masters degree in Marine Engineering from Australian Maritime College, Australia.

LCdr (E) KGC Pathmal currently serves as a lecturer in the Department of Marine Engineering, KDU and graduated from Jawaharlal Nehru University, India, in marine engineering. He devours an exposure on marine diesel engines installed at Fast Attack Crafts and Fast Gun Boats in Sri Lanka naval fleet namely, 16 Cylinders MTU and Deutz. Out of the vast area of marine engineering, he has chosen naval architecture and ship stability as his teaching areas and has an interest in research in the same. He is an associate member of the Royal Institute of Naval Architects (RINA) Institute of Engineers Sri Lanka (IESL).

LCdr (E) VADJV Perera is presently serving as a lecturer in the Department of Marine Engineering, KDU and possesses a BSc in Marine Engineering from General Sir John Kotelawala Defence Unversity, with a 2nd upper class merit. He is well competent in maintaining medium range marine diesel engines namely Yanmar and Cummins, shore based diesel generators and air conditioning systems. Further, he is a competent engine room watch keeper and interested in marine propulsion, propulsion control systes and engine control systems. He is an associate member of the Royal Institute of Naval Architects (RINA) Institute of Engineers India (IEI).

Design Approach to Optimize Water Jet Performance: A Case Study of Coastal Patrol Craft, Sri Lanka Navy

DS Bogahawatte[1#] and LAKR Athukorala[2]

[1]*Department of Mechanical Engineering, Faculty of Engineering, General Sir John Kotelawala Defence University, Sri Lanka*
[2] *Directorate of Naval Design, Sri Lanka Navy, Sri Lanka*

[#]ds-bogahawatte@kdu.ac.lk

Abstract— Commercial water jet manufactures publish their water jet performance curves mostly in the form of thrust/power against boat speed. The common approach is to foresee the performance of craft with candidate water jet(s), to simply plot the developed bare hull drag curve by a Naval Architect against the published power/thrust curves in graphical mode to establish the best fit. Yet this traditional approach does not uncover information of craft performance in the entire speed range or water jet model efficiency as the best choice for a particular local application. This case study incorporates approaches to seek a reduction in the craft bare hull drag, to develop an adequate analysis that shall combine engine RPM analysis to understand the availability of full rated engine power absorbed by propulsor/water jets. Therefore, the research employs a comprehensive mathematical based methodology as compulsory, to evade performance glitches and to outline an accurate and fruitful design structure. Thus, the employment of "universal water jet coefficients" has been considered to validate the design and eliminate the flaws associated with the traditional "thrust-resistance" plotting technique. A naval project designed by the authors was used to demonstrate how the authors averted possible complications and optimized the design through a new calculation methodology.

Keywords: ***traditional approach, water jet efficiency, universal water jet coefficients***

I. INTRODUCTION

The boat propulsion system consists of a marine engine, gearbox, and a suitable propulsor and does not require any design of equipment as Original Equipment Manufacturer (OEM) is entrusted with the same. For marine engines and gearboxes, the Naval Architecture is required to confirm power transmission, power output, and RPMs meet the desired. The Naval Architecture to design hull, propeller styles may be chosen, and be suitably pitch to the engine type. Thus, equilibrium performance relations are upheld.

Figure 1 depicted below identifies the focal study elements as engine – propulsor – hull equilibrium. This necessitates propulsor performance determination with concern on boat speed, Engine/ propulsor RPM, thrust, and torque (or power). The calculated assessments mainly focus on propulsor efficiency, engine fuel consumption, and propulsor cavitation. By this means authors aptitude was to seek, how non-dimensional (same for actual boat and model) associations could use to conduct the above examination for a waterjet thrust (propulsor - hull interaction determination) and torque (engine - propulsor interaction determination).

Figure 1. Equilibrium performance schematic

Cavitation tunnel open water tests usually provide the velocity of advance, RPM, Torque, and Thrust relations of propulsor. A step forward, Propeller Theory is based on models that defines non-dimensional coefficients. With distinctive and complex propeller diagrams, which contain, i.e. J, KT and KQ curves, it is promising to estimate the propeller dimensions, and efficiency. Built around the KT/KQ nomenclature as depicted in Figure 2, it offers a successful methodology which offers the benefit of (a) work with factors rather broad 3D geometry and (b) simple to calculate yet all-

inclusive boat performance study. Thus, this numerically simple task leads to the successful selection of optimum parameters. Yet unfortunately, the methodology is most validated in open water propellers.

$$KT = \frac{T}{\rho . n^2 . D^4}, \qquad KQ = \frac{Q}{\rho . n^2 . D^5}, \quad J = \frac{Va}{n . D}$$

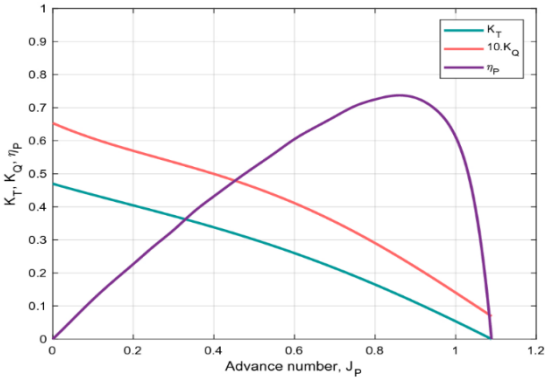

Figure 2. J, KT and KQ curves
Source: Taskar,B., Yum, K.K., Steen, S. and Pedersen, E., 2016

Predicting waterjet performance, in general, the manufacturer of waterjet provides the thrust curves for a region of defined boat speeds, the traditional approach has been the graphical mapping of boat's bare hull resistance curve on it to identify the adequacy of generated thrust to encounter the boat total resistance demand. This traditional approach does hide RPM from power and shall not allow compute and analyze important derivative performance amounts to fuel economy, boat acceleration reserves for manoeuvre/ combat operations which is of paramount importantance for naval operations.

The research problem statement of the study is 'Non availability of comprehensive study approach, which uncover all parameters for military applications' thereby the scope of the study is to develop a 'Design approach to optimize the performance of waterjet driven petrol craft for Naval application'. Thereby research employs a comprehensive mathematical based methodology as compulsory, with objectives: to seek a reduction in craft bare hull drag, to promote an adequate analysis shall combine engine RPM analysis, to understand the availability of full rated engine power absorbed by propulsor /waterjets. The research significance is, the study tries to fill the gap, specially the analysis of power to RPM with a selected prime mover, fuel efficiency, boat acceleration, and treatment of sensible parameters for hull drag.

II. METHODOLOGY AND EXPERIMENTAL DESIGN

Authors scanned the international shelf to shortlist candidate waterjet models with criterions amounts to power to weight ratio, boat speed, transom detail of hull, Glass Reinforced Plastic (GRP) fabrication, and robustness for naval applications etc., as directed by Naval Headquarters.

Authors were then obligated to commence with the information/ specification data provided by all OEMs. In a detail study following were revealed;

a. Nozzle characteristics (transom angle, center of effort, diameter)
b. Impeller characteristics (diameter, pitch variations, number of blades, hub construction)
c. Physical characteristics (weight, geometry, mounting detail, steering/ reversing details)
d. Rating (maximum input power and RPM)
e. Impeller Power (absorbed shaft power) vs. RPM plots, Figure 3.
f. Thrust curves (boat speed vs. thrust/power), Figure 4.

The principal boat design parameters were: Length overall - 20 m, Beam - 5 m, Hull Material – GRP, Draught - 0.95 m, Full Load Displacement - Approx. 27 Ton, Maximum/ Cruising speed - 35/30 Knots, Hull Type - Round-bilge with hard chine, and Endurance - 350 Nm@ 35 kts.
Length, Beam and Depth were kept fixed for this project (GRP mould constraints), but the authors were attentive to see how alterations in weight, Longitudinal centre of buoyancy (LCB), Longitudinal centre of gravity (LCG), deadrise angles and trimming affected bear hull resistance. The authors' presumption on sensible parameters amounts to boat weigh, LCG and deadrise angles was found to be critical in this coastal petrol craft design. Since non availability of precise weights, parametric estimates with educated deduction arrived with the weight estimation of 27 Tons. LCG and LCB were finalized with planning characteristics (Figure 4). Large AFT/stern deadrise angle avoided

improving performance (Figure 4). Further, trim by AFT condition was promoting planning condition to swiftly transfer boat weight to hydrodynamic forces (Figure 5).

However, the authors were cognizant of the fact that an LCG too far forward or too far aft would both have adverse effects. If the LCG is too far forward, the craft would have more power to plane than the same hull shape designed with zero trim or a bit by the stern. However, if the LCG is too far aft, a dynamic instability called "porpoising" would occur, which is primarily caused by concentrating too much weight in the stern. So, you have to reach a good middle ground between keeping weight aft for good planing and keeping it far enough forward to prevent porpoising. Careful analysis was conducted by studying a similar craft and calculating the resistance against the LCG change to reach an adequate balance. The benchmark of these studies was to reach an equilibrium trim angle between 3° to 5° for the whole speed range as indicated in Figure 5.

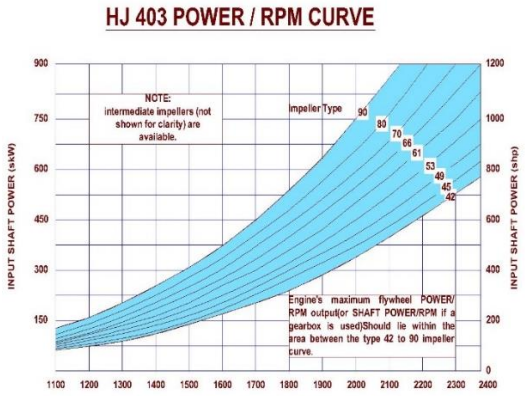

Figure 3. HJ 403 standard impeller power vs. RPM curves
Source: Ms C. W. F. Hamilton & Co. NZ (2019)

Figure 4 depicts a considerable resistance rise near 20 knots (planning of craft), with a wide flat region of the same hull resistance up to 32 knots. Naval application with extreme manoeuvres as the primary design objective, is required to operate the boat above the drag “hollow”. The authors’ initial analysis revealed boat parameter improvement is a necessity. Further, the traditional approach not allowed the visibility of acceleration reserve and efficiency of this operation. Thus, authors opted for complete system analysis with "universal waterjet coefficients" for the steady state performance with boat acceleration study, as promoted in their studies (MacPherson, 2010). Thereby, the authors evaluated possible modifications in hull form in line with performance enhancement. This numerical model provided the characteristics amounts to (a) Parametric - simple and clear define parameters, (b) Universal - applicability to all waterjets, and (c) Computational easiness - easily employed in computer codes.

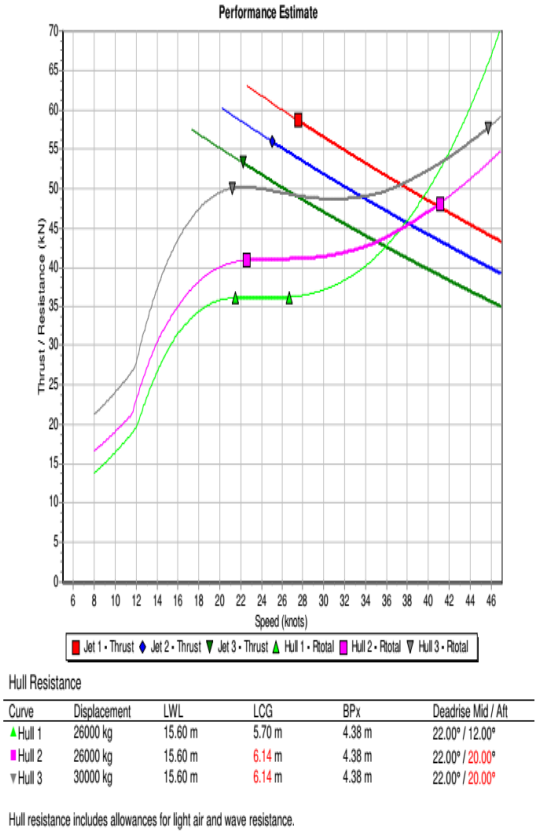

Figure 4. HJ 403 Waterjet thrust and hull drag curves
Source: Ms C. W. F. Hamilton & Co. NZ (2019)

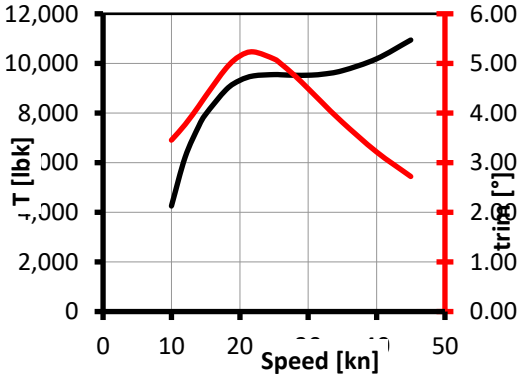

Figure 5. Boat trim conditions
Source: Calculated by authors using algorithm Developed by Dingo Tweedie

III. RESULTS AND DISCUSSION

Three coefficients were utilized by authors to transform the above mentioned commonly available waterjet information provided by respective manufacturers into non-dimensional exemplification of the traditional plots. Thus, complete physics based methodology employing "universal waterjet coefficients".

A. Speed-Thrust-Power coefficients

Figure 4 depicted the thrust curve was collapsed by authors into two coefficients, called C_P (power coefficient) and C_T and (thrust coefficient) is placed in Figure 6. Since Thrust is developed in a waterjet due to the change in the momentum of the water that accelerates through a tunnel, the Thrust could be defined as follows.

$$Thrust = \rho . V_{jet} . A_n . (V_{jet} - V_S)$$

Since the velocity of the waterjet stream can be defined in terms of ship speed using a coefficient, an equation could be developed to obtain C_T. For a given ship speed, the power of the craft is given by the following equation;

$$Power = Thrust \, . V_S$$
$$Power = \rho . V_{jet} . A_n . (V_{jet} - V_S) . V_S$$

Using the same process for C_T a coefficient for Power of the craft, Cp could be developed.

$$Cp = \frac{P}{\rho . An . Vs^3} \quad Ct = \frac{T}{\rho . An . Vs^2}$$

Where, P = shaft power, T = thrust, ρ = mass density of water, An = nozzle discharge area, and Vs = ship velocity, Vjet = Waterjet stream velocity.

Large numbers for C_T and C_P indicate high thrust with low speed. Thus, the waterjet's equivalence of "bollard pull" area. Proposed waterjet manufacturer's charts and geometric data were used to calculate the coefficients as follows to identify the suitability of operation relating to Figure 6. Since the operating range of CPC (35 knots) lies in the region of small X and Y values, waterjet selection could be justified.

Nozzle area (An) = 0.126 m², Impeller diameter (Di) = 0.400 m, Speed (Vs) = 35 kts (18.00 m/s), Power (P) = 1,500 kW Thrust (T) = 45,000 N
CT = 1.077, and CP = 1.99

Further, coefficients were employed to determine one of the most critical parameters "jet efficiency", ηJET, which equals to C_T/C_P (and also TVs/P). Figure 7 provide the plot of ηJET vs. C_P. Thus the arrival of a clearly defined efficiency peak is a possibility. The operating region of the CPC is in at an efficiency of 0.56, almost reaching the peak efficiency as per Figure 7.

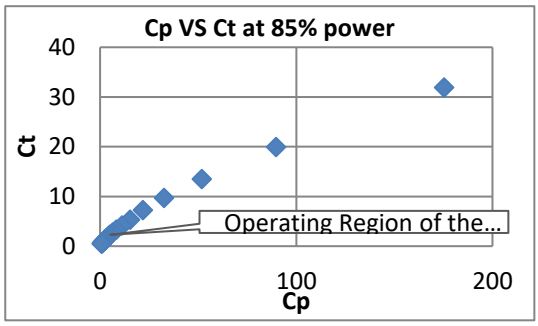

Figure 6. CT vs CP plot
Source: Calculated by authors

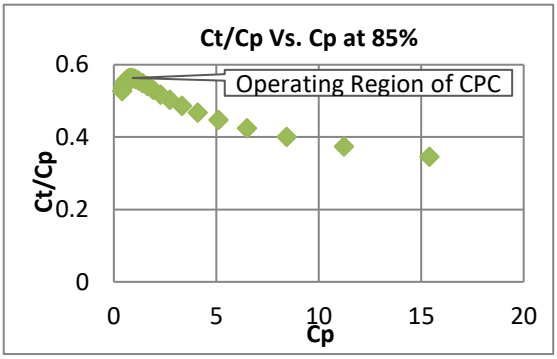

Figure 7. CP/CT (ηJET) vs CT plot
Source: Calculated by authors

One research outcome with employing "universal waterjet coefficients" was the ability to identify the operational location of maximum jet efficiency. Now it is probable to select the best performing waterjet with the greatest efficiency. A "maximum efficiency" track was plot in Figure 8. The authors design is closer to the maximum possible waterjet efficiency. Thus, the selected waterjet is with peak efficiency at a higher speed, which was the requirement. This outcome promote an adequate analysis shall combine engine RPM analysis, an objective of study.

B. Power-RPM coefficient

The authors studied the applicability to employ coefficient KQ (for a conventional propeller) to be suited for the water jet approach. Instead of torque employing power, the formula would be:

Where, P = shaft power, ρ = mass density of water, n = shaft speed, Di = impeller diameter

The torque coefficient KQ is a function of a particular standard impeller and is a fixed number for a separate impeller. Thus, KQ calculation with data from Figure 3. This approach is useful as this stage shaft power, diameter and velocity of advance are known. For impeller type 90 on the Power-RPM curve (Figure 3). Power (P) = 765 (85% Power), RPM (n) = 2150 rpm. Thus, KQ = 0.258. With the calculated KQ value, a plot is to be made in Figure 2 (with a KQ/J^3) on the optimal efficiency line to find RPM envelop. Figure 9 was developed to understand the availability of full rated engine power absorbed by propulsor /waterjets. Thus, another objective was achieved

.

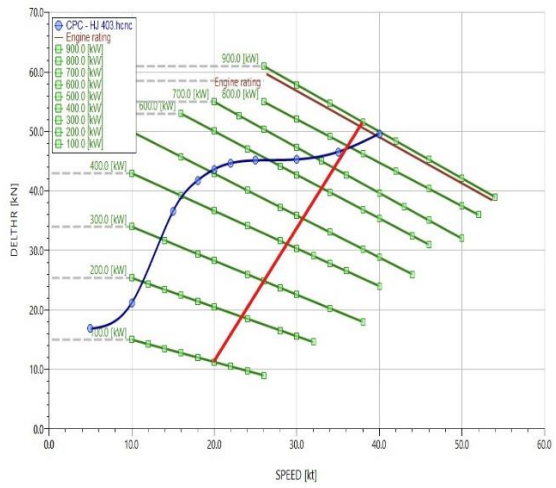

Figure 8. HJ 403 Waterjet thrust and hull drag curves upon parameter improvement
Source: Calculated by authors

C. The power-RPM curve

The matching of the marine engine with selected waterjet with respect to entire operation envelop is required to determine for swift operation. This study will give how good achieve the 'Hitting the Corner' criterion. Further, give a glimpse of manoeuvrability superiority of the design. Figure 10 depict the authors' predictions

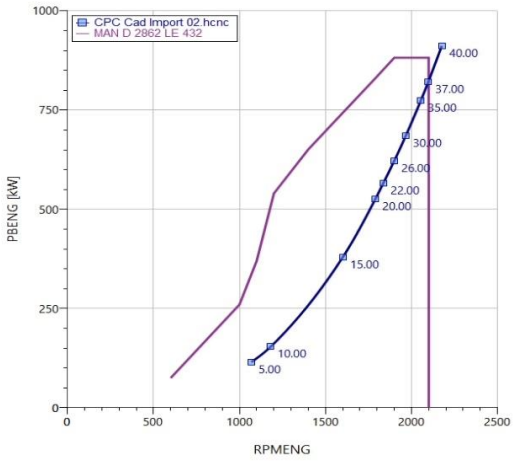

Figure 9. Power vs. RPM Curves
Source: Calculated by authors

D. Vessel acceleration

The "universal waterjet coefficients" did simplify the various powering situations with computer simulations. The boat acceleration analysis was conducted and depicted in Figure 10. The acceleration analysis with a similar waterjet model from another manufacturer was plotted to examine the variance in "time-to-speed" for both choices. The waterjet selected by the authors took approximately 20 seconds while the other unit reached the same speed in 22 seconds, to reach 30 knots. To reach the design speed of 35 knots, the selected waterjet unit took only 32 seconds, while the other unit spent 62 seconds. This information is critical since for a military patrol boat the time to reach its maximum speed is of vital importance. Hence, this approach of assessing the waterjet performance using 'universal waterjet coefficients' is justified

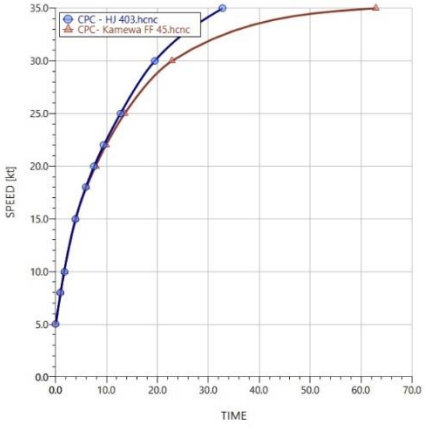

Figure 10. Vessel acceleration comparison
Source: Calculated by authors

The authors considered the cavitation regime with Figure 11 and found design areas are well clear of the cavitation region.

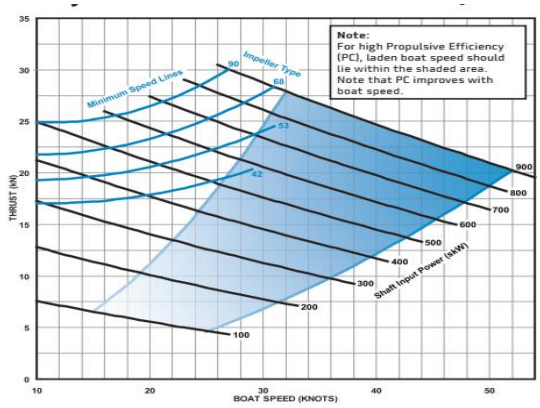

Figure 11. Cavitation study
Source: Ms C. W. F. Hamilton & Co. NZ (2019)

IV. CONCLUSION

Even though most waterjets look suitable for a particular application, waterjets are usually optimized by the manufacturer for separate applications, low speed (yet above 20 knots) and for high speeds. The appropriate selection is the duty of boat building yard Naval Architecture. The actual naval petrol craft design engineering example discussed at this juncture demonstrates why Naval Architecture shall have dependable techniques to assess waterjet performance. Traditional methods are beneficial to ensure particular waterjet will meet some performance requirements, yet the approach is usually inadequate for many virtual assessments of waterjet performance on efficiency, acceleration, entire RPM envelop operation and so forth. The authors exhibit how to employ "universal waterjet coefficients" as methodology, which guide and point the way to the accurate propulsor choice. The outcome is authors found the correct operation point/match of hull, propulsor, engine which is depicted in Figure1.

REFERENCES

C.W.F. Hamilton & Co., *various product brochures*.

MacPherson, D.M., 1999, August. A universal parametricmodel for waterjet performance. *In Proceedings*.

Taskar, B., Yum, K.K., Steen, S. and Pedersen, E., 2016. The effect of waves on engine-propeller dynamics and propulsion performance of ships. *Ocean Engineering*, 122, pp.262-277.

ACKNOWLEDGMENT

Authors would like to acknowledge the Sri Lanka Navy for providing opportunities and required resources for Naval Architectural discipline.

AUTHOR BIOGRAPHIES

Commander, Dinuk Sakoon Bogahawatte, Charted Marine Engineer, perform as Head of Department at KDU. Last six year shoulderd the responsibility of Manager Naval Boat Building Yard, Sri Lanka Navy. Graduated with BSc Eng (Hons) in Marine Engineering from KDU. Possess MBA from University of Moratuwa. Reading Masters in Manufacturing Management at University of Colombo. Expert for Fast Attack Craft & Fast Missile Vessels fleet repairs.

Lieutenant, LAKR Athukorala has graduated from the United States Coast Guard Academy with a BSc. Eng (Honours) in Naval Architecture and Marine Engineering. He currently serves in the capacity of Acting Staff Engineer Officer (Naval Architecture) at the Directorate of Naval Design, Sri Lanka Navy. Further, he has been a Visiting Lecturer on Marine Vehicle Design at the KDU since year 2020

Chronic Kidney Disease of Unknown Aetiology in Sri Lanka: An Implication of Optimizing Recovery Ratio of Brackish Water Reverse Osmosis Plant

MCP Dissanayake#, RS Ginige, KKN Fernando and SD Silva

Faculty of Engineering, General Sir John Kotelawala Defence University, Sri Lanka.

#dissanayakemcp@kdu.ac.lk

Abstract— Drinking water is an essential for human beings. At times, the fresh water from the sources of water in the environment such as streams, wells, and other water bodies cannot be used as drinking water because of the high content of dissolved salts and solids. This is most prominent in areas where water is scarce and areas where fertilizers and chemicals are used for different day-to-day processes such as agriculture. With a high level of environment contamination for a prolong period, the chemicals get into the underground water sources. In rural areas of Sri Lanka, mainly in the district of Anuradhapura, the majority of the people are prone to Chronic Kidney Diseases of Unknown aetiology (CKDu). Reverse osmosis technique is used to remove the dissolved solids from the fresh water and bring it to a drinkable level. Brackish Water Reverse Osmosis (BWRO) plants are present in an industrial scale to provide drinking water from brackish water, but at a higher cost. The main aim of this project is to develop a BWRO plant at a lower operating cost with a high recovery ratio to be implemented in areas where Total dissolved solid (TDS) levels are above the SLS standard (500 mg/L), and where even brackish water is scarce.

Keywords: ***drinking water, brackish water, reverse osmosis, cost, recovery ratio***

I. INTRODUCTION

When considering the planet earth 70% of the area is covered with water bodies but 2.5% of it is fresh water which is suitable for human use and drinking purposes, and only 1% of that is easily accessible, the other is saline water and ocean based. In most countries, lack of fresh water is a huge crisis. Even in the dry zone of Sri Lanka, the freshwater crisis is inevitable with an average rainfall of 1000 mm (Wanasinghe et al., 2018) for a limited period of 3 months and a drought period for 5 months during the mid-year. The water needed for the agricultural activities is obtained using the tank cascade system, which is to be sufficient for the drought period, once filled during the rainy season. But with time it has been observed that Dental fluorosis and Chronic Kidney Diseases of Unknown etiology (CKDu) is a major health issue as a non-communicable disease mainly in parts of North Central, North, North Western, Central, Eastern, Uva, Southern (Dissanayake, 2020) which had resulted in high morbidity and mortality among farmers, agricultural laborer's and their families between the ages 40-60 due to the changes in the drinking water parameters by the contamination of agricultural activities as a probable cause. The dialysis treatment, and kidney transplantation are the only cure for the CKDu patients with a high cost or causing death within two years of getting prone for 80% of the patients.

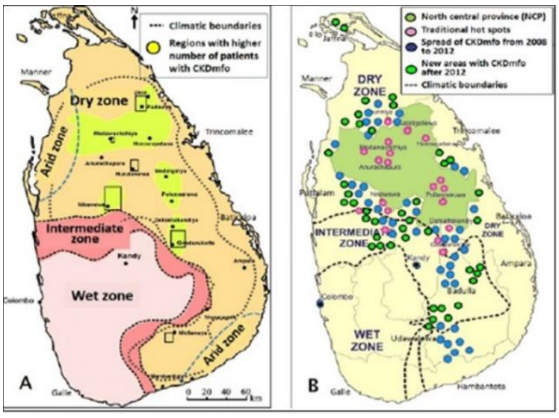

Figure 1.Areas of CKDu spread (Wanasinghe et al., 2018)

The Brackish Water Reverse Osmosis (BWRO) is the process of obtaining purified drinkable fresh water by reverse osmosis through a specially designed semi-permeable membrane comprising

of pre-treatment, post treatment and a cleaning cycle. The feed water temperature, concentration, flow rate, and pressure difference in sides of the semi-permeable membrane are the major factors effecting the process. Reverse osmosis is a technique that extract fresh water from sea water, which is used on board naval vessels to meet the freshwater requirement. The Government of Sri Lanka initiated a program to provide safe drinking water CKDu affected people by importing BWRO plants through National Water Supply and Drainage Board (NWSDB) of Sri Lank, Non-Governmental Organizations (NGO) and establishment of distribution centres in the North Central Province (NCP). Amidst the failure of that program due to practical reasons of unavailability of skilled personnel for defect rectification, repairs and absence of compatible spare parts in the local market. Then, with the involvement of the Sri Lanka Navy, a sustainable solution of in-house BWRO plants was introduced by utilizing the SLN operators to supply safe drinking water to the rural community (Dissanayake, 2020). Consequently, SLN BWRO plants project has been expanded up to 900 plants and providing safe drinking water to more than 2 million people at CKDu impacted areas in the country.

The absence of drinking water quality parameters within acceptable levels (SLS 614: 2013) is the main cause for the spread of CKDu in Sri Lanka. Elimination of CKDu can be done by establishment of BWRO plants. But the Recovery ratio of existing BWRO plants is calculated and identified as around (40-50) % of feed water (Indika et al., 2021). Further, it is understanding that present recovery is not adequate compared to the ground water yield at the dry zone in Sri Lanka. A 75% recovery ratio is a mandatory requirement of a BWRO plant as per the United States Environmental Protection Agency (EPA) due to the scarcity of fresh resources.

II. DESIGN FEATURES

North Central Province (NCP) is the most CKDu affected area in the country. Therefore, 407/ Meegassegama village, Talawa divisional secretariat, Anuradhapura District of the NCP was selected as the study area in this research. The process would differ according to the implementation area because the quality of brackish water, contamination levels, and total dissolved solids (TDS) levels differ from area to area. Then the feed water characterization should be done for the identification of the TDS levels in the feed water for the membrane selection process. In the BWRO process to increase the efficiency by determining the membrane design calculating the effective operative feed water inlet pressures at each stage and the flow rate. The input pressures of pumps should be calculated with trial and error through the closed loop monitoring of the output and inputs by considering the head losses. The whole process is to be automated as PID to control input, output pressures, with the operation of directional valves to maintain constant flowrate, freshwater feed system for membrane flushing at the starting process. The implementation area was selected for the requirement of a low-cost brackish water reverse osmosis (BWRO) plant with the feed water characteristic carried out. The observation of the existing BWRO system with two pressure vessels arranged as single stage parallel configuration was done by measuring the output flows of permeate and concentrate, manually using measuring instruments. The main challenge of coming up with the membrane arrangement was discussed. Mainly the stage array module arrangement and the closed-circuit desalination (CCD) were the most suitable way used to increase the recovery ratio as well as to increase the permeate water quality.

The closed-circuit desalination (CCD) involved higher number of valves and pumps, hence our main objective is to improve the recovery ratio at a lower cost, by the trials carried out on the test rig the concentrate staging array system with two modules had a high recovery ratio. The readings for the output flows of permeate and concentrate were taken manually but even with high pressure pump turned on, the recovery ratios were very low due to the absence of the required osmotic pressure for the RO membrane. The osmotic pressure is developed using flow restrictors.

A. Feed Water Characterization

A feed water characterization of water samples taken from the implementation area was done to identify the water quality in the area.

Following details were obtained through the water quality tests conducted.

National Water Supply and Drainage Board – Water quality test report

Date and time of water sample collected: 0900 hrs on 2020.08.04

Date and time of water sample handed over: 1025 hrs on 2020.08.04

Location of water sample: 407, Meegassegama, Kiralogama

Table 1. Feed Water Characteristics

Parameters	According to SLS 614: 2013 standards		Results Relevant to the Sample	Method of Testing
	Units	Maximum Value		
Physical Characteristics				
Colour	Hazen	15	15	APHA 2120 C
Turbidity	NTU	2	3.0	APHA 2130 B
pH value	25°C ± 0.005°C	6.5-8.5	7.3	APHA 4500-H^+ B
Chemical Characteristics				
TDS	mg/l	500	227	APHA 2540 c
Chloride (Cl-)	mg/l	250	70	APHA 4500 Cl –B
Total bases (as $CaCO_3$)	mg/l	200	140	APHA 2320 B
Total Solubility (as $CaCO_3$)	mg/l	250	130	APHA 2340 C
Nitrate (as NO_3^-)	mg/l	50	0.44	APHA 4500 NO_3^-, E
Nitrite (as NO_2^-)	mg/l	3	0.01	APHA 4500 NO_2^- B
Sulphate (as SO_4^{2-})	mg/l	250	04	APHA 4500 SO_4^{2-} B
Fluoride (as F^-)	mg/l	1.0	0.42	APHA 4500 F^- D
Total Phosphate (as PO_4^{3-})	mg/l	2.0	0.28	APHA 3500 PE
Iron (as Fe)	mg/l	0.3	0.09	APHA 3500-Fe B
Free Ammonia (as NH_3)	mg/l	0.06	-	PAN Method

Sample Drawn by S and D Chemicals (PVT) Ltd.

Test on Heavy Metals

Sample Received date : 21/09/2020

Report Issued Date : 21/09/2020

Table 2. Heavy Metal Indication

Parameter	CAS Number	Result(mg/l)	Limit of Detection (mg/l)
Arsenic as As	7440-38-2	ND	0.05
Cadmium as Cd	7440-43-9	ND	0.05
Copper as Cu	7440-50-8	ND	0.05
Chromium as Cr	7440-47-3	ND	0.05
Iron as Fe	7439-89-6	ND	0.05
Lead as Pb	7439-92-1	ND	0.05
Magnesium as Mg	7439-95-4	8.51	0.10
Manganese as MN	7439-96-5	ND	0.05
Nickel as Ni	7440-02-0	ND	0.05
Sodium as Na	7440-23-5	27.93	0.10
Potassium as K	7440-09-7	0.26	0.10
Calcium as Ca	7440-70-2	31.78	0.10
Silver as Ag	7440-22-4	ND	0.05

B. Pressure Vessel Arrangement

Initially, the pressure vessel/membrane arrangement, which was in two stage parallel configuration, where the water from the pre-treatment stage is fed into two parallel pressure vessels, the concentrate, and the permeate output is also obtained parallelly from the two pressure vessels were modified and tested on the BWRO test rig present at the marine laboratory of KDU as a two stage series arrangement, where the water from the pre-treatment is fed into one pressure vessel, the output concentrate from the first vessel is fed into the second pressure vessel and both permeates from the first stage and the second stage are combined as the final output. Following readings were obtained without controlling the pressure of the concentrate output using a globe valve.

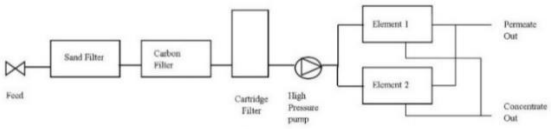

Figure 2. Pressure vessel arrangement before modification

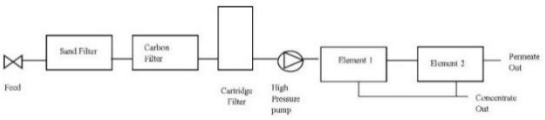

Figure 3. Pressure vessel arrangement after modification

Table 3. Results obtained without concentrate pressure control

Description		Permeate Out (ml)	Concentrate Out (ml)	Feed water (ml)	Recovery Ratio (%)
Before Modification	Without pressure pump	125	4000	4125	3.030303
	With pressure pump	140	4000	4140	3.381643
After Modification	Without pressure pump	350	4000	4350	8.045977
	With pressure pump	600	4000	4600	13.04348

The concentrate output needs to be controlled using a globe valve to build up pressure at the output of the pressure vessel to limit the concentrate flowrate and increase the permeate flowrate increasing the overall recovery ratio per fixed amount of feed water.

C. Recovery Ratio Calculation

The calculation of the recovery ratios for the above module Arrangements are as follows.

- Qfn = Feed flow to RO-n (m^3/h)
- Qpn = Permeate flow of RO-n
- Qbn = Concentrate flow of RO-n
- R = Recovery ratio

Single stage module arrangement

$$Qf1 = Qp1 + Qbl$$

$$R = 100 * \frac{Qp1}{Qf}$$

Multistage parallel module arrangement

$$Qf1 = Qp1 + Qp2 + Qp3 + Qbl + Qb2 + Qb3$$

$$R = 100 * \frac{Qp1 + Qp2 + Qp3}{Qf1}$$

Multistage series module arrangement

$$Qf1 = Qp1 + Qbl$$

$$Qf2 = Qp1 = Qp2 + Qb2$$

$$R = 100 * \frac{Qp2}{Qf1}$$

Multistage series and parallel module arrangement

$$Qf1 = Qp1 + Qbl$$

$$Qf2 = Qp1 = Qp2 + Qb2$$

$$Qf3 = Qb1 + Qb2 = Qp3 + Qb3$$

$$R = 100 * \frac{Qp2 + Qp3}{Qf1}$$

Permeate flow (Qp)

$$Qp = Am * Lp * (\Delta Pm - \sigma \Delta \pi)$$

- Am = Total membrane surface area
- Lp = Hydraulic permeability of the membrane (depends on the type and product of the membrane)
- ΔPm = Average transmembrane pressure
- σ = Reflection coefficient of membrane.
- $\Delta \pi$ = Average osmotic pressure difference between feed $\Delta \eta f$ and permeate $\Delta \eta p$.
- $(\Delta Pm - \sigma \Delta \eta)$ = Average trans membrane net driving pressure, NDP.

Number of membrane elements (Ne)

$$Ne = \frac{Qp}{f * Se}$$

- Qp = Design permeate flow
- F = Flux
- Se = Membrane element surface area

Number pressure vessels (Nv)

$$Nv = \frac{Ne}{Nepv}$$

- Ne = Number of membrane elements
- Nepv = Number of elements in a pressure vessel

- The number of elements and the number of pressure vessels may vary with the manufacturer due to the variation of the Membrane element surface area (Se) and the Number of elements in a pressure vessel (Nepv).

D. Implementation at Talawa (Anuradapura District)

The BWRO facility was built at 407/ Meegassegama village, Talawa divisional secretariat, Anuradhapura District of the North Central Province. 520 families are living in this village.

Figure 4. BWRO Facility building

E. Membrane Installation

The existing BWRO was a single stage single element arrangement figure 6. Therefore, 2nd membrane was purchased and installed serially to this BWRO plant figure 8.

Salient Features of Membarne

a. Modle : LP 440
b. Working Pressure (Max) : 600 psi
c. Working Temperature of feed water (Max): 45 °C
d. Operating PH : 2-11
e. Chlorine concentration : < 0.1 ppm
f. Maximum SDI : 5

The membrane installation is a very delicate procedure if processed wrongly it would result in membrane damage and water leaks. First, the flow side of the membrane should be identified by the marking then the pressure vessel end caps must be adjusted to decide the orientation of the pressure vessel, to define the inlet port, permeate out and concentrate out. When inserting the membrane inside the pressure vessel, the end caps are fixed accordingly at the end of the flow side which contains the 'O' ring to be placed at last to the vessel. Shampoo was applied as lubrication before inserting the element. Then the ½ inch sockets were placed at the feed inlet, permeate out, concentrate out ports, and end cap to the remaining inlet port as there are 2 ports per end cap of the pressure vessel.

Figure 5. Inserting the new BWRO membrane into the pressure vessel

The tightening of the sockets at the end caps with an appropriate amount of thread sealant and PVC gum is necessary to avoid leaks as the membrane is pressured at high pressures. The leaks would also create a drop in pressure and a messy environment around the plant, even creating possibilities for electrical short circuiting. The locking mechanism of the end caps was different from what we have come across. The existing connections were observed and the flow rate of the concentrate was measured before removing it for modification figure 6 & 7.

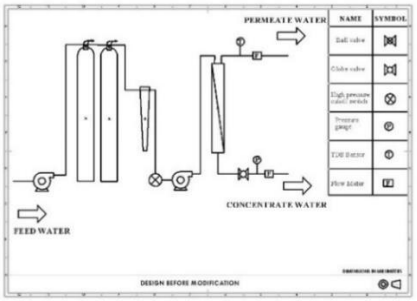

Figure 6. Design before modification

Figure 7. Observation of single stage arrangement

Figure 8. Time taken to fill 4L of concentrate with single stage membrane arrangement

As seen above, only 19.5s was taken to fill 4L amount of concentrate, our main objective was to increase. Which would decrease the flow rate and the amount of concentrate output, simultaneously increasing the permeate output. The union joints at the feed inlet, permeate output, and the concentrate output were detached, and the connections were modified to support the new additional membrane to the system to be modified as two stage series configuration. In addition to the plumbing, the frame structure was modified to hold the second pressure vessel. There was a difficulty of attaching second pressure vessel as there were no compatible brackets, but the team was able to adjust an existing bracket to able to fit the new membrane while supporting the lower part via a temporary fixture, till a suitable bracket is available for installation in figure 9 & 10.

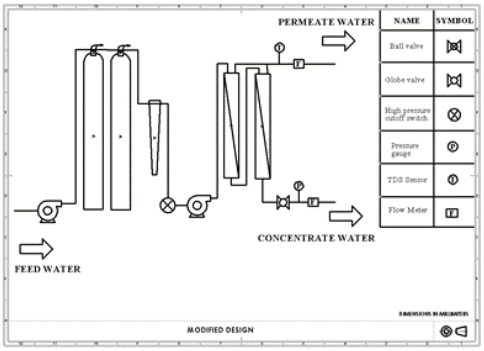

Figure 9. Modified design

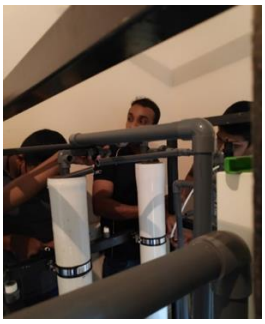

Figure 10. Modifying the plumbing arrangement

Same time, rejected water was tested by hand held conductivity meter and pH meter in Table 4.

Table 4: Comparison of Reject Water Parameters vs Sri Lankan Standard 614

Parameters	Results	SLS 614
pH	7.3	6.5-8.5
Electrical Conductivity	918 ppm	750 ppm
TDS	588 mg/l	500 mg/l
Hardness	518 mg/l	250 mg/l

III RESULTS AND DISCUSSION

Recovery Ratio

The membranes can be used for relatively a longer duration than usual by performing

cleaning cycles in a pre-defined period, chemically and fresh water backwashing. If the process is slowed down or if the recovery ratio is decreased due to membrane clogging, the manufacture has provided with an option of using the membrane in reverse flow direction by using the "O" Ring in the opposite side groove. The modification of the pressure vessel arrangement was successful in increasing the recovery ratio by more than 50% which was present before with the single stage array arrangement by two stage series array arrangement. But the desired 75% recovery ratio was not obtained. The input and the output of the pressure pump were bypassed with a ball valve by creating a pressure difference and a flow path to supply for the water deficit created at the stage array input figure 11 & 12. Then the flow rate of the concentrate was as to fill 4L time occurred was 43.5s. Where the flowrate has decreased compared to the 19.5s that occurred previously with the use of single stage system. The resultant concentrate water also had more salt texture relative to the concentrate obtained before the modification figure 8.

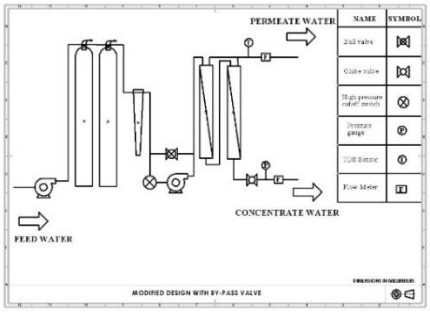

Figure 11. Modified design with by-pass valve

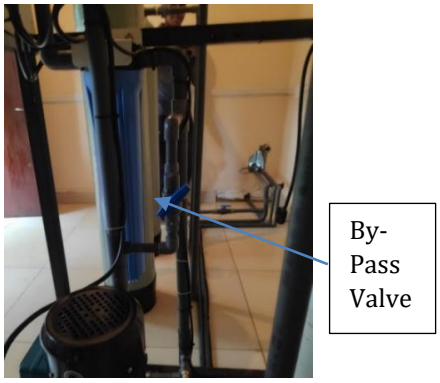

Figure 12. By-Pass valve modification

Figure 13. Observation of Concentration flow after modification

When calculating the recovery ratio, we considered a time of 1 minute for calculations.
For a 1-minute time.
Feed water volume = 25.26 l
Before Modification,
Concentrate Volume = 12.9 l
Therefore, Permeate volume = 25.26 – 12.9 = 12.36 l
Recovery Ratio = 12.36/25.26 ×100% = 48.9%
After Modification,
Concentrate Volume = 6.21 l
Therefore, Permeate volume = 25.26 – 6.21 = 19.05 l
Recovery Ratio = 19.05/25.26 ×100% = 75.4%.

The pH value of reject water was 7.3 and revealed that the pH value was within SLS 614. Further, TDS and Hardness of reject water were above specified SLS 614. Moreover, electrical conductivity was a bit high compare to SLS 614.

IV. CONCLUSION

This resulted in a huge benefit to the villages of Meegassegama by increasing the recovery ratio which would in return reduce the cost per litre of water obtained and reduce in feed water wastage through concentrate. The feed water saving would be mostly affected on times of drought where water is scarce, and the feed water sources are drying up. Recommend to reuse reject water and improve the recovery ratio upto 100% Table 4.

REFERENCES

Dissanayake, M. C. P. (2020). An Air Operated Domestic Brackish Water Reverse Osmosis Plant : Economically Sustainable Solution for Safe Drinking Water Supply for Chronic Kidney Disease of Unknown Etiology Affected Areas in Sri Lanka. 911–920. https://doi.org/10.4236/jwarp.2020.1211053

Indika, S., Wei, Y., Hu, D., Ketharani, J., Ritigala, T., Cooray, T., Hansima, M.A.C.K., Makehelwala, M., Jinadasa, K.B.S.N., Weragoda, S.K. and Weerasooriya, R., 2021. *Evaluation of Performance of Existing RO Drinking Water Stations in the North Central Province, Sri Lanka. Membranes*, 11(6), p.383.

News.navy.lk. (2020). The official website of Sri Lanka Navy - Navy's 250th Reverse Osmosis Plant vested in the General Public. [online] Available at: *https://news.navy.lk/eventnews/2017/09/10/201709101840/* [Accessed 19 Feb. 2020].

Fritzmann, C., Löwenberg, J., Wintgens, T. and Melin, T. (2007). *State-of-the-art of BWRO desalination. Desalination*, 216(1-3), pp.1-76.

Alghoul, M. A., Poovanaesvaran, P., Sopian, K., & Sulaiman, M. Y. (2009). Review of brackish water reverse osmosis (BWRO) system designs. *Renewable and Sustainable Energy Reviews*, 13(9), 2661–2667. https://doi.org/10.1016/j.rser.2009.03.013

Wanasinghe, W. C. S., Gunarathna, M. H. J. P., Herath, H. M. P. I. K., & Jayasinghe, G. Y. (2018). *Drinking Water Quality on Chronic Kidney Disease of Unknown Aetiology (CKDu) in Ulagalla Cascade , Sri Lanka*. 16(1), 17–27.

ACKNOWLEDGMENT

M/S Rashi Water, 724/19/A, Prime Life, Mankada, Kadawatha fully funded this BWRO Project. I would like to acknowledge M.M.A Roshini Nayana (General Mangaer, Rashi Water) for her assistance and cordial relationship throughout this research project.

AUTHOR BIOGRAPHY

[1]Cmde (E) MCP Dissanayake, CEng (India) is currently performs as the Head of Department (Marine Engineering) and hold 2 No's patents for his research papers published so far. He is an inventor and published 06 publications on Brackish Water Reverse Osmosis application, Fan Boat Building, and Oscillation Water Column, Ocean Wave Eenrg Converter. He was the Director in Research & Development at Sri Lanka Navy and has received commendations in number of occasions from Commander of the Navy, HE the President of Sri Lanka for his innovation. Further, he was awarded with prestigious, Japanese, Sri Lanka Technical Award for his own developed low-cost Reverse Osmosis Plant, to eliminate Chronic Kidney Disease from Sri Lanka. Moreover, he has a vast exposure on marine diesel engines and possesses a Masters degree in Marine Engineering from Autralian Maritime College, University of Tasmania, Australia.

Performance Analysis of a Photovoltaic System under Different Configurations

FBYR De Silva[1#], RMPS Bandara[1] and RA Attalage[2]

[1]*General Sir John Kotelawala Defence University, Sri Lanka*
[2]*Sri Lanka Institute of Information Technology*

[#]eng.randana@kdu.ac.lk

Abstract— Solar energy is used worldwide as energy can be harnessed directly from sunlight. Currently, the photovoltaic panel is considered as one of the fastest-growing renewable energy technologies that plays a major role in generating electricity. Sri Lanka receives a significant amount of solar radiation where Global Horizontal Irradiance fluctuates between 1247 kWh/m2 and 2106 kWh/m2 throughout the year. The power output generated by the PV panel depends on the irradiance received by the panel. When the irradiance increases, the power output of the panel also increases. However, as the solar irradiance increases, surface temperature of the PV panel also tends to increase. Higher surface temperatures cause degradation of the panel, and as a result, the lifetime of the same is reduced. Cooling of the PV panel can be used effectively to maintain the surface temperature at a desirable level while maintaining a higher power output. This study investigates the performance of a PV panel in terms of its power output under four different configurations at Ratmalana, Sri Lanka. It is observed that the power output increases substantially around 12 noon when reflectors are used along with the PV panel. However, this configuration records a higher temperature on the surface of the panel. It is observed that air cooling enables only a slight reduction of the panel surface temperature. When both air and water cooling are incorporated, panel surface temperature is reduced substantially while generating a higher power output. It is recommended that the conventional PV panel be used until 12 noon, and then switch over to the configuration that incorporates reflectors with air and water cooling in order to produce a maximum power output while maintaining lower surface temperatures of the panel that will increase the lifetime of the same as well.

Keywords: ***photovoltaic panel, power output, surface temperature, configuration, cooling***

I. INTRODUCTION

The global demand for energy is increasing annually due to the increasing world population and improved access to energy. Fossil fuels (Petroleum, Coal and Natural gas) are still the main source of energy in spite of many challenges and issues. Use of renewable energy has been emphasized in order to mitigate energy-related environmental issues and climate change (Ahmed et al. 2014). In the Sri Lankan context, solar energy has a key role to play compared to other sources of renewable energy. Solar energy will last for millions of years and as a result it will offer a better option for satisfying the future energy demand. In this backdrop, use of solar photovoltaic (PV) panels has increased substantially worldwide. As per current PV technology, the share of solar irradiation converted as productive energy is around 15% to 22% (Palaskar et al. 2014).

A solar cell is a basic p-n junction diode. Solar cells form a photoelectric cell, defined as a device whose electrical characteristics such as current, voltage, and resistance vary when exposed to light. When light reaches the p-n junction, the light photons can easily enter the junction, through a very thin p-type layer (Moharram et al. 2013). The light energy, in the form of photons, supplies sufficient energy to the junction to create a number of electron-hole pairs. The incident light breaks the thermal equilibrium of the junction (Rodrigues et al. 2011). The free electrons in the depletion region can quickly reach the n-type side of the junction. Similarly, the holes in the depletion can quickly access the p-type side of the junction. Once, the newly created free electrons reach the n-type side, they cannot further cross the junction because of potential barrier created in the junction (Arshad et al. 2014). Then the p-n junction behaves as a cell of

a battery. The power output of a solar cell mainly depends on the surface area and is proportional to the intensity of sunlight striking the surface of the cell. Solar irradiance is a key phenomenon that governs the performance of a solar panel (Akbarzadeh and Wadowski, 2014). It is the amount of solar radiation that strike on a specific surface. This is mainly influenced by the orientation of the Sun with respect to the panel (tilt angle), geographical location, cloud cover and reflecting surfaces. When irradiance increases, more packets of photons strike the panel. When photons strike the solar cell, electrons tend to get released from the atoms in the semiconductor material. If electrical conductors are attached to the positive and negative terminals forming an electrical circuit, the free electrons can be captured in the form of an electric current (Tonui and Tripanagnostopoulos, 2007). The electrons collide with adjacent electrons and thus generate heat. This increases the temperature of the panel itself. Increase in temperature leads to increase in resistance to the current flow thereby reducing the power output and also causes degradation of the panel (Kiuth, 2008). It is found that, under concentrated solar radiation, the performance of solar cells is reduced by 50% when its temperature rises from 46 ^{0}C to 84 ^{0}C (Chaniotakis, 2001). Therefore, an efficient cooling system is essential in order to maximize solar cell's performance and to prevent the cell from getting degraded. Photovoltaic panels can be cooled actively or passively (Amelia and Irwan,2016). Active systems require an external power source while passive systems do not need an additional power source. The purpose of present work is to investigate the performance with respect to different configurations as follows.

II. METHODOLOGY AND APPROACH

The study was carried out at Ratmalana, Sri Lanka in July 2019 by using four different configurations as given below:

- Configuration 1: Without reflectors and cooling (with no modifications)
- Configuration 2: With reflectors
- Configuration 3: With reflectors and air cooling
- Configuration 4: With reflectors and by incorporating both air and water cooling

Each case was investigated at three tilt angles: 00, 200 and 300. Output voltage and current of the PV panel were measured to calculate the power output. Surface temperature of the PV panel, cloud cover and ambient temperature at the location were also measured. Data was recorded in every hour from 0800 hrs. to 1700 hrs. for three days for all panel configurations. The study used a polycrystalline silicon PV panel with a maximum rated power output of 500 W.

The PV panel surface was divided into 12 equal rectangular portions and the surface temperature of the panel was measured by taking the mid-point temperatures of each rectangular portion. A non-contact infrared thermometer was used for this purpose. Hourly solar irradiance (total amount of solar energy falling on unit area (MJ/m2)) was obtained with the kind support of the Department of Meteorology. Okta scale and a mercury-in-glass thermometer were attached to the PV system in order to measure the cloud cover and ambient temperature respectively. A cylindrical concave mirror was developed using strips of plane mirrors in order to function as a reflector in Configuration 2.

For Configuration 3, air cooling was introduced. In Configuration 4, both air and water cooling were incorporated. Cooling fins were fabricated using Aluminium sheets and were fixed to the bottom surface of the PV panel. For the process of water cooling, a water supply line was introduced by fixing half split 20 mm diameter PVC tubes to the bottom of the surface of the PV panel using thermal silicon sealant. Water was supplied by using gravity without the presence of any external power source. Data was collected for all four configurations under the same outdoor conditions.

III. RESULTS

Configuration 1: Without reflectors and cooling (with no modifications)

Table 1 presents key operating parameters for Configuration 1 at 00 tilt angle on hourly basis. Similar sets of data have been obtained for the tilt angles 200 and 300 as well. The power output of the PV panel was calculated on hourly basis. For further comparison of performance, graphical representation of results have been done in Figures 2 and 3.

Table 1: Key operating parameters for Configuration 1

Time (hour of the day)	Average Surface Temperature (⁰C)	Voltage (V)	Current (A)	Power Output (W)	Irradiance (W/m²)
0800	28.4	17.2	1.1	18.9	202.8
0900	44.8	20.1	6.2	124.6	277.8
1000	55.4	20.8	7.8	162.2	569.4
1100	57.8	27.1	8.2	222.2	591.7
1200	59.4	28.4	8.2	232.9	783.3
1300	59.9	30.1	9.6	289.0	797.2
1400	55.2	30.0	8.9	267.0	755.6
1500	49.2	18.3	6.6	120.8	644.4
1600	46.7	17.2	6.2	106.6	500.0
1700	43.3	14.6	4.5	65.7	266.7

According to Table 1, it was observed that both voltage and current increased from 0800 hrs. to 1300 hrs. and subsequently reduced from there onwards until 1700 hrs. This is evident for all three tilt angles. Hence, the power output generated by the PV panel reached its maximum around 1300 hrs. as shown in Figure 3. This is mainly due to the maximum irradiance level that the PV panel received during this time of the day. Surface temperature of the solar panel also rises with the increase in irradiance level. It was observed that the increase of average temperature of the PV panel surface follows a similar trend to that of the power output.

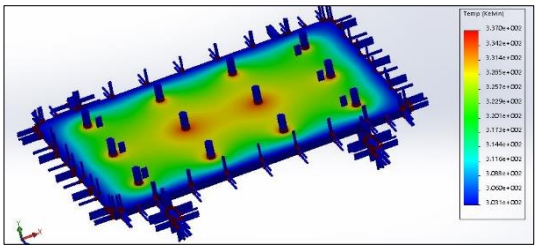

Figure 1. Average temperature distribution on the photovoltaic panel surface.

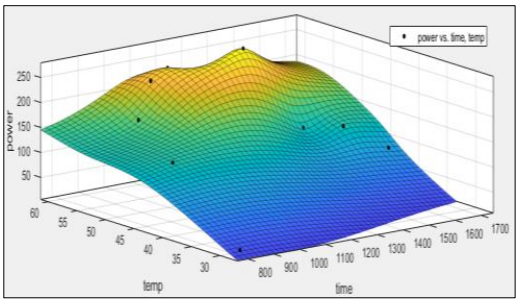

Figure 2. Variation of power output vs time and temperature at 00 tilt angle for Configuration 1

Figures 1 and Figure 2 illustrate the temperature distribution on the PV panel surface and variation of PV power output against time and temperature (3D) respectively.

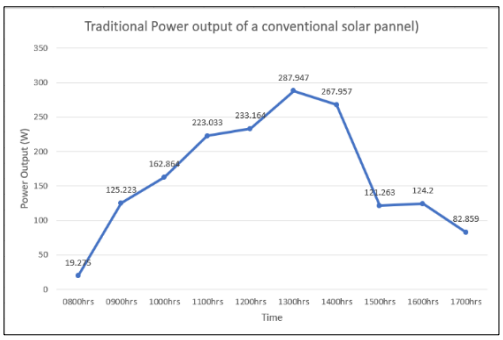

Figure 3. Power output of the photovoltaic panel: Configuration 1

Configuration 2: With reflectors

Table 2. Key operating parameters for Configuration 2

Time (hour of the day)	Average Surface Temperature (⁰C)	Voltage (V)	Current (A)	Power Output (W)	Irradiance (W/m²)
0800	30.4	17.4	1.1	19.1	266.7
0900	37.8	18.3	3.3	60.4	500.0
1000	43.6	24.3	6.3	153.1	519.4
1100	46.7	25.1	7.0	175.7	775.0
1200	55.4	40.1	10.3	413.0	883.3
1300	61.0	42.8	10.9	466.5	969.4
1400	58.3	39.9	10.1	403.0	908.3
1500	56.8	35.8	9.2	329.4	694.4
1600	50.6	30.0	8.3	249.0	588.9
1700	47.6	28.2	7.0	197.4	318.3

As per Table 2, the voltage and current recorded a sudden increase between 1100 and 1200 hrs. This resulted in a large increment in power output as shown in Figure 4.

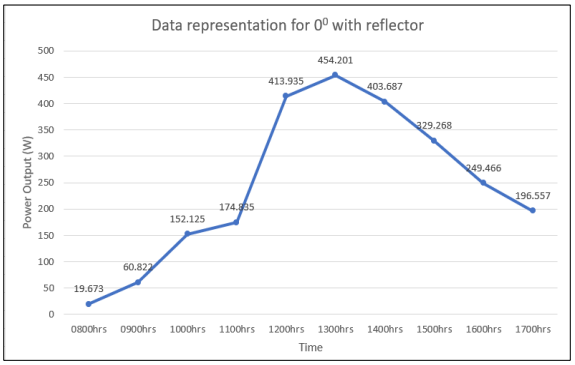

Figure 4. Power output vs. time in Configuration 2

The panel generates maximum power output around 1300 hrs. The impact of the reflector was not evident during the morning hours as the amount of solar radiation that was reflected on to the panel at that time was relatively less. As the amount of solar irradiation increased, the surface temperature of the panel also increased.

Configuration 3: With reflectors and air cooling

Table 3. Key operating parameters for the PV with reflector and air cooling (Configuration 3)

Time (hour of the day)	Average Surface Temperature (⁰C)	Voltage (V)	Current (A)	Power Output (W)	Irradiance (W/m²)
0800	28.3	17.7	1.0	17.7	258.3
0900	35.4	18.3	3.4	62.2	497.2
1000	40.7	24.4	6.3	153.7	627.8
1100	43.7	25.1	7.0	175.7	630.6
1200	51.7	40.1	10.3	413.0	716.7
1300	58.2	41.8	10.9	455.6	797.2
1400	55.6	41.0	10.3	422.3	583.3
1500	52.6	36.3	9.9	359.4	277.8
1600	48.3	32.1	8.7	279.3	133.3
1700	44.4	28.1	7.0	196.7	82.7

According to Table 3, by incorporating the reflectors and air cooling, it was observed that the average surface temperature of the panel had decreased slightly compared to that of Configuration 2. The variation of the power output in Configuration 3 as shown in Figure 5, is fairly similar to that of Configuration 2.

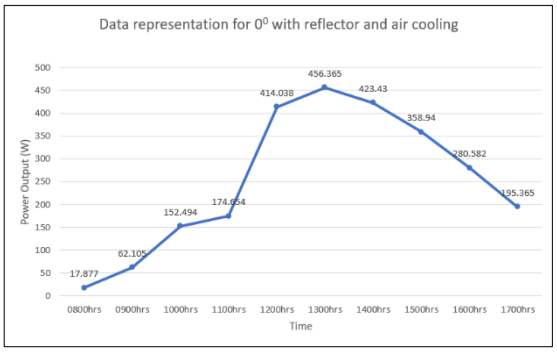

Figure 5. Power output vs. time in Configuration 3

Configuration 4: With reflectors and by incorporating both air and water cooling

According to Table 4, with air and water cooling in place, it was observed that the average panel surface temperature has reduced substantially. The variation of power output during the day is shown in Figure 6.

Table 4: Key operating parameters for the PV with reflector, air and water cooling (Configuration 4)

Time (hour of the day)	Average Surface Temperature (⁰C)	Voltage (V)	Current (A)	Power Output (W)	Irradiance (W/m²)
0800hrs	24.2	17.7	1.0	17.7	258.3
0900hrs	30.9	18.3	3.4	62.2	497.2
1000hrs	36.3	24.4	6.3	153.7	627.8
1100hrs	39.2	25.2	7.0	176.4	630.6
1200hrs	47.4	40.2	10.3	414.1	716.7
1300hrs	52.3	41.9	11.0	460.9	797.2
1400hrs	50.5	41.1	10.3	423.3	583.3
1500hrs	47.7	36.4	9.9	360.4	277.8
1600hrs	43.7	32.2	8.8	283.4	133.3
1700hrs	39.0	28.1	7.0	196.7	82.7

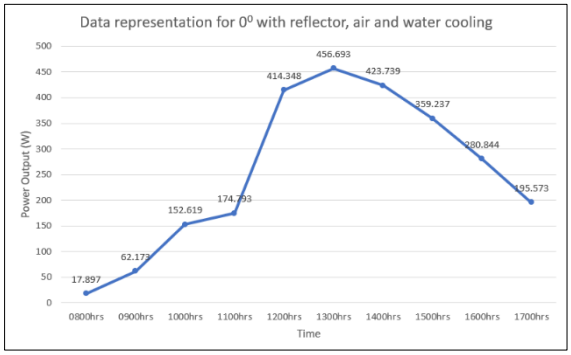

Figure 6. Power output vs. time in Configuration 4

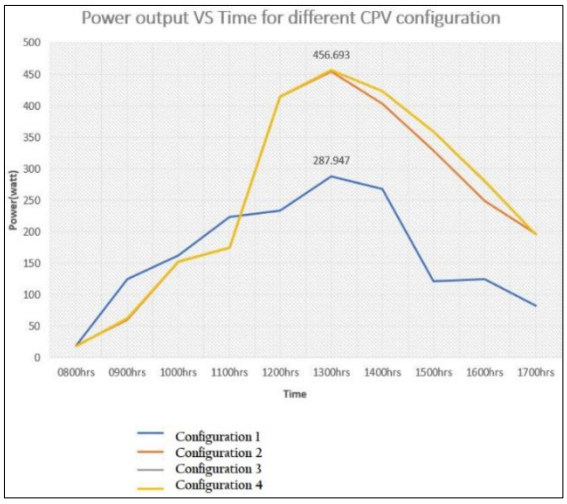

Figure 7. Comparison of power output of all configurations

Figure 7 provides a comparison of power output among all PV panel configurations.

IV. CONCLUSION

As far as the power output is concerned, it is evident that from 0800 hrs. to 1200 hrs., configuration 1 generates a higher power output than other configurations. However, after 1200 hrs. a higher power output is recorded by the other three configurations. By comparing configuration 2 with configuration 3, it is evident that a higher power output can be obtained when the panel cools down due to air cooling. The power output generated by configuration 4 does not show a significant difference to that of configuration 3. However, configuration 4 shows better temperature control due to air and water cooling that mitigates the degradation of the solar panel so that a longer lifetime can be expected for the equipment. The study shows that the conventional PV panel (Configuration 1) can be effectively used until 1200 hrs. and then by switching over to Configuration 4, it is possible to generate a higher power output while mitigating panel degradation due to better control of its surface temperature.

REFERENCES

Ahmed, S., Mia, M.M.A., Acharjee, S. and Ansary, M.A.A., 2014. More efficient use of photovoltaic solar panel using multiple fixed directed mirrors or aluminum foils instead of solar trackers in rural perspective of Bangladesh. International Journal of scientific and technology research, 3(4), pp.294-298.

Palaskar, V.N., Deshmukh, S.P. and Pandit, A.B., 2014. Design and performance analysis of reflectors attached to commercial PV module. International Journal of Renewable Energy Research (IJRER), 4(1), pp.240-245.

Moharram, K.A., Abd-Elhady, M.S., Kandil, H.A. and El-Sherif, H., 2013. Enhancing the performance of photovoltaic panels by water cooling. Ain Shams Engineering Journal, 4(4), pp.869-877.

Rodrigues, E.M.G., Melicio, R., Mendes, V.M.F. and Catalao, J.P., 2011, April. Simulation of a solar cell considering single-diode equivalent circuit model. In International conference on renewable energies and power quality, Spain (pp. 13-15).

Arshad, R., Tariq, S., Niaz, M.U. and Jamil, M., 2014, April. Improvement in solar panel efficiency using solar concentration by simple mirrors and by cooling. In 2014 International Conference on Robotics and Emerging Allied Technologies in Engineering (iCREATE) (pp. 292-295). IEEE.

Akbarzadeh, A. and Wadowski, T., 1996. Heat pipe-based cooling systems for photovoltaic cells under concentrated solar radiation. Applied thermal engineering, 16(1), pp.81-87.

Tonui, J.K. and Tripanagnostopoulos, Y., 2007. Improved PV/T solar collectors with heat extraction by forced or natural air circulation. Renewable energy, 32(4), pp.623-637.

Kluth, A., 2008. Using water as a coolant to increase solar panel efficiency. California State science fair, California, USA.

Moharram, K.A., Abd-Elhady, M.S., Kandil, H.A. and El-Sherif, H., 2013. Enhancing the performance of photovoltaic panels by water cooling. Ain Shams Engineering Journal, 4(4), pp.869-877.

Amelia, A.R., Irwan, Y.M., Leow, W.Z., Irwanto, M., Safwati, I. and Zhafarina, M., 2016. Investigation of the effect temperature on photovoltaic (PV) panel output performance. International Journal on Advanced

Science Engineering Information Technology, 6(5), pp.682-688.

AUTHOR BIOGRAPHIES

Eng. FBYR de Silva obtained his BSc Engineering (Hons.) in Mechanical Engineering from General Sir John Kotelawala Defence University. The author is a Associate Member of the IESL and a Associate Engineer at Engineering Council Sri Lanka. He is currently serving as a Lecturer (Probationary) in the Department of Mechanical Engineering.

Dr. RMPS Bandara graduated with BSc Engineering (Hons.) in Mechanical Engineering from the University of Moratuwa in 1998 and also obtained his Master of Engineering and Doctor of Philosophy in Mechanical Engineering from the same University. He is presently serving as a Senior Lecturer at the Department of Mechanical Engineering, General Sir John Kotelawala Defence University, Sri Lanka. His research interests include Computational Fluid Dynamics, and Energy Engineering. He possesses more than twenty years of academic and industrial experience.

Prof. Rahula Anura Attalage is the former Deputy Vice Chancellor of University of Moratuwa, He is a professor of mechanical engineering, He graduated with BSc in mechanical engineering degree from the University of Moratuwa. He obtained his master's degree in energy technology from the Asian Institute of Technology, Thailand. He also holds a PhD in energy engineering from Ecole des Mines de Paris, France. Currently serving as the Dean – Faculty of Graduate studies & Research at Sri Lanka Institute of Information Technology.

Development of a Robust Fire Boat to Operate at Fishery Harbours

MCP Dissanayake and PMKC Chandimal#

Faculty of Engineering, General Sir John Kotelawala Defence University, Sri Lanka.

#chandimalpmkc@kdu.ac.lk

Abstract— Fires on board of fishing craft at fishery harbours in Sri Lanka have occurred frequently during the last two decades, and in most instances, these spread to nearby fishing craft as well, resulting in heavy damage to property and the lives of the fishermen on-board. The traditional shore-based extinguish methods used to quench the fires proved unsuccessful in every instance. The drawbacks were identified for the existing methods of extinguishing a fire on board of a fishing craft. The most feasible and reliable method was to develop an in-shore patrol craft to hook and tow out the fishing craft on fire away from the other craft, and extinguish the fire with a major firefighting system designed for and installed in the rescuer craft. Thus, a floating fire extinguishing platform was designed and developed in accordance with the international and local fire regulations. The study comprises the designing of the fire main system with the mathematical calculations associated with the designed system and the stability of the craft.

Keywords: *existing methods, fire main system, fishing craft*

I. INTRODUCTION

Sri Lanka consists of 23 fishery harbours including 12 in prominent yet incorporated protective water breakers for the basins. Each and every fishery harbour is registered with minimum of 100 fishing boats and most of them are made of glass reinforced fibre. Approximately 20-30 fishing boats are secured at any given time in a harbour. However, there is no reliable system to extinguish a fire if it occurred onboard a fishing craft. The only available method is seeking assistance from the fire service of a municipal council or the Sri Lanka Navy and they are providing their assistance from the land. It takes time to reach the fishery harbour and to attack the fire. Within that period, in most instances, the fire has converted to a major fire and it did spread out to neighbouring fishing boats due to the windy condition in coastal areas. It has created divastated damage to the rest of the secured fishing boats at the harbour. During the last decade, a large number of fire incidents onboard fishing craft have been reported in many fishery harbours. Figure 1 shows that the fire occurred onboard a fishing boat at Galle fishery harbour[1] (*Sri Lanka Navy*, no date) and trying to extinguish by the fire team of Sri Lanka Navy. In addition to that, few recent incidents are depicted in Table 1 below;

Table 1: Recent fire incidents at fishery harbours

Fishery Harbour	Date	Damaged boats
Cod bay	18th June 2018	05
Tangalle	26th June 2019	20
Galle	09th April 2020	09
Dikowita	30th March 2021	04

Source: (*Department of Fisheries and Aquatic Resources*, no date)

Figure 1: Fire at Galle fishery harbour
Source: (*Sri Lanka Navy*, no date)

Department of Fisheries and Aquatic Resources and Ceylon Fishery Harbours Cooperation had to find a viable solution to counter fire incidents onboard fishing craft. Thus, the institutions had arranged a combined effort with the municipal council at the respective area with the fishery harbour by introducing an emergency telephone number for fire calls onboard fishing craft secured at the harbour. However, it was identified that damages to the fire caught craft and neighbouring craft could not be minimized by fighting the fire by

land based approach, in spite of established fire points equipped with portable fire extinguishers at fishery harbours in the early 2010s. Director General Manager (Harbour Operations)(Personal communication, May 15, 2020) reveals that one reason was identified, as failure to above approach as non availability of sufficient capacities of portable fire extinguishers to extinguish the fires once occurred and leads for an exponential spread in most instances.

Recently, the Department of Fisheries and Aquatic Resources had a discussion with Sri Lanka Navy (SLN) regarding this matter. SLN has been taken up the matter to study in depth. SLN has identified the necessity of a floating platform to hook and tow out the fired craft from the fleet of fishing craft and to carry out the fire extinguishing process in a close quarter periphery in the bay.

Inshore Patrol Craft (IPC), one of the small craft with length 14.5 meters in the Sri Lankan Naval fleet operate in shallow waters effectively and efficiently to prevent anti-smuggling and poaching activities and give security protection for harbour mouths, mainly for Colombo, Galle, Hambanthota, Trincomalee, and Kankasanthurei. IPC is propelled with 250 hp 04 OBMs and achieved the speed of 25 knots at its full load consisting of 2450 litres of fuel. The craft is depicted in Figure 2.

To ensure craft survive and keep floating, moving and fighting, it is highly essential to lay emphasis on fire prevention, keep extinguishing and protection with optimum operation at all times. Therefore, it has been identified the requirement to have a meticulous floating firefighting platform for efficient management of fire fighting operations onboard fishing craft at harbours.

Figure 2: Inshore Patrol Craft in Sri Lanka Navy
Source: Sri Lanka Navy

The research problem statement of the study is non availability of a suitable floating platform in close quarter to extinguish the fires that occured onboard fishing craft secured at fishery harbours. The scope of the study is to develop an Inshore Patrol Craft with a designed major firefighting system that is suited to throw the water flow to extinguish the fire that occurred onboard a fishing craft located at fishery harbours in Sri Lanka. The significance of the research was identified as to fill the gap, once a fire occurs onboard fishing craft secured at fishery harbours, the approach was unsolved until recently for the Department of Fisheries and Aquatic Resources and to the Ceylon Fishery Harbours Cooperation.

II. METHODOLOGY AND EXPERIMENTAL DESIGN

In order to enhance the realism in the firefighting environment simulated onboard IPCs, it is developed a major fire fighting system onboard inshore patrol craft to assist the fishing craft secured at the harbour in an emergency of fire.

It is required to be in par with the international and the local regulatory requirements in designing a fire main fighting system onboard a small craft. Therefore, it has complied with the laid down standards listed below.

a. Merchant shipping act for small craft – craft code 12.6.7
b. Merchant shipping act for small craft – craft code 4.10.4
c. Lloyd's Register – Rule finder part 5, Chapter 1, section 5 2.14.2

Inshore patrol craft has been taken into the consideration to identify the adequacy in operating with a major firefighting systems on afloat conditions. IPC has been designed and built with the following parameters as depicted in Table 2.

Table 2: Design parameters of an IPC

Description	Specification
Length overall	15 m
Beam	3.5 m
Hull material	Glass Reinforced Plastics
Fwd draught	0.7 m
Aft draught	0.6 m
Maximum cruising speed	25 knots at full load
Propulsion system	04 x 250 hp OBMs
Fuel capacity	2450 litres

Source: Sri Lanka Navy

It has been identified the exact location to have the sea chest without obstructing the stream water flow for the hull. Further, there is no disturbance to the water flow for the 04 No's OBMs due to sea chest.

Design parameters were considered to maintain the minimum distance of 20 metres in between two craft and to throw the water column with the required volumetric flow and pressure. Therefore, OEM's fire pumps selection part catalogue has been followed to meet the required specifications for the fire pump. The authors have plotted the system head curve considering the pump head and the flow rate. The pump selection has been carried out by matching the pump head curve and system head curve which is provided by the manufacturer. The details are depicted in Figure 3.

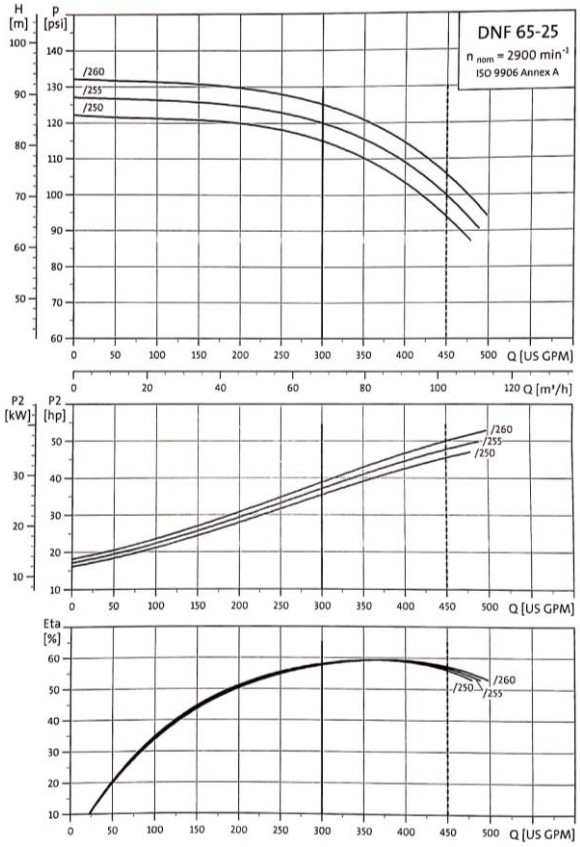

Figure 3: Selection of system operating point
Source: NFPA standard for installation fire pumps

Further, the location has been designed to install a diesel fire pump and its effect on the Longitudinal Center of Gravity (LCG) due to the weight factor of the pump. The stability calculations were carried out to find the stability variations of the craft. The displacement of the IPC is 9 Tons and the actual GZ for the IPC is indicated below in Figure 4.

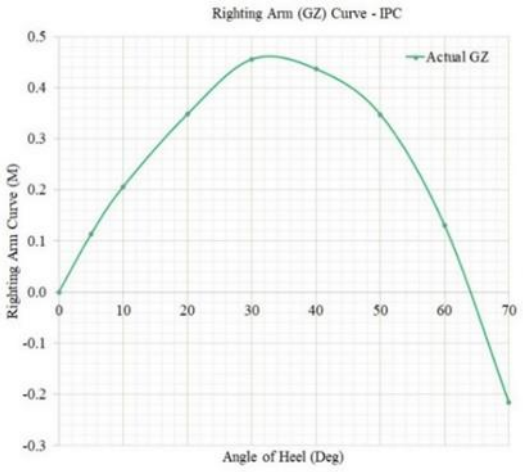

Figure 4: Righting arm curve - IPC
Source: Developed by Authors

The material selection has been carried out in par with the small craft – craft code 12.6.7 and marine quality pipes were selected as per the laid down pipe schedule. In addition, discharging the water has been arranged through a 50 mm branch pipe consisting of a jet and spray nozzle. And also, a branch pipe is installed on the strengthened mount with a rotation of 120 degrees. The authors have designed a single line firemain system to install an onboard fire boat to extinguish a fire that once occurred in a fishing craft at the harbour.

III. RESULTS AND DISCUSSION

Mainly, it has been focused to develop an Inshore Patrol Craft with a designed major firefighting system that is suited to throw the water flow to extinguish the fire that occurred onboard fishing craft located at fishery harbours in Sri Lanka.

A. Fire pump pressure head and flow rate

The discharge velocity of the flow is calculated by Bernoulli's equation.

$$P + 1/2\,\rho V^2 + \rho g h = Constant \ldots. (1)$$

Thereby, the volumetric flow rate is calculated using the following equation.

$$Q = \upsilon A \ldots (2)$$

Where, Q = Volumetric flow rate, υ = Flow velocity and A = Cross sectional area

Considering the minimum distance of 20 metres in between two craft, the output pressure and the flow rate is calculated. The pressure head = 68 psi and flow rate = 244 GPM.

Therefore, it has been analysed the condition with the performance curves of the pump head curve, power curve and efficiency curve and selected the pump with a pressure head of 70 psi with a flow rate of 250 GPM to cater for the minimum requirement. However, the pump should have a sufficient pressure head and flow rate to extinguish the fire. Since the pump is producing 300 GPM and 120 psi at 255 mm diameter impeller and also near to the maximum efficiency, selection has been done as per the curves in figure 3. Further, it was able to maintain the required distance and continuous water flow rate to extinguish the fire.

As per the Merchant shipping act for small craft – craft code 4.10.1, marine quality steel was selected and the seawater suction line outer diameter was 112.5 mm according to the pipe schedule. The associated 2 valves also matched with the steel. A 65 mm diameter jet and spray branch pipe was installed at the mount to maintain the distance in between the craft during the fire extinguishing operation.

B. Stability of the craft

The effect of the addition of the weight of the pump for the stability of the craft has been studied while changing the pump location at the forecastle area of the craft. The aft of the craft is not considered for pump locating to get the maximum advantage while engaging with the fire. The authors designed the pump bed after calculating the stability of the craft and changes of LCG and the Vertical Center of Gravity (VCG). The change of VCG is 0.2 m and it is a positive value. Therefore, VCG increases. Further, Change in LCG is 0.01 m and stability remains as previous. The comparison of righting arm (GZ) curve is depicted in Figure 5 below.

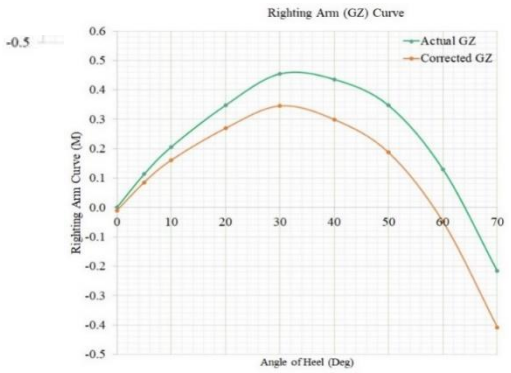

Figure 5: Righting arm curve
Source: Developed by Authors

IV. CONCLUSION

The fires onboard fishing craft at fishery harbours was an unsolved problem for the last two decades. Though, it has been taught many lessons learnt from those incidents, all of them were failed to provide a lasting sustainable solution. The development of an Inshore Patrol Craft with a designed major firefighting system which is suited to throw the water flow to a minimum distance of 20 meters to extinguish the fire that occurred onboard fishing craft. It will fulfil the gap of the requirement of a viable fire extinguishing method onboard fishing craft at harbours in Sri Lanka. With that, authors have pointed out the benefit and the suitability of the floating platform as an Inshore patrol craft to extinguish a fire once occurred onboard fishing craft and to prevent the spread of fire to neighbouring fishing craft.

REFERENCES

Department of Fisheries and Aquatic Resources (no date). Available at: *https://www.fisheriesdept.gov.lk/web/index.php?lang=en* (Accessed: 9 June 2021).

Sri Lanka Navy (no date). Available at: https://news.navy.lk/eventnews/2020/04/09/20200409140 0/ (Accessed: 4 June 2021).

Developing an Explosive Laden Unmanned Waterborne Vehicle to Eliminate Liberation Tamil Tiger Elam (LTTE) Suicide Boat Attacks at Sea

MCP Dissanayake

Department of Marine Engineering, Faculty of Engineering, General Sir John Kotelawala Defence University, Sri Lanka

dissanayakemcp@kdu.ac.lk

Abstract— The LTTE was one of the most ruthless terrorist groups, which had operational sea capabilities. In the early 1980s, the LTTE formed a naval wing called sea tigers. Subsequently, the sea tiger leader introduced an elite and highly trained suicide carders to this special element to carry out attacks against Sri Lanka Navy (SLN) ships, using explosive laden boats. The Sri Lanka Navy, thus, was faced with a unique challenge. The highly developed maritime guerrilla warfare, which the SLN faced, had to be fought and won in close proximity to the enemy, at visual range, where speed and manoeuvrability took precedence over long-range weapons and endurance. Then, the SLN decided to build an unmanned waterborne vehicle (UWV), to counter suicide boat attacks of the LTTE without harming its own men. This UWV was unique and operated at a wide range of both shallow and deep waters effectively. Further, it was fixed with 120 kg high explosive claymore mines that could be detonated remotely. The speed, manoeuvrability, and explosion impact of UWV were investigated by ramming it to the LTTE target. It was found that significant damage to the enemy was done by the explosion and shock wave during the test. Consequently, the LTTE suicide boat launching dramatically reduced.

Keywords: ***Sri Lanka Navy (SLN), Unmanned Waterborne Vehicles (UWV), Unmanned Arial Vehicle (UAV), Rapid Action Boat Squadrons (RABS).***

I. INTRODUCTION

The LTTE was one of the most ruthless terrorists, which consisted of operational sea capabilities. In the early 1980s, LLTE has formed a naval wing, called sea tigers. Subsequently, the sea tiger leader introduced elite and highly trained suicide carders to this special element to carry out attacks against Sri Lanka Navy (SLN) ships, by explosive laden boats. Initially, the SLN was suffered heavily and tried to make counter attacks by available resources. Further, the SLN fleet was upgraded by supreme boats with new technologies, as per proposals of expert fighters on board SLN ships. Though it was not enough to evade the LTTE suicide boat attacks and SLN was losing their boats during sea battles against the enemy.

The Sea Tigers were designed and developed a new tactic called "wolf pack" attacks. In these attacks, the formation was gradually built up and identified a target by command vessel. Then, directed a bunch of smaller boats to approach the target vessel and attack from all directions, and ensure to prevent it from fleeing the area. Subsequently, an explosive laden boat was moved towards the target with a cover of the larger command vessel and rammed the target by losing a single Black Tiger, in this mission. Generally, two types of boats were utilized against SLN, one was stealth craft which was operated at high seas atmore than 40 knots speed, another type was Explosive Laden Floating Device that was used at shallow water against SLN patrol craft,

Figure 1. Liberation Tamil Tiger Elam suicide boat

Figure 2. Explosive Laden Floating Device

SLN realized that the bigger Dvoras were not enough to hunt down the smaller in size, vary fast moving, shallow water operating and highly maneuvered LTTE suicide boats. Therefore, SLN elite force, Special Boat Squadron was testing out smaller versions of boats against LTTE suicide boats, though it was not fully succeeded.

An unmanned vehicle that can be controlled remotely has been a matter of military curiosity. Advancement in automation technology made such an idea a practical reality of such a vehicle capable of travelling in air or water. where the terrain obstruction does not interfere with the line of sight control has been of particular significance. Thus the development of unmanned vehicles for military use has been progressing at a fierce pace all over the world during the last few decades. Though, development of unmanned aerial vehicles has outpaced their waterborne counterparts due to their distinctive usefulness for surveillance waterborne unmanned vehicle, on the other hand, could not make the same place for itself in a maritime arena that is predisposed towards airborne surveillance, long-range weapons and prolonged endurance. A scenario for which waterborne unmanned vehicle is intrinsically not suited. Therefore, worldwide, the development of remotely controlled unmanned waterborne vehicles (UWV) is restricted for roles such as target boats, mine clearance vehicles, deep sea submersibles, etc. (Ebken J, Bruch M, Lum J 2005).

Sri Lanka Navy, however, was faced with a unique challenge of a very different kinds. The highly developed maritime guerilla warfare, which the SLN faces, had to be fought and won in near close to the enemy, at visual range, where speed and maneuverability were taken precedence over long-range weapons and endurance. Therefore, the utility of UWV was of special consequence for SLN. Naturally, as the challenge faced by SLN was very unique and unprecedented in technologically developed parts of the world, the expertise needed for such an enterprise had to be home grown rather than imported.

The UWV was primarily designed to mislead the LTTE boats during sea battles. A secondary purpose of the UWV was to use it as the first line of the battle and avoid human casualties. The main objective of this research project was to stop LTTE suicide attacks by operating and triggering this UWV with a safe distance, and minimum damage to the SLN during sea confrontations.

II. DESIGN FEATURES

Explosive Laden Unmanned Waterborne Vehicles (UWV).

A. Material Selection and Design of Hull

Fiberglass was chosen to make this arrow boat due to low cost, light weight, minimal elongations, and availability of experts and infrastructure facilities at SLN. Subsequently, type of the hull was decided after conducting number of trails, utilizing 18-foot dinghy, 16-foot arrow boat and 18-foot arrow boat with 200 kg pay loads. Eventually, a planning hull was selected for this UWV considering the fact that ability to push through the water and skim across the water's surface. According to preliminary design, construction of the 18-foot arrow boat was begun with the fabrication of a hull in figure 1. Since stability of the 18-foot arrow boat is one of the very important criteria in this design, to destroy the enemy targets by ramming without hindering the mission. The length of the arrow boat is restricted to 18' and maximum breadth is curtailed with 5' 3". The height is 2' 7" with both sides angled out, at an angle determined from the difference in the beam and bottom widths of the hull in figure 2. Fabricating a transom is vital, and considered as the back panel of an arrow boat hull. Consequently, the angled sides are generating additional depth to the planning hull and an increase in the displacement. Therefore, it leads to enhance the capacity of the arrow boat to accommodate a heavy load of explosives to destroy the enemy target with surprise.

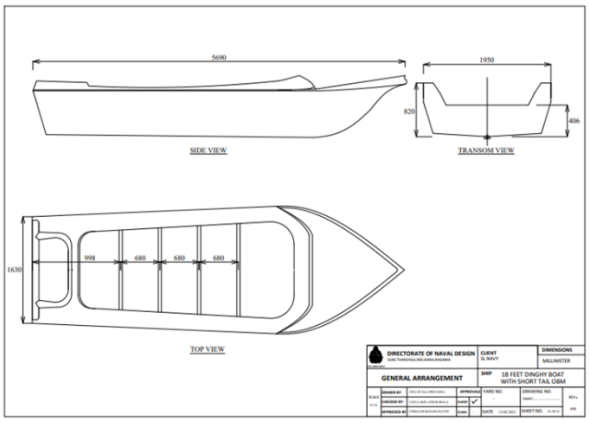

Figure 3. Detail Design of 18' arrow Boat

Salient Features

a.	Type of Boat	- Arrow (18')
b.	Propulsion Plant	- 75 HP OBM
c.	Pay Load Capacity	- 150 Kg

d. Max Speed - 40 / 50 knots (Sea State 1/3)
e. Actuating Mechanism - Hydraulic
f. Remote Link - VHF (Handheld Communication Set)
g. Remote Control Range - 6/ 15 Nm (Max / Practical)

B. Propulsion System

Short tailed 2-stroke, 75 HP Outboard Motor (OBM) was chosen as a propulsion system for this arrow boat due to easy handling in shallow water, to achieve maximum speed, destroy the enemy target with surprise and availability of work shop facilities within SLN in Table 1. In this context, many options were had with SLN to select suitable engines for the designed arrow boat. Both inbuilt engines and separate propulsion systems or inbuilt engines and water jet systems are generally used for this kind of water borne application, to achieve design speeds.

Table 1: Selecting the right size hp for outboard motor for this 18' arrow boat

Motor HP	Boat length (feet)	Boat length (metres)
2hp – 10hp	8' – 12'	up to 3.5m
5hp – 15hp	8' – 14'	up to 4.2m
9hp – 20hp	11' – 16'	up to 4.5m
20hp – 40hp	13' – 18'	up to 5.0m
40hp – 75hp	14' – 20'	up to 5.5m
90hp – 140hp	16' – 25'	up to 6m +

Figure 4. Short tailed 75 HP Outboard Motor

C. Selection of Correct Propeller

Propeller size is expressed with two numbers, diameter and pitch, with diameter always stated first. The diameter is two times the distance from the center of the hub to the tip of any blade. Smaller prop diameters generally go with smaller engines, or with fast high performing boats. Therefore, in this context, a smaller size propeller was fixed with 75 HP OBM as per guidelines of Yamaha Manufacturer to meet SLN requirements such as speed and surprise (Savitsky, 2003). In addition, Rake is the degree that the blades slant forward or backward in relation to the hub. Rake can affect how water flows through the propeller, which can make a difference regarding boat performance. Aft rake helps to lift the boat's bow, decreasing the hull's wetted surface area and improving top end planing speed. Eventually, SLN decided to take enemy targets by using UWV within the 2 nm range to dodge enemy swam attacks.

D. Trim Angel

Trim angle is a very important aspect, fixing an OBM to the arrow boat and leads to maintain stability of the vessel. Further, it depends on the vessel's handling characteristics, the size of the outboard, the sea, and loading conditions. In this design, the trim pump played major role to correct the trim angle during the operation of the arrow boat figure 5 & 6.

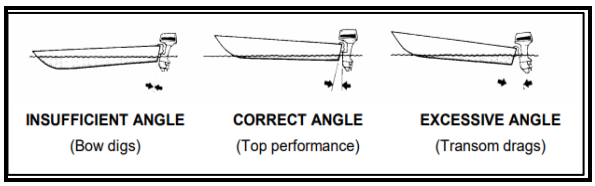

Figure 5. Correct Trim Angle

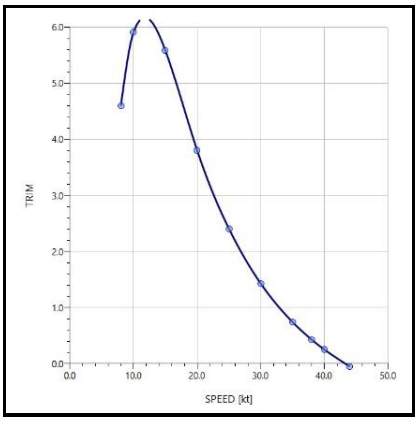

Figure 6. Characteristics of Trim vs Speed

E. Control System

The development process of this successful prototype had gone through long and arduous rigours seven failed model tests and many fundamental changes in technological approach itself. To begin with a purely mechanical control system based on automobile window winding mechanism was tried. Though, due to inconsistent performance and lack of robustness this approach had to be abandoned. Eventually, a hydraulic actuating system assembled from a discarded hydraulic mechanism of Out Board Motor (OBM) was found to be suitable and was successfully integrated into a functional remote control aggregate. After developing a reliable control system, an initial scaled down model with only steering control (Without throttle control) was developed and tried on a 23' FGD. With subsequent insight gained into the practicalities of such a development and with the lessons learnt, the final prototype was based on a 18' Arrow Boat which is powered by a 75 HP OBM. The steering system was developed, utilization of trim pump and both port and starboard could be achieved maximum up to 30o, without harming to the stability of the UWV. Similarly, the speed control mechanism was incorporated with another trim pump and hydraulically controlled the acceleration and retardation during the experiment. The trim pump was powered by 24 DC and ensured to keep the batteries, fully charged throughout the test (Ford, D.W. and Juve, E.K., Nautamatic Marine Systems Inc, 1996). A steering system was very special in this UWV and hydraulically operated with the utilization of additional trim pump, that was actuated by VHF signals and associated with fluid communication through a hydraulic cylinder, that connected to the OBM (Treinen, K.J., Amerling, S.J. and Fisher, B.L., Brunswick Corp, 2001). Then, the prototype model had both steering as well as throttle control and was remotely controlled through a VHF link based on handheld VHF communication set. The control was exercised by pressing the Power Transmitting Toggle (PTT) switch and quantum of control signal was determined by the duration for which the PTT was pressed. For differentiating between different types of commend, different channels of the communication set were used. It may be pertinent to mention that the remote control circuit had been exclusively developed for this requirement and was quite different from a normal remote control toy. While, the vehicle could be remotely controlled up to a range of 15Nm, practical difficulties of sighting and precise control limits the useful range of remote control to 6 Nm. The prototype model was operating with a dummy load of 120 Kg but could carry and payload up to 150 Kg. the prototype had been extensively tried a sea and can travel up to 40 knots speed.

Figure 7. Trim Pump

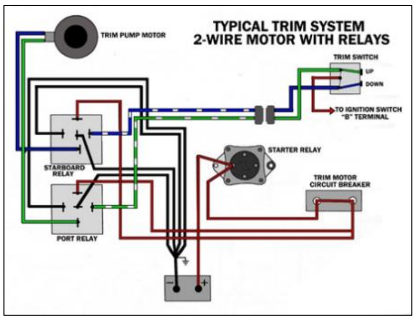

Figure 8. Wiring diagram of Trim Pump

Figure 9. Prototype an explosive laden unmanned waterborne vehicle (initial testing)

F. Test Procedure

The UWV was fixed with 120 kg of high explosive and amalgamated with a trigger mechanism to carry out explosion by VHF communications. An operator was on board another arrow boat at sea and selected the target as abandon merchant vessel called Fara III, which was grounded at LTTE controlled area at Pudumatalan. Subsequently, the operator was identified a distance to the target from the operating platform by a radar and prepared the UWV for the assigned task. Then, the UWV was operated at speed of 40 knots, at seas

state 1-2 and reached the target within 5 minutes and carried out the attack by ramming. This complete operation was observed by the Unmanned Arial Vehicle (UAV) and recorded all the events to make further improvements of UWV.

G. Launching Platform

Special Boat Squadron (SBS) of SLN had 23 foot arrow boats which were operated at more than 45 Knots speed with high maneuverability. Therefore, SLN decided to strengthen SBS boats with one or two Explosive Laden UWV for missions against LTTE.

Figure 10: Special Boat Squadron Launching Pad

Figure 11. Launching Unmanned Waterborne Vehicle at Sea

Figure 12. Moving Unmanned Waterborne Vehicle to the LTTE target

Figure 13. Unmanned Waterborne Vehicle was rammed into the Fara III

III. RESULTS AND OUTCOMES

Sea trials were carried out using three different types of boats, different weight conditions, erratic capacities of OBM, and different sea states in table 2.

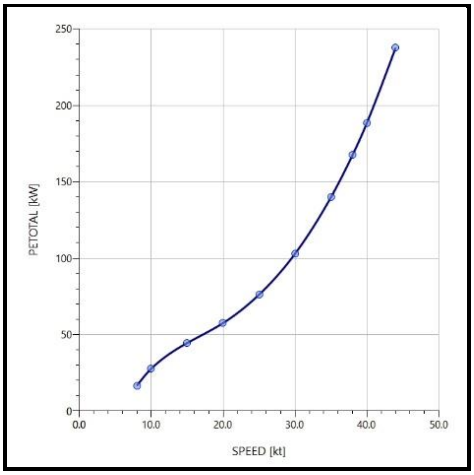

Figure 14. Comparison of Power vs Speed

Power of OBM and speed of boat were calculated at sea state 1-2 figure 14.

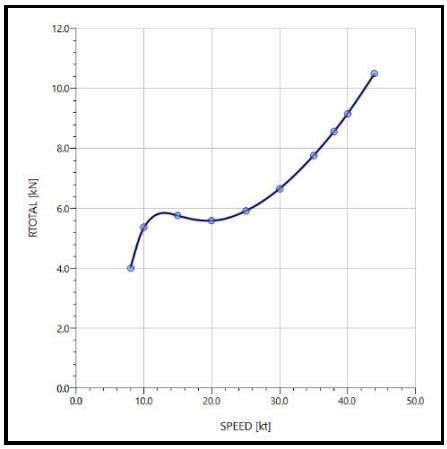

Figure 15. Comparison of Resistance vs Speed

Arrow boat hull resistance and speed were calculated at sea sate 1-2 figure 15.

A bearable level of noise and bit vibration was generated during the UWV operation. The UWV was steady at sea state 1-2 with a speed of 40 knots. The hydraulic control and data acquisition systems were produced very reliable outcomes. The maneuverability of UWV was very high and reached the target accurately. The explosion impact was immense and Fara III was parted into two pieces.

IV. DISCUSSION

Table 2. Details of Sea Trails in Three different Models

Date	Type of Boat	Weight	OBM	Sea State	Speed	Remarks
23/03/2007 24/03/2007 26/03/2007	23' FGD	500 kg	25 HP	1-2 1-2 1-2	12 knots 11 knots 12 knots	Less speed, taking large turning circle, stable, operated 16 hrs and very reliable control system
07/04/2007 08/04/2007 19/04/2007 23/04/2007 24/04/2007 27/04/2007	23' FGD	600 kg	75 HP	1-2 2 3-4 1-2 2 2	23 knots 20 knots 15 knots 24 knots 19 knots 18 knots	Moderate speed, Taking large turning circle, stable, operated 64 hrs and very reliable control system
16/05/2007 17/05/2007 20/05/2007 03/06/2007 06/06/2007 12/06/2007 20/06/2007 09/07/2007 10/07/2007 12/07/2007 20/07/2007	16' Arrow Boat	420 kg	75 HP	1-2 2-3 3 1-2 2 2 3 1-2 2-3 1-2 2-3	34 knots 28 knots 20 knots 34 knots 24 knots 24 knots 19 knots 33 knots 26 knots 35 knots 27 knots	High speed, Taking small turning circle, steady and stable, operated 108 hrs and very reliable control system
16/08/2007 19/08/2007 23/08/2007 25/08/2007 02/09/2007 14/09/2007 22/09/2007 25/09/2007 26/09/2007 28/09/2007 29/09/2007 02/10/2007 06/10/2007 10/10/2007 12/10/2007 14/10/2007 15/10/2007	18' Arrow Boat	280 kg	75 HP	1-2 1-2 1-2 2 1-2 1-2 1-2 3 3-4 3 1-2 1-2 1-2 2 2 2 1-2	48 knots 48 knots 47 knots 43 knots 49 knots 48 knots 48 knots 41 knots 39 knots 40 knots 48 knots 47 knots 48 knots 44 knots 43 knots 45 knots 48 knots	High speed, Taking small turning circle, stable (bit unstable above seas state 3), operated 146 hrs and very reliable control system
13/11/2007 19/11/2007 25/11/2007 26/11/2007 02/12/2007 10/12/2007	18' Arrow Boat	420 kg (with high explosive)	75 HP	1-2 1-2 2 1-2 2-3 2	40 knots 40 knots 36 knots 41 knots 32 knots 37 knots	High speed, Taking small turning circle, steady and stable (bit unstable above seas state 3), operated 48 hrs and very reliable control system

The mission was conducted in day time and completely visible weather conditions. This was the first time the explosive laden UWV, used against enemy target. Further, it was created an utter panic state for sea tigers, and ended up with a disastrous situation. Moreover, this low profile UWV could not detect by the enemy radars or look outs, until the explosion.

Initialy UWV was at rest, the weight of the arrow boat was stayed entirely by the water in which it's sitting, known as "static buoyancy." Subsequently, the arrow boat started to move forward through the water, speed created hydrodynamic lift. Eventually, more power was applied, lift increased, and reduced wetted area and thus reducing drag. At this point, the boat was said to be "planing" and steadily reached up to 45 kt. In addition, 12 knots

to 20 knots region that the arrow boat had maximum drag and that was why speed drop came into place in figure 14 &15.

V. CONCLUSION

LTTE suicide boat launching was dramatically reduced. A remote controlled unmanned waterborne vehicle was potent and can be used for a variety of task ranging from benign use as target boats to an offensive platform. One of the most potent uses of this platform could be to match the suicide boat tactics of the enemy during sea confrontations. The remote control boats with explosive payload could be made part of 'Rapid Action Boat Squadrons' (RABS) and unleashed in the form of a swarm attack on an unsuspecting enemy at a decisive moment during the battle. This only envisions one of the many such scenarios where an unmanned vehicle could be effectively used without putting the valuable human resource in harm's way. Therefore, possibilities of potential use are many and are only limited by creative imagination rather than the limitation of the hardware.

REFERENCES

Ebken J, Bruch M, Lum J (2005). Applying UGV technologies to unmanned surface vessels. SPIE Proc. 5804, *Unmanned Ground Vehicle Technology VII*, Orlando.

Ku, B.Y., Strong Engr Consulting Co Ltd, 2002. Modularized unmanned marine surface vehicle. *U.S. Patent* 6,427,615.

Ruszkowski Jr, R.A., Lockheed Martin Corp, 2006. Immersible unmanned air vehicle and system for launch, recovery, and re-launch at sea. *U.S. Patent* 7,097,136.

Mulhern, F.M., US Secretary of Navy, 2005. Unmanned watercraft retrieval system. *U.S. Patent* 6,883,453.

Brooks, B. and Mateer, J., 2007. Automated trim tab adjustment system method and apparatus. *U.S. Patent* 7,311,058.

Ford, D.W. and Juve, E.K., Nautamatic Marine Systems Inc, 1997. Automatic steering apparatus and method for small watercraft. *U.S. Patent* 5,632,217.

Ford, D.W. and Juve, E.K., Nautamatic Marine Systems Inc, 1996. Small watercraft automatic steering apparatus and method. *U.S. Patent* 5,509,369.

Treinen, K.J., Amerling, S.J. and Fisher, B.L., Brunswick Corp, 2001. Integrated hydraulic steering actuator. *U.S. Patent* 6,276,977.

Dissanayake, M.C.P. and Gunarathna, T.M.S., 2020. Design of a Wind Propelled Planning Hull Craft for Shallow Water Operation.

ACKNOWLEDGMENT

I would like to acknowledge Admiral (Rtd) RC Wijegunaratne, Rear Admiral (Rtd) MUKV Bandara, and Rear Admiral YN Jayarathna to provide guidance and assistance throughout this research project.

AUTHOR BIOGRAPHIES

Cmde (E) MCP Dissanayake, CEng (IEI), Associate Member (IESL), Fellow (FRINA) is currently performs as the Head of Department (Marine Engineering) and hold 2 No's patents for his research papers published so far. He is an inventor and published 06 No's publications on Brackish Water Reverse Osmosis application, Fan Boat Building and Oscillation Water Column, Ocean Wave Energy Converter. He was the Director in Research & Development at Sri Lanka Navy and has received commendations in number of occasions from the Commander of the Navy, HE the President of Sri Lanka for his innovation. Further, he was awarded with prestigious, Japanese, Sri Lanka Technical Award for his own developed low-cost Reverse Osmosis Plant, to eliminate Chronic Kidney Disease from Sri Lanka. Moreover, he has vast exposure on marine diesel engines and possesses a Master's degree in Marine Engineering from Australian Maritime College, University of Tasmania, Australia.

Inductively Coupled Plasma Optical Emission Spectrometry in Effective Condition Based Maintenance Engineering Plan

DMPM Dasanayaka# and EN Fernando

Naval Headquarters, Colombo 01, Sri Lanka

#dasanayakamilinda@gmail.com

Abstract— The Inductively Coupled Plasma Optical Emission Spectrometry (ICP-OES) is a powerful tool for the determination of many wear down elements in a variety of different sample matrices. The Sri Lanka Navy commenced analysis of used lubricating oils in on-board main machineries and shore-based generators since the year 2017 which assists to implement Condition Based Maintenance (CBM) philosophy in the Sri Lanka Navy as a vital component in the P-F curve of machinery maintenance reliability. As per ASTM D 5185, the testing has been carried out. Results of the analysis capture only the particle sizes below 10 microns where the elements are necessary to be oil-solvable. In this, soluble residues are not counted. The paper is focuses on appraising the process practiced by the SLN to study the elemental behaviour of machineries fitted on-board to support the CBM development plan. The annual oil condition monitoring schedule has been published, and sample testing is done according to the promulgated directives. The findings of the analysis are plotted against each of the machinery, and the machinery health is monitored accordingly. Several failures were pre-identified and preventive actions were initiated. The numerical results against each similar type of engines with respect to the running hours of the machinery are compared and specific limitations against each make/model are identified. This will enable us to find the safe operating parameters as a baseline measurement and to promulgate the threshold limits.

Keywords: ***inductively coupled plasma optical emission spectrometry, oil analysis, condition monitoring***

I. INTRODUCTION

Machinery maintenance is a vital role of an Engineer which involves measuring, servicing, carryout functional tests, overhauling, repairing, etc. Various maintenance categories have been introduced to optimize the schedules according to the industrial /user requirements. The Condition Based Maintenance is a strategy that monitor the real time condition of the machinery/equipment which is an asset that decides the real maintenance requirement. Inductively Coupled Plasma – Optical Emission Spectrometer (ICP-OES) is a widely used analytical tool that is used globally as a versatile method of inorganic analysis. This is used as one of the main components of Condition Based Monitoring in SLN Oil analysis for wear down analysis. This will identify and quantify the element presence in the provided oil sample.

A. The Operating concept of ICP-OES

A plasma is a gas, in this case argon, which contains a significant number of argon ions. The plasma is formed by seeding the argon gas passing through a plasma torch with electrons. The electrons are accelerated and collide with argon atoms releasing more electrons and forming argon ions. Elements, in the form of atoms, are introduced into the plasma. A proportion of these atoms will be become ionized within the plasma. When an atom or ion is excited within the plasma, its electrons jump from a lower to a higher energy level (Figure 1). Upon relaxation of these electrons to their initial 'ground' state, energy is emitted in the form of photons. The emitted photons possess wavelengths that are characteristic of their respective elements.

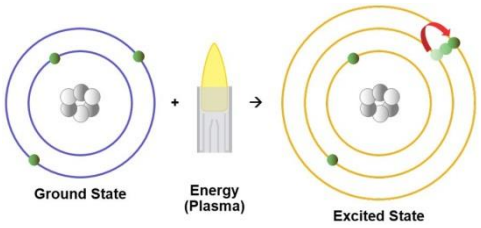

Figure 1. Excitation of an atom by a Plasma

One element can have multiple electron excitations and relaxations; therefore, it can have wavelengths with multiple characteristics. However, during the analysis, the Analyst will select the most suitable wavelength which will not interfere with any of the other elements that exist in the provided oil

sample. An example of an emission spectrum for calcium is shown in figure 2.

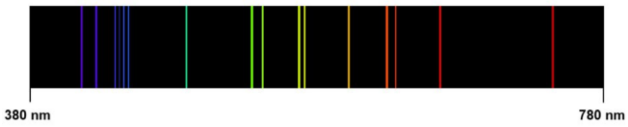

Figure 2. Emission of spectrum of Calcium in visible range

The main aim of this wear down analysis is to formulate safety margins for machinery fitted on board fleet units and also to identify unforeseen failures prior major failures. The oil analysis spectra assessment is to be performed during each oil draining interval, major repairs, major routines or installation of new equipment to understand the elemental behaviour of specific regimes.

II. METHODOLOGY

The wear elements presence in provided oil samples are tested through ICP-OES. Following methods are identified as the essential components of the testing;

A. Sampling & Sample / Equipment Preparation

The objective of sampling is to obtain a test specimen that represents the entire quantity. Therefore, the sampling procedure is done according to the laid down ASTM D 4057 standard.

The samples were prepared as per the Laid down procedure in ASTM D 5185. The following elements are tested by ICP-OES and results were recorded accordingly. The elements determined and tested wavelengths are as follows;

Table 1. Elements Determined and Suggested Wavelengths

Element	Wavelength, nm
Aluminium	308.22, 396.15, 309.27
Chromium	205.55, 267.72
Copper	324.75
Iron	259.94, 238.20
Lead	220.35
Nickel	231.60, 227.02, 221.65
Silicon	288.16, 251.61
Tin	189.99, 242.95

As an example, the Figure 3 indicates how the elements will interfere against other elements presence in the sample. It is visible that Vanadium (V), Antimony (Sb), Barium (Ba), Radium (Ra), Tungsten (W), Tantalum (Ta) elements interfere with the Iron (Fe) (252.851) element. However, that can be neglected due to none of the wear elements which need to be tested are present in the interference list.

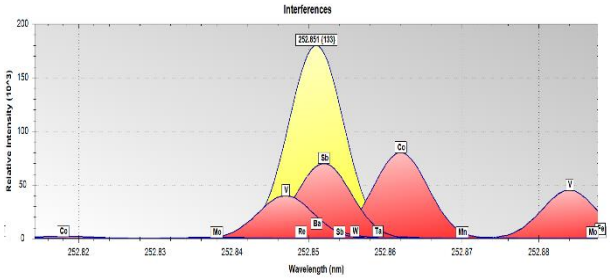

Figure 3. Interference between elements

However, in the ICP-OES plasma temperature is above 9000 K which is considered as higher in temperature, which will help to chemical interferences, This will be sufficient to break down the most spices into the atoms or irons for excitation and subsequent emission.

B. Calibration

The instrument calibration is one of the most important factors in which the linear range must be maintained. This is performed prior to each analysis. At the beginning of the analysis blank, three specimens of Oil Analysis standards were prepared.

The concentration of the Oil Analysis standard was 1000ppm. Therefore, three specimen samples will be prepared to perform three-point calibration.

Following mathematical calculation was used to prepare the specimen samples.

$$c_1 \times V_1 = c_2 \times V_2$$

where,
c_1 = Initial concentration or molarity
V_1 = Initial volume
C_2 = Final concentration or molarity
V_2 = Final volume

Therefore, 2.5 ppm, 5 ppm and 10 ppm sample specimens are prepared and by running the samples in ICP-OES as per the procedure, the calibration curves were plotted as per Figure 4 to Figure 8. Therefore, the linearity will confirm the calibration process.

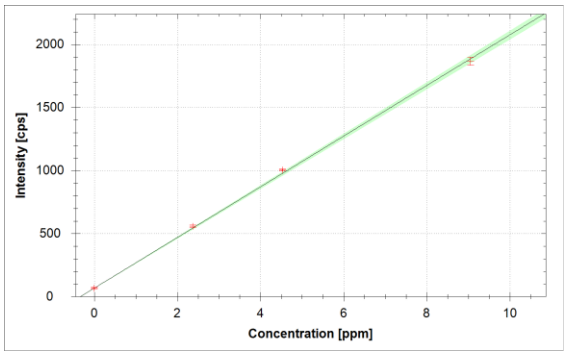

f(x) = 200.8345*x + 67.7000
R^2 = 0.9993
LoD = 0.0817 ppm

Figure 4. Calibration curve of "Al" element

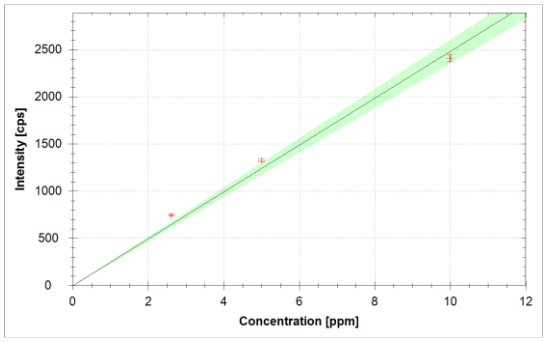

f(x) = 209.2875*x + -15.6444
R^2 = 0.9988
LoD = 0.0526 ppm

Figure 5. Calibration curve of "Cr" element

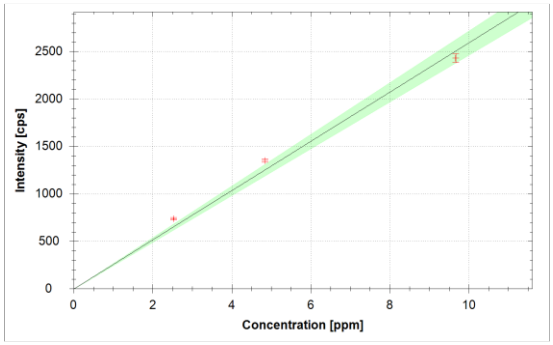

f(x) = 259.3706*x + -4.2986
R^2 = 0.9929
LoD = 0.0195 ppm

Figure 6. Calibration curve of "Cu" element

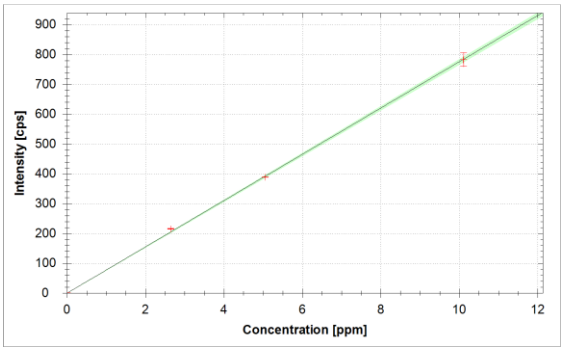

f(x) = 77.5786*x + -0.1661
R^2 = 0.9996
LoD = 0.0554 ppm

Figure 7. Calibration curve of "Pb" element

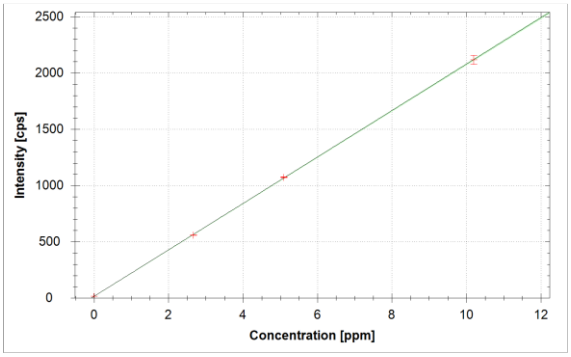

f(x) = 206.3070*x + 15.0743
R^2 = 1.0000
LoD = 0.0114 ppm

Figure 8. Calibration curve of "Sn" element

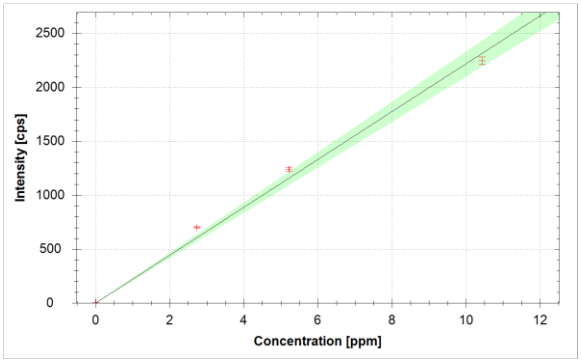

f(x) = 221.7207*x + 0.1000
R^2 = 0.9923
LoD = 0.0215 ppm

Figure 9. Calibration curve of "Fe" element

If the R^2 value is closer to 1 the calibration is considered as accepted. If the calibration curve is not passing through the origin or the blank shows some amount of count, then there is a possibility of

having low concentration or having analyte in the sample which will show negative results if the blank is different or use a different weight/volume of blank. Mostly it is recommended to have a low Limit Of Detection (LOD). However, if the analysis results are lower than the LOD value, those results should not be considered. If the results are not large negative numbers that indicate the element(s) which are measured is not present in the particular oil sample.

Basically, the calibration curve is plotted to understand the relationship between concentration and intensity.

C. Testing frequency

In order to standardize the oil sample testing intervals (except specific cases), an oil analysis schedule has been introduced which recommends the time interval for oil sample testing for ships/craft (main engines, gear boxes and generators). Therefore, the end-users will forward the oil samples as per the prescribed schedule.

D. International Standards Followed

The ASTM D 5185 method "Standard Test Method for Determination of Additive Elements, Wear Metal, and Contaminants in used lubrication oils and determination of selected Elements in base oils by Inductively Coupled Plasma Optical Emission Spectrometry (ICP-OES)" are practised as the international standardized test method.

III. RESULTS AND DISCUSSION

The focus was mainly placed on the wear metal concentrations of Fe, Cu, Al, Si, Pb, Cr, Sn, Ni elements in the oil samples to prevent unforeseen failures. Basically to find out the wear metal presence in lubricating oil samples.

The analysis was carried out for 16 cylinder V type reciprocating engines as per the promulgated schedule. Both the engines had clocked approx. 40000 Hrs. All the wear metals were found within acceptable regimes in the initial stage of analysis and it was noticed that the "Cu" elemental concentration in Port Main Engine was abnormal compared to Stbd Main Engine. Therefore, it was recommended to flush the entire lubricating oil system of Port Main Engine and re-fill with fresh oil to address this abnormality.

Port Main Engine

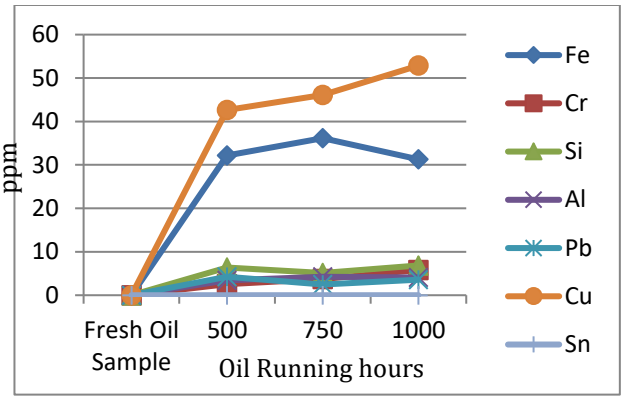

Figure 10. Variation of element concentrations in the lubricant oil as a function of engine operating hours in Port Main Engine

Stbd Main Engine

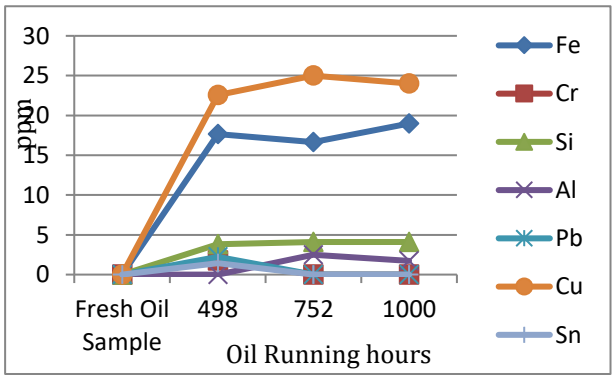

Figure 11. Variation of element concentrations in the lubricant oil as a function of engine operating hours in Stbd Main Engine

The general standard guidelines for this type of engine series elemental concentration are as follows;

Port Main Engine

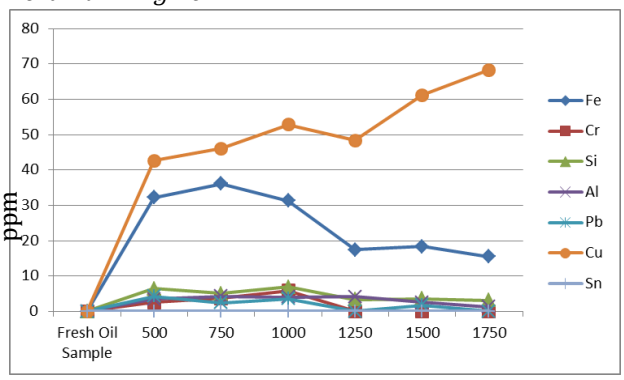

Figure 12. Variation of element concentrations in the lubricant oil as a function of engine operating hours in Port Main Engine

Comparing results with this particular series of engines, Port Main Engine values were beyond the

general referred guidelines as well as the previous trend pattern.

The wear rate of "Cu" element concentration was carried out by using the following formula;

$$Wear\ Rate = \frac{(ppm\ of\ wear\ metal)}{(Total\ Hours)} x \left(1 + \frac{(oil\ added)}{(sump\ capacity)}\right)$$

Therefore, it was found that the wear rate also increasing with the running hours. Hence, it was recommended the repair authority to carry out in depth investigation to find root causes for this specific metal wear down giving special attention to inspecting bearings, bushes, sleeves, bearing cages, coolant core tubes, valve guides, thrust washers, alloyed with Si-Ti.

The inspections were carried out by the repair authority and found heavy metal deterioration in Main bearings as shown below;

Figure 13. Metal wear down of No 09 bearing lower half

Table 2. Standard safety limits of wear element concentration of 16 cylinder V type reciprocating engine

Element	Maximum permissible limits
Fe	80
Cr	10
Si	15
Al	20
Pb	20
Cu	25
Sn	10
Ni	10

Figure 13. Metal wear down of No 01 bearing upper half

The second stage of oil analysis was carried out on completion breakdown repairs and a similar trend analysis pattern to Stbd Main Engine was observed. Therefore, these particular findings confirmed the metal wear down of bearings of a particular engine. The statistical data of the first stage and second stage are shown in Table 3.

Table 3. Statistical data of the first stage and second stage

	Stage 01						
Element	Oil R/H Fresh oil sample	500	750	1000	1250	1500	1750
Fe	< 1.000	32.178	36.153	31.257	17.446	18.344	15.51
Cr	< 1.000	2.54	3.74	5.82	< 1.000	< 1.000	< 1.000
Si	< 1.000	6.404	5.121	6.851	3.36	3.56	< 1.000
Al	< 1.000	3.455	4.255	4.056	2.529	2.529	1.305
Pb	< 1.000	4.254	2.457	3.587	1.7	1.7	< 1.000
Cu	< 1.000	**42.628**	**46.083**	**52.857**	**61.153**	**61.153**	**68.248**
Sn	< 1.000	< 1.000	< 1.000	< 1.000	< 1.000	< 1.000	< 1.000
	Stage 02						
Element	Oil R/H Fresh oil sample	50	250	500			
Fe	< 1.000	22.147	18.141	17.217			
Cr	< 1.000	1.78	< 1.000	< 1.000			
Si	< 1.000	4.584	3.5013.851				
Al	< 1.000	2.415	1.215	1.946			
Pb	< 1.000	4.414	3.417	3.457			
Cu	< 1.000	**50.248**	**30.013**	**25.204**			
Sn	< 1.000	< 1.000	< 1.000	< 1.000			

With these statistics, it was evident that the "Cu" element concentration increment is due to the bearing failure and the replacement of the particular bearing had normalised the elemental behaviour.

The SLN plan is to transfer the existing maintenance schedules to condition based predictive maintenance in which at present the oil will be drained on completion of OEM recommended intervals. This case was one of the key instances in which the findings had paved the path to prevent a catastrophic failure to an engine. These specific findings will also be utilized to systematically extend the Oil Draining Intervals (ODI) of machinery fitted on board the SLN fleet.

IV. CONCLUSION

Many of the findings of wear down analysis, had helped MTTU of SLN to reveal the information on machinery health. This instance had identified the developing malfunctions, damages to the machinery at the initial stage which had finally led to prevent catastrophic failures to the particular machinery. With the help of the findings, it will be beneficial to the relevant repair authorities of SLN to carry out a root cause analysis to identify the process environment, uneven mechanical loads such as stresses and strains or surface oil chemistry.

These findings will be correlated with the vibration analysis, thermography, ultrasound and non-destructive testing results as a productive approach to maximise the life of machinery. When conducting these techniques independently, only a portion of machinery fault is identified, therefore, integrating all these concepts will be more beneficial to predict the failure and also to extend the life cycle of the machinery.

ACKNOWLEDGMENT

Providing the facility of conducting wear down analysis using the ICP-OES in the Sri Lanka Navy is acknowledged. The technical assistance and the guidance received from the Department of Mechanical Engineering, University of Moratuwa and other key industrial laboratories, are highly acknowledged.

REFERENCES

Diane Beauchemin (2000), Sample Introduction System in ICPMS and ICP-OES, 1st Edition

Augustus Herman Gill (2008), *A Short Hand-Book Of Oil Analysis*

ASTM D 5185 - Standard Test Method for Determination of Additive Elements, Wear Metal, and Contaminants in used lubrication oils and determination of selected Elements in base oils by Inductively Coupled Plasma Optical Emission Spectrometry *(ICP-OES).*

AUTHOR BIOGRAPHY

Commander (E) Milinda Dasanayaka is presently serving as the Officer In Charge of Machinery Testing and Trials Unit of the Sri Lanka Navy. He earned his BTech in Mechanical Engineering from Sri Jawaharlal Nehru University, India and MPhil in Mechanical Engineering from the University of Moratuwa. He is a certified RCM Analyst from Mobius Institute, Australia.

Lieutenant Commander (E) Eric Fernando is presently serving as the Marine Engineer (Machinery Testing and Trials Unit) of the Sri Lanka Navy. He earned his BTech in Mechanical Engineering from Sri Jawaharlal Nehru University, India. He is a certified RCM Analyst from Mobius Institute, Australia.

Cost Effective Method to Analyse Lubrication Oil

TNA Rathnayake

Directorate of Naval Design, Sri Lanka Navy, Sri Lanka

nuwan1705@yahoo.co.uk

Abstract— The lubricating oil analysis is the most common method to identify the condition of any machinery. There are various ways to analyse lubricating oil based on an individual examination of lubricant properties such as Viscosity, Total Base Number (TBN), Total Acidic Number (TAN), Water Content, Impurities (element analysis) etc. However, the equipment required to conduct these analyses are costly, need specific environmental conditions, and generally time consuming. The time consumption of this whole process hampers the maintenance program efficiency. Hence, an onsite, cost-effective, and faster results-giving method to analyse lubricating oil would be a valuable asset. A comprehensive literature survey was carried out to understand the current trends in lubricating oil analysis. Accordingly, the analysis techniques could be categorized as Physical, Chemical, Electro-magnetic, and Optical. The proposed design is based on an optical technique that deals with the Refractive Index (RI) since it is an indicator of the physical as well as the chemical property characteristic of a substance. The critical angle of a material is directly related to RI. Monitoring the critical angle changes leads to an understanding of the quality of the lube-oil. The performance of a proposed lube-oil analyser was assessed using Shell Gardenia 40 (lubricating oil used in high-speed marine engines of Fast Attack Craft) lubricant at different operating hours. The results obtained from the proposed device were compared with the tests carried out according to the American Society for Testing and Materials (ASTM) standards and through a viscometer. Both tests confirm the effectiveness of the proposed device.

Keywords*: *lubricating oil analysis, refractive index, cost-effective lubricating oil analyzer

I. INTRODUCTION

The relative movement of rubbing parts creates resistance. This resistance is called friction between the rubbing surfaces, and it causes a lot of wear and tear and could also convert a part of the energy of motion into heat. Lubricants are used to reduce this resistance and the other adverse effects caused by it.

At present, Sri Lanka Navy practices Planned Preventive Maintenance (PPM) or scheduled maintenance procedures to maintain machinery condition. The manufacturer of the machine will indicate a schedule (specific time period) to change the lubrication oil without considering the usability of the used oil.

In Condition Based Preventive Maintenance (CBPM) method it is used similar to blood samples are used in diagnostics, lubrication oil analysis of a machine can be used to detect or predict the machine failures.

The contemporary methodology of analysis of the lubrication oil using laboratory-based methods takes considerable time. The current practice is based on specific property analysis of lubricating oil such as viscosity, impurities available (carbon content, dilution, water content, and material particles) etc. These lab-based investigation methods require special conditions such as controlled environments (temperatures, humidity, etc.) and proper sampling methods. Hence, the requirement of a cost-effective lubrication oil analysis method that will not require controlled environmental conditions can enhance the cost-effectiveness of maintenance. This in turn facilitate decision making with lesser delays.

It is essential to replace the lubrication oil with an early notice during industrial applications because an unexpected failure of any machinery will affect the process of the product directly and also the particular machine requires to be stopped to minimize further damages or wear.

The performance parameters are under the variations of optical, electrical, chemical and physical properties which will affect the

characteristic changes of a particular lubrication oil towards its degradation. The performance parameters could be identified as viscosity, water content, Total Acid Number (TAN), Total Base Number (TBN), particle counting, flash point, spectrometric oil analysis, etc.

The objective of the study is to identify the functions of lubricants in a lubrication oil system including these main properties of a lubricant. Further to design and fabricate a cost-effective lubrication oil analyzer to check the condition of lubricating oil.

II. UNDERSTANDING THE LUBRICANTS

A. Main Functions of Lubricants

The main functions of lubricants during the rubbing between the surfaces are as follows;

i. It avoids direct metal to metal contact between the surfaces and reduces wear and tear (Lubricants will create an oil film within the surfaces).
ii. Heat is generated due to friction and it destructs the material. Lubrication oil reduces the expansion of metal due to generated heat.
iii. Acts as a coolant since it is a medium to heat transfer.
iv. It avoids rough conditions of the relative movement of surfaces (due to unevenness of the surfaces).
v. Minimizes the cost of maintenance since increases the life expectancy of the equipment.

B. Important Properties of Lubrication Oil

The most important properties that could be used to analyse the condition of the lubrication oil are as follows;

i. Viscosity and Viscosity Index (VI)
ii. Flash point and Fire point
iii. Cloud point and Pour point
iv. Oxidation stability
v. Aniline point
vi. Corrosion stability

III. METHODOLOGY

A. The Constraints of Available Lubrication Oil Analysis Methods

The available lubrication oil analyzing methods are based on the degradation of lubrication oil. These methods are based on identifying the changes in a single property of lubricating oil or calculating the amount of impurities added to lubrication oil. Hence, the lubricating oil analysis reports are providing only the quantitative values of changes related to the aforesaid lubricating oil properties or added impurities. The decision to change the oil or to analyze the condition of the machine is based on these analysis reports. The main disadvantages of this analyzing system are the high cost to analyze a single method of lubrication oil and also the time duration to obtain the reports. Also due to a large number of sampling carried out by the service providers, mishandling of provided sample, adding impurities to the sample, and misplacing of provided samples could result in inaccuracies of the reports.

The available lubricating oil analyzing methods, could be categorized into physical, electrical (magnetic), chemical, and optical techniques. After scrutinizing, it was decided to use an optical method to design a cost-effective lubrication oil analyzing device. The device is to be designed based on the Refractive Index (RI) which is a physical property with the characteristic of a pure compound.

B. The Working Principle of the Designed Lubricating Oil Analyzer

Any visible light changes its direction when it passes through a material with a higher Refractive Index (RI) to that with a lower Refractive Index. As the incident ray angle, Alfa (α) increases, the refractive angle, Beeta (β) will increase in accordance with Snell's Law, and when the refractive angle 'β' (where the incident ray angle 'α') reaches the critical angle (=90°), the total refraction will occur at the boundary between the prism and the lubricating oil sample. However, when the incident ray angle increased beyond 'α_c' (critical angle), the light cannot enter the medium (which is the oil sample) and reflects to the prism. The special feature of this action is the critical angle of the lubrication oil sample will vary with the Refractive Index (RI) of the particular sample. The RI of a lubrication oil sample will be based on the properties of it such as viscosity, suspended particle density, dilutions (liquid impurities), water content and chemical properties.

When we use a divergence beam of light towards the lubrication oil sample through the prism, a fraction of light rays will have an incident angle higher than the critical angle. A schematic diagram of the working principle of the designed lubrication oil analyzer is shown in Figure 1. Because of that, the internally reflected light could be obtained as an image to a separate plane. This image will have a brighter and darker region due to the partial internal reflection of light. When the critical angle changes with a refractive index of the lubrication oil sample, the brighter and darker region of the internally reflected image will change. Further, the appearance of the internally reflected image will vary as per the quality of the lubrication oil sample.

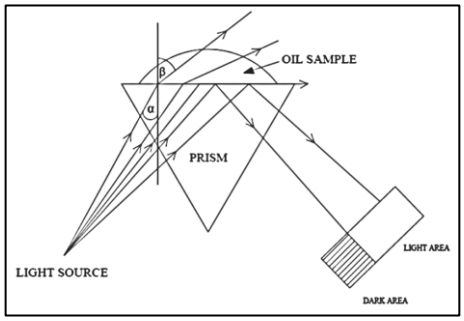

Figure 1. A schematic diagram of the working principle of the designed lubrication oil analyzer

The proposed design of lubrication oil analyzing equipment is based on the reflection theory. It has the capability of comparing the internally reflected image of the original lubrication oil (brand new oil or unused oil) and used lubrication oil. The internally reflected image that is going to be obtained by analyzing unused oil will be examined to understand the main features of the image.

The internally reflected image of the unused oil sample, the area of the brighter region will indicate the quality of the lubrication oil sample where it will depend upon the refractive index. It can be taken as a reference to check the used oil samples which have been taken from the engines. However, the used oil samples are going to be obtained as per pre-defined time frames to identify the variation in the internally reflected image until the Original Equipment Manufacturer (OEM) given lubrication oil changing intervals.

A separate comprehensive computer programme could be used to identify and calculate the variations of the brighter area of the image to analyze the original oil and the used oil. This programme could be used to analyze the condition of any given lubrication oil sample by understanding the internally reflected image comparing with the image of the original oil. However, the reference image is to be obtained by using fresh oil/ new oil samples of any kind of lubrication oil before starting the checking of the used oil samples.

C. Practical Application of the Equipment

During the testing of the designed cost-effective lubrication oil analyzer, the lubrication oil (Shell Gardenia 40) is used in MTU 12 V 396 TE 94 engines because these engines are high speed marine engines. For MTU 12V 396 TE 94 engines, the oil changing interval is 500 operating hours (where centrifugal filters are fitted) as indicated by the OEM. Engine Oil Requirements are selected as per the Original Equipment Manufacturer (OEM). Viscosity class selection is determined in accordance with the engine oil temperature at the time of starting.

IV. FABRICATION OF LUB OIL ANALYZER

A. Components used to Design the Oil Analyzer

i. Prism
ii. Wiring system
iii. Converging lens
iv. Camera
v. Computer
vi. Computer programme

B. Construction Process of the Analyzer

The sample of the used lubrication oil should have the capability to remain within the position even in rough environmental conditions. Therefore, the prism is positioned on the top most part of the equipment (horizontally). Further, there is a circular groove on the upper most plate to pour the lubrication oil samples and the prism is fixed to the cover with a rubber packing to stop leaking of lubrication oil.

A light beam is produced with the help of a Light Emitting Diode (LED) bulb and the direction of the light beam was designed to be adjustable. In addition, a converging lens is fixed to the end of the

screw to focus the light beam towards the prism and it will enhance the intensity of the light beam by improving the quality of the internally reflected image.

The electrical circuit is powered by 230 V electric power supply through a power pack and it consists of a variable resister and a switch. Further, the camera is fixed in a side wall of the lubrication oil analyzer, where it can be adjusted to get a clearer image to the computer. The lubrication oil analyzer functions with an optical method and it is mandatory to remove the effect of natural light and other light sources to get an effective outcome of the results. Hence, the equipment is fabricated in a box-shaped arrangement, covering all sides as shown in Figure 2.

Figure 2. Box-shaped arrangement of the designed lubrication oil analyzer

V. DATA PRESENTATION AND ANALYSIS

The fabricated lubrication oil analyzer is tested using the lubrication oil samples obtained through the MTU 12V 396 TE 94 marine engines. Shell Gardenia 40 mono grade lubrication oil is used for these engines. The samples are collected from the relevant engines at an interval of 100 hrs (from 0 hrs- 500 hrs) for 3 different oil samples per each time interval. The internally reflected image obtained without pouring the test samples through the lubrication oil analyzer is a single elliptic shaped image since the camera is not in-line with the image. The obtained image is shown in Figure 3.

Figure 3: Internally reflected image without pouring oil samples to the designed analyzer

The design lubrication oil analyzer is highly depending upon the original oil condition (fresh oil sample of the particular lubrication oil). Hence, 03 new lubrication oil samples of Shell Gardenia 40 were analyzed through the designed analyzer and captured the images of the oil samples (03 Nos samples) are shown in Figure 4.

Figure 4. The captured images of the new lubrication oil samples (Shell Gardenia 40)

The second stage is to obtain the internally reflected image for the first used oil sample, after 100 operating hours. A significant difference can be observed between the images for the new lubrication oil sample and the 100 hours operated lubrication oil sample. The images after 100 operating hours are shown in Figure 5.

Figure 5. The captured images for the 100 hours operated used lubrication oil samples (Shell Gardenia 40)

The comparison of the images obtained through the designed lubrication oil analyzer for the new Shell Gardenia 40 oil sample and 100 operating hours used oil is shown in Figure 6. A considerable deviation in the area of the bright region between the two images can be identified.

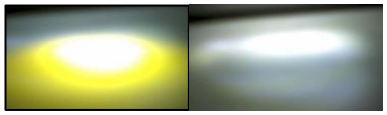

Figure 6. Comparison of the received images of new oil and 100 hours operated used oil sample

The third stage is to check the used oil after 200 operating hours. However, a vast difference between the images of 100 hours operated used oil and the 200 hours operated used oil may not be observed during the comparison. The images of the three samples (200 operating hours) are shown in Figure 7.

Figure 7. The captured images for the 200 hours operated used lubrication oil samples (Shell Gardenia 40)

Similarly, the other samples at 300 hrs, 400 hrs, and 500 hrs were compared with the obtained images using the fabricated lubrication oil analyzer.

A. Comparison of the Results

The results obtained for the 100 hrs used oil to 500 hrs used oil are similar to each other. It indicates the condition of used oil up to 500 hrs operating hours is suitable to operate for a longer period. Thus, even though the OEM recommended Oil Draining Interval (ODI) is after 500 operating hours, depending on the condition of the lubrication oil operating hours can be extended. However, to cross examine whether the obtained readings through the designed lubrication oil analyzer is accurate, the same lubrication oil samples are analyzed with the help of under mentioned lubrication oil analyzing methods.

1) *Viscosities of the samples through Viscosity Comparator*

2) *ASTM Standards*

i. ASTM D 5185 – 05 (Standard test method for Determination of Additive Elements, Wear Metals, and Contaminants)
ii. ASTM D 445 – 06 (Standards test method for Kinematic Viscosity)
iii. ASTM D 4739 – 06a (Standard test method for Base Number)
iv. ASTM D 7899 – 13 (Standard test method for Measuring the Merit of Dispersancy)
v. ASTM D 893 – 05a (Standard test method for Insolubles in Used Lubricating Oils)
vi. ASTM D 92 – 05a (Standard test method for Flash and Fire Points)
vii. ASTM D 95 – 05 (Standard test method for Water in Petroleum Products)

As per the viscosity readings of each used lubrication oil sample, the viscosity is within acceptable limits for the used lubrication oil samples up to 500 operating hours. To finalize the performance evaluation of the lubrication oil analyzer, ASTM standards checking were carried out for the used oil samples of 50 hrs, 250 hrs and 500 hrs.

Table 1. Element Concentration after 50 operating hours

Elements	Method	Maximum Permissible Limit	Fresh Oil Sample	Port Main Engine	Stbd Main Engine
Fe	ASTM 5185	80	< 1.000	19.344	30.921
Cr	ASTM 5185	10	< 1.000	< 1.000	1.107
Si	ASTM 5185	15	< 1.000	1.498	2.955
Al	ASTM 5185	20	< 1.000	< 1.000	< 1.000
Pb	ASTM 5185	20	< 1.000	3.320	4.026
Cu	ASTM 5185	25	< 1.000	13.690	17.313
Sn	ASTM 5185	10	< 1.000	< 1.000	1.196
Ni	ASTM 5185	10	< 1.000	< 1.000	< 1.000

Table 2. Analysis for other ASTM Standards after 50 operating hours

Description	Method	Fresh Oil	Port M/E	Stbd M/E
Viscosity @ 40^0 (cSt)	ASTM D 445	139.00	133.25	132.73
Viscosity @ 100^0 (cSt)		14.40	14.00	14.14
Viscosity Index	ASTM D 2270	103	101.94	103.68
Total Base No. mg KOH/g	ASTM D 4739	10.48*	6.78	6.43
Water Content	ASTM D 95	<0.2	<0.1	<0.1

Table 3. Element Concentration after 250 operating hours

Element	Method	Maximum Permissible Limit	Fresh Oil Sample	Port Main Engine	Stbd Main Engine
Fe	ASTM 5185	80	< 1.000	10.422	9.776
Cr	ASTM 5185	10	< 1.000	< 1.000	< 1.00
Si	ASTM 5185	15	< 1.000	1.738	1.532
Al	ASTM 5185	20	< 1.000	< 1.000	< 1.00
Pb	ASTM 5185	20	< 1.000	< 1.000	< 1.00
Cu	ASTM 5185	25	< 1.000	5.482	5.083
Sn	ASTM 5185	10	< 1.000	< 1.000	< 1.00

Ni	ASTM 5185	10	< 1.000	< 1.000	< 1.00

Table 4. Analysis for other ASTM Standards after 250 operating hours

Description	Method	Fresh Oil	Port M/E	Stbd M/E
Viscosity @ 40⁰ (cSt)	ASTM D 445	139.00	133.25	132.73
Viscosity @ 100⁰ (cSt)		14.40	14.00	14.14
Viscosity Index	ASTM D 2270	103	101.94	103.68
Total Base No.	ASTM D 4739	10.48*	6.78	6.43
Water Content	ASTM D 95	<0.2	<0.1	<0.1

Table 5. Element Concentration after 500 operating hours

Element	Method	Maximum Permissible Limit	Fresh Oil Sample	Port Main Engine	Stbd Main Engine
Fe	ASTM 5185	80	< 1.000	10.422	9.776
Cr	ASTM 5185	10	< 1.000	< 1.000	< 1.00
Si	ASTM 5185	15	< 1.000	1.738	1.532
Al	ASTM 5185	20	< 1.000	< 1.000	< 1.00
Pb	ASTM 5185	20	< 1.000	< 1.000	< 1.00
Cu	ASTM 5185	25	< 1.000	5.482	5.083
Sn	ASTM 5185	10	< 1.000	< 1.000	< 1.00
Ni	ASTM 5185	10	< 1.000	< 1.000	< 1.00

Table 6. Analysis for other ASTM Standards after 500 operating hours

Description	Method	Fresh Oil	Port M/E	Stbd M/E
Viscosity @ 40⁰ (cSt)	ASTM D 445	139.00	126.96	120.96
Viscosity @ 100⁰ (cSt)		14.40	13.36	13.24
Viscosity Index	ASTM D 2270	103	101.94	103.68
Total Base No. mg KOH/g	ASTM D 4739	10.48*	6.78	6.43
Water Content	ASTM D 95	<0.2	<0.1	<0.1

After the comparison of the results obtained through the viscosity comparator and the ASTM standards, it is observed that the condition of lubrication oil samples is good. Moreover, it is observed that the results obtained through the lubrication oil analyzer is also accurate since it shows that the lubrication oil samples are in usable condition.

The results through the designed lubrication oil analyzer could be finalized with a help of a computer programme by considering the features of the obtained internally reflected images for a lubrication oil. A computer programme is written to identify the area of the brighter region of the internally reflected image of each lubrication oil sample. The computer program will identify the number of pixels within the area of the brighter region. The interface of the computer program is shown in Figure 8.

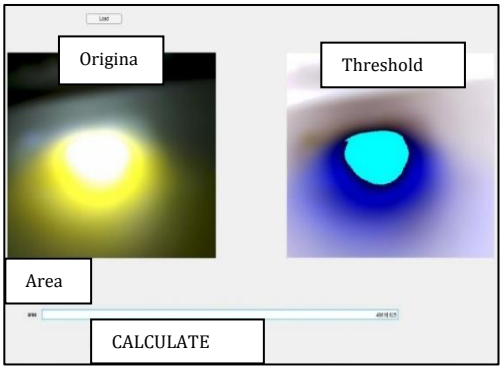

Figure 8. Computer program interface to calculate the area of brighter region for an oil sample.

The variation of the area (brighter area) can be identified for the fresh oil sample and all other used oil samples to visualize the changes of the image area. As per the images obtained for the Shell gardenia 40 lubrication oil samples, the calculated details of areas are indicated in Table 7.

Table 7. Area of the brighter part of the images obtained for Shell gardenia 40 oil samples.

Operated hours	New oil (0 hrs)	100 hrs	200 hrs	300 hrs	400 hrs	500 hrs
Area of brighter region	116337	73369	71310	72258	71062	75374

The used lubrication oil samples which are obtained from the MTU 12V 396 TE 94 marine engines are within the acceptable limits even after 500 operating hours in accordance with the

visualized processes mentioned below. The results of the designed lubrication oil analyzer also could be justified with the following reports.

i. Viscosity reading of the viscosity comparator (for sample intervals of 100, 200, 300, 400, and 500 hours).
ii. ASTM standards checking for lubrication oil samples (for sample intervals of 50, 250, and 500 operating hours).

However, the readings obtained through the designed lubrication oil analyzer could be further justified by understanding the correlation between the usable lubrication oil and the diluted oil (mixed with diesel). A usable lubrication oil sample of Shell Gardenia 40 is diluted forcibly with 25%, 50%, and 100% diesel quantities separately. After these lubrication oil samples are analyzed through the designed lubrication oil analyzer.

Table 8. Areas of the brighter part of the images obtained for Shell gardenia 40 diluted lubrication oil samples

Dilution of lubrication oil (%)	Used oil (>1)	25%	50%	100%
Area of brighter region (No of pixels) of the image	23778	28525	34170	39686

It is obvious that the brighter area of the internally reflected image is increasing (compared to good quality used lubrication oil) with the percentage increment of mixed diesel.

VI. CONCLUSION

The results have been obtained through the designed lubrication oil analyzer are cross examined with the results obtained by using viscosity comparator and also with the ASTM standards lubrication oil analyzing methods. During the comparison, it is understood that the readings which are obtained through the designed cost-effective lubrication oil analyzer are accurate.

Further, the results obtained through the lubrication oil analyzer for the correlation between the dilution in a particular lubrication oil (mixing with diesel) samples and usable used oil samples are also confirming the accuracy of the analyzer.

VII. RECOMMENDATION

The requirement of a cost effective lubrication oil analyzing technique is to identify the condition of lubrication oil which will not require any special considerations on the environmental conditions (temperature and other atmospheric conditions) and also to fulfil the feasibility to conduct the lubrication oil analysis at the location where the machinery is installed will enhance the effectiveness and the efficiency of the production process which is the particular machinery is required. The fabricated equipment could be used to fulfil the above requirement since the output results are accurate when compared to prevailing lubrication oil testing methods.

Further, the ODI of a particular machine can be extended beyond the OEM provided oil changing interval after analyzing the results obtained through the designed cost-effective lubrication oil analyzer. However, it is recommended to further improve the system by automating the analysis entirely to assess the condition of lubrication oil where it will not require human involvement and monitor the degradation trend of lubrication oil cost-effectively.

REFERENCES

Feldman, A., 1983. Refraction through a prism. *American Journal of Physics*, *51*(10), pp.929-931.

Gunshore, P.M. and Ishler, L.W., General Electric Co, 2001. *Method and apparatus to extend the operating interval between oil changes for an internal combustion engine*. U.S. Patent 6,283,082.

Nousiainen, T., Kahnert, M. and Veihelmann, B., 2006. Light scattering modeling of small feldspar aerosol particles using polyhedral prisms and spheroids. *Journal of Quantitative Spectroscopy and Radiative Transfer*, *101*(3), pp.471-487

Winge, R.K., Peterson, V.J. and Fassel, V.A., 1979. Inductively coupled plasma-atomic emission spectroscopy: prominent lines. *Applied Spectroscopy*, *33*(3), pp.206-219.

Zhang, Y., Wei, Y., Chen, C., Huang, W., Wang, X. and Xu, H., 2016. Self-mixing interferometer based on frequency

analysis method for accurate refractive index measurement. *IEEE Photonics Journal*, *8*(2), pp.1-6.

ACKNOWLEDGMENT

The author would like to acknowledge the guidance and assistance provided by Dr. D.A.S. Amarasinghe (Senior Lecturer, Department of Materials & Engineering, University of Moratuwa) for the successful completion of this research project.

AUTHOR BIOGRAPHY

Commander, Nuwan Aravinda Rathnayake, Marine Engineer, of Sri Lanka Navy and currently holding appointment as Manager (Naval Boat Building Yard) and Manager Naval Design (Naval Architecture) of Directorate of Naval Design. Graduated with BSc Eng (Hons) Marine Engineering from Kotelawala Defence University. Possess MSc. in Material Science from the University of Moratuwa.

ID 159

Optimization of Industrial Manipulation Tasks Using Parallel Manipulators

IM Akarawita#, BGMS Senadheera, HSG Samarasinghe and WSP Fernando

Department of Mechanical Engineering, Faculty of Engineering, General Sir John Kotelawala Defence University, Sri Lanka.

#iakarawita@gmail.com

Abstract— Small-scale product handling industries are at the cusp of increasing their efficiency and effectiveness, where optimization is a considerable factor. Though regular pick and place tasks are nonvalue added steps, it can replace expensive manual labour by increasing efficiency. Hence, this paper discusses the optimization of regular pick and place tasks using parallel manipulators. Out of the evaluations, on alternative manipulators, the 3-link parallel manipulator was of the focus. A simulation and a real-time operation were conducted for the comparison of the two designs in relation to robot workspace. The robot kinematics were derived to define the robot workspace, and for the dimensions of the mechanical components which were equally designed and tested using SOLIDWORKS. Fabricating was done using lathe machining and 3D-printing. The servo and visual systems were decided accordingly for the pick and place application. Control and functionality with the input visual system and kinematics model were mapped and generated in MATLAB, and then transferred to Arduino which drives the motors of the manipulator. This makes the robot end effector to actuate and perform the picking and placing using the solenoid gripper. An accurate result in object detection, mapping, picking, and placing by the delta robot is thereby achieved. The presented model is feasible to be used in the industry which can accommodate regular pick and place tasks in a facility.

Keywords: *pick and place, parallel manipulators, delta robot, kinematics, workspace, visual servo system, MATLAB*

I. INTRODUCTION

Requirement for automation is in the verge of being an industrial necessity due to various challenges faced by modern day industries. Labour shortage, complex customer orders, cost of labour, idle times, inaccuracy, and compliance standards are few instances which promotes the need for automating various processes in a regular production flow. Automating the task of pick and place products from assembly lines shares common interest in multiple industries mainly due to it being a nonvalue added task, and with no direct effect to the quality standards of the production.

The current automation solutions of utilizing robotic manipulators to achieve this task consist of major draw backs. Recent advancement of parallel robots has shown greater potential towards finding solutions to this problem. Because, parallel manipulators are of higher precision, stiffness, and dynamic capacity due to closed links, lower maintenance cost, efficient in attaining higher accelerations due to lower inertia and lower space taken-up with comparison to serial robots for pick and place applications. Some of these have also been discussed from comparisons by Deshmukh and Patil (2015) in the review paper. Furthermore, the initial and implementation cost for a series robot manipulator is mostly not viable for industries with small scale product categories mainly due to afore mentioned factors.

Above challenges were the main motivation for this project on optimizing general pick and place tasks commonly available in the small-scale product category industry. Pick and place objects on a moving conveyor, which is a commonly seen application has been selected. The focus was more on the object identification, recognition, picking and placing accurately with a considerable speed of operation. The proposed method also considered optimization on the minimum cost paths.

This paper describes the designing, fabricating and testing of a visual servo based parallel manipulator, and these defined areas concurrently being the main objectives of the project. The application of the parallel robot, was to focus on a generaized

pick and place task found commonly in industries, along with a design comparison in order to achieve a minimum manipulator workspace.

II. LITERATURE REVIEW

Azmoun et al. (2018) have proposed a similar design for a 4-DOF delta robot in SimMechanics environment of MATLAB software, by studying the performances of Sliding Mode Control (SMC) mechanism and the PID controlling based on the Inverse Kinematic Problems (IKP).

Chen et al. (2018) have presented a simulation study of optimizing for delta robots. That is for the improvement of pick and place route based on lame curves to smooth the right angles of transitions. Thereby they have established the overall trajectory in the cartesian plane with good performance in comparison for the virtual prototype in ADAMS and MATLAB. Abduraimov et al. (2017) have proposed an algorithm for the forward kinematics method with one root for delta robots. Where the conventional method is to solve forward kinematics by 3 sphere method and finding the intersection point. Out of which one is selected. But in their calculation algorithm, the solution gives only one. They have verified the method, by doing an analytical substantiation and a numerical experiment with the results obtained. A thesis by Rosquist (2013) describes on the modelling of the kinematics and forward dynamics for the IRB340 FlexPicker parallel robot and the implementation control by software and hardware from B&R Automation. This was referred for the system, mathematical model in this paper. Peng et al. (2019) have studied 35 combinations of the same topology for a linear delta robot, on which they have obtained by changing the dimensional parameters. The kinematics model for all the combinations have been analysed, thereby revealing the coupling relationship between the output parameters of 2 parallel mechanisms. The article by Clavel (1998) have proposed 2 kinematics calibration models an shows that the accuracy of the parallel robot can be improved by means of calibration. The mechanical development, kinematic analysis along with simulation for the training of the delta robot Caertec rk 2010 have been proposed by Bulej et al. (2012) using CATIA software. A vision servo-based delta robot has been developed by Lin et al. (2016) to pick and place objects on a moving conveyor with a vacuum suction clamping method, where they have used Canny and Sobel edge detection methods for object recognition in a C++ based program. By the proposed algorithm, only when the object is fully present in the screen, the coordinates of the object is calculated and sent to the delta robot via TCP/IP protocol.

III. EXPERIMENTAL DESIGNS

Through comparison of serial and parallel robots, another comparison was done to select 3-link parallel manipulator among 2-link and 4-link manipulators. The 3-link delta robot satisfied the minimum requirements to complete a regular pick and place task with 3-DOF for X,Y and Z translation. Based on this, a further study was done to improve the optimization and workspace of delta robot.

Figure 1. Design 1

Figure 2. Design 2

Hence, conceptual designs were designed with a new configuration by altering the motor orientation relative to the base plate. Motors were placed parallel to the tangent of the circumference of the base plate as shown in Figure 1. The other design is where the motor is mounted so that the arm is in perpendicular to the circumference of the circle, which is shown in Figure 2. In both the designs, the motor shafts are placed at 120° apart. This is considered as the standard configuration of the delta robot. Both configurations were fabricated to implement real-time kinematics. Also, manipulator workspace simulation was done and the unique advantages and disadvantages of each design is presented in Section V.

IV. SYSTEM OVERVIEW

The specific application selected was, pick and place screws through a vision-based system which additionally requires an operation of sorting based on the colour or size of the screw or both. The presented system uses a direct operating solenoid as the gripping mechanism. Sectional headings A, B, C, D and E shows the phases followed in this working procedure.

A. Mathematical Modelling

In pick and placing, the delta robot changes its 3 motor parameters to move the end effector to the desired position where either the angles of the motors or the coordinates of the end position are

to be decided. In inverse kinematics - if the desired position is known, the motor angles can be generated. In forward kinematics - if joint angles are known, the end effector position can be generated. One general observation is: for serial chains, the forward kinematics is generally straightforward while inverse kinematics may be complex and for parallel mechanisms, it is vice versa.

The calculations to determine the manipulator kinematics and motor torques were done based on the design criteria. A thorough calculation on forward kinematics inverse kinematics, and dynamics regarding parallel robots and series robots were studied and compared. The forward and inverse kinematic model given by Tsai et al. (2016) was referred for building up the inverse kinematics model. The kinematics and dimensions of the design were simultaneously taken into consideration for the simulation and the model, in determining the most practical parameters.

Robot-arms and base-plate-revolute-joints relative to the fixed base plate, revolute joints relative to the end effector and the end effector location relative to base plate {x,y,z} were taken to derive the vector loop closure equation for the delta robot. Geometrically, these legs are considered as the intersection of 3 spheres of radii of the length of links and arms of the robot.
Eventually, the 3 contriant equations were obtained deriving the kinematic equations for the 3 legs of the delta robot. Mentioned below is the generalized equation used for the independent scalar inverse position kinematics.

$$A_i\cos\theta_i + B_i\sin\theta_i + C_i = 0 \qquad \text{where } i=1,2,3$$

This equation is further solved by taking A_i, B_i, and C_i as of the results obtained from loop closure equation which also involves dimensions. Thus, deriving the arc tan angles for the 3 individual motor parameters. The singulairties were avoided at the final stage by eliminating the extreme and impossible values.

B. Design Specification and Simulation

Evaluation of alternative serial and parallel robots were done and conceptual designs were brought up prior to finalizing on design specifications. By Design 1 and 2, a calculational procedure was followed to arrive at the final machine designs. The calculations and the material analysis were done to obtain the final design parameters and verified if the design system can withstand all loads and deformations acting on the design parts. The material stress analysis, bending moment analysis and twist analysis for components were done prior to selecting a material and with the availability of materials, aluminium was selected as the most suitable material for almost all components. The analysis done for the robot arm and the robot base plate is shown in Figure 3 and Figure 4. With the obtained designed values, software based 3D modelling was done. The components were drawn partwise and assembled to form the required design, which gave a visual representation of the system designed. A motion study was performed to depict the complete motion of all the components of the system.

After finalizing the structure of the base plate and the type of rod end ball bearings, the length of the robot arms and links were decided according to the required workspace of the robot. The required workspace of the robot was decided upon the requirement of our application. Accordingly, it was decided to come up with the following workspace of the robot in the 3 axes to suite the requirement: X: -135mm to 135mm, Y: -135mm to 135mm and Z: 600mm to 300mm. Using the kinematics models with the above values, the length of the arm and link (forearm) was derived: Length of the arm = 200mm and Length of the link (forearm) = 450 mm. The intermediate shaft used to join the arms with the links was designed to be of 6mm diameter to suite the bearing shell and a length of 70mm. The base plate was decided according to the design proposed in the preliminary design and its diameter was chosen in a way that it can comfortably accommodate the three motors chosen. Finally, it was decided to design the base plate with a diameter of 300mm and 6mm thickness. 3 Motor brackets to hold the motors were also designed. A structure was designed to hold the whole robot vertically.

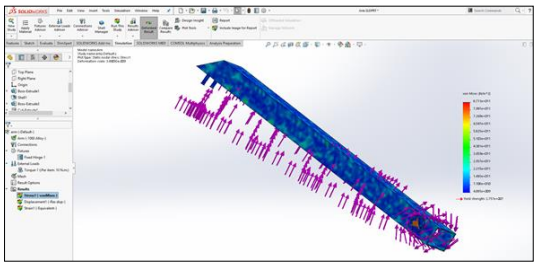

Figure 3. Stress and displacement analysis of magnitude 25N twisting moment on the robot arm

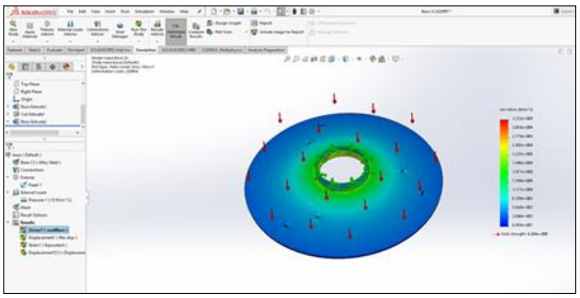

Figure 4. Stress and displacement analysis of magnitude 30N axial force on the robot base plate

C. Fabrication

After finalizing the design parameters and dimensions, the fabrication of the project was initiated part by part. The robot base plate, 3 robot-arms of 200x6x4mm (lxbxh), 6 robot-links (forearm) of 6mm diameter, motor brackets of 3mm thickness and 6 intermediate rods of 10mm diameter and 70mm length were fabricated in aluminium. The three arms were drilled with holes of 6mm diameter for the intermediate shaft to pass through. The other end of the arm was drilled with 5 holes with a diameter of 3mm to hold the motor coupling. Threads were made in robot-links (forearms) in both ends to a suitable length to attach the rod end ball bearings. For the base plate, set of 4 holes each were drilled 120 degrees apart at the edge of the plate for smooth, fast and error free operation of the robot. Finally, the end effector was 3D printed using PLA polymer which is light weighted and even has a high strength. The appropriate electromagnetic gripper for the end effector was selected for the application.

The mounting structure is used to hold the manipulator in place for its functioning. As per the requirement, it needed to be portable and withstand movements of the robot. It was designed and fabricated using 1.5x1.5inch aluminium box bars. This cuboid structure comprised the dimensions of 65x65x70cm (lxbxh) and had extra two crossed bars at the top to mount the robot. Finally, the fabricated components were assembled with the camera module mounted to the mounting structure and the solenoid gripper was attached to the middle of the end effector for the completion of delta robot.

D. Image Processing

Logitech C310 web camera was selected as per the required specifications of minimum of 60° viewing angle, coloured, a reasonable resolution and with a USB connection. The camera input is directly taken to model for image processing. Initially, surf feature was used to detect the object. However, the points of the image the function acquired was not strong enough in identifying the same object among other objects and mixed up the relative points. Hence, the colour of the object was taken as the next approach with the use of colour thresholding app in available with the software. Lab colour scheme was used for this, and it was successful in identifying the object based on its specific colour.

To move the end effector, the system requires the location of the object. The code was written to locate the centre of mass based on the area of the image with the given colour. The web camera connected to the system sends a 160 x 120-pixel frame from the video output to the mathematical model with the script file for detecting the object and for locating that object. The model calls another function for processing the above-mentioned task and the output video stream is given from another function model. Locating this object was done through the blob analysis technique with the computer vision systems toolbox, by creating a persistent variable.

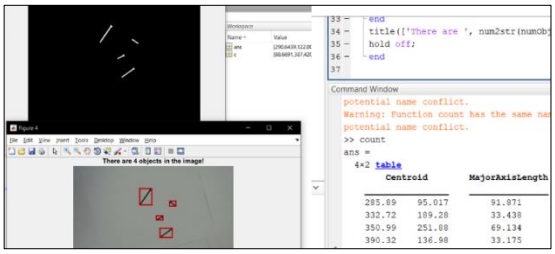

Figure 5. Image processing object detection

For the application, to detect screws of varying lengths, morphological operations were used. The RGB image was first converted to binary. This image was then subjected to morphological erosion and dilation through the construction of a structuring element. The number of screws laid were correctly detected. Finally, the centre points of the screws and the length of each of the screws were obtained accurately because of this procedure. The programmed Simulink model shows the exact x and y location of the centre of the object in pixels. The pixel coordinates were then mapped to the real x and y coordinates of the plane. The GUI shows the centroid of the object in pixels as well as the converted value in meters. Depicted in Figure 6. These coordinates were then passed on to the kinematics model.

E. Control and Functionality

Position based and Model based control methods are 2 available control strategies for robotic manipulations. In position-based control, each joint is separately considered in motor controlling whereas in model-based control the complete system dynamics are considered. Therefore, the model-based controller yields higher positional accuracy without the use of additional sensors. By considering the computational capacity of this process, the following physical components were required: Vision Sensor, PC, Microcontroller, Motor Driver and different softwares for the modelling and simulation. Initially, ROS (Robot Operating Software) was taken too for the implementation. The image processing and kinematics have been done in Simulink. The camera is taken as an input to the modeul and the generated motor angles are passed on to the controller where the motors are connected via motor drivers.

The weights were calculated via simulation by giving the proposed material. The simulation was done to examine the motion study of the robot, with weights and gravitational force. This motion study was done for the modelling; the motor torques were calculated. Since servo motors are more precise and accurate compared to stepper motors a DC servo motor of 20kg/cm was selected as the three motors for the delta robot.

F. Testing and Optimizing

For testing the system, a raspberry pi with ROS as an interface was selected as the controller for its better performance. However, as this selected controller lacked both computational capacity and multi-sequential PWM signal generation for the 3 motors in the delta robot, an Arduino controller was used. Which is a more cost effective and a simpler version for the system.

Ensuring the reachable area of the robot, camera is mounted and pointed out to the area where the screws are located. The program written in Simulink, executes image processing and kinematics model to generate the coordinates. This data is then sent to the controller to actuate the motors thereby achieving the picking task by the delta robot. Image processing and predefined locations determines the placement of the object by the delta robot. The customized GUI created, allows some basic operations for the user and to run the algorithm for sorting operation making it more user-friendly.

V. RESULTS

Workspace of a parallel robot is less compared to a serial type of robot. When the system is running, unlike in serial robots, the positional error gets averaged without accumulating. Parallel robots can achieve higher accelerations and is the ideal system for pick and placing tasks when a quicker response is required and also when a limited workspace is available.

Table 1. Results obtained from the system

Placement of screws underneath the delta robot (using 640x480 pixels video stream)	**Location in pixels (x, y)**	**Location in mm (x, y, z)**	**Computed motor angles**		
			θ1	**θ2**	**θ3**
	(282.6, 125.4)	(185.5, 81.5, -550)	60.9°	23.5°	64.7°
	(314.5, 119.3)	(206.4, 77.6, -550)	64.0°	23.9°	70.0°

Design 1 and Design 2 were compared in real time analysis and mainly using workspace simulation. This was due to the complexity in creating the kinematics code for the Design 1. Both designs showed similar workspaces. Design 1 has a better advantage over design 2 when considering the robot arm workspace, which is the ideal solution for a system that has limited area for functioning. Thereby, more robots can be placed inline within the production system achieving more tasks within a limited space, which will cut out lengthy conveyors and the time taken for a process to finish the entire task. But when the robot end effector workspace is considered, the design 2 is more flexible since that orientation gives the minimum strain on bearings.

The quantity, lengths, colours and coordinates of the screws and mapping were accurately done by using the created image processing code. Thereby, generating the motor angles via the kinematics model. The results are tabulated in Table 1.

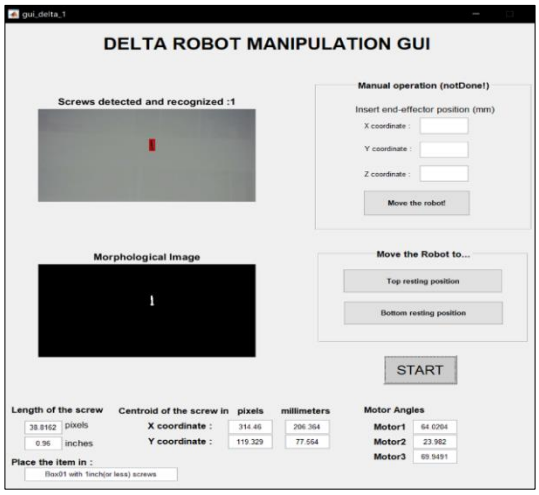

Figure 6. GUI

The fabrication and testing were done as of the method discussed in this paper. This produced accurate results in object detection, mapping, pick and placing by the robot as of the sequence of operation mentioned in Figure 7.

VI. DISCUSSION

The intermediate shafts are passed through the shell of the rod end ball bearings freely. Therefore, once the robot is in operation, the length of all the shafts will not be equal unless fixed. The intermediate shafts started to fall off the bearings and due to the shaft being passed into the bearings freely. Hence, intermediate shafts of 10mm diameter were taken and were threaded at the ends to a lesser diameter. By this, it was able to pass through the bearings freely and then they were tightened with a nut to achieve equal length.

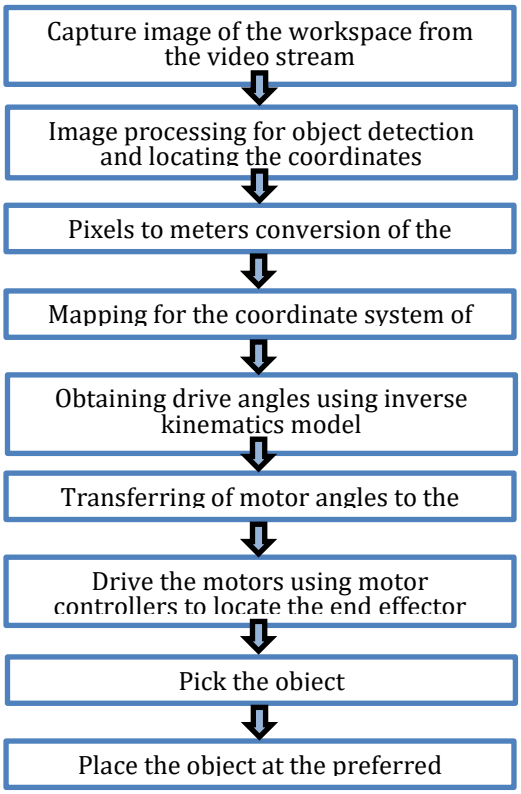

Figure 7. Control Flow

The initial decision was to undergo the manufacturing of links using carbon fibre due to its light weight and strength. Due to its fair of constraints of availability, cost, and fabrication, Aluminium was selected as the alternate material because of its lightweight and strength. However, the material stress analysis, bending moment analysis and twist analysis done for each component for both carbon fibre and aluminium yielded well above the required value.

Singularities were common at the initiation of the system.

The strength of the end effector solenoid should withstand the acceleration of the system.

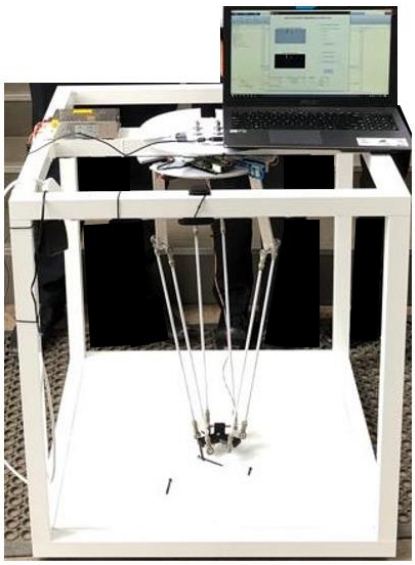

Figure 8. Fabricated, visual servo delta robot for sorting screws

VII. CONCLUSION

Since the functionality and the objectives of the prototype model were to its expected level, a scaled-up model is feasible to be used in the industry to accommodate regular pick and place tasks.

REFERENCES

Abduraimov, A. et al., 2017. Delta robot forward kinematics method with one root. s.l., IEEE.

Azmoun, M., Kalhor, A., Masouleh, M. T. & Rouhollahi, A., 2018. Kinematics and Control of a 4-DOF Delta Parallel Manipulator. s.l., IEEE.

Bulej , V., Poppeova, V., Rejda, R. & Uricek, J., 2012. THE DESIGN AND SIMULATION OF TRAINING DELTA ROBOT. Dubai, s.n.

Chen, Z., Geng, Y., Wu, J. & Xu, S., 2018. The simulation study of optimization of pick-and-place route for delta robot based on lame curves. s.l., IEEE.

Clavel, R. & Vischer, P., 1998. Kinematic calibration of the parallel Delta robot. Robotica, Volume 16, pp. 207 - 218.

Deshmukh, M. P. & Patil, M. J., 2015. A Review Paper on Introduction of Parallel Manipulator and Control System. International Journal of Engineering Research & Technology (IJERT), 4(2), pp. 959-963.

Kim, J., Liu, X.-J., Oh, K. & Wang, J., 2004. A New Approach to the Design of a DELTA Robot with a Desired Workspace. Journal of Intelligent and Robotic Systems, Volume 39, pp. 209-225.

Lin, C., Liu, C. C., Shaw, J. & Tsou, P. C., 2016. Vision servo based Delta robot to pick-and-place moving parts. s.l., IEEE.

Peng, B., Zhu, S., Khajepour, A. & Huang, Y., 2019. Kinematics and orientation capability of a family of 3-DOF parallel mechanisms. Mechanism and Machine Theory, Volume 142.

Rosquist, K., 2013. Modelling and Control of a Parallel Kinematic Robot, s.l.: s.n.

Tsai, C.-S.et al., 2016. Design and Simulation of a Delta Type Robot. s.l., IEEE

Auto Balancing Ambulance Stretcher with Active Control to Mitigate the Discomfort of the Patient

KKVPM Kalyanapriya#, CON Ratnayake, AMAB Adikari, WSP Fernando and KDPR Jayatilaka

Department of Mechanical Engineering, General Sir John Kotelawala Defence University, Sri Lanka

#mihirangapinindu@gmail.com

Abstract— During a medical emergency, the time taken to transport a critically ill or injured patient to the closest medical centre is a key factor determining the life and death of the patient. Although the current ambulances have attained the capability of passenger transport at a higher rate, the inability of the same designs to cater to the level of comfort during this journey has led to an increase in the mortality rates. The solutions for the above problem are either to build an ambulance, or to improve the design aspects of the stretcher, in order to ensure the required level of comfort to the critical patient. This study suggests a stretcher design capable of three degrees of freedom, which is used to counteract the discomfort caused by centrifugal accelerations and vibrations. The tests conducted have proven the capability of the stretcher to reduce the vibrational effect experienced by the subject by 58%, while bringing the maximum vibration well below 2Hz, the effect due to inertial accelerations by 92%, and effect due to centrifugal acceleration by 88%. Considering the ergonomic characteristics and lower cost associated, the suggested design shows feasibility of using the apparatus in developing countries like Sri Lanka.

Keywords: ***auto-balancing ambulance stretcher, mitigate discomfort, inertial forces, 3-DOF***

I. INTRODUCTION

In medical emergencies, the ambulances are used as the main mode of transport of patients from the scene of the incident to the hospital or from one hospitals to another. In order to save lives of patients who are transferred from ambulanaces, time taken for the task must be shortened as much as possible. While treating this aspect as the main factor, safety and comfortability of the patient during the journey to the hospital are also considered as other critical factors that affect the life of the patient. However, when rushing patients to the hospitals becomes the priority, both safety and comfort of patients during the journey are often compromised. In the current ambulance designs and the patient supporting set up inside ambulances, there are ineffective devices are available which fail to reduce the discomfort of patients inside a fast moving ambulance. Hence, this study aimed to develop an auto balancing ambulance stretcher to mitigate the discomfort of the patients inside a ambulance during the visit to the hospital.

II. LITERATURE REVIEW

Illnesses and injuries are unpredictable and could cause at any place or any time. For such instances, ambulances are placed under the broad umbrella of Emergency Medical Services commonly known as EMS (T.ZobelJ, 2004). Ambulance development has come a long way since the first encounter of carrying a patient in 1497, where the patient was carried on carts using horses (Bell, 2009). In the latter part of the 19th century, the development of motorized systems induced the use of motor vehicles as ambulances. The structure of ambulance was laid down during the world war period, incorporating a physician and medical equipment, which is mandetory inside the ambulance since it resulted in a significant reduction in mortality rate during travel (Bell, 2009). Lieutenant Clifford Peel came up with a fixed wing aircraft design named as 'Air Ambulances' in 1917 (King, 2004). With the evolution in technology, modern day ambulances have four major categories (Gainor, 2015). They are classified as Type I, Type II, Type III and Type IV. Type I ambulance is used in scenarios such as advanced life support and mobile intensive care. Type II ambulances are used for basic life support. Type III has a custom built van chassis and a rear compartment. Type IV is built under international standards, but have the capability to travel through restricted areas (HAMPSON, 2007). CEN1789 is the regulation published by the European Committee for standardization for the compliance level required to be adhered for

Ambulances. United States follows KKK-A-1822F which is published by the General Services. NFPA 1917 issued by the National Fire Protection Association is a globally recognized report, suggesting the design standards for ambulances. These were further influenced by the national ambulance standards for countries like Sri Lanka and India. It is noted that reduction in the patient compartment area while keeping minimum height of the patient compartment is due to the presence of only type II ambulances for emergency medical services (COUNCIL, 2013). Most of the current developments in the ambulance design had been unable to address the effects to the patient during travel. These include inertial forces caused by acceleration and deceleration, centrifugal forces due to ambulances taking bends at higher speeds and by vibration generated due to the roadside deformations and those transmitted from the mechanical components of the ambulance. According to the study (Waddel, 1975), the mortality rate of patients who suffered from hypertension is around 67%, hypotension is 50%, and delayed hypotension is around 29% (G.Waddel, 1975). Wheble (1987) further stated that, patients who arrive at the hospitals experience worse medical conditions than that prevailed before they were transported. Snook (1972) stated that the health condition of the patient can be directly and indirectly affected by the movement of the vehicle. The body sway causes physical and psychological effects, which may cause a rise or fall of blood pressure, critical heart arrest and cardiac arrythmia (Snook, 1972). As the main factor to be mitigated during travelling, the body sway caused by inertia, centrifugal forces and vibrations play a major role in minimalizing the mortality rates of patients. According to Ono, these external forces cause variation in blood pressure and body sway (Ono & Inooka, 2009). Pre-surgery hypertension plays a critical factor in determining the outcome of any surgery. Around 75% of the patients transported through ambulances undergo surgery procedures, thereby if a patient is to be affected by blood pressure variations in the pre-surgery stage, he/she will face serious consequences. Several notable designs had been developed with the aim of mitigating the effect on a patient due to vibration, centrifugal forces caused due to ambulances taking bends at higher speeds, inertial forces caused due to instant acceleration and deceleration (Abd-El-Tawwab, 2001). Ono and Inooka (2009) have proposed an active-controlled bed for the ambulances as shown in Figure 1.

Figure 1. Active Control Bed (Ono & Inooka, 2009)

According to them the discomfort caused due to the inertial acceleration and deceleration degrades the medical condition of the patients. The ACB is designed to be able to move in two axes of rotations. These two rotations will permit the cancellation of the longitudinal and lateral acceleration of the patient.

A special air suspension system was installed in this system so that the vibration and shocks induced by the road are absorbed. To reduce the impact of engine vibration and shocks, a low pass filter was added to the data acquisition model thereby these noises do not affect the readings taken by the system. In the implementation of the proposed design, several constraints were added to the system to prevent any discomfort to the patient. The constraints were added in order to prevent bed's motions inversely affecting on the subject.

The Active-Controlled bed suggested by Ono and Inooka (2009) does not meet the International standards for stretcher dimensions. Additionally, hard braking leads to nose driving which causes a rebound motion of the stetcher which is uncomfortable to the patient.

The prime goal of present work is to devise a mechanism to mitigate the impact on patients travelling on an ambulance stretcher due to inertial, centrifugal accelerations and vibrations. The research focusses upon the 3 degrees of freedom, where platform is considered as the main mechanism which is to be used to provide the desired motion for the ambulance stretcher. Three Degrees of freedom platforms belongs to the sector of parallel robots (Staicu, 2005). The limbs are composed of prismatic actuators giving the capability to the 3 DOF platform to increase and decrease the length between the two platforms. Generally, the joints used in the mechanism are revolute joints and ball joints. The presence of 3 revolute joints provides the capability to the platform to tilt in 3 degrees of freedom namely Roll, pitch and rotation around the z-axis.

III. METHODOLOGY

This research mainly focuses on mitigating the forces acted upon the patient throughout the journey in the ambulance. An initial study in this regard revealed that, only the suspension system supports to mitigate the discomfort caused during travel. Majority of ambulance stretchers are firmly attached to the chassis of the vehicle, thereby subjected to the movements of the ambulance, upon the patient. These movements that act upon the patient causes physical and psychological changes which could lead to mortality, and thereby causing substantial impact on mortality rates of critical patients, during transport. Methodology of the study is show in Figure 2.

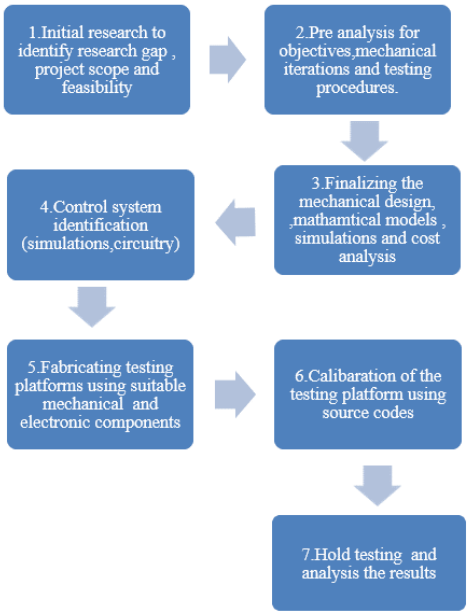

Figure 2. Flow Diagram showing the methodology

From the literature review, publications related to the effects of ambulance on critically ill patients (Waddel, 1975) and actively-controlled beds for ambulance (Ono, 2009) were studied further to lay the foundation for the proposed design. However, in this study, 6 main directions of movement which are left, right, upwards, downwards, slope up and slope down were considered. Mechanical simulations were conducted initially. Here, the iterations were done for the active control bed model developed by Ono and Inooka (2009). Analysis was conducted using the statistical analysis model suggested by Ono and Inooka (2009).

IV. DESIGN AND FABRICATION

A. Mathematical Model

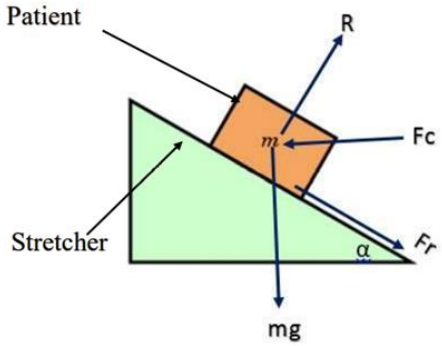

Figure 3. Free body diagram

The tilt of the stretcher is one of the key factors determining the level of comfort experienced by the patient. Figure 3 shows the free body diagram of the forces exerted on the patient's body, when the upper platform is turned by an angle of α.

The terminology used in the calculation are as follow:

R- Normal reaction on the patient's body from the stretcher

F_c- Centrifugal force acting upon the patient

F_r- Frictional Force acting on the patient

m- Mass of the patient

g- Acceleration due to gravity

μ- Coefficient of friction

θ_d- Desired tilt angle

The equilibrium condition was taken into consideration by applying Newton's second law along and in perpendicular directions. Considering the equilibrium in the direction perpendicular to the plane (Direction of R),

$R - mg\cos\alpha + Fc\sin\alpha = 0$ ------- (1)

Considering the equilibrium in the direction along the plane (Direction of F_r),

$F_r = F_c \cos\alpha - mg\sin\alpha$ ---------- (2)

By equating these equations, the following kinetic model was obtained (Here $\theta_d = \alpha$).

$$Desired\ platform\ tilt = \theta_d = \tan^{-1}\left[\frac{(F_c - \mu mg)}{(mg - \mu F_c)}\right] \quad G. \text{ ----- (3)}$$

Free body diagram shown in Figure 4 represents forces exerted on the patient's body when the upper platform is turned by an angle of θ when subjected to linear acceleration.

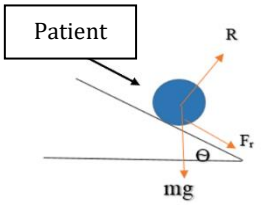

Figure 4. Freebody Diagram of patient on stretcher

By applying F=ma perpendicular and horizontal to the stretcher:

$$\theta = \frac{1}{2}Sin^{-1}\left(\frac{\alpha-\frac{\mu g}{2}}{\frac{g}{2}\sqrt{1+\mu^2}}\right) - \frac{1}{2}Sin^{-1}\left(\frac{\mu}{\sqrt{1+\mu^2}}\right) \quad \text{--- (4)}$$

Equation 4 gives, the required angle of tilt during an event of linear acceleration:
Additionally, for the mechanical design, the required torque for the motors were calculated as 1.718 Nm. Required motor speed was calculated as 1875 rpm. The natural frequency of the system was calculated as 8.1 Hz. The required minimum spring constant for 2 Hz was obtained as 2962.59 Nm^{-1}.

B. Mechanical Design

Stewart platform, which is one of the main prismatic actuators, feedback control system with a gyroscopic sensor and accelerometer were the main mechanisms in this study. Final design was established from the conceptual design, simulation results and, structural analysis of the design conducted using SolidWorks2018. The functions of the design, specifications of the components and the mechanical structure of the design were given as inputs. Figure 5 gives the stress analysis of the design.

I. Figure 5. Stress Analysis

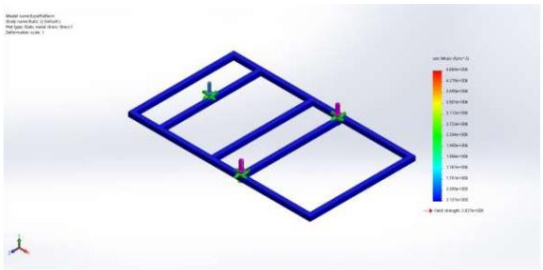

Name	Type	Min	Max
Stress1	VON: von Mises Stress	3.137e+000N/m^2 Node: 471	4.668e+006N/m^2 Node: 16883

Properties such as material density, low brittleness, high tensile and compressive strength, cost effectiveness, desirable ductililty and malleability were considered. It was decided that the most suitable metal for this design is low carbon steel. Railing mechanism, guiding device and locking mechanism were the most critical points of the mechanical design. Ball bearing slider, vertical and horizontal guides and auto lock while inserting mechanisms have been used since the process of entering patient into the ambulance should be an urgent matter. According to the analysis, a customized linear actuator was obtained to satisfy the needful. This actuator has a stroke of 300 mm, 24V DC output, maximum load of 250 N and a speed of 45 mms^{-1}. Additionally, dampers which suited the requirement were selected.

C. Control System Design

Gyroscopic and accelerometer readings were taken as main inputs. Developing an algorithm for prismatic actuation and elevation which has 3 linear actuators based on the gyroscopic and accelerometer reading was the main part of the coding. Here, the feedback of the system is the encoder reading of the motor.

D. Wiring connections

Circuitry was developed using two microprocessors which are RaspberryPi B3+ and Arduino Mega 2560. Additionally, two accelerometers (MPU 6050) were used to obtain analog readings of orientation and acceleration on the stretcher and the ambulance separately. Further, RaspberryPi 3B+ was used in the HMI system. Arduino Mega 2560 was used in the electrical system due to the high-speed data transfer rate of MPU 6050. Accordingly, the device was programmed using Python and Arduino for the required operations. The, gyroscopic and the accelerometer readings were taken as the inputs for the system. A propotional movement was developed from the coding system. Executing proper "if" conditions to the gyroscopic readings, the tilt angle was calculated and the feedback was added to the calculation, thereby, enhancing the motion of the ambulance bed. The HMI was coded afterwards while debugging the system and conducting the necessary tests. A Kalman filter was used as the elevation angle reading library to enhance the reading values of the MPU6050. Figure 6 shows the final fabricated design of the active control bed.

Figure 6. Final Fabricated Design of the Active Control Bed

V. TESTING AND RESULTS

Analysis was conducted using the statistical analysis model suggested by Ono and Inooka (2009). For this, the subject selected for the tests was a dummy that weighed 50 kg. Type II ambulance was used for the test and the airport road in-front of the Ratmalana airport was selected as the location to conduct the test. Accordingly, the following tests were conducted.

Test 1: Evaluating the design dimensions

When evaluation the design dimensions, the limitations provided by the International Standards NFPA 1917 and the Guideline for Government and Private Ambulance Services of Sri Lanka were taken into consideration. The minimum distance of the walkway between the ambulance stretcher and the paramedic sheet is 300 mm. The minimum distance from rear doors to the rear edge of the ambulance stretcher is to be 254 mm. Additionally, maximum allowable height of the stretcher in the loading position is to be 700 mm. After the design was attached to the ambulance body, the required measurements were taken as follows. Minimum distance of the paramedic walkway was 320 mm. This is a 6.67% positive variation from the required value. Minimum distance from the door to the stretcher was 340 mm. This is a 33.86% positive variation. Also, the maximum allowable height during operation was measured as 720 mm. This is a 2.86% positive variation from the required value.

Test 2: Evaluating the performance of dampers

For this test, two gyroscopes of model ICM42605M were used. Here, the application developed by RWTH Aachen University, Phyphox was used in order to gather data. One accelerometer was set to the developed device and the other was attached to the stretcher frame. The difference in the readings taken from the stretcher and the stretcher frame was considered as the evaluation here. The tests were mainly conducted for 2 different speeds, 50 kmph^{-1} and 75 kmph-1. The speed was maintained for 15 seconds and the data was gathered. For the purpose of comparison, the results obtained from 75 kmph^{-1} was considered. According to the results obtained, with respective to the conventional stretcher, the active control bed was able to obtain 58% reduction in vibration throughout the session at 75 kmph^{-1}.

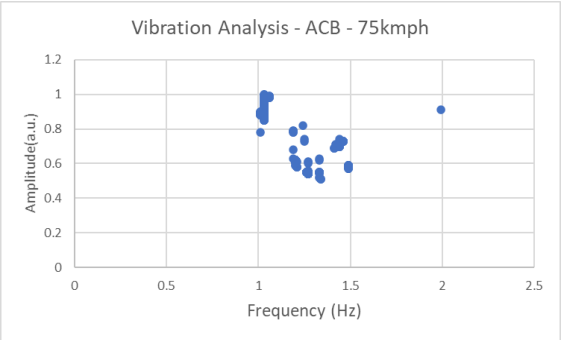

Figure 7. Vibration Analysis of Active Control Bed at 75 kmph

Test 3: Evaluating the stretcher response for the instant acceleration

According to the mathematical model and the constraints set by the dimensions of the design, the maximum tilt that the device should allow is 20 degrees. Here, the data retrieved from MPU6050 and the acceleration data gathered form the phyphox application using ICM42605M were compared. The ambulance was tested against an acceleration until it reached a speed of 75 kmph^{-1}. Ambulance took 20 seconds to reach the targetted speed. Within this time, the acceleration achieved and the tilt obtained were recorded separately. From the acceleration, the required tilt was calculated, and the required tilt was compared with the achieved tilt.

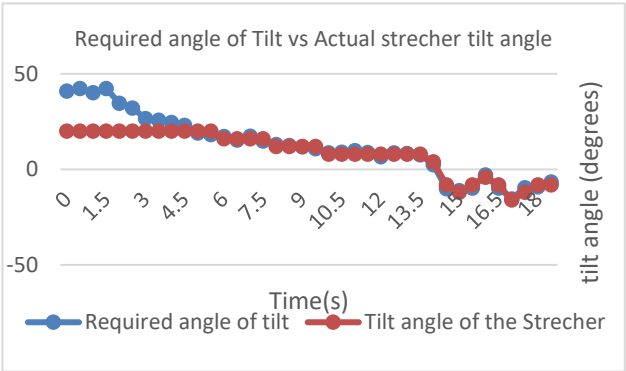

Figure 8. Required Tilt Angle vs Actual Tilt Angle on Instant Acceleration

The required tilt of more than 20 degrees was considered as the uncontrollable region. A deviation of 66.8% from the required tilt was observed. However, in the controllable region, only a deviation of 2.17% was observed. Within this range, the stretcher performed with a

maximum error of 2 degrees. Therefore, it was calculated that the stretcher responds with an accuracy of 92% of the recorded inertial acceleration.

Test 4: Evaluating the stretcher response against instant deceleration

Here, the test was similar to Test 3, but the ambulance was brought to a halt from a speed of 75 kmph and the data was recorded. Similar to Test 3, the required tilt angle of the recorded de-acceleration was calculated and compared with the achieved tilt. Here a percentage variation of 23.1% was observed between the required and the achieved tilt. The calculated ambulance stretcher response efficiency was 77%. It should be noted that here the stretcher was restricted to nose driving. Hence a reduction was expected in the efficiency. Maximum deviation of tilt was recorded as 3 degrees for this session.

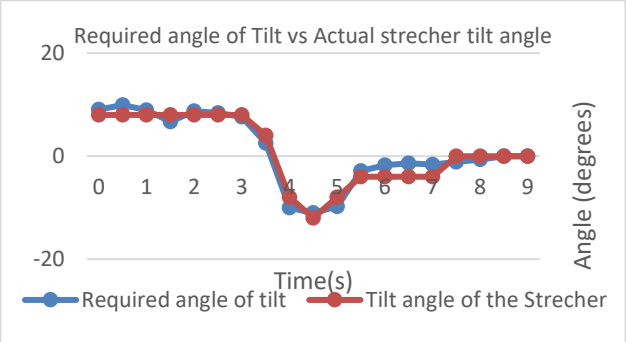

Figure 9. Required Tilt Angle vs Actual Tilt Angle on Instant Deceleration

Test 5: Evaluating the stretcher response against centrifugal acceleration

For this test, the ambulance was tested against a bend acquiring 50 $kmph^{-1}$ and 75 $kmph^{-1}$. Here, the data was recorded for 12 seconds and from the acceleration data gathered, the required tilt of the stretcher was obtained. Shown below is the tilt comparison for 75 $kmph^{-1}$.

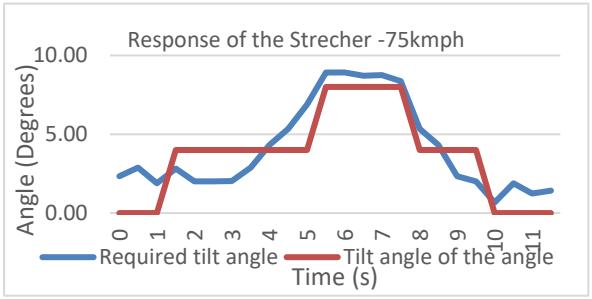

Figure 10. Required Tilt Angle vs Actual Tilt Angle on Centrifugal Forces

The responsiveness for accelerations above 1 ms^{-2} stands at 88% at 75 kmph. It showed a responsiveness of 82% for 50 kmph indicating that the bed is more responsive for higher changes in acceleration.

VI. DISCUSSION

The objective of this research is to design, fabricate and evaluate the performance of an autobalancing ambulance bed with the capabaility of absorbing intertial and centrifugal forces upon the patients. In this study, steward platform has been utilized as the basis for mechanical design. The final fabricated apparatus was able to exhibit 3-DOF which is essential in counteracting the interial and centrifugal forces. In the performance evaluation phase of the apparatus, 5 tests were conducted.

Design ergonomics of the fabricated design has shown a variation of 6.67% related to the distance from the paramedic walkway. All the other ergonomic factors attributed were within the threshold.

Tests were conducted in order to verify the functional aspects predetermined against the international standards published on the comfort and safety of patients travelling in ambulances. The statistical analysis model suggested by Takahiko and Inooka (2009) was used in this regard. From the test results, it was found that the active control bed designed was complied with the limitations provided by the International Sandards NFPA of 1917 and the Guideline for Government and Private Ambulance Services of Sri Lanka. The designed active control bed showed a 58% reduction in vibration compared to the conventional stretcher used in the ambulance. The bed was able to operate under 92% accuracy for the responsiveness against instant acceleration. When the ambulance was taken into halt with an instant deacceleration, the bed was able to operate under an efficiency of 77% accuracy. The action against centrifugal accelerations provided a responsiveness of 88% by the active control bed, thereby it was able to improve the patient comfort and to mitigate the discomfort compared to that of the conventional stretcher.

VII. CONCLUSION

It can be concluded that the stretcher is capable of absorbing majority of inertial forces acting on human body when the ambulance is driven at 75 kmph. The overall cost of the apparatus shows that

auto balancing strecher proposed in this study can be locally manufactured at a cost similar to NF A9 emergency stretcher (Without the auto balancing capability), making it a feasible remedy for the fatalities and discomfort caused due to the inertial, vibrational and centrifugal accelerations.

REFERENCES

Abd-El-Tawwab, A. M., 2001. Ambulance Stretcher With Active Control. Journal of Low Frequency Noise, Vibration and Active Control, 20(4), pp. 217-228.

Bell, R. C., 2009. The ambulance : a history. 1 ed. Newyork : Jefferson, N.C. : McFarland & Co..

COUNCIL, H. S. R., 2013. GUIDELINE FOR GOVERNMENT & PRIVATE AMBULANCE SERVICES, Colombo : Ministry of Health , Sri Lanka .

G.Waddel, P. S. N. L. I. M. L., 1975. Effects of Ambulance Transport in Critically Ill Patients. British Medical Journal, Issue 1, pp. 386-389.

Gainor, D., 2015. Ambulance Vehicle Design Specifications Revision, Falls Church: Nebraska EMS.

HAMPSON, J., 2007. Federal Specifications for the Star-of-Life Ambulances KKK-A-1822F, Washigton DC : GSA-Federal Acquaition Service .

King, D., 2004. Patrick O'Brian: A Life. 10 ed. Ohio: Diane Pub Co.

SNOOK, R., 1972. Medical Aspects of Ambulance Design. British Medical Journal, 3(1), pp. 574-578.

Stefan Staicu, D. Z. R., 2005. Dynamic modelling of a 3-DOF parallel manipulator using recursive matrix relations. Robotica, 24(1), p. 125–130.

T.ZobelJ, O., 2004. Factors of importance in identification and assessment of environmental aspects in an EMS context: experiences in Swedish organizations. Journal of Cleaner Production, 12(1), pp. 13-27.

Takahiko Ono, H. I., 2009. Actively-controlled Beds for Ambulances. International Journal of Automation and Computing, 1(6), pp. 1-6.

WHEBLE, V. H., 1987. Ambulance transport : a question of patient comfort. Engineering in Medicine, 16(1), pp. 230-238.

ACKNOWLEDGEMENT

We would like to thank Police offciers at Rathmalana police station and Reginoal director of Health services Monaragala in providing the necessary clearance, knowledge and support that made this study a success.

AUTHOR BIOGRAPHIES

K.K.V.P.M. Kalyanapriya

BSc. (Hons) in Mechatronics Engineering Graduated from Mechanical Department of General Sir John Kotelawala Defence University.

C.O.N. Ratnayake

BSc. (Hons) in Mechatronics Engineering Graduated from Mechanical Department of General Sir John Kotelawala Defence University.

A.M.A.B. Adikari

BSc. (Hons) in Mechatronics Engineering Graduated from Mechanical Department of General Sir John Kotelawala Defence University

K.D.P.R Jayathilake

K.D.P.R. Jayathilake is graduated from University of Moratuwa , Sri Lanka and M.Sc. in Engineering and Technology in Thammasat University, Thailand, 2015.

W.S.P.Fernando

W.S.P.Fernando graduated from University of Moratuwa,Sri Lanka and specialized in the field of Computer Science and Engineering and followed M.Phil from University of Moratuwa.

Design of a Magnetostrictive Bimorph for Micromanipulation

KNM Perera[1], HAGC Premachandra[2#] and YWR Amarasinghe[1,2]

[1]*Centre for Advanced Mechatronic Systems, University of Moratuwa, Katubedda, Sri Lanka*
[2]*Department of Mechanical Engineering, University of Moratuwa, Katubedda, Sri Lanka*

[#]charithp@uom.lk

Abstract— Micromanipulation within a lab-on-a-chip (LOC) device enables precise manipulation of cells, paving the way to diverse biomedical applications. In this research, the design of a magnetostrictive microactuator for micromanipulation is presented. The proposed microactuator is a cantilever-type bimorph consisting of a Poly-methyl methacrylate (PMMA) layer between a Terfenol-D and Samfenol-D layer, which have high magnetostrictive properties, and a Silicon probe tip at the free end. The microactuator characteristics were evaluated through numerical simulations. The designed microactuator can operate under frequencies up to 146.12 kHz. The sensitivity range of the microactuator is 77.6-11323.6 nm/T, while it can exert pressures up to 15.55 MPa for magnetic fields from up to 800 kA/m, demonstrating that it is capable of micromanipulation of cells in LOC devices.

Keywords: ***lab-on-a-chip, magnetostriction, MEMS, microactuators, microrobotics***

I. INTRODUCTION

A lab-on-a-chip (LOC) is a micro-electro-mechanical system (MEMS) device that integrates one or several laboratory functions onto a single chip. These are often microfluidic devices consisting of microfluidic channels, pumps, droplet generators and reservoirs. When it comes to LOCs in genomics and proteomics, it is essential to manipulate biological particles to observe, analyze and enumerate components at cellular level. Using microrobots for manipulation increases the throughput and repeatability of processes outperforming human manipulation.

In literature, there are basically two types of micromanipulators in terms of interaction: contact and non-contact. Atomic Force Microscopy (AFM) and Scanning Tunneling Microscopy (STM) have been promising contact type micro/nano manipulation methods since 1990s (Pavliček & Gross 2017; Sitti 2001; Sitti & Hashimoto 1999). STM probes use electric pulses to manipulate particles, whereas AFM probes can perform more mechanical tasks such as pushing/pulling, cutting, touching, and indenting. The AFM probe is a cantilever/tip assembly which interacts with the sample. Usually, a separate mechanism controls the up and down and lateral motions of the probe. On the contrary, optical tweezers is a non-contact manipulator which uses a highly focused laser beam to create an optical trap (Xie et al. 2019). Existing approaches of LOCs for cell manipulation are different from AFM and STM. In most of the cases, they are polarizing particles using electric fields for cell manipulation (Medoro et al. 2003; Medoro et al. 2007). In addition, LOCs incorporate mechanical structures such as microgrippers to manipulate cells (Somà et al. 2017).

Magnetostriction effect is the phenomenon where a ferromagnetic material expands or contracts in response to an external magnetic field, as illustrated in Figure 1. Hence, utilizing this phenomenon in an actuator paves the way for wireless actuation and control. Researchers have created magnetostrictive bimorphs in millimeter scale and were able to achieve displacements up to 4 mm with static magnetic fields (Arai & Honda 1996). Despite their nonlinear material properties, magnetostrictive materials are deemed to perform better than piezoelectric and shape memory alloys due to inherent characteristics: fast response time, relatively large strokes, high resolution and bandwidth (Zhao & Lu 2018; Niu et al. 2017).

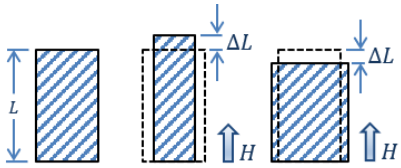

Figure 1. Schematic illustrating the positive and negative magnetostrictive effects.

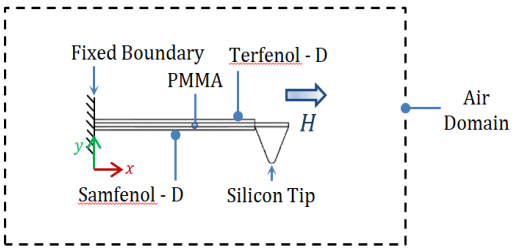

Figure 2. Layout of the proposed magnetic microactuator. The bimorph is 100 µm in length. *H* is the spatially uniform external magnetic field in the x-

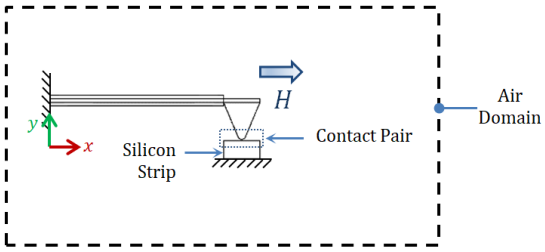

Figure 3. Schematic diagram of the contact simulation.

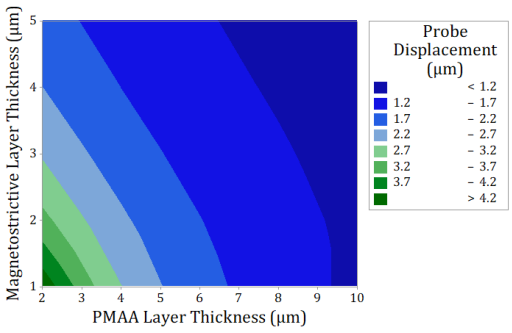

Figure 4. Variation of bimorph tip displacement with PMMA and magnetostrictive material layer thicknesses.

In this research, the design of a magnetostriction based micron-scale bimorph for micromanipulation is presented. The basic mechanical structure was inspired from the AFM probe. Through analyzing the characteristics of the microactuator, the capability of using magnetostriction based microactuators in micromanipulation is investigated. Significant design parameters such as accuracy, range of motion, and linearity were evaluated using numerical simulations to this effect. The abstract introduces the proposed magnetostrictive microactuator and describes the methodology of investigating microactuator characteristics. The microactuator characteristics obtained through numerical simulations are discussed, along with the conclusions.

II. MATERIALS AND METHODS

The conceptualized single degree of freedom (DOF) magnetostriction based cantilever-type microactuator is shown in Figure 2. It consists of a Poly-methyl methacrylate (PMMA) layer sandwiched between a Terfenol-D and Samfenol-D layer. Here, PMMA was selected due to its flexibility as a result of the low Young's modulus, the value of which is 3 GPa. From this, the stiffness of the bimorph is reduced. At the free end of the cantilever is the probe tip. In terms of magnetostriction, Terfenol-D and Samfenol-D have significant positive and negative magnetostrictive properties respectively. Hence, when an external magnetic field *H* is applied, the beam acts as a bimorph due to the strain difference of the two magnetostrictive elements. The saturation magnetization of Terfenol-D is 800 kA/m while for Samfenol-D it is 560 kA/m. Saturation magnetostriction of Terfenol-D and Samfenol-D are 820 ppm and -1258 ppm respectively. The initial magnetic susceptibility of both the materials were taken as 14. By selecting one magnetostrictive layer to have positive

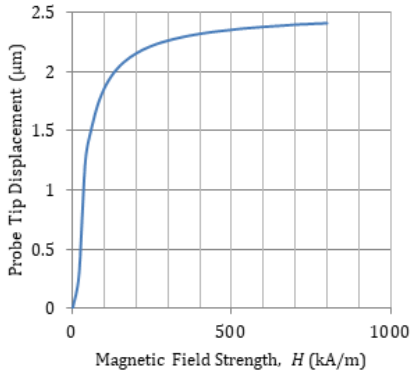

Figure 5. Probe tip displacement in the y-direction with varying magnetic field strength.

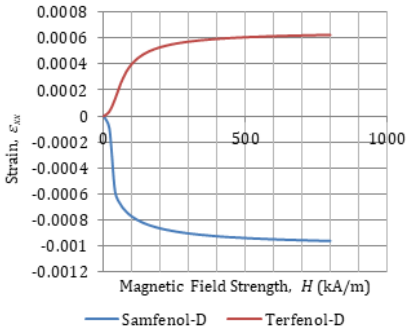

Figure 6. Direct strain of the magnetostrictive materials in the x-direction (ε_{xx}) variation with magnetic field strength.

magnetostriction and other to have negative magnetostriction, the tip displacement of the bimorph can be increased.

The behaviour of the proposed microactuator was analyzed through 2-dimensional numerical simulations using COMSOL Multiphysics. The length of the bimorph is set as 100 µm. First, a parametric study was carried out without the probe tip to select the layer thicknesses of the bimorph by analyzing the probe displacement variation with the thicknesses of the PMMA and magnetostrictive element layers. The thickness of the PMMA layer was varied in the range 2-10 µm, while thickness of the magnetostrictive layers was varied in the range 1-5 µm. The applied uniform magnetic field in the x-direction for this study is the saturation magnetization of Terfenol-D, i.e. 800 kA/m.

After selecting suitable material layer thicknesses for the bimorph, a modal analysis using numerical simulations was conducted to find the first mode frequency and shape. Furthermore, numerical simulations were done to obtain the range of motion and sensitivity of the microactuator. For this, the uniform external magnetic field was varied in the range 0-800 kA/m and resulting probe tip displacement in the y-direction was computed. The pressure exerted by the actuator on an object was analyzed for different magnetic field strengths through computing the contact pressure between a Silicon strip and the probe tip using the penalty contact algorithm (see Figure 3). The initial gap between the probe tip and the strip is zero. The material of the probe tip is also Silicon. The applied external magnetic field strength was varied up to 800 kA/m in the aforementioned study.

III. RESULTS AND DISCUSSION

For any actuator, the range of motion is an important parameter that exhibits the capabilities and limitation of the actuator. The layer thicknesses of both the PMMA layer and magnetostrictive layers affect the bending of the bimorph. Therefore, it is desirable to analyze the behaviour of bimorphs with different layer thickness and select suitable values. From Figure 4, it is observable that the bimorph tip displacement in y-direction is high at low PMMA and magnetostrictive layer thicknesses. Therefore, to obtain a maximum probe tip displacement above 2 µm, both the PMMA and magnetostrictive layer thicknesses were selected as 2 µm.

The first mode frequency of the microactuator is 146.12 kHz. Hence, the excitation frequency should be less than 146.12 kHz in order to obtain the expected bending mode shape. The range of motion of the microactuator, which is the probe displacement in the y-direction, can be defined as 0-2.41 µm for applied magnetic field strengths in the x-direction up to 800 kA/m (see Figure 5). The sensitivity of the microactuator can be obtained by computing the gradient of the relationship between probe tip displacement and magnetic field strength. Overall, the microactuator shows a nonlinear relationship between probe tip displacement and applied magnetic field strength, where the sensitivity gradually decreases. However, in the considered magnetic field strength range are 77.6 nm/T and 11323.6 nm/T respectively. This sensitivity is more than sufficient for cell manipulation since the average human cell size is around 100 µm in diameter (the minimum of which is red blood cells with 8 µm diameter). Furthermore, it was observed that the Samfenol-D layer has a higher direct strain in the x-direction ε_{xx} than the Terfenol-D layer for a given magnetic field strength (see Figure 6).

The maximum contact pressure between the Silicon strip and probe tip is shown in Figure 7. Overall, it is observable that the exerted pressure increases nonlinearly with the magnetic field strength. This behaviour exhibits a saturation of the contact pressure. However, in the range 0-80 kA/m, this relationship is approximately linear. Hence, if the operating region is within this range, one can obtain linear actuator force characteristics. Consequently, the force controlling would be relatively easier in this region. The microactuator can exert a maximum pressure of 15.55 MPa at 800 kA/m and 11.82 MPa at 100 kA/m. Thus, the microactuator is able to manipulate a payload of 1 ng, which is the average weight of a human cell (assuming a 100 µm

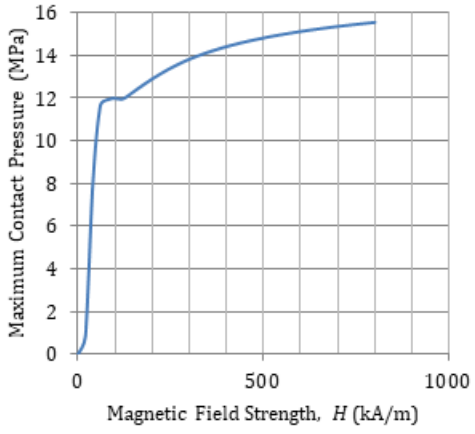

Figure 7. Maximum contact pressure variation with magnetic field strength.

diameter circular cell area). Furthermore, since the bimorph deflects in the y-direction, no additional mechanism is required to control the movement of the probe in the y-direction unlike in the AFM probe.

IV. CONCLUSION

A cantilever-type magnetic microactuator based on the magnetostriction effect is proposed for micromanipulation. The actuator consists of a bimorph that deflects due to magnetostriction and a probe tip at its free end. The probe tip interacts with the objects inside a lab-on-a-chip (LOC) device. The microactuator has sensitivity in the range between 77.6-11323.6 nm/T for magnetic fields up to 800 kA/m. The microactuator is able to operate up to 146.12 kHz, which is the first mode frequency of the system. Furthermore, contact pressures up to 15.55 MPa can be exerted using the proposed microactuator. Therefore, the nanometer sensitivity with higher force output verifies the possibility of magnetostrictive bimorph to be used for micromanipulation of cells in LOC applications.

REFERENCES

Pavliček, N & Gross, L 2017, 'Generation, manipulation and characterization of molecules by atomic force microscopy', *Nature Reviews Chemistry*, vol. 1, no. 1.

Sitti, M 2001, 'Survey of nanomanipulation systems', *IEEE Conference on Nanotechnology*, Maui, HI, USA, 30 October, 2001, pp. 75-80.

Sitti, M & Hashimoto, H 1999, 'Teleoperated Nano Scale Object Manipulation', *Recent Advances on Mechatronics*, pp. 172–178.

Xie, M, Shakoor, A, Shen, Y, Mills, J & Sun, D 2019, 'Out-of-Plane Rotation Control of Biological Cells With a Robot-Tweezers Manipulation System for Orientation-Based Cell Surgery', *IEEE Transactions on Biomedical Engineering*, vol. 66, no. 1, pp. 199-207.

Medoro, G, Manaresi, N, Leonardi, A, Altomare, L, Tartagni, M & Guerrieri, R 2003, 'A lab-on-a-chip for cell detection and manipulation', *IEEE Sensors Journal*, vol. 3, no. 3, pp. 317-325.

Medoro, G, Guerrieri, R, Manaresi, N, Nastruzzi, C & Gambari, R 2007, 'Lab on a Chip for Live-Cell Manipulation', *IEEE Design & Test of Computers*, vol. 24, no. 1, pp. 26-36.

Somà, A, Iamoni, S, Voicu, R, Müller, R, Al-Zandi, M & Wang, C 2017, 'Design and experimental testing of an electro-thermal microgripper for cell manipulation', *Microsystem Technologies*, vol. 24, no. 2, pp. 1053-1060.

Arai, K & Honda, T 1996, 'Micromagnetic actuators', *Robotica*, vol. 14, no. 5, pp. 477-481.

Zhao, R & Lu, Q 2018, 'Design and Experiments of a Galfenol Composite Cantilever Beam-Driven Magnetostrictive Micro-gripper', *Iranian Journal of Science and Technology, Transactions of Mechanical Engineering*, vol. 44, no. 1, pp. 1-10.

Niu, M, Yang, B, Yang, Y & Meng, G 2017, 'Dynamic modelling of magnetostrictive actuator with fully coupled magneto-mechanical effects and various eddy-current losses', *Sensors and Actuators A: Physical*, vol. 258, pp. 163-173.

ACKNOWLEDGEMNT

The authors would like to express their gratitude to the Accelerating Higher Education Expansion and Development (AHEAD) - Development Oriented Research (DOR) grant of the Centre for Advanced Mechatronic Systems (CFAMS), University of Moratuwa, Sri Lanka for their financial contribution and the CFAMS for their valuable advice and guidance towards the success of the research.

BIOGRAPHY OF AUTHORS

K. N. M. Perera received the B.Sc. degree in mechanical engineering from the University of Moratuwa, Sri Lanka, in 2020. He is currently a Research Assistant in the Centre for Advanced Mechatronic Systems, University of Moratuwa, Sri Lanka. His research interests include mobile robotics, microrobotics, and dynamics & control.

H. A. G. C. Premachandra received the B.Sc. degree in mechanical engineering from the University of Moratuwa, Sri Lanka, in 2020. He is currently a Lecturer in the Department of Mechanical Engineering, University of Moratuwa, Sri Lanka. His research interests include micro/nano sensors and actuators, robotics, and mechatronics.

Y. W. R. Amarasinghe received the B.Sc. degree in mechanical engineering from the University of Moratuwa, Sri Lanka. He received the master's degree in information science and systems engineering and the Dr.Eng. degree in micro-electro-mechanical systems from Ritsumeikan University, Japan. He

served as a Post-Doctoral Fellow under the Japan Society for the Promotion of Science and as a Chair Professor with the Department of Micro Systems Technology, Ritsumeikan University, Japan. He is currently a Professor with the Department of Mechanical Engineering, University of Moratuwa. He is also working as the Director of Centre for Advanced Mechatronic Systems (CFAMS), a multidisciplinary research centre of University of Moratuwa. His research interests include design and development of MEMS/NEMS-based devices and systems, micro/nano sensors and actuators, microrobotics, and micromechatronics.

Framework for Aviation Safety Cost Optimization through Risk Mitigation Tolerance Analysis

WTS Rodrigo and WDT Fernando#

Department of Aeronautical Engineering, Faculty of Engineering, General Sir John Kotelawala Defence University, Sri Lanka

#dakshinafdo@kdu.ac.lk

Abstract— The aviation industry depicts itself to be one of the topmost safety-conscious industries where thorough emphasis is focused on safety management systems as a toolbox for hazard identification and risk mitigation. The promulgation of regulatory safety measures for in-air and on-ground operations has collated additional time and operational costs for all types of aviation establishments. The risk probability and severity aspects of safety models have been vastly studied in previous research mainly through qualitative analysis and risk matrix formulation. In conventional studies, the "risk tolerance" has been mainly incorporated with the probability and the severity of the risks where less or no emphasis is laid on the cost-benefit analysis. Hence, this study focuses on the implications of the "cost variable" on risk mitigation tolerance analysis in a collaborative approach of qualitative and quantitative analysis. The study converges the theoretical relationship of the "safety tolerance levels", towards the "overall safety cost" which aims to bridge a significant gap in the contemporary aviation safety literature. In bridging the unpredictability of the post-failure cost, the optimization of the cost of safety assurance enables expanded forecast ability by mathematically calibrating the strategic positioning of the safety threshold. The scale of the airline and the regulatory mandates have been considered in developing the conceptual ideology. Moreover, the study will span through to the development of a data-driven mathematical model for the cost to tolerance variation. Hence, the theoretical framework of this study proposes a more generalized approach that can be customized for the safety cost-benefit analysis and resources allocation policies of diversified airline operations spanning from low-cost carriers to high-end niche markets with utmost safety concerns.

Keywords: ***Safety Management Systems (SMS), Safety Risk Management (SRM), aircraft maintenance cost benefit, risk mitigation, risk tolerance.***

I. INTRODUCTION

As aviation is considered as a safety-critical industry the overall measures are developed as such supports and manipulates every operation to be supportive of reaching an acceptable range of safety. (Smith, 2005) Delivering a safer product consists of not only operational safety but the primary safety aspects such as design and maintenance safety measures. Due to the requirement of critical safety consideration, the International Civil Aviation Organization (ICAO) has developed the global standard safety risk probability value table as per the following Table 1.

Table 1. Safety risk probability table
Source: SMM (ICAO)

Likelihood	Meaning	Value
Frequent	Likely to occur many times (has occurred frequently)	5
Occasional	Likely to occur sometimes (has occurred infrequently)	4
Remote	Unlikely to occur, but possible (has occurred rarely)	3
Improbable	Very unlikely to occur (not known to have occurred)	2
Extremely improbable	Almost inconceivable that the event will occur	1

The maintenance aspect of aviation operations has developed various means of safety management options and policies throughout the years of air travel. (Fumero, 2018) The

development of tolerance levels and risk matrix are two key aspects of semi-quantitative approaches of aircraft maintenance safetyassessment.

The conventional approach in developing the risk matrix revolves around the comparative analysis of severity vs likelihood. Due to its biased nature under differential expectations and varied understanding of the data sources, a quantitative measure has been developed through time. (Song and Lee, 2015) The validation has been enumerated through qualitative measures, by comparison, quantitative measures by value assigning, and hybrid methods by risk calculation and matrix development.

In most conventional systems, the cost factor depending on the tolerance level has been overlooked through the intervention of insurance or post-accident recovery measures. (Xie, 2017) Under the said conditions the operators have given minimal consideration towards optimizing the selection of tolerance levels. (Čavka and Čokorilo, 2012).

J. Conditional liability sharing/transference

One of the most common mislead methods integrated into the aviation industry in terms of safety cost management is the reliance on insured entity.

This method deemed to be an indemnifying scheme in the sense of risk transference rather than risk mitigation. A third party transference may build a one-off occurrence assurance but will not guarantee a continuous safety process.

The cost benefit of safety assurance will not be met in liability sharing and transference. Thus, the process improvement can be emphasised as an optimal method in improving the safety tolerance to be in a continuous basis.

Table 2. Example safety risk severity table
Source: SMM (ICAO)

Severity	Meaning	Value
Catastrophic	• Aircraft / equipment destroyed • Multiple deaths	A
Hazardous	A large reduction in safety margins, physical distress or a workload such that operational personnel cannot be relied upon to perform their tasks accurately or completely • Serious injury • Major equipment damage	B
Major	A significant reduction in safety margins, a reduction in the ability of operational personnel to cope with adverse operating conditions as a result of an increase in workload or as a result of conditions impairing their efficiency • Serious incident • Injury to persons	C
Minor	• Nuisance • Operating limitations • Use of emergency procedures • Minor incident	D
Negligible	• Few consequences	E

The Table 2 depicts the most general definitions of the severity of occurrences derived by the International Civil Aviation Organization.
The systematic explanation has been contemplated in accordance with the previous occurrences and anticipated incidences. In such case the direct tolerability require task wise as well as operation wise broader scope in decision making.

II. CONCEPTUAL DEBRIEF

The capping of tolerance ranges to differentiate the regions does not possess a global standard optimal position. (Čokorilo et al. 2010) Thus, the capping margin has been varying from operator to operator without a standard means of variance. This has driven the majority of operators to overlook the tolerance levels and highly depend solely on the risk analysis (Lališ et al. 2018). With respect to the cost factor, this measure has been overlooked. (Cavka, Petrović and Cokorilo, 2014)

Safety Risk		Severity				
Probability		Catastrophic A	Hazardous B	Major C	Minor D	Negligible E
Frequent	5	5A	5B	5C	5D	5E
Occasional	4	4A	4B	4C	4D	4E
Remote	3	3A	3B	3C	3D	3E
Improbable	2	2A	2B	2C	2D	2E
Extremely improbable	1	1A	1B	1C	1D	1E

Figure 2. Risk Matrix
Source: SMM (ICAO)

In this study, the variance of the optimal position for the tolerance range is objectified as the primary output of the study in aspects of mathematically calculable means.

III. THEORETICAL FRAMEWORK

A. Overview and Rational

When considering the regional disposition, the range varies under the three sectors of risk management namely, Unacceptable region, Tolerable region, and Acceptable region (Zhang et al., 2018). The optimal positioning of the safety threshold could be derived on par with the cost factor consideration whereas the cost of safety could be brought to a reasonable balance by addressing the production and protection dilemma.

The generalized tolerance is globally depicted as per the following Figure 2 is derived from the aforementioned matrix in Figure 1 and risk analysis methods.

Suggested Criteria	Assessment Risk Index	Suggested Criteria
Intolerable Region	5A, 5B, 5C, 4A, 4B, 3A	Unacceptable under the existing circumstances
Tolerable Region	5D, 5E, 4C, 4D, 4E, 3B, 3C, 3D, 2A, 2B, 2C	Acceptable based on risk mitigation. It may require management decision
Acceptable Region	3E, 2D, 2E, 1A, 1B, 1C, 1D, 1E	Acceptable

Figure 2. Generalized Safety Tolerance Levels

B. Objectives

i. To identify the conditional variations of risk tolerance levels.

ii. To mathematically model the variations subjected to a generalized form.

iii. To introduce the cost benefit factors in supporting any type of airline through the derived model

iv. To suggest the optimal safty engagement achievable by any airline withrespect to its financial position.

IV. CONCEPTUAL FRAMEWORK

A. Unacceptable region - (Beyond High upper tolerable limit)

The range can be considered to be the standard specific upper limit where the disposition is limited to increment of the range under practical conditions. With respect to the organization policies, this range could be increased under the capacity to control the cost aspect in a higher range.

B. Tolerable Region - ALARP Principle

In accordance with the tolerable region, the upper limit can only be reduced with respect to the limitation of the unacceptable range and the lower limit could vary with either a positive or negative gradient (Jaiswal et al., 2018). With respect to the organization's focus on production and protection, this region could be kept at a reasonably practicable range according to the ALARP principle.

As Low as Reasonably Practicable or well known as ALARP principle signifies the economically viable and socially desirable range of safety. (Yasseri, 2013) In risk based safety management the range in favour and range in imminent failure is averaged from ALARP principle.

In generalized form the overall risk is defined as the summation over all conceivable vulnerabilities towards their respective consequences. Whereas, the ALARP depicts the pressure on the practical condition with respect

to cost and benefit to the operator in attaining safer operation. (Rus, 2021)

C. *Acceptable region (Below Lower tolerable limit)*

With the intervention of the direct and indirect cost factors, for the positioning of the acceptable range, the threshold may differ. The variance of the region may differ with respect to the capability of the organization to manage the secondary costs.

In retrospect, the experimental design could be developed in such a way as to model the variance of the upper tolerable threshold and lower tolerable threshold.

V. EXPERIMENTAL DESIGN

The following assumptions have been made in the derivation of a calculable model for the subject conditions.

i. The unacceptable region cannot be reduced from a set point due to the set hazardous margins by the manufacturer and unavoidable safety risks taken in general operations.
ii. The acceptable region cannot be zero as it is improbable to reach a hundred percent safe operational conditions.

The cost factor of the aircraft operation directly incorporates with the safety cost against the marginal profit towards the same. In set conditions higher profit margin will provide the organization to expand towards its safety expenses. The same conditions may vary among the threshold of risk mitigation without overlooking any and all factors.

The tolerability segmentation according to the operational safety may differ with respect to the engagement of the airline towards its safety assurance engagement. This could be varying from socio-economic factors to financial stability of the enterprise.

In this study the focus has been towards the general contribution measurmant by any scale of airlines to improve its safety. The contributing factor considered is the cost benefit towards tolerability region variation.

Prior to addressing the cost factor the tolerability variance is studied in this stage crossfitting the first two objectives as prior mentioned. Further, the qualitative cost condition is introduced to support the third objective of the study.

The variance of tolerability ranges can be signified under the following five conditions as per Table 3. While benchmarking the generalized model as per Figure 2, the differentiation between the conditions has been mathematically promoted by specifying the ALARP range in accordance with Table 3.

Table 3. Risk tolerance conditions

Generic Tolerance Levels	Condition 1
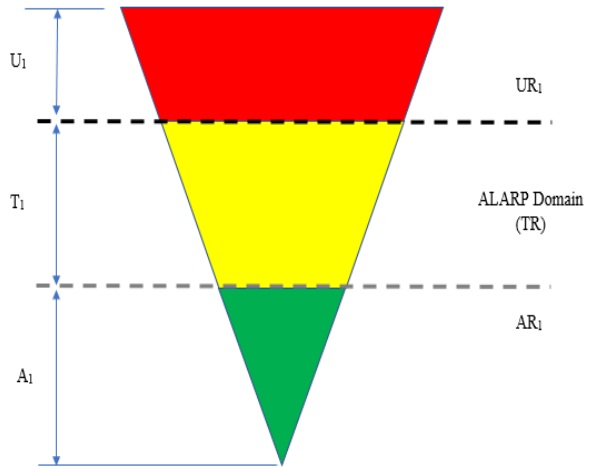	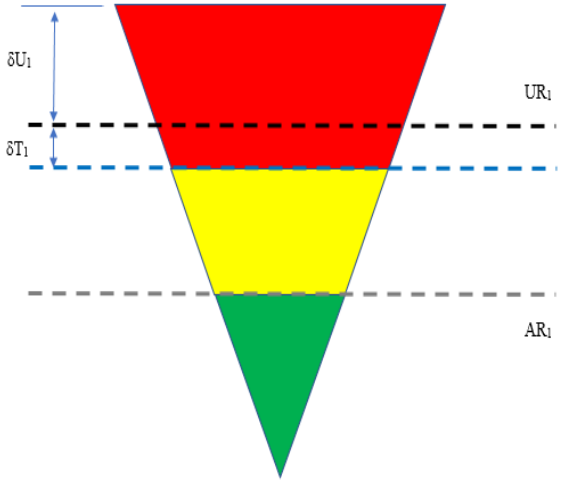
Condition 2	**Condition 3**
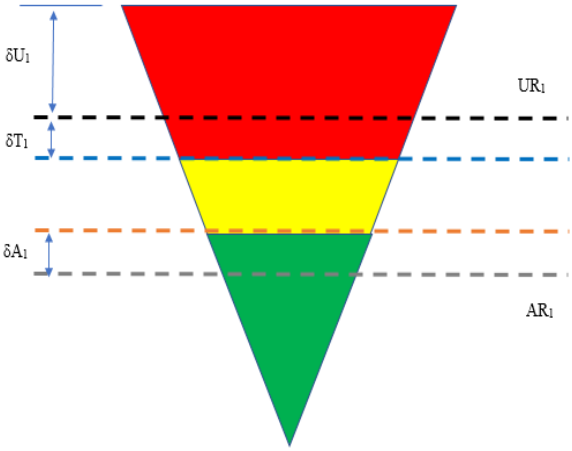	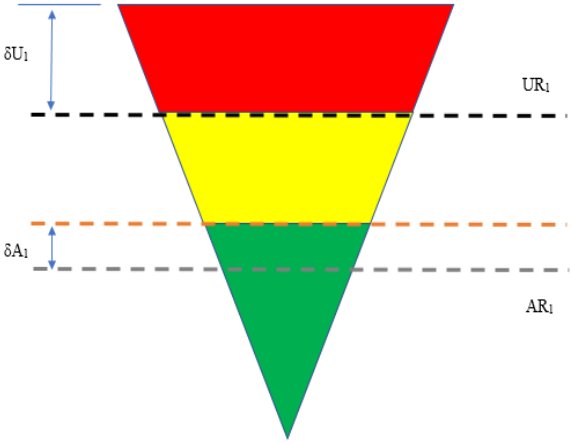
Condition 4	**Condition 5**
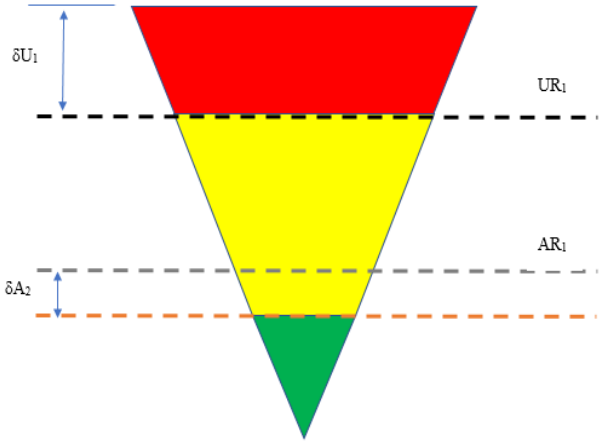	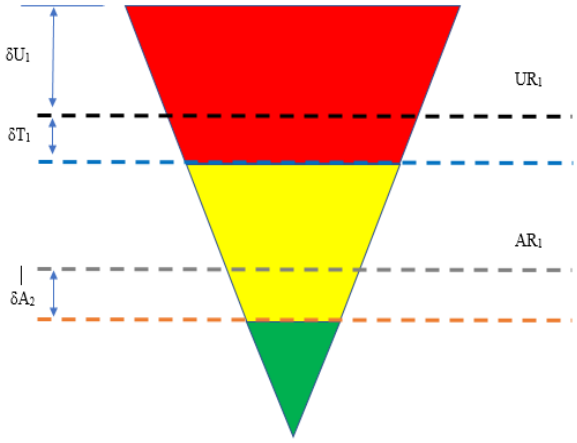

K. Nomenclature

UR_1 –Unacceptable Region tolerance level
TR (T_1) – Tolerance Range (ALARP Domain)
AR_1 – Acceptable Range tolerance level
U_1 – Unacceptable Range
A_1 – Acceptable Range

δU_1 – The change in Unacceptable Range
δT_1 – The change in Unacceptable Region tolerance level
δA_1 – The negative change in Acceptable level
δA_2 – The positive change in Acceptable level

L. Derivation

Considering the two base levels of ALARP Domain,

From UR1 base level δT_1 as (↓ +)

From AR1 base level δA_2 as (↓ +) and δA_1 as (↑-)

$f(TR) = T_1, \delta T_1, \delta A_1, \delta A_2$ ..... (1)

$\delta T_1 \geq 0$ ..... (2)

From generic ALARP principle,

$AR_1 - UR_1 = TR$ ..... (3)

From eqⁿ (1), eqⁿ (2) and eqⁿ (3)

For Condition 1,

$TR = T_1 - \delta T_1$ .....(4)

The primary means of variance for the generic model can be the increase of the unacceptable range while promoting a constant acceptable range. This will impact directly on the cost of safety depicting the limited expenditure and high liability.

For Condition 2,

$TR = T_1 - (\delta T_1 - \delta A_1)$ ..... (5)

The equilibrium state of the cost and tolerance can be depicted in this condition. The increase of unacceptable range and the safety cost that need to overcome the same may be balanced off. This can be done through the profitability incurred by increase of acceptable region in secondary means.

For Condition 3,

$TR = T_1 + \delta A_1$ .....(6)

With respect to safety wise secondary profit making the condition provide the best approach an airline may reach. The increase in acceptable range while sustaining the unacceptable range of generic operation depicts pure profit.

For Condition 4,

$TR = T_1 + \delta A_2$ ..... (7)

The initial condition of loss making portrays substantially from the reduction of the acceptable range while the unacceptable range stays consistent. This interprets the inability to generate revenue to support safety cost.

For Condition 5,

$TR = T_1 - (\delta T_1 - \delta A_2)$ ..... (8)

The poorest condition in terms of cost vs safety tolerance is contrasted by the increase of unacceptable region and the reduction of acceptable region. The unattainable safety cost with respect to revenue generation devices the scenario to be addressed under excessive means through cost benefit analysis.

Assuming,

$|\delta A_2| = |-\delta A_1| = \delta A$ ..... (9)

The general equation without the cost factor can be written as,

$TR = T_1 - (\delta T_1 - \delta A)$ ..... (10)

VI. DISCUSSION

The dominant factor of tolerance range variation with cost need to be derived with respect to each scenario and the type of operational properties. The derived general equation denotes the overall tolerance range of all scales of operators. This contemplates the optimal reference range to be the ALARP.

The forthcoming study will expand towards cost clustering towards safety expenses integrating with the generalized tolerance.

A. Cost Interaction

The cost interaction can be primarily derived among the tolerance regions with respect to the primary as well as secondary costs. Which could further clarify into safety assurance costs and post-incident costs.

i. Primary Costs

The costs pertaining to operation, quality, maintenance, labour, and Lease & Depreciation can be entailed as primary costs in aviation. In all

these aspects the safety cost of each is intertwined with the overall amount.

ii. Secondary Costs

The secondary costs occur in inefficient utilization of primary costs. These cannot be depicted directly in books but will reflect in long term financial performance and brand competition of the organization.

Some of the major secondary costs can be named as customer satisfaction, quality of operation, consumer confidence, and environmental effect.

The introduction of better exploitation of safety costs incorporated with the primary costs converges into reduction of the negative effect on the secondary costs.

iii. Safety Assurance Costs

In terms of safety assurance, the expenses an airline is willing to spend may differ on number of conformities. Safety assurance under each cost frame of the primary items may differ with company policies. This will develop the said generic tolerance levels that company will incorporate towards its operations. Which in terms depicts the company engagement in risk mitigation.

iv. Post-incident Costs

The post-incident cost does not necessarily mean the recovery of incidents or accident in which it is not only the turnaround or compensation. But the cost of recovery from a market breakdown and consumer contradiction.

B. Integration to Tolerance Levels

The overall ideology on the safety cost and tolerance ranges contrasts the following;

i. Unacceptable range

The higher the organization invests on the critical safety conditions the more stable the unavoidable safety hazards become. Which will then be limited to the safety threshold where any and all flights has to bargain in operation.

ii. Tolerable Region

The optimal variability stands on the tolerable region with respect to safety cost. This region is prone to the intentional variation of the operator with respect to the revenue generated.

iii. Acceptable Range

The increase of acceptable range brings the best option for the organization as it evidently brings the capita to cover the safety cost as well as reducing the secondary cost by developing consumer confidence on the brand.

VII. CONCLUSION

The aviation safety tolerance is directly intrigued by the cost of safety the organization is willing to spend. Which in ethical means, safety has been delivered as a vague unit. The Implied Cost of Averting Fatality (ICAF) is the key consideration in aviation where a certain level of risk being persevere towards economic gain.

Due to the vague nature of safety the optimization of the tolerance levels is critical.

The price worth paying concept demarks the ALARP principle for the range of tolerance.

Thus, the change in the safety tolerance levels can be optimized through the inclusion of cost to general equation through quantitative modelling under real time data simulation benchmarking residual.
The importance of enhancing the ALARP over the acceptable range with respect to cost could be promoted in qualitative means. This may validate through cost benefit analysis in a further macro scale.

This framework can be concluded as cost of achieving optimal life safety through risk reduction.

VIII. FUTURE STUDY

The introduction of cost factors when promulgating safety can be rationalized by identifying the correlation of cost of safety assurance. Thus, future study can be carried out by quantitatively analysing the cost of achieving different levels of safety assurance.

Furthermore, insurable expense reduction can be

calculated by risk liability management analysis. This could be curated by considering the surreal norm of post-accident assurance in aviation safety managment.

REFERENCES

Čavka, I. and Čokorilo, O. (2012) 'COST - BENEFIT ASSESSMENT OF AIRCRAFT SAFETY', International Journal for Traffic and Transport Engineering. City Net Scientific Research Center Ltd., Belgrade, 2(4), pp. 359–371. doi: 10.7708/ijtte.2012.2(4).06.

Cavka, I., Petrović, J. V and Cokorilo, O. (2014) '(PDF) Superjumbo Aircraft Safety: Cost - Benefit Assessment', in 17th Annual World Conference, Air Transport Research Society (2014 ATRS) World Conference. Bordeaux: Air Transport Research Society.

Čokorilo, O. et al. (2010) 'Išlaidos, patiriamos aviacijoje del nesaugumo', Technological and Economic Development of Economy. Taylor and Francis Ltd., 16(2), pp. 188–201. doi: 10.3846/tede.2010.12.

Fumero, S. (2018) AVIATION SAFETY Challenges and ways forward for a safe future. Brussels. doi: 10.2777/37074.

Jaiswal, K. et al. (2018) 'Safety culture in aircraft maintenance organizations of United Arab Emirates', 2018 Advances in Science and Engineering Technology International Conferences, ASET 2018. IEEE, pp. 1–7. doi: 10.1109/ICASET.2018.8376809.

Lališ, A. et al. (2018) 'Conditional and unconditional safety performance forecasts for aviation predictive risk management', IEEE Aerospace Conference Proceedings, 2018-March, pp. 1–8. doi: 10.1109/AERO.2018.8396648.

Rus, G. d (2021) (PDF) Introduction to Cost-Benefit Analysis: Looking for Reasonable Shortcuts. Second edition, 2021. 2nd edn. Camberley: Edward Elgar.

Smith, S. D. (2005) 'Safety management systems - New wine, old skins', Proceedings - Annual Reliability and Maintainability Symposium. IEEE, pp. 596–599. doi: 10.1109/RAMS.2005.1408428.

Song, K.-H. and Lee, D.-K. (2015) 'Study on Calculation Methodology for National Aviation Safety Cost', Journal of the Korean Society for Aviation and Aeronautics, 23(2), pp. 21–31. doi: 10.12985/ksaa.2015.23.2.021.

Xie, Z.-H. (2017) 'Air Operators' Safety Assurance System', ITM Web of Conferences. EDP Sciences, 12, p. 03026. doi: 10.1051/itmconf/20171203026.

Yasseri, S. (2013) (PDF) The ALARP Argument.

Zhang, Y. et al. (2018) 'Change Risk Management in Civil Aviation', Proceedings - 12th International Conference on Reliability, Maintainability, and Safety, ICRMS 2018, pp. 179–184. doi: 10.1109/ICRMS.2018.00042.

AUTHOR BIOGRAPHIES

Dr Thusitha Rodrigo is a passionate aeronautical engineer and a senior lecturer with more than 16 years of aviation experience with first-hand experience in the rotor and fixed-wing aircraft maintenance management including production planning, quality assurance, structural repairs, modifications and safety management. His aviation specific academic & research interests cover a diverse array of specializations including aviation maintenance resource optimization, engineering workforce scheduling, airline supplychain process improvement and aviation engineering education standardization.

Mr Dakshina Fernando who is a driven researcher in aircraft maintenance engineering have completed his Bachelors degree in 2018 and has been actively engaging in research related to the areas of aircraft maintenance resource management, aviation manpower and work efficiency optimization, aircraft controllability and performance enhancement and intelligent aircraft manouering. He is a fresher in the field of aviation with nearly 3 years of academic experience as an Instructor in aeronautical engineering.

Impacts of Changing Rainfall Patterns on Hydropower Generation: A Case Study of Kehelgamu Oya Sub-basin

RWMNT Lokubandara# and WCDK Fernando

Department of Civil Engineering, Faculty of Engineering, General Sir John Kotelawala Defence University, Sri Lanka

#nuwanthi5678@gmail.com

Abstract— Hydropower, the largest renewable energy source in Sri Lanka, generates approximately 50% of the total energy requirement. The annual electricity generation fluctuates greatly due to the variation of rainfall. Thus, the daily rainfall at Castlereagh and Norton stations of the Kelani River basin during the period 1960-2016 has been analysed on an annual, seasonal, and monthly basis. The aim of this research is to identify the impact of rainfall patterns on hydropower generation in Sri Lanka. Variability of the time series is assessed by detecting the trend using Spearmen's correlation coefficient test. Sen's slope estimator test was used to estimate the magnitude of the trend. Pearson correlation coefficient was used to find the relationship between rainfall and hydropower generation. A significant decrease in the annual rainfall and South-West monsoon rainfall observed at Norton and Castlereagh also shows a similar but not significant decreasing trend. A decreasing trend of monthly rainfall was also found at both stations. The results revealed that the future hydropower generation is in an alarming situation due to the decreasing trend of rainfall.

Keywords: ***climate variability, rainfall trends, Spearman's Rho trend test, Sen's slope, hydropower***

I.INTRODUCTION

Energy is one of the essential requirements in day-to-day life and hence surviving without energy would be a major challenge (Gray, 2017). On the way to sustainable development, Sri Lanka too considered energy as one of the focal points and thus took initiatives for ensuring access to affordable, reliable, sustainable and modern energy to all(GOSL, 2018). Nearly 50% of the national energy requirement of Sri Lanka is generated using renewable energy. According to Ceylon Electricity Board, main hydropower plants generated 34% and mini-hydropower plants generated 9% of the total capacity (CEB,2017). In general, there is a clear relationship between rainfall and hydropower generation; however, it was shown that hydropower generation would decrease due to climate change impacts especially in line with temperature and rainfall (Harrison & Wittington, 2002). Moreover, Beheshti *et al*., (2019) indicated that local studies are needed to study the climate change impacts on hydropower generation due to its regional behaviour.

Rainfall being one of the major factors on hydropower generation, Khaniya *et al.,*(2018) investigated the impact of rainfall on hydropower generation at Denawaka Ganga in Ratnapura district. Perera and Rathnayake (2019) also studied the climate variability and its effect on run-of-the-river hydropower plants in Ratnapura. These shows that local studies have been conducted in Sri Lanka at different locations.

The objective of this paper is to find the impacts of changing rainfall patterns on hydropower generation at plants located in Kehelgamu Oya, an upstream tributary of the Kelani river (Figure 1).

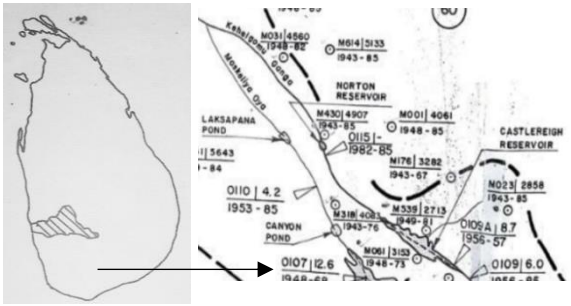

Figure 1. Study area in Kelani river basin
Source: CEB, 2014

This study covers two rainfall stations – Castlereigh and Norton - located in theKehelgamu Oya catchment. For both stations, daily rainfall data are available from 1960-2016 (57 years). The general

characteristics of the two stations are given in Table 1.

Table 1 - General Characteristics of Selected Stations

Station	Latitude (N)	Longitude (E)	Elevation (m)	Catchment area (km^2)
Castlereigh	06 50 40	80 36 00	1027	114
Norton	06 54 56	80 31 06	893	131

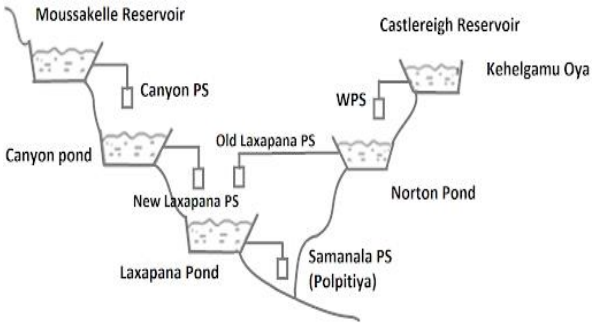

Figure 2. Reservoirs and hydropower plants at the study area
Source: http://www.laxapanacomplex.lk/oursys.html

Figure 2 shows that the Wimalasurendra power plant operates from rainwater collected at the Castlereigh reservoir and after the operation, water is collected at the Norton pond to generate power at the Old Laxapana power station (CEB,2017).

Rainfall variation is usually studied by detecting the trend pattern by using parametric or non-parametric tests. The parametric tests are not generally used for trend detection due to non-normality data series which is common in most hydro-meteorological data(Beheshti*et al.*, 2019). The use of non-parametric tests has been used in Sri Lanka at different locations for annual, seasonal and monthly time series(Alahacoon & Edirisinghe, 2021; Wickramaarachchi *et al.*, 2020).

A non-parametric test, Spearman's Rho (SR) or Spearman rank correlation method is widely used by many researchers to detect a trend in rainfall series(Ahmad *et al.*, 2015). More details on the SR test can be found in Dahmen & Hall (1990). Sen's slope method is generally used to estimate the magnitude of the slope of the data series (Khaniya *et al.*, 2018).

II. METHODOLOGY

Daily rainfall data at Castlereigh and Norton rainfall stations were collected for 57 years from 1960 – 2016 from the Department of Meteorology. After screening the rainfall data, annual, monthly and seasonal data series were prepared. The seasonal data series were prepared as North-East monsoon (NEM) from December to February, 1st Inter monsoon (1stIM) from March to April, South-West monsoon (SWM) from May to September and 2nd Inter monsoon (2ndIM) from October to November.

SR test was used to identify the trend pattern of the above data series. The rank correlation coefficient, R_{sp} is defined as follows:

$$R_{sp} = 1 - \frac{6\sum_{i=1}^{n} D^2}{n(n^2-1)} \quad (1)$$

where n is the total number of data, D is the difference between ranking, $D = K_{xi} - K_{yi}$, K_{xi} is the rank of the variable, in which x is the sequential order number of the observations and K_{yi} is the rank of the variable (y) in which y is the rank.

rainfall series in the ascending order of magnitude. The standardized test statistic is given in equation (2) (Dahmen and Hall, 1990),

$$t_t = R_{sp}\left(\frac{n-1}{1-R_{sp}^2}\right)^{0.5} \quad (2)$$

where t_t has student t-distribution with v= n-2 degree of freedom. A positive value of t_t shows an increasing trend while a negative t_t describes a decreasing trend. At a significance level of 5%, the two-sided critical region t_t is bounded by (Dahmen and Hall, 1990), $t\{v,2.5\%\} < t_t < t\{v,97.5\%\}$ and for a 57- year data series t_t should lie between -2.005 and 2.005.

To predict the magnitude of the slope of the rainfall time series,Sen's slope method was used(Perera and Rathnayake,2019).

$$d_k = \frac{(X_j - X_i)}{(j-i)} \quad (3)$$

For (1<i<j<n), where d_k is the slope, X_i and X_j are data values at time i and j, respectively, and n is the number of data. The median of n values of $d_k$is given as Sens slope estimator (Q_i) and given by,(Perera and Rathnayake,2019)

$$Q_i = \begin{cases} d\_((n+1)/2) \text{ (n is odd)} & (4) \\ \frac{1}{2}\left(d_{\frac{n}{2}} + d_{\frac{n+1}{2}}\right) \text{ (n is even)} \end{cases}$$

Due to the limitations of getting hydropower generation data, the rainfall-runoff graph method was used to estimate the generated hydropower during 2006- 2016 as explained by Harvey (1993). Finally, the Pearson correlation coefficient method is used to find the correlation between annual rainfall and hydropower generation data.

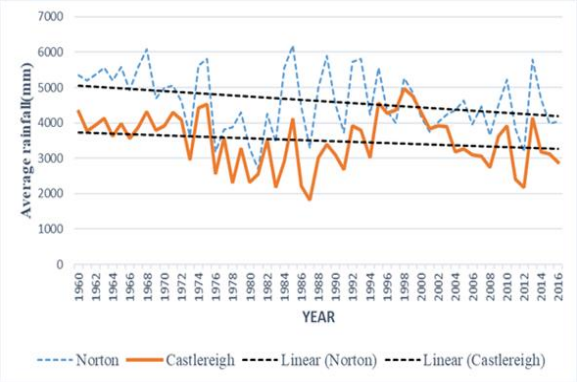

Figure 3. Annual rainfall trend analysis at Norton and Castlereigh

III. RESULTS AND DISCUSSION

The annual rainfall of 57 years at Norton and Castlereigh are shown in Figure 3 with the linear trend analysis. Figure 3. Annual rainfall trend analysis at Norton and Castlereigh

During the selected period, the maximum annual rainfall at Castleriegh and Norton is 4966 mm in 1998 and 6179 mm in 1985 respectively. The minimum annual rainfall observed at Castleriegh and Norton are 1812 mm in 1987 and 3291 mm in 1980 respectively. The annual average rainfall during the study period was 3499mm at Castlereigh and 4613mm at Norton.

Tables 2 and 3show the summary of trend analysis test results for the time series of selected rainfall stations for annual and seasonal rainfall respectively.

Table 2. Results of trend analysis for annual rainfall

Station	Test	Annual	Annual (1960-1987)	Annual (1988-2016)
Castlereigh	t_t	-1.51	**-3.77***	-1.77
	Q_i	-10.5	-14.6	-6.4
Norton	t_t	**-2.36***	**-2.47***	**-2.88***
	Q_i	-17.7	-10.5	-14.5

*Significant trends

Table 3. Results of trend analysis for seasonal rainfall

Station	Test	NEM	1st IM	SWM	2nd IM
Castlereigh	t_t	-0.37	0.23	-1.89	-1.24
	Q_i	-0.63	0.22	-9.19	-2.12
Norton	t_t	-1.31	-0.47	**-2.62***	-0.43
	Q_i	-1.74	-1.01	-14.67	-0.77

*Significant trends

At a significance level of five percent, the two sided critical region t_t is bounded by, $t\{v,2.5\%\} < t_t < t\{v,97.5\%\}$ and for a 57 years of data, $-2.005 < t_t < 2.005$.

Significant decreasing trends on annual and SW monsoon rainfall were observed at Norton. Although Castlereigh shows a somewhat decreasing trend on annual and SW monsoon rainfall, it is not significant at the 95% confidence level.The highest slope of the trend of annual rainfall was found at Norton as -17.7 mm/year. The maximum slope for decreasing trend of seasonal rainfall was indicated as -14.67 mm/year at SW monsoon season of Norton.Having observed the significant decreasing trend in annual rainfall, the analysis was extended by splitting the time series into two series from 1960 – 1987 and 1988 - 2016. It was clearly seen that both subsamples at Norton demonstrated a significant decreasing trend. However, at Castlereigh, a significant trend was observed only in the first subsample.

In general, the SW monsoon provides the major portion of the annual rainfall in the wet zone of Sri Lanka and therefore, the decrease in SWM rainfall indicates a regional climate variation.

The trend analysis was further carried outconsidering monthly time series and the results are indicated in Table -4.

Table 4. Trend results for Monthly rainfall

Month	Castlereigh		Norton	
	t_t	Q_i (mm/month)	t_t	Q_i (mm/month)
January	-0.20	-1.06	-0.09	-0.60
February	-0.96	-0.59	-1.78	-1.19
March	0.92	0.45	-0.67	-0.37
April	0.04	-0.19	-0.81	-0.74
May	-0.38	-0.68	-0.74	-1.68
June	-0.25	-0.35	-1.14	-2.35
July	-1.68	-2.61	-1.62	-2.94
August	**-3.05***	-3.19	**-2.14***	-3.66
September	-1.17	-1.82	**-2.16***	-4.18
October	-1.63	-2.05	-0.98	-1.02
November	-0.06	-0.105	0.49	0.71
December	0.03	-0.02	0.01	-0.04

*Significant trends

Table 4 clearly shows that a significant trend was detected at both stations in August. Further, Norton shows a significant trend during September too. Although the test statistic is not significant during July for both stations, it indicates more towards a significant negative trend. Monthly rainfall results clearly demonstrated the decreasing trend during SW monsoon rainfall. In contrast, a small-scale positive trend occurs during March to April (1st IM) at Castlereigh and the same scale upward trend in November and December at Norton. The highest slope of decreasing trend, (-4.18 mm/month) was observed in September at Norton.

The correlation between annual rainfall and the generated hydropower is illustrated in Figure 4. The results show that the correlation is 0.96 considering both stations.

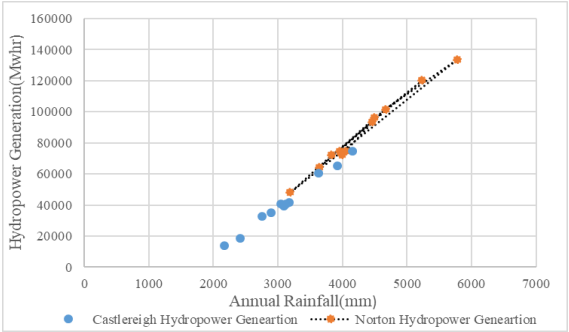

Figure 4. Hydropower generation over the annual rainfall

IV.CONCLUSION

This study investigated the trends in annual, seasonal and monthly rainfall using the Spearman's Rho test from 1960 to 2016 at Castlereigh and Norton rainfall stations in Kehelgamu Oya basin, which is a major tributary of the Kelani river. The magnitude of the trend was estimated using Sen's slope method. The trend results of the annual series showed a downward trend at both stations however at Norton, it was a significant trend. Although the South West monsoon greatly contributes to the annual rainfall, the findings emphasized that there is a significant reduction in the seasonal rainfall. The magnitude of the maximum decreasing seasonal trend was -14.67 mm/season at South-West monsoon while the maximum increasing trend was 0.22 mm/season at 1st Inter Monsoon period.

According to the results, an alarming situation can be anticipated in future for hydropower generation due to significant decreasing trends on annual and south-west monsoon seasonal rainfall. The correlation between rainfall and hydropower generation may be changed with the availability of monthly generated hydropower data.

REFFERENCES

Ahmad, I., Tang, D., Wang, T., Wang, M., and Wagan, B., (2015)Precipitation Trends over Time Using Mann-Kendall and Spearman's rho Tests in Swat River Basin, *Advances in Meteorology*, 2015, https://doi.org/10.1155/2015/431860

Alahacoon, N. and Edirisinghe, M. (2021)Spatial Variability of Rainfall Trends in Sri Lanka from 1989 to 2019 as an Indication of Climate Change. ISPRS *Int. J. Geo-Inf.*, 10, 84. https://doi.org/10.3390/ijgi10020084

Beheshti, M., Heidari, A., Saghafian, B., (2019)

Susceptibility of hydropower generation to climate change: Karun III Dam case study. *Water* (Switzerland) 11. https://doi.org/10.3390/w11051025

Ceylon Electricity Board (CEB)(2014). CEYLON ELECTRICITY BOARD Supply Services Code.

Ceylon Electricity Board (CEB) (2017) Sales and generation data book 2017, Statistical Unit Corporate Strategy & Regulatory Affairs Branch.

Dahmen, E.R., and Hall, M.J., (1990)Screening of hydrological

data: Tests for stationarity and relative consistency, *International Institute for Land Reclamation and Improvement,* 49, https://edepot.wur.nl/71119

Government of Sri Lanka (GOSL) (2018) Voluntary National Review on the status of implementing the Sustainable Development Goals, *Ministry of Sustainable Development, https://sustainabledevelopment.un.org/content/documents/19677FINAL_SriLankaVNR_Report_30Jun2018.pdf*

Gray, R. (2017)The biggest energy challenges facing humanity, *Futurehttps://www.bbc.com/future/article/20170313-the-biggest-energy-challenges-facing-humanity*

Harrison, G. P. and Whittington, H. W. (2002) Susceptibility of the Batoka Gorge hydroelectric scheme to climate change, *Journal of Hydrology,* 264, 230-241.

Harvey, A. (1993) Micro-hydro design manual:a guide to small-scale water power schemes, London.

Khaniya, B., Priyantha, H.G., Baduge, N., and Rathnayake, U., (2018). Impact of climate variability on hydropower generation : A case study from Sri Lanka. ISH J. Hydraul. Eng. 00, 1–9. https://doi.org/10.1080/09715010.2018.1485516

Perera, A. and Rathnayake, U. (2019) Impact of climate variability on hydropower generation in an un-gauged catchment : Erathna run-of-the-river hydropower plant, Sri Lanka. Appl. Water Sci. 9, 1–11. https://doi.org/10.1007/s13201-019-0925-9

Royal Geographical Society, 2019 A Guide to Spearman's Rank 20–23.

Wickramaarachchi, W.W.U.I., Peiris, T.U.S. and Samita, S. (2020) Rainfall Trends in the North-Western and Eastern Coastal Lines of Sri Lanka Using Non-Parametric Analysis. *Tropical AgriculturalResearch*,31(2):41-54.

ACKNOWLEDGEMENT

The authors wish to thank the officials of the Department of Meteorology for their assistance in supplying the relevant data.

AUTHOR BIOGRAPHY

[1]Author graduated with BSc Engineering degree in Civil Engineering from General Sir John Kotelawala Defence University, Sri Lanka.

[2]Author is a senior lecturer of Civil Engineering at General Sir John Kotelawala Defence University, Sri Lanka. She graduated with BSc Engineering degree in Civil Engineering and also received MEng and PhD degree in Civil Engineering from the University of Moratuwa, Sri Lanka.Her research interests include Water Resources Management, Dam safety and Engineering Education.

Identifying Current Trends in Source Selection of Household Water Use in Pohaddaramulla, Kalutara

ETD Ediriweera# and NK Gunasekara

Department of Civil Engineering, Faculty of Engineering, General Sir John Kotelawala Defence University, Sri Lanka

#tharakaediriweera@gmail.com

Abstract— Sri Lankan Drinking Water Supply Policy is committed for the sustainable use of drinking water, while addressing reliability and safety of the resource. . In this research, trends in the selection of water sources for household use in Pohaddaramulla area are addressed. Tube wells, open wells, and mains supply from the National Water Supply and Drainage Board (NWS&DB) are the main water sources used in the area. However, some areas are not covered by the NWS&DB services as yet. Various trends in selecting water sources by the consumers are found. Ground water sources are used while using the mains supply. Data collected through a questionnaire, rainfall data, evapotranspiration data, runoff calculations, and various other sources were used to analyse the current trends and identify their sustainability. Several types of trends are found in this area. Out of the families that use mains supply, 35% is using the mains supply as their only source of water. Remaining 65% uses other water sources while using the mains supply. A 40% of the sample does not use the mains supply. From them, 66% uses tube wells and 31% uses open wells with pumping. Only 3% of them uses tube wells and open wells. Our analysis points out that the current trend is not sustainable even at present. In the future, it will not be sustainable as the ground water demand by the residents cannot be fulfilled by the current conditions. There is no recharge to the ground water storage. Therefore, alternative water sources are needed. Also, there is a risk of saltwater intrusion. These issues can be further studied in the future researches. The information obtained from this study can be used by NWS&DB for planning the extension of service area.

Keywords: water sources, tube wells, open wells, mains supply, ground water

I. INTRODUCTION

As one of the most consumed resource by the mankind, water is becoming scarcer. With the development and the increase of population this has become a great concern. Many factors have to be considered when using water for various purposes. Also, various sources of water are available. In this research, water sources used in the Pohaddaramulla area are discussed. Pohaddaramulla is a village in the coastal belt of Sri Lanka which belongs to the Kalutara district. Population is around 750 families (2700 people).

Different water sources are used in Pohaddaramulla. Mainly, mains supply for most of the houses. There is a preference of using tube wells over open wells even when the mains supply connection is there. These trends may be unsustainable as the ground water usage is more. As ground water takes time to replenish, there is danger of saltwater intrusion. Not many researches are found on selection of water sources other than Kaleel (2017). Ground water quantification is not available in previous studies often.

Demand for ground water has not been addressed much. Therefore, a study on these matters was necessary. Research area is limited to Pohaddaramulla village. Household water usage is only considered for this study.

Objectives

- To compare the trends in selection of water sources used in the area.
- To find why tube wells are preferred over the other sources.
- To find why the tube wells are used even when there is the mains supply from the NWS&DB.
- To find the sustainability of the current trends considering the population increase.

II. LITERATURE REVIEW

Research studies have been carried out regarding water sources and their sustainability. Water sources like tube wells and open wells are described in these studies. They discuss about the ground water; about the quality of the water. Issues occurred when using wells as water sources.

The research carried out by Dharmaratna and Parasnis (2012) presents an analysis of the cost structure of the pipe borne water supply in Sri Lanka. The total cost is the addition of operating cost for the capital expenditure. Operating cost is the short run cost which is the sum of monthly expenditure on labour, chemical, electricity, maintenance and other costs. They are not restricted by any authority. Ground water can be drawn for any purpose and no charges are levied for that. This analysis assumes that the operational cost for different districts does not vary substantially. The other fact is that NWS & DB does not charge for extracting raw water, which should be added. By this analysis it could be seen that the all the marginal cost for the water supply are higher than the current average volumetric charges. Thus, water is under-priced in Sri Lanka. Although Sri Lanka receives average annual rainfall of 1850 mm, there is not enough water for drinking because the water supply is not managed properly. Only 14% of the rural area receive the mains supply from the NWS & DB (Dharmaratna and Parasnis, 2012).

In the article published by Kaleel (2017), it is mentioned that there is an increase in the pipe borne water consumption by the residents in the Panadura area for household work. Pipe borne water is preferred over the other water sources. This depends on factors such as population, lifestyle changes and modern machinery utilization. As it shows, water consumption for water for various purposes are as follows. Washing clothes – 22.26%; bathing – 23.27%; washing utensils – 16.67%; cooking – 8.17%; drinking – 9.84%; sanitary – 15.77%; watering home garden – 4.03%. Rise in the pipe-borne water consumption depends on income level increment (Kaleel, 2017).

Research by Boone, Glick and Sahn (2011) presents the choices of water sources and time allocation for water collection in a rural area. Choices of water sources depend on many household characteristics and distance to source as well. The time spent to collect water varies with gender, age, and distance to water. Household's choice of water source is sensitive to the distance. The water sources are used by the people, when the distance to the water source decreases. There is a relationship between the distance to the water source and the time spent for collection by individual household members. Factors like quality and quantity are not discussed(Boone, Glick and Sahn, 2011). Another study by Arouna and Dabbert (2009) analyses the factors determining the use of water sources in rural areas in Benin, Nigeria. The differences and similarities between the purchased water sources and free water sources are described. Purchased water demand is price in elastic due to the scarcity of water. Size and the composition of the household, access to water sources, income and time used for fetching water; are the determining factors for choosing water sources. But these factors can be challenged due to the reasons like seasons, policy changes and household types.(Arouna and Dabbert, 2009)

III. METHODOLOGY AND EXPERIMENTAL DESIGN

A.Data used for the study

Population data were gathered from the Grama Niladhari. A brief introduction about the village and trends of using water sources were gathered. Observations were made by visiting the village.
The main source of data was the questionnaire survey. Information regarding identifying the trends and factors determining the selection of water sources were found using the data from the questionnaire survey. Rainfall data were obtained from the Department of Meteorology which were used to calculate the rainfall trend. The ground water calculations were done by using these data.

B.Methodology adopted

First, the data was gathered from the Grama Niladhari. Brief idea of the village and water sources and trends were taken from him. Also, population data were gathered to plot the population trend.

Questionnaire survey was carried out to obtain the data for the analysis of the trends. It consisted of 40 questions and two main section for the people who uses mains supply and who does not. Both open ended and closed ended questions were used. Sample size was 58 families. Questionnaire was translated to Sinhala for ease in understanding. Residents were interviewed personally, and their responses were noted.

Questionnaires were analysed, and classified qualitatively and quantitatively using MS Excel software. Population trend and rainfall trend were also obtained. Data from the questionnaire survey and the visits, were used in creating the map in Google Earth Pro software. Boundary, area and mains supply distribution area were clearly marked on the map. Locations of houses of the residents who participated for the survey were marked as shown in the figures in the results chapter.

The net annual replenishment of the ground water available is calculated in order to find the

sustainability of using ground water in the area. Water balance principle is used for this calculation (Zhang, Walker and Dawes,2002).

$$\Delta S = P - I - ET - RO - DD \ldots\ldots\ldots (1)$$

ΔS	=	Change in the ground water
P	=	Precipitation
I	=	Interception loss
ET	=	Evapotranspiration
RO	=	Surface runoff
DD	=	Deep Drainage

Here it is assumed that the interception loss is negligible as the calculation is done for a long period of time (a year).

Deep drainage is a small percentage of the precipitation. Roughly about 5% (Zhang, Walker and Dawes, 2002). Therefore it is not been taken for the calculation.

$$\text{Ground water contribution} = P - RO - ET \ldots\ldots (2)$$

Precipitation is taken form rainfall data gathered. Evapotranspiration values are found using the nearest river basin. Evapotranspiration value of Kalu Ganga river basin is 1315mm for the year (Bastiaanssen and Chandrapala, 2003).
Runoff is calculated using the rational method.

$$Q = CIA/360 \ldots\ldots\ldots (3)$$

Runoff is given as a volume per unit time. This value is then converted to annual runoff volume, to be used in the water balance equation where the evapotranspiration and the rainfall are taken in volumes. This represents the water surplus or deficit clearly. Runoff coefficient is taken considering the soil type and topography. It is 0.4 for Pohaddaramulla area as the soil is sandy loamy and a residential area (Najim). Rainfall intensity is given in the rainfall data. The village area is taken as the catchment area, which is found using the Google Earth Pro software.
Net annual groundwater replenishment is considered here, as the remainder, from the ground water contributed to the selected area from rainfall, after the usage by the residents.

$$\textit{Net annual groundwater replenishment} = \textit{Ground water contribution} - \textit{Ground water usage} \ldots\ldots\ldots (4)$$

Ground water usage should be calculated to find the net annual groundwater replenishment. For this total water usage and mains supply water usage are found.

$$\text{Ground Water usage by the residents} = \text{Total water usage} - \text{Mains supply usage} \ldots\ldots\ldots (5)$$

$$\text{Total water used} = \textit{per person water consumption x population}\ldots (6)$$

Per person water consumption is taken as 135 l per day. (*The Sundaytimes*, 2013). This value ranges from 100 l to even 600 l depending on factors and region (Lo, Wong and Mui, 2018). This value is relevant to our region. Assumptions were made as to whether this value is not changing for gender or age, and stays the same for future years.
Mains supply water usage is found using the average mains supply water usage in a family.

$$\text{Amount of water used in a family} = \text{No. of units used in a house} \ldots\ldots (7)$$

$$\text{Amount of water used by the mains supply} = \text{water usage in a family x no. of families} \ldots\ldots\ldots (8)$$

Average monthly water bill for a house is calculated. From that the number of units of water used is found by referring to the water tariff (Prins, 2009).That amount is considered constant for every month and for the future years as well. Volume of water usage per house is calculated. The number of families are found using the population data. Number of members in a family are found from the questionnaire survey. Average number of members in a family is calculated as five (5) members and considered same for the future. Number of families change as per the change in population. From these values net annual groundwater replenishment (equation 4) could be found. Projections of the data were estimated assuming linear trends from 2017 to 2022 and 2027.

IV. RESULTS AND DISCUSSION

Results of the analysis done with the questionnaire survey, the calculation for the ground water availability and the results from the Google Earth software are discussed here.

A. Results from the questionnaire analysis

From the chart below, it is obvious that the other water sources are used by the majority (60%) of the population. Mains supply is used by only 40%. Other

water sources are used by the residents, where there is no connections to the mains supply.

Other water sources are used while having the mains supply by 65 % of the families. Mains supply alone is used by only 35% of the families. The trend in the present is using other sources while having the mains supply. Sustainability of this trend is identified through this research.

Those who do not use the mains supply, uses other water sources to fulfil their needs. Those water sources and their usage by the residents are presented in the chart below. These people use either tube wells or open wells. All these people use those wells with a pump. From that 66% use tube well with a pump. 31% use open well with a pump.

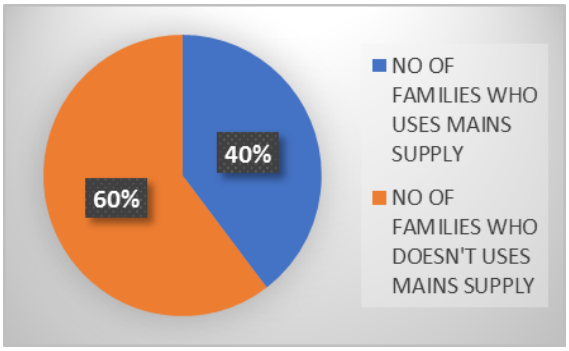

Figure 2. Usage of mains supply by the residents

Minority of 3% use both well and tube well for their water consumption.

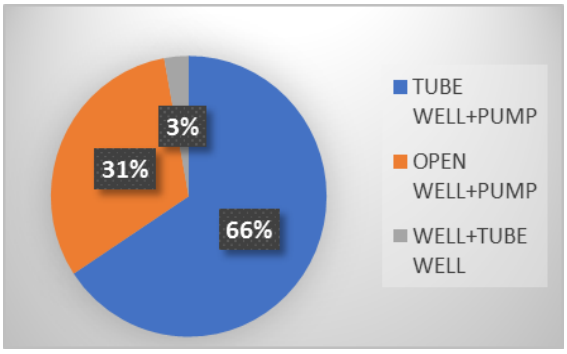

Figure 2. Use of other water sources while using the mains supply

As mentioned below, other sources are used while using mains supply. Type of water sources used with the mains supply are mentioned in the chart below. Tube with or without the pump are used by 60%. Pumps are used to lift water from the wells as it is easier than manually. These are some trends found in the area.

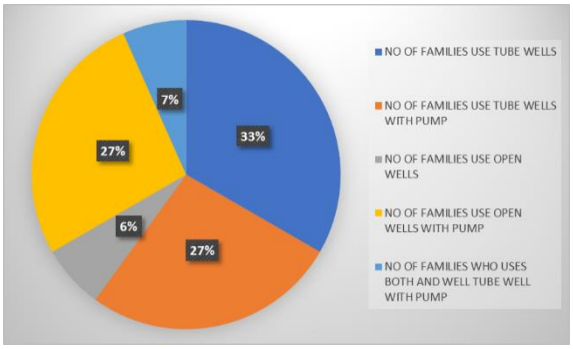

Figure 1. Use of other water sources while using the mains supply

B.*Results from the Google Earth Pro software*

The following are the results obtained by the data analyzed using Google Earth Pro software. Using its tools, boundary and the Area of Pohaddaramulla village found. Regions where the mains supply connections are laid were marked. GIS Locations of the residents who participated for the survey are marked. Rainfall trend is obtained as shown below. Annual rainfall data have been used to plot this graph. As seen in figure 7, there is a reducing trend with time. That means the rainfall is decreasing with time. As per the trend line, rainfall is likely to reduce further in the future.

Figure 4. Area of Pohaddaramulla village

Figure 5. Regions according to the availability of mains supply

Figure 6. Locations of the residents who took part in the survey

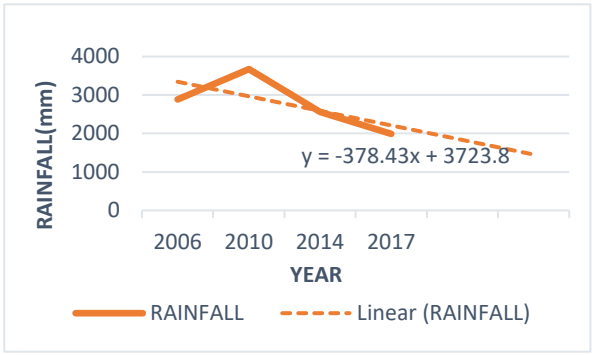

Figure 7. Rainfall trend in Pohaddaramulla Area

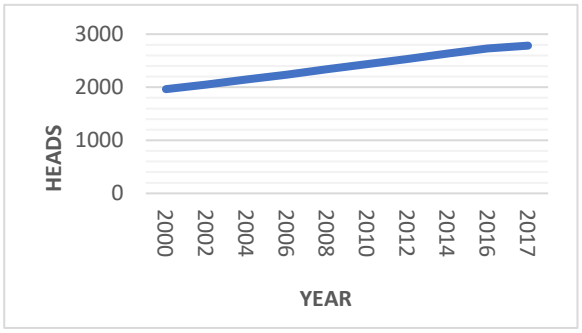

Figure 8. Population trend in Pohaddaramulla Area

Population chart of the Pohaddaramulla area is given in figure 8. This is plotted using the population data from the year 2000 up to 2017. There is an increasing trend of 48 heads per year on average. This will increase further in the future, as the trend increases with time. Population in 2017 is 2784.

iv. Results of the calculation of ground water contribution

Ground water usage in 2017, 5 years and 10-year time are mentioned in the Table 1. This gives the results of the calculation of ground water usage annually. It represents the future values for 5 and 10 years ahead. It is visible that the usage is increasing due to the population increase.

Table 1. Ground water usage of the people in Pohaddaramulla

Years	Population	No. of houses	Total water usage(m^3)	Mains supply usage(m^3)	Ground water usage(m^3)
2017	2784	557	137181.6	58798.1	78383.5
2022	3831	766	188810.8	80927.1	107883.7
2027	4059	812	200034.6	85737.8	114296.8

Run off volume for 2017 is calculated using the Rational method. Runoff volume is taken to compare it with the precipitation and evapotranspiration volumes in the water balance equation.

Table 2. Runoff volume with respect to time

Years	Rainfall (mm)	Rainfall Intensity	C	A(ha)	Runoff (m^3/s)	Runoff Volume $x10^3$ (m^3)
2017	1990.1	0.227	0.4	103.58	0.0261	824.54
2022	652.4	0.074	0.4	103.58	0.0085	270.30
2027	206.5	0.024	0.4	103.58	0.0027	85.56

Table 3. Ground water available

Year	Runoff Volume $x10^3(m^3)$	Rainfall volume $x10^3(m^3)$	Evapotranspiration volume $x10^3(m^3)$	Ground water contribution$x10^3(m^3)$
2017	824.54	2061.38	1362.09	-125.26
2022	270.30	675.77	1362.09	-956.63
2027	85.56	213.90	1362.09	-1233.76

Table 4. Ground water contribution

Year	Ground water contribution $x10^3$ (m^3)	Ground water usage $x10^3$ (m^3)	Net annual groundwater replenishment $x10^3$ (m^3)
2017	-125.26	78.38	-203.64
2022	-956.63	107.88	-1064.52
2027	-1233.76	114.30	-1348.06

As shown in Table 4, remaining volume of ground water after the usage is a deficit. This deficit is increasing with the time is shown in the Figure 9. In this case, what will be extracted by residents will be the paleo-groundwater in underground aquifer systems, which is unarguably unsustainable.

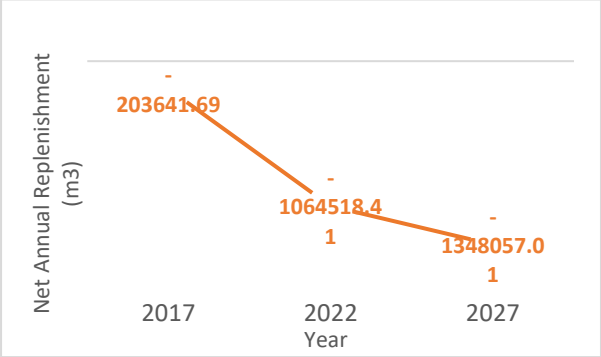

Figure 9 Variation of net annual ground water replenishment with time

V. CONCLUSION

This study was done to find out the current trends in source selection in Pohaddaramulla area. Comparison among the current trends is done in parallel. Rainfall data, population data, data from the questionnaire survey are used in the study. Visits to the village and identifying the water sources was also useful in getting a clear idea on this study. MS Excel software is used in analysing the questionnaire survey and plotting the rainfall and population trends. Calculations were done to find the sustainability of the current trend of using ground water with the mains supply.

From the study, several conclusions regarding these matters were obtained. Mains supply is used by minority of 40% of the population. Ground water sources are used by 60%. Other sources are used while using the mains supply by 65% of the population. Cost effectiveness and easiness of usage at failure of the mains supply are main reasons behind this trend. Mains supply alone is used by 35%. Tube wells are preferred over the open wells because of the less space required and easiness in handling.

From the calculations, it is obvious that the current trend is unsustainable. At the end of the year, the change in the storage is a deficit. Higher runoff and evapotranspiration volumes are the reasons for this case. Ground water is drained from the storage rather than recharging. This will worsen in the future with the current conditions. Then there occurs a danger of saltwater intrusion since this area is in the coastal line. However, the paleo-groundwater in underground aquifers were not considered in fulfilling the demands, as this data is unavailable for the region and for most parts of the country. Even if these unrenewable resources were considered, still the ground water usage in the area can be considered to become unsustainable. It will only be a question of when it will become a deficit.

Rainwater harvesting could be a good solution for this issue. It will reduce the ground water usage. Studies developing solutions to afore-mentioned issue can be carried out in the future.

ACKNOWLEDGEMENT

The assistance given by the Gama Niladhari of Pohaddaramulla, in providing the guidance and information is appreciated. The Meteorological Department is acknowledged for providing the data necessary as well.

REFERENCES

Arouna, A. and Dabbert, S. (2009) 'Determinants of domestic water use by rural households without access to private improved water sources in Benin : A Seemingly Unrelated Tobit', (September 2009), pp. 1–17. doi: 10.1007/s11269-009-9504-4.

Bastiaanssen, W. G. M. and Chandrapala, L. (2003) 'Water balance variability across Sri Lanka for assessing agricultural and environmental water use', 58.

Boone, C., Glick, P. and Sahn, D. E. (2011) 'Household Water Supply Choice and Time Allocated to Water Collection : Evidence from Madagascar Collection : Evidence from Madagascar'.

Dharmaratna, D. and Parasnis, J. (2012) 'An analysis of the cost structure of water supply in Sri Lanka', *Journal of*

the Asia Pacific Economy, 17(2), pp. 298–314. doi: 10.1080/13547860.2012.668092.

How much water does an urban citizen need? | The Sundaytimes Sri Lanka (2013). Available at: http://www.sundaytimes.lk/130217/education/how-much-water-does-an-urban-citizen-need-32913.html (Accessed: 22 October 2018).

Kaleel, M. I. M. (2017) 'Pipe-borne water consumption and its wastage: A study based on Panandura Urban Area in Sri Lanka', *World Scientific News*, 66, pp. 250–262

Lo, Y. F., Wong, L. T. and Mui, K. W. (2018) 'Mosaic analysis for personal water consumption in residential buildings in Hong Kong Mosaic analysis for personal water consumption inresidential buildings in Hong Kong', pp. 0–5.

Najim, P. M. M. M. 'Runoff', pp 14-16.

Prins, B. (2009) 'Handbook for water consumers', pp 8.

Zhang, L., Walker, G. R. and Dawes, W. R. (*2002*) 'Water Balance Modelling : Concepts and Applications', (84), pp. 31–47.

ID 567

Impact of COVID-19 Lockdowns on Air Quality in the South Asian Region

MT Gunasekara# and VS Waraketiya

Department of Civil Engineering, Faculty of Engineering, General Sir John Kotelawala Defence University, Sri Lanka

#thyaga5@hotmail.com

Abstract— Air pollution has become a common problem in most urbanized cities in the world. South Asia is a pollution hot spot since most countries in the region qualify to be categorized as developing nations with poor monitoring and control of industrial-related pollution. The recent outbreak of the COVID-19 pandemic led many countries to lock-down to control the spread of the virus. This resulted in the complete shut-down of most sources of industrial emissions and a heavy reduction in vehicular emissions. Accordingly, most South Asian countries witness a notable reduction in air pollution and significant improvement in air quality. This study measures and compares the change in pollution levels in the first six months of 2020 while using 2018, and 2019 as points of reference. The analysis includes an investigation of daily, weekly, and monthly trends of air pollution concentrating on PM2.5 levels in six countries of the region. Based on the observations of the analysis, significant factors affecting the level of change in air quality were identified. Most cities recorded significant change in the pollution level only after 30 days into the lockdown while the Source of pollution, topography, and location were identified as the main factors which affected the dispersion rate of pollution.

Keywords: ***air pollution, COVID-19, Sri Lanka, South Asia***

I. INTRODUCTION

Most countries in the south Asian region qualify as developing countries consisting of low or middle-income attributes. As history suggests the cost of development includes heavy adverse impacts on the surrounding environment. Air pollution and worsening of Air Quality have been a constant headache in the region. According to IQAir report on global air quality, 18 out of the top 20 most polluted cities in the world are from the South Asian region (AirVisual, 2019). According to expert research, most of the pollution in the region occurs in the form of particulate matter (Hopke *et al.*, 2008; Aryala *et al.*, 2009; Begum and Hopke, 2018). Particulate Matter (PM) refers to microparticles of solid pollutants if inhaled over long exposure periods could be of deadly results. It is identified that the PM originate mainly from industrial emissions and vehicular emissions (Ali and Athar, 2010; Seneviratne *et al.*, 2011; Gurjar, Ravindra and Nagpure, 2016). Initial research into PM dates back to the late 18th century and early 19th century (Brimblecombe, 1999). Researchers have identified that the major reasons for increased emission of PM through industrial and vehicular emissions are due to weak emission control regulations and primitive fuel types (Bekir Onursal and Gautam, 1997; Singh, V. *et al.*, 2020). World Health Organization defines 25 $\mu g/m^3$ as the standard exposure condition for 24-hour mean for PM2.5. The recent pandemic resulting from the COVID-19 outbreak devastated the way of life across the world. As of 31st of May 2021, 177 million individuals have reported contracting the virus worldwide while the death toll has reached 3.82 million, while 382,000 of these deaths are reported from India. Most countries turned towards 14-day shutdowns during the first wave of the pandemic to stop the spread of the disease. This resulted in an immediate halt in most production and manufacturing. Strict travel restrictions resulted in streets being practically empty in most countries. Though governments only introduced mandatory lockdowns in the latter part of March in 2020 in most South Asian countries, from February onwards a decrease in general activities was visible due to the initial measures. When the South Asian region is concerned, these restrictions were first imposed by Sri Lanka on the 20th of March 2020. This lasted till the 28th of June 2020 (Erandi *et al.*, 2020), India commenced its nationwide lockdown on 25th March 2020 and lasted till 03rd May 2020 while conditional lockdown was in place till 30th May 2020 (Sharma, S. *et al.*, 2020). Pakistan went into a nationwide lockdown from 1st April to 09th May 2020 (Mumtaz, 2020). while Bangladesh imposed strict restrictions on travel from 05th April to 28th April 2020. Nepal went through a cycle of nationwide lockdown from

24th March to 21st of July 2020 (Sharma, Banstola and Parajuli, 2020). For the study, the first 06 months of 2017, 2018, 2019 and 2020 are used.

Decrease in industrial and travelling related activities resulted in a phenomenal drop in all forms of pollution (Collivignarelli *et al.*, 2020; Menut *et al.*, 2020; Mousavinezhad, Lops and Seyadali, 2021). Resource consumption levels from the region indicate a steep decline in rates of resource utilization due to the limited activity during the period. Reports indicate that levels of air pollution and water pollution reached a recorded minimum during this period. Several articles suggest that the most decreased form of environmental pollution during this period is Air Pollution (Mousavinezhad *et al.*, 2021). Studies even indicate that the Ozone levels in the upper atmosphere have improved due to the temporary halt in anthropological emissions (Xing *et al.*, 2017; Sharma *et al.*, 2020). Decreased emissions have reduced the number of respiratory illnesses recorded during the period (Bourdrel *et al.*, 2021).

Since the South Asian region is prone to dangerous levels of air quality, reviewing the impact of COVID-19 lockdowns on air quality is a timely topic. This review focuses on variation in air quality during the lockdown, before and after, focusing on several key cities in the region. Unlike the East-south Asian region, South Asian countries have limited resources when air quality monitoring is concerned. India, being the largest economy in the region has already invested significantly in monitoring air pollution since 2017 due to the disturbing experience of high mortality rates due to air pollution (Vikas Singh *et al.*, 2020) . Sri Lanka only has 04 industry-grade operational automated air quality monitors in place. Another concern in studying Air Pollution trends is the outlying meteorological conditions over a period of time in focus. It is believed that the quality of air can drastically change due to severe and long-term meteorological events in the surrounding region (Micro, Meso and Synoptic scale)(Cheng *et al.*, 2017; Li *et al.*, 2019). Seasonal variation in air quality trends in most countries also associates with these seasonal meteorological changes. However, as for the previously conducted research on COVID-19 impact on air pollution over India, it is determined that the meteorological conditions during the large part of March and April seem to share the same meteorological characteristics over the four years from 2017 to 2020 (Vikas Singh *et al.*, 2020).

To perform time series analysis on air quality, the data sets used should be uniform, consistent, and reliable. However, except for the data sets from the Central Pollution Control Board of India, other countries lack consistent air pollution monitoring data required for the study. Lack of data is a common struggle faced in all air quality-related research. For the study, air pollution data is gathered through the Automated Air Quality Monitoring Stations located in the United States Embassy (airnow.gov, 2020) and Consulates in the region. The study primarily focuses on how PM2.5 concentration varied during the period of study.

II. METHODOLOGY

A. *Analysis of overlaying Meteorological and Climatic Circumstances*

Though the lockdown occurred generally in the same period over the south Asian region, the meteorological characteristics at the time vary drastically even within one country when analyzed closely. To overcome the difficulties of synchronizing the meteorological parameters is to use reference data from the same period for comparison. This will eliminate the impact of climatic conditions on air quality variation while significantly reducing the impact of seasonally driven meteorological parameters.

Even this method of analysis could be unfruitful if any major meteorological events had occurred during the overlaying period. Previous research suggests that the general meteorological parameters over the Indian subcontinent and the Bay of Bengal remained somewhat unchanged. This was confirmed through the analysis of MERRA-2 meteorological parameters from 2017 to 2020 as suggested by Vikas Singh *et al.* (2020).

B. *Data Collection and Filtration*

Availability and the method of collection of air quality data vary significantly due to different available technologies. Availability and non-availability of different parameters limit the scope of the study significantly. Kandari and Kumar (2021), Investigates variation of air quality over 08 south Asian countries using data from different sources including websites (aqicn.org; worldometers.info; iqair.com, etc.) and other sources like the World Health Organization, United Nations Environment Programme, National Aeronautics and Space Administration. This can create non-uniformity in the collected data. Manikanda et al., (2020) look decisively at air quality variation over more than 10 Indian cities

concerning multiple parameters. Data uniformity is protected by utilizing data sets from uniform means of measurement. Central Pollution Control Board, India (CPCB) has provided data for the above study. However, the research compares overall yearly air quality trends from reference years 2017 to 2019 against 2020. Since the identified decrease in air quality only occurs in the lockdown periods, this approach can undermine the decrease in air quality significantly. Vikas Singh et al. (2020), used data from 134 different caliber measurement devices belonging to CPCB to analyze the decrease in air pollution over different regions of India due to the lockdown. This study aims to utilize a similar methodology to identify a decrease in air pollution. However, this research utilizes data sets from similar caliber measurement devices (Automated Air Quality Monitoring Stations) to increase the reliability of the comparison. Sharma, S. *et al.* (2020) also uses data from the countrywide CPCB air quality monitors to study several parameters while focusing on Air Quality Index (AQI) substantially. Sharma, S. *et al.* (2020) believes that AQI better reflects the change in air quality than any other individual parameter.

This study utilizes data from the network of Automated Air Quality Monitoring Stations maintained by the State Department of the United States of America. Data from the 2018 to 2020 period is used, primarily concentrating on the regional dominant pollutant, PM2.5. The granularity of the raw dataset is hourly averaged data points. In order to conduct a proper analysis, the raw data was cleaned and pre-processed to ensure quality and consistency. The data was observed to have outliers and Instrument codes for when the measuring device had been in calibrating stage or indicating errors. Since the dataset contains time series data, the error codes were not considered as invalid. Instead, data cleaning and transformation methods were applied to cleanse the corrupted data points. The timestamps with outliers were smoothed by using the quantile clipping method, which is an anomaly smoothing method that replaces the data points with values higher or lower than the 95^{th} or 5^{th} percentile respectively, with the percentile point value. The first step towards cleaning the instrumental codes was replacing them with missing values string (NaN) and next linear interpolation was applied to fill in the NaN. The pre-processing and analysis were all conducted using python libraries, mainly pandas, matplotlib and statsmodels. The cleansed data were finally resampled into daily averages and used for the analysis.

C. Time Series Analysis of the Air Quality

Cleaned and pre-processed data averaged per day is used to study the variation of air quality over the years. This initial analysis is done through a time series analysis in form of a graph. Selected 08 locations in 05 South Asian countries will be graphed for 2018, 2019 and 2020 separately. Macro analysis of the trend will be concluded by using combined 2018 to 2019 monthly data as reference and the data from 2020 as a comparison. Quantitative values of the variation are obtained through the following equation in terms of percentage. M_c refers to the 2020 data set while M_r refers to the reference data set. It is expected that the largest decrease in air pollution will occur overlaying the months of lockdown for each country.

$$Change\ in\ Air\ Pollution = \frac{M_c - M_r}{M_r} \times 100$$

III. RESULTS & DISCUSSION

A. Climate and Meteorological Circumstances

From literature review and data from the MERRA-2 platform indicates the variation in wind levels directions and precipitation levels over the Indian subcontinent and the Bay of Bengal remains stable throughout 2018 to 2020. No long-term or significant meteorological events were present during the period.

B. Data Collection

The study obtained hourly PM2.5 values from the Automated Air Quality Monitoring Stations, located in 08 locations over 05 countries in the South Asian Region.

C.Time Series Analysis

A clear decrease in recorded air pollution levels can be seen in the early half of the year 2020. It is already established that this occurred due to the lockdown which was enforced to stop the spread of the COVID-19 pandemic. In the case of some countries, the period in focus is recognized as the most concerning period when it comes to Air Quality.

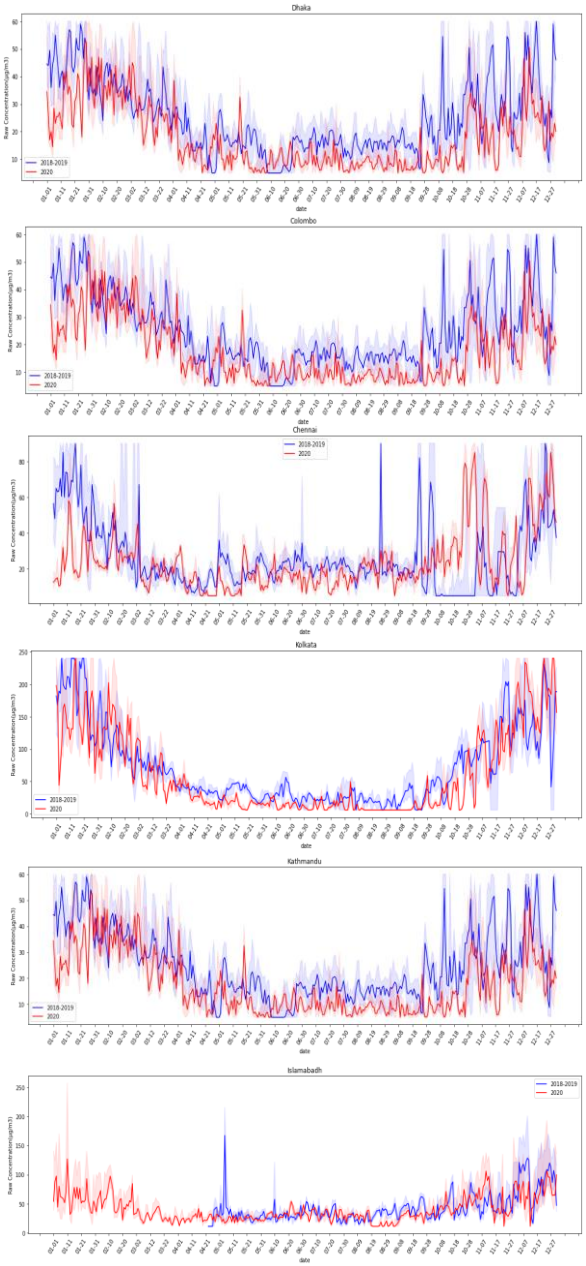

Figure 3. Behaviour of the daily median of reference years (2018 and 2019) and observed year (2020)

This enables the comparison to be more fruitful. In most cases, the lockdown was enforced for 30 days or similar. Hence, the box and whisker plots illustrate in Figure 1 the variation of Air Pollution over the first 06 months of the calendar year in each of the selected cities. It is observed that a decrease in pollution level and increase in air quality overlapping the period where the lockdowns were initiated is present. The most decreased pollution levels were recorded from the cities with a history of air pollution-related complications such as Delhi, Kolkata, Dhaka and Colombo. Figure 2 clearly illustrates the behavior of the daily median during the combined reference years and 2020. The reference years were grouped by month-day and the daily median was lotted in a clear single line plot while the interquartile range (Q_3 -Q_4) was plotted and filled in.

1) Sri Lanka: City of Colombo

Colombo is located on the west coast of Sri Lanka and is considered the financial hub of the country. It is identified that the dominant pollutant in the region is particulate matter (Seneviratne *et al.*, 2011). Premasiri *et al.* (2016) suggest that the visible pollution in the city is lower than the reality because most of the pollution is carried inwards through the strong coastal winds, away from the city. Previous research has also determined that the pollution landscape of the city is also affected by transboundary elements (Gunasekara and Waraketiya, 2020). According to the analysis results during the lockdown period, since the enforcement of the lockdown at end of March, 28.03% reduction in average monthly air pollution April, 30.3% reduction in May and 10.65% decrease in June is evident (Figure 03). The pollution trend in Colombo suggests that the city's highest pollution is recorded through the period of December to February. Slightly lower pollution is recorded from March to May.

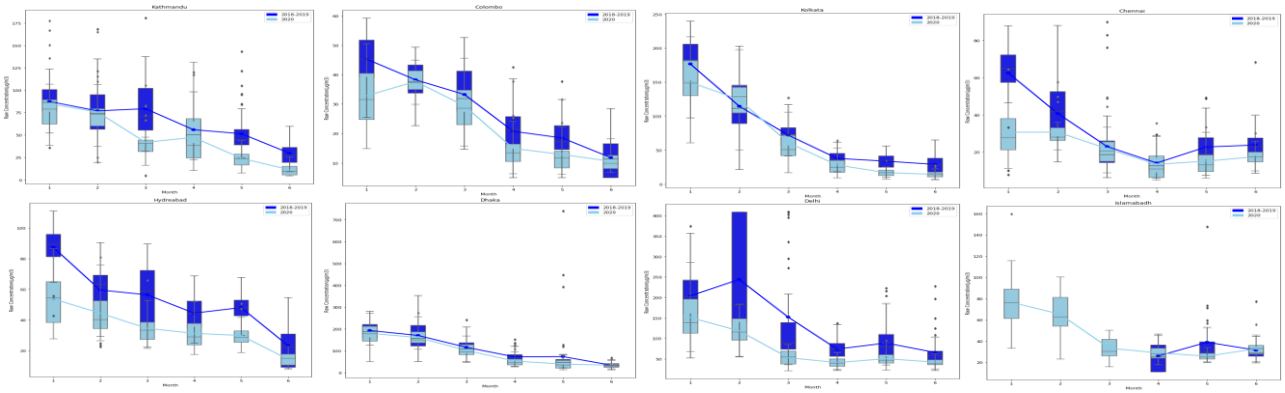

Figure 4. Box Plot Diagrams for Monthly Average

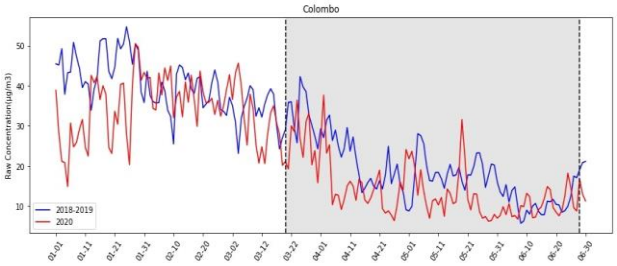

Figure 3: Air pollution variation in Colombo

2) India: Cities of Kolkata and Delhi

Both these cities are located in the northern part of India where the climate is dry, and the winds are moderate. As industrial cities with heavy population densities, Delhi and Kolkata are recognized as pollution hotspots of India (Gurjar, Ravindra and Nagpure, 2016). As per the air pollution trend observed in the reference years, the highest pollution in Delhi and Kolkata is recorded from November to January (Figure 04 and 05). Research links paddy field burning across the northern parts of India for this pattern (Gadde *et al.*, 2009; Lohan *et al.*, 2018). After the lockdown was enforced at end of March, the decrease in air pollution is staggering. The following table provides a quantitative decrease in air pollution compared with the mean of the reference years.

Table 1: Decrease in pollutant levels in Delhi and Kolkata.

Month	Decrease in Delhi	Decrease in Kolkata
April	25.69%	44.39%
May	49.98%	42.86%
June	50.39%	35.75%

3) India: Cities of Chennai and Hyderabad

These two cities are located in the southern part of India. Chennai is a coastal city while Hyderabad is not. Compared to the previous megacities, pollution levels in Chennai and Hyderabad is quite low (Manikanda *et al.*, 2020). These cities are known more as urban cities rather than industrial establishments. Chennai's pollution trends show peaks in November, December and January while Hyderabad's pollution trend is generally increasing from September and peaks in December January then decreases reaching the lowest in June to July (Figure 06 & 07). In general, the monthly average pollution levels in Hyderabad are higher than in Chennai. The monthly average pollution levels for the year 2020 are lower compared to the reference years. The following table provides a quantitative decrease in pollution levels for the two cities.

Table 2: Decrease in pollutant levels in Chennai and Hyderabad

Month	Decrease in Hyderabad	Decrease in Chennai
April	29.67%	5.08%
May	37.96%	33.57%
June	38.34%	26.53%

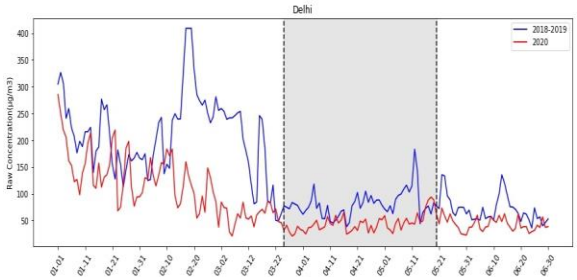

Figure 5: Air pollution variation in Delhi

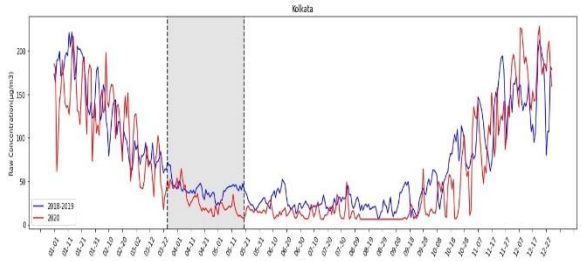

Figure 5: Air pollution variation in Kolkata

4. Bangladesh: City of Dhaka

Dhaka is the capital city of Bangladesh. As the mercantile hub of the country and the administrative capital, the population density in Dhaka is one of the highest in the world (Begum and Hopke, 2018). Pollution in Dhaka is identified to be caused by two major pollutants, PM2.5 and Lead (Begum, B.A., Hopke and Markwitz, 2013). According to previous research, the major source of pollution in Bangladesh is caused by the Brick Kilns and Vehicular Emissions (Begum, B.A. *et al.*, 2014). The pollution trend in Dhaka seems to be moderate throughout the year. Slightly elevated levels are recorded in the first 3 months of the year (Figure 08).

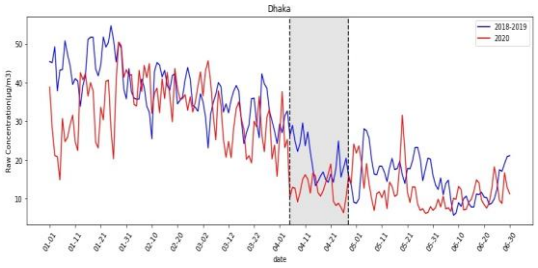

Figure 8: Air pollution variation in Dhaka

Strict lockdown in Bangladesh was only enforced from the first week of April to the last. Less than the other countries in the region. The decrease in pollution levels was also low compared to the regional average. The decrease in April was only 26.76%, Then the decrease increased to 47.32% in May then again returned to general pollution levels with only a reduction of 0.04% in June. Soon after the lockdown was over, pollution levels increased and reached those of the reference years.

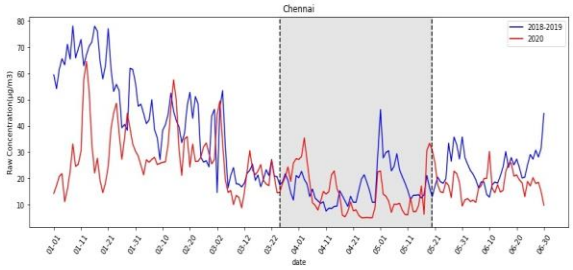

Figure 6: Air pollution variation in Chennai

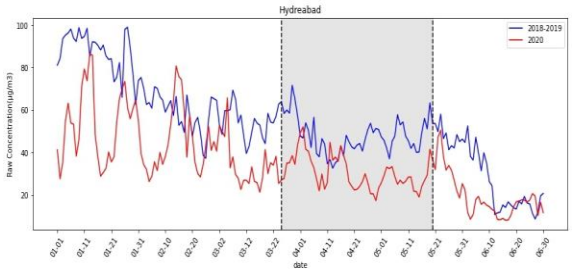

Figure 6: Air pollution variation in Hyderabad

5) Nepal: City of Kathmandu

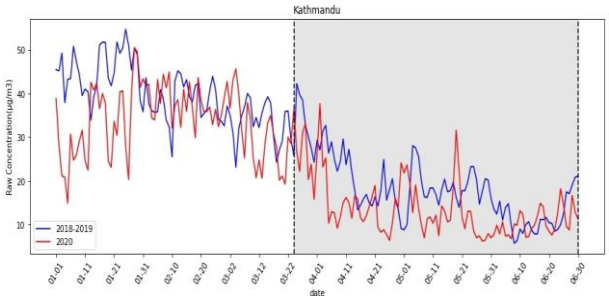

Figure 9: Air pollution variation in Kathmandu

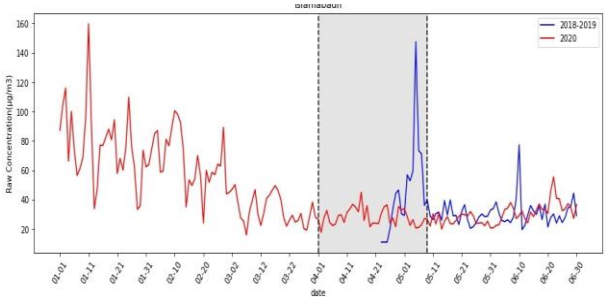

Figure 7: Air pollution variation in Islamabad

Nepal is landlocked by the two industrial giants in the region, India and China. The unique topography and meteorological characteristics of Kathmandu have uniquely contributed to the pollution levels in the city. The city of Kathmandu is located in the Kathmandu valley, surrounded by the Himalayan Mountain range. This bowl-like topography surrounding the city traps pollution in and decreases air quality further. Research has identified that the prominent pollutant in the region is again to be PM2.5 (Saud and Paudel, 2018).. Biomass burning and Vehicular emissions are found to be the major pollutant source in Nepal (Ramanathan *et al.*, 2010; Stone *et al.*, 2018). Researchers hint at the evidence of trans boundary pollution in the region but comprehensive research into pollutant dissemination is yet to be concluded (Aryala *et al.*, 2009; Bong Mann Kim *et al.*, 2015). Similar to Indian conditions, air pollution in Kathmandu increases in the latter part of the year which reaches its peak in December and slowly decreases (Figure 09). Nationwide lockdown in Nepal was enforced from the last week of March and extended till June. In April the monthly mean air pollution levels only decreased by 15.3% even though all activities in the valley were halted. Then the following month, air pollution dropped by a staggering 53.33% and again by 61.98% in June.

6) Pakistan: City of Islamabad

Climatic conditions in Pakistan are mostly dry. Pakistan is as intensely industrialized as India yet shows considerably high pollution concentrations in urban regions. Over the years pollution trend in Pakistan has slowly increased (Colbeck, Nasir and Ali, 2009). The major source of air pollution is identified as vehicular emissions and PM2.5 is the key pollutant. Other vehicular emission-related gaseous pollutants such as SO2, NO2 and Lead is also identified in large concentrations (Ghauri, Lodhi and Mansha, 2007; Ali and Athar, 2010). Studies concluded in Islamabad identifies as Afghanistan and Western India to be the source area through back-trajectory studies. Pollution concentration was highest at the city center, confirming that the major pollution source is vehicular emissions (Rasheed *et al.*, 2014). The lockdown period for Pakistan 1st of April and ended on the 9th of May. A much-relaxed restriction was in place afterward. No decrease in pollution levels was recorded in April (Figure 09). Following months recorded a decrease in monthly average pollution level by 33.77% which was then again increased in June when all imposed restrictions were removed. It is also essential to mention that only 2019 data

starting from April was available for Islamabad to conduct the analysis.

IV. CONCLUSION

As expected, all the cities in the focus group recorded lower pollution levels and better air quality in 2020 compared to the two previous years. Trend analysis concludes that from the start of the year, recorded pollution levels were below what was expected. This could be motivated by the overall air quality improvement in the world. Most European countries and China imposed lockdowns before the threat was identified in the South Asian region. This observation can be evidence of long-range transboundary pollution, which is yet to be comprehensively studied in the South Asian region. European studies into Long-range Transboundary Pollution have proven that the upper atmosphere could transfer pollutants over incredibly long distances (Tørseth *et al.*, 2012).

Analysis of monthly average PM2.5 pollution levels provides us with evidence that the decrease in pollution levels over highly industrialized cities is higher than the others, except for Kathmandu and Dhaka. The lockdown period over Dhaka was only a month. Lowered pollution levels were only recorded the following month which again increased. Hence, the visible drop in pollution level is low. Though Dhaka is a heavily industrialized city, a short lockdown period resulted in only a slight decrease in pollution levels. Pollution in Kathmandu is found to be closely linked to vehicular emissions and biomass burning. However, the rate of decrease in pollution levels soon after the lockdown is lowest in the city of Kathmandu. This could be due to the topography of the city. Entrapped topography reduces ventilation and decreases the speed of pollutant removal. Coastal cities such as Colombo and Kolkata recorded a considerable improvement in air quality soon after the lockdown is enforced. These two observations provide clear evidence of how topography, location and climate influence the decrease in air pollution landscape over the study period.

In conclusion, the highest reduction in PM2.5 pollution levels in south Asia was recorded in Kathmandu during June 3 months after the lockdown was enforced and immediately before the lockdown was lifted the following month. The low rate of pollution decrease is associated directly with the topography and the location of the city. Chennai and Colombo are comparatively less industrialized in comparison to Delhi, Kolkata, or Dhaka. Pollution levels in these cities only slightly decreased which is less significant in comparison.

Most cities recorded the highest levels of PM2.5 pollutant decrease rates exactly about 30 days after the enforcement of the lockdown. This directs towards the assumption that generated pollution concentrations in urbanized cities tend to dissipate slowly. Environments with higher dispersion rates such as comparatively less urbanized coastal cities constantly recorded lower pollution values than inland cities, this is another observation that supports the above assumption. The trend of pollution decrease during the lockdown period suggests that optimum dissipation takes about 20 to 30 days in an urbanized city. Generally, for each city, the lowest pollution concentration was recorded 3 to 4 weeks after the lockdown was enforced. This is evidence that South Asian countries are suffering from passive air pollution and air pollution aggregation.

REFERENCES

airnow.gov (2020) *US Embassies and Consulates Air Quality*, *airnow.gov*. Available at: https://www.airnow.gov/international/us-embassies-and-consulates/#India$Chennai (Accessed: 1 July 2020).

AirVisual (2019) *2018 World Air Quality Report*.

Ali, M. and Athar, M. (2010) 'Impact of transport and industrial emissions on the ambient air quality of Lahore City, Pakistan', *Environmental Monitoring and Assessment*, 171, p. 353.

Aryala, R. K. *et al.* (2009) 'Dynamics of PM2.5 concentrations in Kathmandu Valley, Nepal', *Journal of Hazardous Materials*, 168(3), p. 732.

Begum, B.A. *et al.* (2014) 'Identification and apportionment of sources from air particulate matter at urban environments in Bangladesh', *Journal of Applied Sciences and Technology*, 4.

Begum, B.A., Hopke, P. K. and Markwitz, A. (2013) 'Air Pollution by Fine Particulate Matter in Bangladesh.', *Atmospheric Pollution Research*, (4), p. 75.

Begum, B. A. and Hopke, P. K. (2018) 'Ambient Air Quality in Dhaka Bangladesh over Two Decades: Impacts of Policy on Air Quality', *Aerosol and Air Quality Research*, 18, p. 1910. doi: doi: 10.4209/aaqr.2017.11.0465.

Bekir Onursal and Gautam, S. (1997) *Vehicular Air Pollution: Experience from Seven Latin American Urban Centers*. Washington: The World Bank.

Bong Mann Kim *et al.* (2015) 'Source apportionment of PM10 mass and particulate carbon in the Kathmandu Valley, Nepal', *Atmospheric Environment*, 123, p. 190.

Bourdrel, T. *et al.* (2021) 'The impact of outdoor air pollution on covid-19: A review of evidence from in vitro, animal, and human studies', *European Respiratory Review*. European Respiratory Society, 30(159), pp. 1–18. doi: 10.1183/16000617.0242-2020.

Brimblecombe, P. (1999) 'Air Pollution and Health History', in *Air Pollution and Health*, pp. 5–18. doi: 10.1016/B978-012352335-8/50077-6.

Cheng, N. *et al.* (2017) 'patiotemporal variations of PM 2.5 concentrations and the evaluation of emission reduction measures during two red air pollution alerts in Beijing.', *scientific Reports*, 7, p. 8220.

Colbeck, I., Nasir, Z. . and Ali, Z. (2009) 'The state of ambient air quality in Pakistan—a review', *Environmental Science and Pollution Research*, 17(1), p. 49.

Collivignarelli, M. C. *et al.* (2020) 'Lockdown for CoViD-2019 in Milan: what are the effects on air quality?', *Science of the Total Environment*, p. 732.

Erandi, K. K. W. . *et al.* (2020) 'Effectiveness of the Strategies Implemented in Sri Lanka for Controlling COVID-19 Outbreak', *Journal of Applied Mathematics*, 2020, p. 10.

Gadde, B. *et al.* (2009) 'Air pollutant emissions from rice straw open field burning in India, Thailand and the Philippines', *Environmental Pollution*. Elsevier Ltd, 157(5), pp. 1554–1558. doi: 10.1016/j.envpol.2009.01.004.

Ghauri, B., Lodhi, A. and Mansha, M. (2007) 'Development of baseline (air quality) data in Pakistan', *Environmental Monitoring and Assessment*, 127, p. 237.

Gunasekara, M. and Waraketiya, V. (2020) 'Analysis of Air Pollution Trend and Identification of Possible Transboundary Influence: A Case Study of Colombo Sri Lanka', in *13th International Research Conference of General Sir John Kotelawala Defence University*. Colombo: General Sir John Kotelawala Defence University, p. 08.

Gurjar, B. R., Ravindra, K. and Nagpure, A. S. (2016) 'Air Pollution Trends over Indian Megacities and thier Local-to-global Implications', *Atmospheric Environment*, 142, pp. 475.

Hopke, P. K. *et al.* (2008) 'Urban air quality in the Asian region', *Science of the Total Environment*, 404(1), pp. 103–112. doi: 10.1016/j.scitotenv.2008.05.039.

Kandari, R. and Kumar, A. (2021) 'COVID-19 pandemic lockdown: effects on the air quality of South Asia', *Environmental Sustainability*. Springer Science and Business Media LLC, 1, p. 3. doi: 10.1007/s42398-020-00154-6.

Li, L. *et al.* (2019) 'Evaluation of the effect of regional joint-control measures on changing photochemical transformation: a comprehensive study of the optimization scenario analysis', *Atmospheric Chemistry and Physics*, 19. doi: https://doi.org/10.5194/acp-19-9037-2019.

Lohan, S. K. *et al.* (2018) 'Burning issues of paddy residue management in north-west states of India', *Renewable and Sustainable Energy Reviews*. Elsevier Ltd, 81(June 2017), pp. 693–706. doi: 10.1016/j.rser.2017.08.057.

Manikanda, B. K. *et al.* (2020) 'Air pollution improvement and mortality rate during COVID-19 pandemic in India: global intersectional study', *Air Quality, Atmosphere & Health*, 13.

Menut, L. *et al.* (2020) 'Impact of Lockdown Measures to Combat Covid-19 on Air Quality over Western Europe.', *Science of the Total Environment*.

Mousavinezhad, M. *et al.* (2021) 'Impact of the COVID-19 outbreak on air pollution levels in East Asia', *Science of the Total Environment*, 754. doi: https://doi.org/10.1016/j.scitotenv.2020.142226.

Mousavinezhad, M., Lops, G. Y. and Seyadali, Y. C. (2021) 'Impact of the COVID-19 outbreak on air pollution levels in East Asia', *Science of the Total Environment*, 754.

Mumtaz, M. (2020) 'COVID-19 and Mental Health Challenges in Pakistan', *International Jounral of Social Psychiatry*, 67(3), pp. 303–304.

Premasiri, H. *et al.* (2016) 'Influence of Climatic and Geographical Conditions on Urban Air Quality of Major Cities in Sri Lanka', *NBRO Internatonal Symposium 2016*, pp. 203.

Ramanathan, E. A. *et al.* (2010) 'Characterization of emissions from South Asian biofuels and application to source apportionment of carbonaceous aerosol in the Himalayas', *Journal of Geophysical Research: Atmospheres*, 115. doi: 10.1029/2009JD011881.

Rasheed, A. *et al.* (2014) 'Measurements and analysis of air quality in Islamabad, Pakistan', *Earth's Future*, 2(6), p. 303.

Saud, B. and Paudel, G. (2018) 'The Threat of Ambient Air Pollution in Kathmandu, Nepal', 2018.

Seneviratne, M. C. S. *et al.* (2011) 'Characterization and source apportionment of particulate pollution in

Colombo, Sri Lanka', *Atmospheric Pollution Research*. Elsevier, 2(2), pp. 207–212. doi: 10.5094/APR.2011.026.

Sharma, S. *et al.* (2020) 'Effect of restricted emissions during COVID-19 on air quality in India', *Science of the Total Environment*. doi: 10.1016/j.scitotenv.2020.138878.

Sharma, K., Banstola, A. and Parajuli, R. . (2020) 'Assessment of COVID-19 Pandemic in Nepal: A Lockdown Scenario Analysis', *Frontiers in Public Health*, (1).

Sharma, S. *et al.* (2020) 'Effect of restricted emissions during COVID-19 on air quality in India', *Science of the Total Environment*. Elsevier B.V., 728, p. 138878. doi: 10.1016/j.scitotenv.2020.138878.

Singh, V. *et al.* (2020) 'High resolution vehicular PM10 emissions over megacity Delhi: relative contributions of exhaust and non-exhaust sources.', *Science of the Total Environment*, 699. doi: https://doi.org/10.1016/j.scitotenv.2019.134273.

Stone, T. *et al.* (2018) 'Nepal Ambient Monitoring and Source Testing Experiment (NAMaSTE): emissions of particulate matter from wood- and dung-fueled cooking fires, garbage and crop residue burning, brick kilns, and other sources', *Atmospheric Chemistry and Physics*, 18, p. 2259. doi: 10.5194/acp-18-2259-2018.

Tørseth, K. *et al.* (2012) 'Introduction to the European Monitoring and Evaluation Programme (EMEP) and observed atmospheric composition change during 1972-2009', *Atmospheric Chemistry and Physics*, 12(12), pp. 5447–5481. doi: 10.5194/acp-12-5447-2012.

Vikas Singh *et al.* (2020) 'Diurnal and temporal changes in air pollution during COVID-19 strict lockdown over different regions of India', *Environmental Pollution*, 266.

Xing, J. *et al.* (2017) 'Impacts of aerosol direct effects on tropospheric ozone through changes in atmospheric dynamics and photolysis rates', *Atmospheric Chemistry and Physics*, 17, p. 9869.

ACKNOWLEDGMENT

Environmental Protection Agency and State Department of the United States of America for their involvement in monitoring and archiving worldwide air quality data.

Indigenously Designed and Developed Control System for Sri Lankan Naval Vessels "Naval Propulsion and Steering Control" System

K Bombugalage and AB Arachchi#

Sri Lanka Navy

#akilalawan@gmail.com

Abstract— Obsolescence of spares for Leader In Propulsion System (LIPS), Netherlands engine/steering control system Fast Attack Craft (FACs) of Sri Lanka Navy (SLN), will be non-operational in the near future, and the manufacturer has provided a proposal for upgrading these at a cost of approximately Rs 93,9 Mn per craft in year 2017. Hence, this effort has been made by studying the existing system with the automation knowledge accessible. This study presents aspects of the engine and steering controls onboard P47 series FACs, by analysing the existing systems based on automation and the use of modern propulsion based on Programmable Logic Controllers)PLC .(Human Machine Interfaces)HMI (have been integrated for advanced monitoring and calibrating purposes which comprised a PLC based control system integrating sensors and actuators with commands given at the engine room, wheelhouse, and open bridge command panels .Processed command data are fed to actuators and the feedback have been obtained, thus forming a closed loop control system. These commands, feedback, and sensor readings are fed to PLCs and interfaced with the HMIs which indicate parameters in real time .Alarms and shutdowns have been set at the specific reference values and indicated on the monitoring displays. Controls are available at the engine room, wheel house, and open bridge for easy manoeuvrability as per operational requirement. The study covers the designing process, implementation process and PLC programming, HMI programming, simulation process, commissioning process, and testing process. Used PID controls in the feedback mechanism to optimize the control process variables are the most accurate and stable controller .The designed system was installed onboard P471 and tested several times under close supervision by experienced Senior Electrical Engineers as well as Senior Marine Engineers of SLN, prior to placing the craft as operational on 03rd January 2019. The cost for the project was only approximately a total of Rs. 3.6 Million which will save approximately Rs. 91.4 Million per craft.

Keywords: ***MMM (Mini Micro Module) and LMP (Lips Micro Processor), Machine Interface (HMI)***

I. INTRODUCTION

Designing and developing engine or steering control systems in the marine field is to be undertaken at a high standard where it needs to have proper insulations and a higher level of vibration resistance value. SLN Fast Attack Crafts are specially armed and they are equipped with highly standardized control systems and possess with above said qualities and from highly developed European countries. Carrying out deep studies about these systems and the gained experience during the past decade with marine control systems, made our way so clear about understanding the basics of control systems practically.

Omron CP1H high end type PLC which is an IP 65 rated and certified for the marine environment. Analog/digital external modules, relays, relay bases and RTC 100 (04 mA to 20 mA converting) modules were chosen for meeting the above requirement. The designed system was installed onboard P470 in the initial stage for more than 02 years and no major failures or defects occurred due to simplicity and also a depth of study about securing and proper mounting of the system make easy for background works.

Control signals from existed LIPS controls were bleached to the PLC based new control system. Interlocks and safeties were interfaced using the Ladder diagrams as appropriate. Important functions for armed craft such as **Battle override**, **Emergency Start/Stop**, **Backflush**, etc. were also

given practically introduced and given major apprehension on them.

In addition to the existed LIPS features, newly introduced numbers of features such as Engine Alarms Log which can store the last 4000 alarms from each engine, Standby mode for the control system which saves power and lifetime of the essential components, home screen facilitated with steering and both engine critical parameters, etc. (Beckert, 2015).

Maintain the operational state of the LIPS control system is very difficult due to the obsolete of main PCBs such as MMM (Mini Micro Module) and LMP (Lips Micro Processor), also the Original Equipment Manufacturer (OEM) – Wartsila Netherlands Propulsion Services Pte, indicated that the production of above PCBs is no longer available. Hence, they forwarded a quotation for upgrading of 02 craft cost Rs. 178,977,684.43 in the year 2017.

II. APPLICATIONS

The Indigenously designed system is consisting with Engine controls as well as Steering controls. The marine engine is available with various types of pressure sensors (4mA to 20mA), temperature sensors (PT100/1000), limit switches, tachos, solenoids, etc. which are providing indications, alarms and shutdowns for the safety of the engine. This engine control system can be introduced for various types of marine engines of SLN such as,

1) 12V 604 Deutz
2) 12V 620 Deutz
3) 08V MTU TE 93
4) 12V MTU TB 94, etc.
5) Onan-Cummins Generator engine
6) Nothern-lights Generator engine

The designed steering control system also facilitates the smooth operation of solenoids for hydraulic cylinder operations and feedback from marine type potentiometers. Further, the system can install on a somewhat type of hydraulic driven steering system onboard identified types of Fast Attack Craft available in the Sri Lanka Navy. (marineinsight, 2017)

1) Marine Jet Power– Water jet propulsion- Sweden
2) Kamewa Water Jet – Rolls-Royce, German
3) LIPS – Watsila Netherlands
4) Pneumatic systems – Chinese

III. LITERATURE REVIEW

As per the internet surveys, PLC development began in 1968 in response to a request from a US car manufacturer (GE). The first PLCs were installed in the industry in 1969 and communications abilities began to appear in approximately 1973. The latest standard "IEC 1131-3" has tried to merge PLC programming languages under one international standard. We now have PLCs that are programmable in function block diagrams, instruction lists, C and structured text all at the same time.

The functionality of the PLC has evolved to include sequential relay control, motion control, process control, distributed control systems, and networking. The data handling, storage, processing power, and communication capabilities of some modern PLCs are approximately equivalent to desktop computers. PLC programming combined with remote I/O hardware, allows a general-purpose desktop computer to overlap some PLCs in certain applications.

The main difference from most other computing devices is that PLCs are intended for the tolerance of more severe conditions (such as dust, moisture, heat, cold) while offering extensive Input/output to connect the PLC to sensors and actuators. PLC input can include simple digital elements such as limit switches, analog variables from process sensors (such as temperature and pressure), and more complex data such as that from positioning or machine vision systems. PLC output can include elements such as indicator lamps, sirens, electric motors, pneumatic or hydraulic cylinders, magnetic relays, solenoids, or analog outputs. The input/output arrangements can be built into a simple PLC, or the PLC may have external I/O modules attached to a computer network that plugs into the PLC.

IV. CERTIFICATE OF COMPATIBILITY

1) PLC

PLC Brand	: Omron
PLC model number	: CP1H
Country of Origin	: Japan
Shock resistance	:30 g, 3 pulse each axis
IP rating	:IP54
Max. working temp.	:-20C to + 60C
Vibration withstand	:10-500Hz, 3 g, 0.015" max peak-peak

2) Touch Panel – HMI

HMI Brand	: Samkoon
HMI model number	: Samkoon AK& SK

Country of Origin	: China
Shock resistance	:20g, 3 each axis
IP rating	: Front IP65, Back IP54
Max. working temp.	: -10C to + 70C
Vibration withstand	:10-500Hz, 3g

3) Control Relays

Brand	: Schindler Electric
model number	: Zelio series
Country of Origin	: China
Mechanical durability	: 30,000,000 cycles
Electrical Durability	: > 100,000 cycles for resistive loads at 12A, 250V
Max. working temp.	:-10C to + 70C
Vibration withstand	:10-500Hz, 3g

Device certificates:UL 508, CSA C22-2, EN/IEC 61810-1

V. DESIGN SPECIFICATIONS

The large engine control cabinet of LIPS, located in the engine room which faced high temperatures, moisture, smoke, etc. Hence the manufacturer; LIPS had many difficulties rectifying any defect on this while sailing.

Designed system wire connections were taken distinctly and decided to locate inside an Air Conditioning compartment next to the engine room (OIC/2IC Cabin) which facilitates and provides a longer lifetime as well as increased working efficiency to the system. Further, a designed Engine room control panel was introduced with a touch screen display (HMI) for monitoring all the parameters of the engines.

Figure 1. Designed Control Box for Engine Room

The designed control panel was including all the critical functions such as Engine Start/Stop, RPM increase/decrease, etc. with the Jog switches, selector switches. For the steering system, introduce 12.1 inches common HMI for Closed Bridge to monitor both the engine and steering parameters in one screen and 7 inches common display for Open Bridge for easy operation which simplifies the control panel and can identify the details/data at the real time.

Figure 2. New Control and Monitoring Panel

The control system architecture consists of 02 No's of PLCs with required sensor inputs at Engine Room panel and 04 No's of PLCs at Wheel House (Closed Bridge) to work as engine data transmitting to HMIs and for the steering system. All the Analog/Digital inputs from Engine Room and Wheel House/Open Bridge throttles were sent to the Engine Room through intermediate PLCs and processed within the Engine Room PLCs.

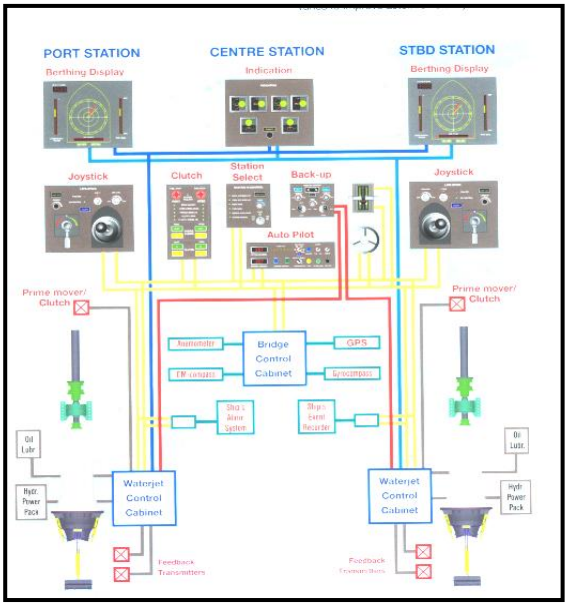

Figure 3. Existing LIPS Block Diagram

Other Inputs/Outputs of Wheel House and Open Bridge will be controlled via the Wheel House PLC and connected to the Engine Room PLC using serial

communication interfaces. PLC to PLC communication made using RS 485 protocol.

A. Designing of Engine Control System

Used sophisticated panel boxes at Engine Room for mounting of designed engine controls to avoid vibration and mounting losses and laid wiring connections from engine sensors to engine room control panel and numbered as our NPSC diagrams.

Figure 4. Introduced Engine Control Panel

B. Designing of Steering Control System

LIPS consists of analog indication gauges in Open Bridge and Wheel House compartment for steering, bucket and RPM. It required calibration one by one when replacing of PCB or module when occurred any defect on it. Hence, the designed system introduced a touch screen display for indications such as steering, bucket and RPM also for the calibration. However, remain separate analog gauge for RPM at both locations.

Figure 5. Designed HMI for Closed Bridge

The introduced HMI at Closed Bridge is also designed to give Steering as well as both engine data on its home page. When it touches an upper potion, shall shift to a separate Steering data page and when it touches the lower left and lower right, shall shift to Port engine data and Stbd engine data respectively. Furthermore, introduced 7 inches HMI for Open Bridge to give clear steering indications and only critical engine data.

Separate 02 PLCs were used for the Steering Control system (Port & Stbd) where it connected to all sensors of the water jet system from one end and Steering Wheel & Throttles from the other end. (Arneson, 2020). The PLCs are mounted on the top of the previous LIPS mounted plate where the Air Conditioning environment is located to the system.

VI. PERFORMANCE

Carried out considerable sea trials successfully at the inner harbor as well as the outer harbor at Trincomalee since 02nd December 2017. Engine parameters are monitored separately by mechanical gauges, non-contact IR tacho-meters and observed same values are displaying on the monitoring display (HMI). Also steering parameters were monitored such as hydraulic oil working pressure, temperature by mechanical gauges and all were under the permissible level.

Turning circles and maneuvering of the craft is very much easy and smooth compared to existed system LIPS. Performance has been monitored from Open Bridge visually and the speed of the craft compared to other craft when operating a single engine, it is very much efficient and the speed of the craft also higher than the LIPS.

Engine parameters are monitored separately by mechanical gauges, non-contact IR tacho-meters and observed same values are displaying on the monitoring display (HMI). Also steering parameters were monitored such as hydraulic oil working pressure, temperature by mechanical gauges and all were under the permissible level.

Turning circles and maneuvering of the craft is very much easy and smooth compared to existed system LIPS. (Anon., 2020). Performance has been monitored from the Radar onboard and the speed of the craft compared to other craft of the same series is higher than the LIPS.

Table 1. Engine Parameters recoded during Sea Trials

Location	**Engine RPM (in load condition)**	**Speed by GPS**
Trincomalee harbor	700	8.5 Knots
	800	9.2 Knots
	900	10.3 Knots
	1000	11.5 Knots
	1100	12.3 Knots
	1200	13.2 Knots
	1300	15.8 Knots
	1400	17.1 Knots
	1500	22.0 Knots
	1600	27.9 Knots
	1700	30.8 Knots

VII. REDUNDANCY IMPLEMENTATION

There is a backup control panel board at Engine Room, Wheel House and Open Bridge. All the inputs and output of the designed engine control panel (either PORT or STBD) can be switched to the backup controller to completely isolate the normal PORT or STBD controller. This enables the boat to operate in case of a failure in any of the systems within the engine controller and enables the components to be replaced at the operational stage. (www.crossco.com, 2020).

The same works for the Wheel House and Open Bridge. The redundancy PLC unit takes all the I/O from the general PLC unit and operates the same way as the general PLC. The HMI panels and indicator panels are not redundant. But a failure of one of these components will not affect the running operation of the engine as the engines can operate without indicators or touch panels.

The key operations (Start PB, Stop PB, Emergency PB,etc) are supplied at the redundancy controller interface so that separate Start, Stop, Emergency PBs will be installed at the HMI panels to be used at redundancy operation.

VIII. CONCLUSIONS AND FUTURE WORK

An indigenously designed Engine/Steering control system is a cost saving of 1/8 compared to an existed system made obsolete by the manufacturer. Also, this designed system can be separated into two independent systems like Steering Control System and Engine Control System with some modifications both the systems can installed many types of existing control systems use in SLN.

1) SLNS Sayura D86 System Engine/Alternator/Axially Equipment, etc.
2) SLNS Shakthi Engine Control System
3) SLNS Udara/Prathapa Engine Control System
4) P47 Series Fast Attack Craft Engine/Steering Control System
5) P46 Series Steering Control System
6) Various Generators/Alternators

Programmable Logic Controllers developing day by day. (www.crossco.com, 2020). Hence the designed system also has to be modified and standardized day by day. Knowledge about programming and designing has to improve with technology and it will help to make standardized and higher quality systems for Sri Lanka Navy.

REFERENCES

Beckert, B., Ulbrich, M., Vogel-Heuser, B., Weigl, A.: Regression verification for programmable logic controller software. In: Butler, M., Conchon, M., Zaïdi, F. (eds.) ICFEM 2015. LNCS, vol. 9407, pp. 234–251. Springer, Heidelberg (2015)

Procedure of testing steering gears on ship, July 2020 Available: https://www.marineinsight.com/guidelines/procedure-of-testing-steering-gears-on-ship/

Articles "Howard Arneson 2000 Hall of Fame", May 19 2020.
Available:https://www.howardarneson.com/articles/articles.as
.

Introduction to CX-Programmer. Aug 2020. Available: https://www.fa.omron.com.cn/data_pdf/mnu/r132-e1-05_cx-programmer.pdf?id=1605

PLC Upgradation benefits. Aug 2020. Available: https://www.crossco.com/blog/benefits-upgrading-or-maintaining-omron-plcs/

AUTHOR BIOGRAPHY

Akila Bamunusinghe Arachchi was born in Balangoda, Sri Lanka in 1988. He received his BTech degree in Electrical and Electronics Engineering from Jawaharlal Nehru University, New Delhi, India. From 2014, he has engaged in many research and development (R&D) activities in electrical and electronic field. He has served in Sri Lanka Navy as an Electrical and Electronic Engineer in R&D and fleet units. He is presently serving as a senior Electrical and Electronic Engineer of Electrical New Design Center (E) of Sri Lanka Navy.

A Methodological Literature Review on Non-Invasive Blood Group Detection

MDVAG Jayawardena

Department of Electrical, Electronic and Telecommunication Engineering, Faculty of Engineering, General Sir John Kotelawala Defence University, Sri Lanka.

varsha.anarkali@gmail.com

Abstract— Blood grouping is the method of determining the type of blood inherent in an organism's body based on the unique types of molecules present in their body- namely antigens and antibodies. Blood groups are differentiated based on the general ABO classification system. Identification of the blood group is a key factor, specifically in the field of healthcare. Organ transplantation and blood transfusion require the blood groups of the individuals to be determined rapidly, in case of diseases or accidents. The standard method of blood grouping requires samples of blood to be extracted from the person, which is then directed for further chemical processing. This conventional method is painful and time-consuming; thus, the introduction of a novel non-invasive method would bring convenience to most humans. The proposed systems have generally used visible light for voltage detection, image processing and deep learning algorithms, NIR spectroscopy, and methods of molecular detection in order to yield results. But limited literature based on this subject exists. Hence, this methodological literature review focuses on the existing peer reviewed literature that explores methods related to non-invasive blood grouping. Out of the methods reviewed, voltage detection using visible light and NIR spectroscopy proved to have the highest rates of success.

Keywords: ***ABO blood grouping, non-invasive, methodological review***

I. INTRODUCTION

Accurate blood grouping is a mandatory process in the medical field, since mismatches in blood typing can lead to hemolysis which could be fatal (Rudlof *et al.*, 2011). Blood grouping is a prime factor to be considered during blood transfusions, identification of suspects or victims using blood samples in crime scenes and organ transplantations. During critical conditions like diseases and accidents, where the medical practitioners do not have access to the patient's blood group, but urgent blood transfusions are required, the patient's blood type must be detected rapidly and accurately. Apart from this, people with certain blood groups are more prone to contract certain diseases. This is backed up by the results of a study conducted using 454 patients with gastric ulcers, in which 217 people had the blood group O (Mentis *et al.*, 2014). So, it's of utmost importance that the blood group is determined accurately.

The conventional ABO and Rh detection tests are performed to determine the type of blood. Humans can have the blood groups A, B, AB or O and the Rhesus (Rh) factor can be positive or negative. The genes inherited from one's parents will determine the antigens on the surface of the Red Blood cells and the antibodies in plasma, which in turn will determine the blood group of a person. To perform a traditional blood typing test, a blood sample must be withdrawn from a vein of the patient using a syringe. The blood samples are reacted with monoclonal antibodies and any occurrence of agglutination will be inspected. Commonly used tests are slide tests, tube tests, microplate method and column or gel centrifugation.

This conventional process takes from 10-20 minutes and modern detectors can minimize this time to achieve results within 5 minutes. But devices that minimize the time taken will be expensive (prices ranging above 7000USD) (Zhang *et al.*, 2017). Apart from the added cost, withdrawal of blood samples from a patient under a clinical setting causes discomfort to the patient. This might lead to symptoms like nausea, fainting and in rare conditions, even anxiety attacks can be observed in hemophobic patients. According to statistical data, 2.5% of the human population tends to faint after or during the withdrawal of

blood. ('How Blood Collection Errors Impact Patients', 2021) Moreover, needles can cause bruising at the site of puncture and cause excessive loss of blood in patients with high blood pressure and other blood related diseases, such as hemophilia. Additionally, lacerations and arterial damages can occur, and poorly sanitized needles can increase the risk of pathogens entering the body. The spread of bloodborne pathogen diseases like HIV, malaria and syphilis can escalate when using poorly disinfected syringes.

Given the profusion of the health and safety risks, the cost effectiveness and the length of the detection period, it is comprehensible that non-invasive blood grouping methods will indeed reduce the risk of disease spread. It's a real time procedure, meaning that the time delay in displaying the results will be minimal and it does not pose any of the side effects that invasive methods do. Thus, developing a non-invasive blood group detection method will be beneficial to society. Existing research has used detection methods like optical signaling and spectroscopy, which will be discussed in detail throughout this review. The feasibility of these procedures cannot be accurately guaranteed since a limited amount of literature is available and no successful device or prototype has yet been output to the market. However, existing methods do reveal a promising future in developing this model. This literature review aims to discuss an advanced yet economical method of blood typing, which will elevate the quality of the existing healthcare systems. Furthermore, the limitations of the existing research that have been performed in this field will be identified in order to assist future research.

II. METHODOLOGY

Health based research benefits from methodological literature reviews, mainly because they highlight the methods utilized in their research, their potential benefits and drawbacks. This enables t he researchers to reduce the time utilized in scanning the resources.

Table 1. Comparison Methods

Method	**Invasive**	**Time taken**	**Mean Sample size**	**References**
Visible light-(Voltage Detection, Image processing , Deep learning)	No	Low	103 for voltage detection, undefined for image processing, deep learning	(Patel, Joshi and Khambhati, 2019) (Kumar,Soundariya,Yuvasree and Balasundaram, 2019) (Gayathri , Rekha , Akmha and Nithyakalyani, 2018) (NON-INVASIVE BLOOD GROUP DETECTION, 2016) (Sornalatha, Yamuna , Vasanthi and Yuvarani, 2021) ('Blood Group Measurement using Light Emitting Diode', 2019) (Mehare et al., 2014) (Agarwal *et al*, 2020)
Maternal samples	Partially invasive	High	400	(Mari *et al.*, 1995; Daniels *et al.*, 2009; Hyland *et al.*, 2009; Clausen, 2014; Rieneck, Clausen and Dziegiel, 2016; *Noninvasive fetal blood group genotyping of rhesus D, c, E and of K in alloimmunised pregnant women: evaluation of a 7-year clinical experience - Scheffer - 2011 - BJOG: An International Journal of Obstetrics & Gynaecology - Wiley Online Library*, 2015) (Scheffer *et al.*, 2011)
Body fluids	No	High	60	(Metgud *et al.*, 2016) (KAUR and SHARMA, 1988; Motghare *et al.*, 2011; BoKhedher *et al.*, 2020; *Effects Of Fabric Materials On Abo Blood Grouping Of Blood Group A And B From Blood*, 2018)
Antibodies	No	High	120	(Boettcher and Kay, 1973)
Spectroscopy	No	Low	70	(Sultan *et al.*, 2018)

Thus, to perform this literature review an effective, methodological approach was used. To compile the literature review, a meta-ethnography was conducted- following the Noblit and Hare's seven stepped technique.(Cunningham *et al.*, 2019)

A. Step 1-Focus of the Review

The research scope was initially established; in this case, it was the feasibility of several non-

invasive blood grouping approaches. Methods which were partially invasive were also examined due to the limitation of resources.

B. Step 2-Area of Relevance

To study the area of interest, peer reviewed articles and scientific journals that explore blood grouping and non-invasive methods were explored. Initially the keywords were noted down and their synonyms were listed. The keywords were chosen to be 'blood-grouping', 'non-invasive', 'spectroscopy' and 'ABO classification'. The listed synonyms were 'blood typing', 'spectrometry', 'spectroscopic analysis', 'spectrographic analysis', 'non-intrusive', and 'minimally intrusive'. To narrow down the search results, Boolean operators including 'and' and 'or' were employed.

This resulted in keyword combinations such as "Blood grouping and non-invasive methods", "Blood Types and spectroscopy", " Non - invasive ABO classification " , " Minimally intrusive or non-invasive detection methods" and "Spectrographic analysis and blood grouping". The titles and abstracts of recently written and published (most were peer-reviewed) research articles were skimmed and scanned, to obtain the latest literature. To obtain the relevant research articles, databases including google scholar, PubMed, Science Direct and ResearchGate were used.

C. Step 3- Examining the Studies

Out of the 50 results that were obtained, the articles of controlled studies that were frequently cited were chosen. To compose the literature review, the articles were ordered based on the relevance after scanning the abstracts of all articles. The number of citations were also considered. Only 22 research articles were chosen based on these criteria.

D. Step 4-Relationship Between Studies

The recurrent methods of blood grouping were identified along with their properties. A table was set up to compare the identified approaches (Table 1).

E. Step 5- Translating Between Studies

The data were critically analyzed and tabulated based on methods used, increasing frequency of occurrence of the method, time taken for detection and sample sizes.

III. LITERATURE REVIEW

The following review depicts the final two stages of Noblit and Hare's approach - the synthesis and the expression of the translations. Recent developments in the medical field have introduced non- invasive methods of blood group detection. Limited resources were available in analyzing this approach since it is a novel method. The following will analyze the relevant literature, based on the methods used.

A. Visible Light

Out of the 22 unique research articles that were analyzed, 8 used non-invasive optical methods.

1) Voltage Detection: In 5 of the proposed systems, (Patel, Joshi and Khambhati, 2019) (Kumar,Soundariya, Yuvasree and Balasundaram, 2019)(Gayathri , Rekha , Akmha and Nithyakalyani, 2018)(NON-INVASIVE BLOOD GROUP DETECTION, 2016) ('Blood Group Measurement using Light Emitting Diode', 2019) voltage detection techniques were used, with a mean sample size of 103 individuals. Light was passed through the finger and the photodetector at the receiving end detected the transmitted signal. The detected signal was converted into a digital format and the change in voltage was detected. The signals were processed in order to identify the voltage ranges by an Arduino (Uno) board or a Node MCU. Depending on the voltage range, the type of blood was determined. To minimize the scattering of light these methods used LEDs. The voltage ranges that were commonly observed across multiple researches are summarized in Figure 1.

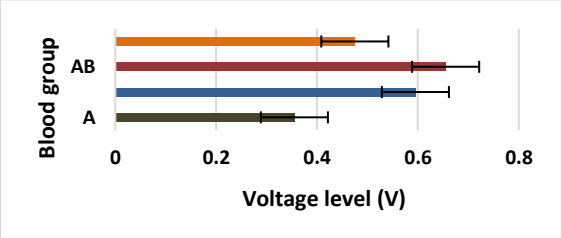

Figure 3. Voltage ranges identified for different blood groups

2) Image Processing: Two studies employed image-processing systems (Sornalatha, Yamuna, Vasanthi and Yuvarani, 2021) (Mehare et al., 2014), where the image obtained using a digital camera was converted to a digital format and pre-processed. The image was developed and structured and the noises were eliminated by filtering. The intensity was adjusted, and the image was broken down into pixels to be displayed on a

screen. The pathway of the absorbed light due hemoglobin and the scattered light due to the antigens was monitored, which represents the unique blood group. The results are depicted in Figure 2. This method is rapid and can be used in any setting due to its non-invasive nature. These apparatuses are lightweight, cheap and do not pose any side effects. But its accuracy is limited due to variation in factors like blood pressure, finger size and colour and the limited sensitivity of the camera used by the image processing technique. The sample size was also undefined. These optical devices are still at the research level and none of these prototypes have yet been manufactured at an industrial scale.

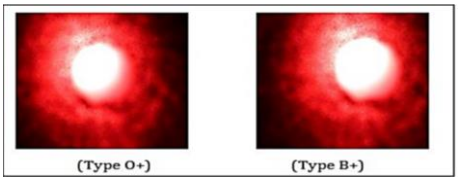

Figure 2. Blood groups identified by image processing
Source: (Mehare *et al.*, 2014)

3) Deep Learning: A rare study (Agarwal *et al*, 2020) used deep learning algorithms to process the data. In this research, a high-resolution camera captures 100-200 images of the fingertip placed over a light source. The dimensions of the image were fixed, and image thresholding was performed. The images were preprocessed by gray scaling, denoising and enhancing the contrast and were converted into binary images. Pixel locations were obtained for the focused area. The model was trained by the input of pre-set values obtained from hospitals. This was used to extract the features using the Gray scale co-occurrence matrix. Depending on the morphological features the output will vary, which can detect the blood group. But the accuracy of this method cannot be validated since only a single study was conducted on this topic and morphological differences can affect the image acquired. The results obtained and sample size were not clearly expressed.

B. Maternal/ Fetal DNA

As it was revealed by 7 different studies, it is evident that maternal plasma contains traces of fetal DNA and antigens. Several researchers obtained samples of maternal and sometimes paternal plasma or cord blood, which were then filtered to obtain fetal DNA samples and amplified by PCR techniques. Employing several DNA extraction and identification processes, the fetal components were analyzed. The results were used to determine the blood group of the fetus, to perform RHD genotyping and to identify any blood related diseases. Methods including genotype testing, next generation sequencing and doppler ultrasound were employed for this process. These methods could only be used for the detection of fetal DNA, to diagnose the blood type and any blood related condition, but postnatal detection cannot be performed by using maternal samples. The level of accuracy was identified as extremely high; in one research where the RHD was determined, out of the 140 samples tested 135 were diagnosed with RHD positive accurately (Mari *et al.*, 1995). This is further substantiated by the large mean sample size that was used, which was 400. But this still requires chemical processing; thus, the time taken to provide the results would not be effectively decreased. Though this method is non-invasive to the fetus, it will be an invasive process for the mother. Another limitation observed through one research (Scheffer *et al.*, 2011) was that the results from genotyping or cord blood serology could be observed in only 59% of the women, thus the feasibility is jeopardized. Also, in early stages of gestation (below 11 weeks) the concentration of fetal DNA is extremely low in the maternal blood, which could lead to false results.

C. Body Fluids

Body fluids can also assist in the detection of blood types. Saliva, urine, vaginal samples and amniotic fluid contain traces of antigens in secretory groups of people. Once the fluid samples were collected by spitting/ excreting, they were isolated by centrifuging and conventional chemical tests were run to isolate the antigens and to detect the blood group. 80% of the human population were proved to be secretors, meaning that they secrete antigens into the body fluids (Motghare *et al.*, 2011). A study involving 80 individuals (Metgud *et al.*, 2016) obtained saliva samples and by using absorption-inhibition/elution methods, it was proven that blood groups A and O were absolute secretors (100%) and 95% of AB and B were secretors. The results of this research are represented in Figure 3. This evidence was backed up by 5 other studies. (KAUR and SHARMA, 1988; Motghare *et al.*, 2011; BoKhedher *et al.*, 2020; *Effects Of Fabric Materials On Abo Blood Grouping Of Blood Group A And B From Blood*, 2018). However, not all individuals are secretors and certain blood types may or may not secrete the antigens. Thus, this method cannot be used for all patients. Furthermore, the sample sizes used in

these researches were inadequate and the validity cannot be assured. Though the method is fully non-invasive, the use of chemical tests would increase the time taken to detect the blood group.

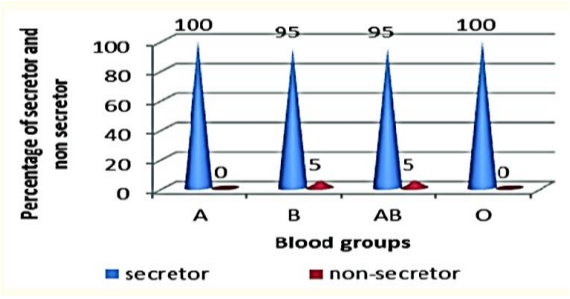

Figure 3. Secretor comparison for each type of blood.
Source: (Metgud *et al.*, 2016)

D. Radioactive Antibodies

One interesting research (Boettcher and Kay, 1973) was conducted using Radioactive antibodies from hair samples obtained from humans. The hairs were crushed, radioactively marked and was used to develop x-ray films after adding reagents which are used for blood grouping. The results were compared with standard ABO blood samples (Table 2). However, this research did not produce results for the blood group O and antigen A and insufficient amount of research has been done by using this method. Moreover, preparation of samples took a large amount of time.

Tabel 2. Accuracy of the results obtained for radioactive antibodies

ABO RBC type	Number of subjects	Number of subjects showing results						
		H	A	B	A+H	B+H	A+B+H	NR
A	5	1						4
AB	3	1				1	1	
B	4			1		3		
O	5	3						2
A_2	3	1						2
A	8	1	3		4			
B	9			3		6		
O	6	6						
A	3		1					
O	4	4						
O	2	1			1			

Source: (Boettcher and Kay, 1973)

E. Spectroscopy

NIR photon transmission spectroscopy is based on the concept that different antigens have unique interaction of photons, thus creates varying levels of scattering and absorption. (Sultan *et al.*, 2018) In this the 850 nm transmitter was placed as a cuff around the lower arm and the RF absorption levels were measured by using the receiver. Modulation and demodulation is performed by the network analyzer. The changes in wave amplitude and phase were displayed (Insertion and phase losses) as a spectrogram for each type of blood, in which the Rh factors for each blood type were also considered unlike the optical method. These in vivo values were compared with values from an experiment performed in vitro. The two results had a correlation greater than 0.95, indicating that non-invasive blood typing provided accurate results similar to invasive processes. Among the methods that were explored, this displayed the highest level of accuracy, with least complications and lowest detection time. However, the sample size that was used was relatively low (70).

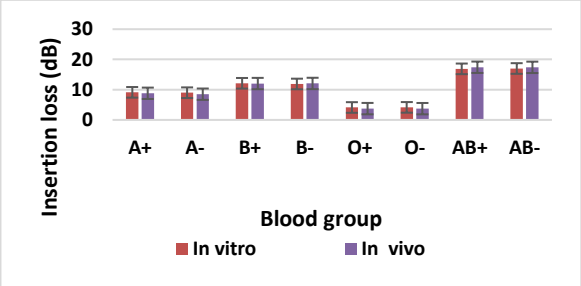

Figure 4. In vivo /In Vitro results from NIR photon transmission.
(Sultan *et al.*, 2018)

IV.DISCUSSION

Out of all the literature that were reviewed, it can be deduced that the visible light-voltage detection method of blood grouping had the highest reliability because it was the only method which had 8 research-based evidence out of the non-invasive techniques, and it took less time for detection. However, no prototype has yet been introduced to the society and all models are still at the primary trial levels due to the limitations posed; the sensitivity of the instrument should be very high to obtain an accurate measurement of light that is detected after passing through several layers of the body. This will increase the cost of production and make it undesirable. The variations in morphology will also affect the results. The sample sizes used for image processing and deep learning techniques were undefined. Despite its advantages, the validity of the deep learning method proved to be inconclusive since the results were not displayed. The NIR photon transmission method that was discussed proved to have the highest accuracy and detection speed based on the results, and the Rh factors were also considered, unlike the optical method. Yet its validity is inconclusive due to the shortage of literature and it did not use a considerably large sample size to validate the accuracy. Limited evidence was available to prove

the effectiveness of the detection methods using body fluids and antibodies, they did not yield results for all blood groups, and were time intensive. Maternal fluid testing which was carried out to determine the blood group of the neonate produced successful results, with the highest reported sample size. However, it requires maternal samples; thus, it is not fully non-invasive.

V.CONCLUSIONS

Significant amount of evidence exists to prove that the development of a method to detect blood groups non-invasively is successful. The major problem is the accessibility of the antigens from the external environment, since the human body is composed of several layers. If this barrier could be overcome, more accurate results could be obtained. This would also require cheaper yet highly precise detection instruments that could be used as an alternative to the expensive detectors that are currently proposed. The visible light-voltage detection method had the highest reliability, but NIR spectroscopic analysis proved to have a high accuracy in detection (due to the comparison of in vivo and in vitro samples producing a large correlation value of 0.95), with the least detection time. If more research-based evidence existed and a larger sample size was used to back up the method, it can be concluded that NIR spectroscopy has the highest feasibility out of all the methods considered. The development of a functional NIR spectrometer for blood group detection would be a major breakthrough in the healthcare sector. Thus, my area of research will be based on a low-cost, lightweight, and an accurate wearable NIR spectrometer that can non-invasively detect blood groups in clinical and forensic settings, crime scenes and war zones, using an embedded signal transducer and receiver that can detect the blood type in a small time span with high accuracy. This innovation could contribute to a colossal development in the fields of biomedical engineering, computer science and medicine.

REFERENCES

A non-invasive way to determine blood type based on antigen property - (2021). Available at: https://docplayer.net/210565621-A-non-invasive-way-to-determine-blood-type-based-on-antigen-property.html (Accessed: 17 June 2021).

An approach towards Non Invasive blood group detection -(2018). Available at: https://docplayer.net/142125002-An-approach-towards-non-invasive-blood-group-detection.html (Accessed: 17 June 2021).

'Blood Group Measurement using Light Emitting Diode' (2019) *International Journal of Recent Technology and Engineering*, 8(4), pp. 11339–11342. doi: 10.35940/ijrte.D5408.118419.

Boettcher, B. and Kay, D. J. (1973) 'ABO Blood Grouping of Human Hair Using Radioactively-Labelled Antibodies', *Vox Sanguinis*, 25(5), pp. 420–425. doi: 10.1111/j.1423-0410.1973.tb03533.x.

BoKhedher, R. *et al.* (2020) 'Effect of gender and ABO blood groups on frequency of ABH antigens secretor status', p. 3.

Clausen, F. B. (2014) 'Integration of noninvasive prenatal prediction of fetal blood group into clinical prenatal care', *Prenatal Diagnosis*, 34(5), pp. 409–415. doi: 10.1002/pd.4326.

Cunningham, M. *et al.* (2019) *Stage 1: methodological review*, *Developing a reporting guideline to improve meta-ethnography in health research: the eMERGe mixed-methods study*. NIHR Journals Library. Available at: https://www.ncbi.nlm.nih.gov/books/NBK537432/ (Accessed: 17 June 2021).

Daniels, G. *et al.* (2009) 'Noninvasive prenatal diagnosis of fetal blood group phenotypes: current practice and future prospects', *Prenatal Diagnosis*, 29(2), pp. 101–107. doi: 10.1002/pd.2172.

Dikshita Agarwal, A. N. Kalyani (2020) 'Blood Group Detection Using Deep Learning', International Journal of Advanced Science and Technology, 29(9s), pp. 499–507.

Effects Of Fabric Materials On Abo Blood Grouping Of Blood Group A And B From Blood (2014) *Issuu*. Available at: https://issuu.com/ijiras/docs/paper_1_fca85f9d82c70f (Accessed: 27 October 2020).

'How Blood Collection Errors Impact Patients' (2013) *Center for Phlebotomy Education*. Available at: https://www.phlebotomy.com/phlebotomyblog/blood-collection-errors-and-their-impact-on-patients.html (Accessed: 8 August 2021).

Hyland, C. A. *et al.* (2009) 'Evaluation of non-invasive prenatal RHD genotyping of the fetus', *Medical Journal of Australia*, 191(1), pp. 21–25. doi: 10.5694/j.1326-5377.2009.tb02668.x.

Kaur, g. And Sharma, v. K. (1988) 'comparison of absorption-inhibition and absorption-elution methods in the detection of abo(h) antigens in sweat stains', *Current Science*, 57(22), pp. 1221–1223.

Mari, G. *et al.* (1995) 'Diagnosis of fetal anemia with Doppler ultrasound in the pregnancy complicated by maternal blood group immunization', *Ultrasound in Obstetrics & Gynecology: The Official Journal of the International Society of Ultrasound in Obstetrics and Gynecology*, 5(6), pp. 400–405. doi: 10.1046/j.1469-0705.1995.05060400.x.

Mehare, G. S. *et al.* (2014) 'A Non-invasive Way to Determine Blood Type Based on Image Processing', 05(04), p. 4.

Mentis, A. *et al.* (2016) 'ABO blood group, secretor status and detection of Helicobacter pylori among patients with gastric or duodenal ulcers', p. 9.

Metgud, R. *et al.* (2016) 'Evaluation of the Secretor Status of ABO Blood Group Antigens in Saliva among Southern Rajasthan Population Using Absorption Inhibition Method', *Journal of Clinical and Diagnostic Research : JCDR*, 10(2), pp. ZC01–ZC03. doi: 10.7860/JCDR/2016/11598.7161.

Motghare, P. *et al.* (2011) 'Efficacy and Accuracy of ABO Blood Group Determination from Saliva', *Journal of Indian Academy of Oral Medicine and Radiology*. Edited by S. Kailasam, 23, pp. 163–167. doi: 10.5005/jp-journals-10011-1120.

Non Invasive Blood Group Detection (2017). Available at: https://www.jetir.org/view?paper=JETIRCU06029 (Accessed: 17 June 2021).

Non Invasive Blood Group Detection Using Light Emitting Diode - (2018). Available at: https://docplayer.net/92811071-Non-invasive-blood-group-detection-using-light-emitting-diode.html (Accessed: 17 June 2021).

Noninvasive fetal blood group genotyping of rhesus D, c, E and of K in alloimmunised pregnant women: evaluation of a 7-year clinical experience - Scheffer - 2011 - BJOG: An International Journal of Obstetrics & Gynaecology - Wiley Online Library (2019). Available at: https://obgyn.onlinelibrary.wiley.com/doi/full/10.1111/j.1471-0528.2011.03028.x (Accessed: 27 October 2020).

Patel, T., Joshi, G. and Khambhati, D. (2019) 'Identification of Voltage Level Present in Blood during Mistransfusion of Blood', *International Journal of Engineering Trends and Technology*, 67(3), pp. 96–99. doi: 10.14445/22315381/IJETT-V67I3P218.

Rieneck, K., Clausen, F. B. and Dziegiel, M. H. (2016) 'Noninvasive Antenatal Determination of Fetal Blood Group Using Next-Generation Sequencing', *Cold Spring Harbor Perspectives in Medicine*, 6(1). doi: 10.1101/cshperspect.a023093.

Rudlof, B. *et al.* (2011) 'Mismatched transfusion of 8 AB0-incompatible units of packed red blood cells in a patient with acute intermittent porphyria', *Saudi Journal of Anaesthesia*, 5(1), pp. 101–104. doi: 10.4103/1658-354X.76497.

Scheffer, P. G. *et al.* (2011) 'Noninvasive fetal blood group genotyping of rhesus D, c, E and of K in alloimmunised pregnant women: evaluation of a 7-year clinical experience', *BJOG: an international journal of obstetrics and gynaecology*, 118(11), pp. 1340–1348. doi: 10.1111/j.1471-0528.2011.03028.x.

Sultan, E. *et al.* (2018) 'Novel optical biosensor method to identify human blood types using free-space frequency-modulated wave of NIR photon technology', *Medical Devices (Auckland, N.Z.)*, 12, pp. 9–20. doi: 10.2147/MDER.S181796.

Zhang, H. *et al.* (2017) 'A dye-assisted paper-based point-of-care assay for fast and reliable blood grouping', *Science Translational Medicine*, 9(381). doi: 10.1126/scitranslmed.aaf9209.

ACKNOWLEDGMENT

The author would like to express her gratitude to Dr PPCR Karunasekara for the valuable guidance. The author would also like to thank Mr. IAMP Ileperuma for the extended support.

AUTHOR BIOGRAPHY

Varsha Jayawardena is currently a BSc Biomedical Engineering undergraduate in the Department of Electrical, Electronic and Telecommunication Engineering of the Faculty of Engineering at General Sir John Kotelawala Defence University.

ID 456

Supersaturation Controlled Wet Synthesis of Nanohydroxyapatite for Biological Applications

GS Dhananjaya#, TGD Madusanka and SU Adikary

Department of Material Science and Engineering, University of Moratuwa, Sri Lanka

#eng.gs.dhana@gmail.com

***Abstract*—** In this study, the effect of supersaturation for wet chemical synthesis of Nano-hydroxyapatite HA [$Ca_{10}(PO_4)_6(OH)_2$] was investigated. The nano-hydroxyapatite powder was synthesized using $Ca(OH)_2$ and H_3PO_4 as precursors at five different supersaturations while the temperature for the whole study remained at 30^0C. The supersaturation for hydroxyapatite was caused by changing the concentration of precursors maintaining the constrained molar ratio near 1.67 between Calcium and Phosphorus Ca/P. The H_3PO_4 was added to the $Ca(OH)_2$ suspension at a constant acid addition rate of 4ml/min using a burette under vigorous stirring having maintained the final pH at 10. During the synthesis, the variation of pH of the mixed precursor suspension was measured and analysed. After 48 h aging, the precipitate was separated by centrifuging at room temperature. Then the resulting wet powder samples were dried and characterized. The particle size distribution was obtained by Laser Particle Size Analyzer and Fourier Transform Infrared (FTIR) spectroscopy investigated the bonding structure of pure hydroxyapatite. In addition to that, morphological and chemical analysis was done by Scanning Electron Microscopy (SEM). As a measurement, the time taken by the final precursor mixture to start reducing pH value increased with the supersaturation decreasing. It was clearly observed that the particle size and the standard deviation of the distribution or a broader distribution had increased with decreasing supersaturation. Finally, this model could be used to predict the particle size distribution of hydroxyapatite resulting from a wet chemical routine with the supersaturation which depends basically upon precursor concentrations.

Keywords: ***nano-hydroxyapatite, wet chemical precipitation, supersaturation, particle size distribution***

I. INTRODUCTION

Recently, different phosphates of calcium are the materials being used for a variety of medical applications like controlled drug formulation and delivery, tissue engineering, and implants in dentistry as mentioned by Uskoković and Wu (2016). Apart from the medical applications, hydroxyapatite is used in fuel cells (Gross, Berndt, et al. 1998) and column chromatography as packing material (Morales, Burgues, et al. 2001) Among calcium phosphates, Naruporn M (2008) expressed the views on hydroxyapatite as a bioactive and biocompatible ceramic which has a similar mineral structure and composition to the naturally occurring hard tissue in bone and teeth of humans. Materials having higher crystallinity and chemical stability like hydroxyapatite are good candidates to be a productive biomaterial. With respect to mechanical properties, hydroxyapatite (HA) has poor hardness, low tensile strength, low compressive strength which makes it suitable for applications that require little or no-load bearing functionality as described by Liu and Troczynski (2001). Naruporn M (2008) reviews that there is a broader diversity of preparation methods of hydroxyapatite like solid state synthesis, hydrothermal methods, sol-gel methods, electro crystallization, sonochemical synthesis, spray pyrolysis and wet chemical precipitation. Although there are so many techniques to synthesis hydroxyapatite, *Guzm'an V' azquez, et al* (2005) emphasized that the wet chemical precipitation method is the most predominant one in terms of the ease of experimental procedure, lower synthesis temperature, yield, and cost of required equipment.

However, the diversified application of hydroxyapatite needs to be tailored based on the application. Basically, different researchers all over the world have altered and customized its properties such as stoichiometry, size and distribution, tensile properties, morphology, sinterability and solubility. As Sudip and Apurba (2016) states, the property customization can be done by varying the synthesis methodology along with controlling parameters such as pH, precursors and their concentrations, temperatures, etc. Based on the parameters above mentioned, some

mathematical and kinetic models have been established depending upon kinetics (Thanh, Maclean, et al. 2014). As they derived analytically based on the classical nucleation theory, the nucleation rate is basically a function of temperature and supersaturation.

For spherically nucleating particles, the homogeneous nucleation rate is given by,

$$\frac{dN}{dt} = Aexp\left(-\frac{16\pi\upsilon^2\gamma^3}{3(k_BT)^3(\ln\ (S))^2}\right) \text{..... (1)}$$

where, the nucleation rate, dN/dt is dependent upon pre-exponential factor A, molar volume υ, interfacial energy between the growing phase and solution γ, Boltzman's Constant k_B, absolute temperature T, and Supersaturation S.

Supersaturation gives an indication about how many times the ionic activity product is greater than the activity product in its saturation.

$$S = Q/K_{sp} \text{..... (2)}$$

where, Q is the ionic activity product of precursor ions in the solution for the given stoichiometry (Dragan, Vuk et al. 2010)

The Q was calculated by considering ionic activities of Ca^{2+} , PO_4^{3-} and OH^- in the solution as given in EQ03

$$Q = [\boldsymbol{a}_{Ca^{2+}}]^5[\boldsymbol{a}_{PO_4^{3-}}]^3[\boldsymbol{a}_{OH^-}] \text{..... (3)}$$

In medical implantations and orthopedic and orthodontic application in tissue engineering like scaffolds, the medical grade hydroxyapatite must be osteoconductive, which means it must be compatible with hard tissue in the body for the continuum (Ferraz, Monteiro, et al. 2004). For the osteoconductivity, two major important factors are particle size and purity of the hydroxyapatite synthesized. Nano size and wet chemical precipitation is thereby preferred for biological grade hydroxyapatite. Therefore, in this research work, the wet chemical process was chosen for the synthesize of hydroxyapatite particles additionally because it offers a molecular level of mixing to improve the chemical homogeneity of the product which affects the uniformity of nucleation. Basically, this study focused on the particle size and its distribution depending upon the supersaturation which was calculated based on concepts from analytical chemistry. Although there are so many studies in the literature to have a nano-size particle distribution from different synthesis methods, the particle size tailored to the synthesis variable parameters has not been well established. Hence, the main objective of this work was to tailor the particle size to precursor concentration based-parameter, supersaturation, leaving the working temperature, Ca/P molar ratio and acid addition rate constant.

II. METHODOLOGY

A. Chemicals and reagents

Analytical grade Calcium hydroxide [$Ca(OH)_2$, 98%] was procured from VWR, orthophosphoric acid [Assay (H_3PO_4), min 88%], ammonium hydroxide [NH_4OH, 28%], Ethanol [C_2H_5OH] were procured from MERCK Specialties Private Limited. During the synthesis, deionized water (DI) was used as the solvent.

B. Experimental procedure

As the Table 1 shows, five samples of from different precursor concentration (in $moldm^{-3}$) were prepared.

Table 1. Precursors' concentration for five Samples.

Sample / Reagent	1	2	3	4	5
$Ca(OH)_2$	0.1670	0.3400	0.6300	0.8400	1.0400
H_3PO_4	0.1000	0.2000	0.3710	0.4940	0.6000
Ca/P	1.67	1.7	1.70	1.70	1.73

First 250 ml suspension of $Ca(OH)_2$ was magnetically stirred for 1 h in a beaker. Then 250 ml of H_3PO_4 was poured in a burette and added dropwise to calcium hydroxide suspension with a flowrate of 4 ml/min under continuous mechanical agitation. After the completion of acid addition, the reactant mixture was subjected to ultrasonic stirring for 30 mins. Then, quick and dropwise addition of ammonia hydroxide was made to raise the reactant mixture pH to 10 under magnetic stirring. After setting the final pH to 10, pH was noted for every 30 second interval under mechanical agitation. After a time-independent and constant pH suspension was observed, mechanical agitation was stopped, and the sample was placed in 48 h aging. Then the water layer above the deposition was removed and the sample was centrifuged at 5000 rpm for 6 mins at 30 ^{0}C with DI water. Finally, the precipitation in centrifuging

tubes was carefully separated to a petri dish. One specimen of this wet precipitate was analyzed with laser particle analyzer (HMK-CD2, 0.02 - 2000 um). This wet sample of synthesis was placed in the oven at 60 ^{0}C for 2 ½ hr. Then, the resulting powder was diluted in ethanol and sonicated in order to prepare a drop cast for the SEM analysis. The molecular bond structure or the functional groups present in the hydroxyapatite powder was determined by Fourier transform infrared spectroscopy (Bruker Alpha-T) in the scanning range of 4000 - 400 cm^{-1} using a cold pressed pellet of KBr containing 1% hydroxyapatite.

III. RESULTS AND DISCUSSION

The supersaturations (S) for five samples were calculated and the values of ln (S) are graphically shown by the Figure 1.

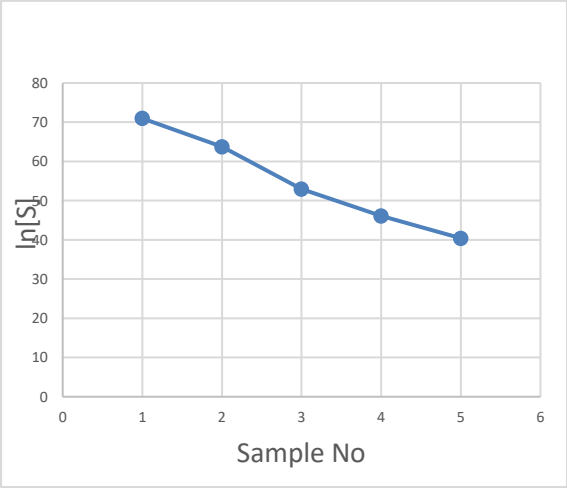

Figure 4. Calculated supersaturations for five Samples.

One may be surprised because in this study the highest supersaturations have been recorded by the sample with lowest precursor concentrations. In conventional calculations, the ionic interactions in highly charged suspensions are not considered. But in this study, all the analytical calculations were based on the electrostatic interactions that occur in solutions between the various charged ionic species. With high precursor concentrations, the electrostatic interactions are at maximum and it will reduce the totally decomposed ionic concentrations like PO_4^{3-}. Therefore, for the supersaturation calculations ionic strengths have been considered with Debye-Huckel equation for aqueous solutions. Accordingly, the highest ionic strength has shown by sample 05. Hence highest activity coefficients have shown in sample 01 giving rise to supersaturation.

With the dropwise acid addition to the calcium hydroxide suspension, the final pH of the mixture came near 6. Figure 2 shows the pH variation for the first synthesis after the pH adjustments of the final mixture to 10. It shows after 300 seconds, the first sample started to drop pH. According to the kinetic theory in classical nucleation, that rest time of the reaction is called the induction time (τ) and during that period nucleation takes place within the suspension. The chemical reaction taking place during the HA formation can be suggested as follows.

$$10\ Ca(OH)_2 + 6H_3PO_4 \longrightarrow Ca_{10}(PO_4)_6(OH)_2 + 18H_2O$$

The formation of hydroxyapatite particles from the supersaturated solution consumes OH^- ions reducing the pH in the suspension.

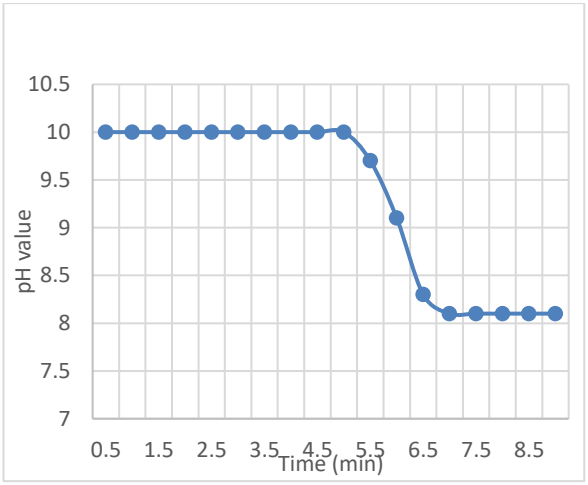

Figure 2. pH Variation with the reaction time of first Sample

As Figure 3 illustrates, the induction time has increased with reducing supersaturation. The least induction time was reported for the highest supersaturated solution 01. Dragan and Vuk et al (2010) modeled the nucleation rate in terms of induction time. As they suggested the induction time is a measure of nucleation rate which cannot be directly measured. It is obvious that with increased nucleation rates, the particle size will decrease which ultimately means that the lower induction time results in reduced particle sizes. This phenomenon will support the formation of reduced particle size with higher supersaturation.

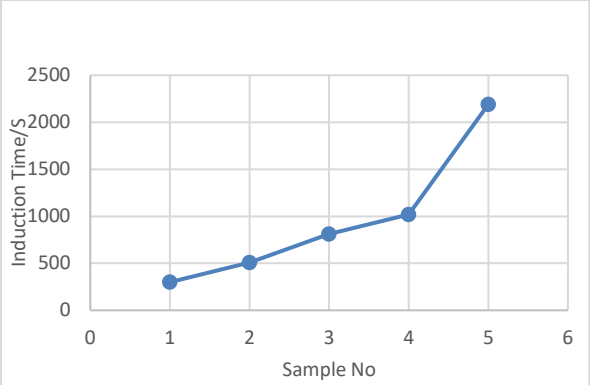

Figure 3. Variations of induction time for five samples

FTIR absorption spectrum of hydroxyapatite is shown in the Figure 4. As Sahebali Manafi and Seyyed (2008) concluded, the narrow bands located at around 472, 575, 963 cm^{-1} are attributed to the characteristic bands of PO_4^{3-}. The absorption band appeared at 472 cm^{-1} represents the v2 bending vibration. The narrow band near at 963 cm^{-1} corresponds to v1 vibration of PO_4^{3-} ions in hydroxyapatite. The absorption bands appeared at 575 cm^{-1} and 601 cm^{-1} can be attributed to the n4 fundamental bending mode of phosphate ions. The range of band appeared in between 1089-1036 cm^{-1} are dealt with n3 vibrations of phosphates. The band revealed around 1459 cm^{-1} is evident for the presence of a little amount of CO_3^{2-} in the sample as Tampieri and celotti (1997) showed. The IR absorption bands appeared around 3573 cm^{-1} and 632 cm^{-1} are stretching and vibration modes of OH^- ions respectively present in the hydroxyapatite.

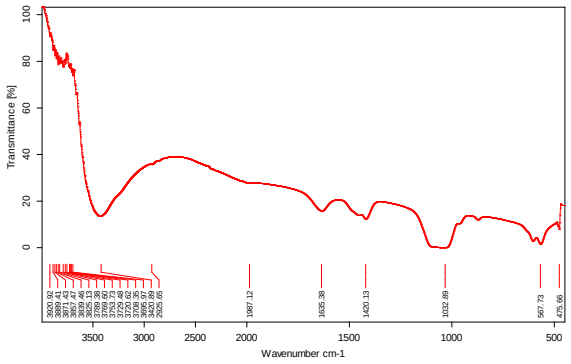

Figure 4. FTIR spectrum pattern of Synthesized first sample

Laser particle analyser recorded the particles beyond 20nm. This technique was selected because it gives the real particle size containing very small number of crystallites while powder x ray diffraction gives the crystallite size. The Figure 5-9 demonstrate the particle size distribution curves obtained from the laser particle analyser. The mean and the stand deviation of each distribution are tabulated in Table 2. This experimental work basically focused on the nucleation rate which is inversely proportional to the induction time. But in the pH dropping period, the nucleated particles are growing up to the solubility limit of the hydroxyapatite. As the pKsp value which is 117.3 at 37^0C for HA suggests the growing of particles will predominantly occurs because the experiment deals with higher supersaturations. Therefore, the mode can be given as a good parameter to interpretate the particle size distributions obtained. Therefore, the lowest modal particle size was obtained for the first sample with highest supersaturation. This decrease in size with increasing supersaturation can collaboratively be explained by the above-mentioned nucleation theory. When the supersaturation is very high, the nucleation is promoted with higher nucleation densities leading to smaller particles and shorter induction time as the shortest induction time for the first sample. It can be considered as an experimental validation for the theoretical concepts generated. The distribution for the first sample is cut off from the left-hand side because it has the limitation of cut off size as 20 nm only. But the Gaussian curve is also established there. The Gaussian fitting is applicable for all distributions. The standard deviation has increased with sample number resulting in a broader distribution. This can be caused by the higher concentrations of precursors with loosing supersaturations after rapid nucleation. In broader distributions, particles have grown to greater extent.

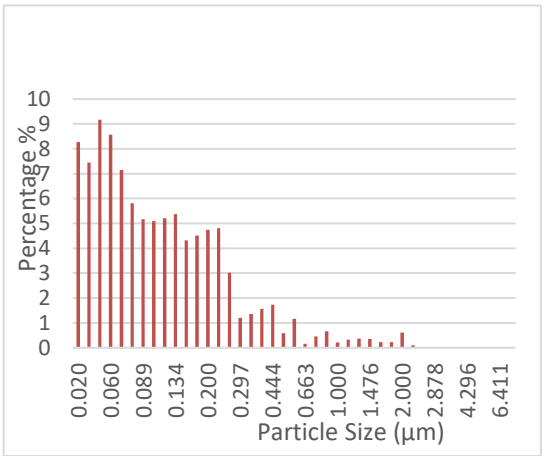

Figure 5. Laser Particle analyzer results for sample 01

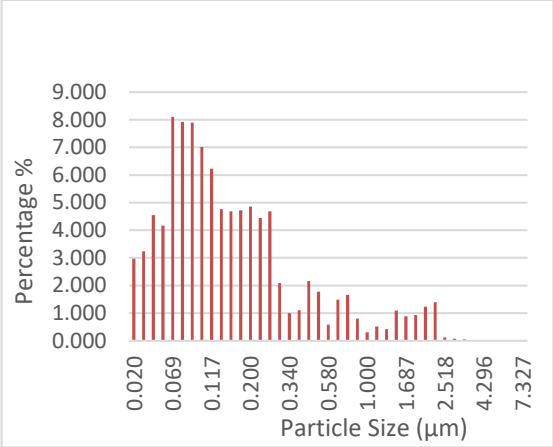

Figure 6. Laser Particle analyzer results for sample 02

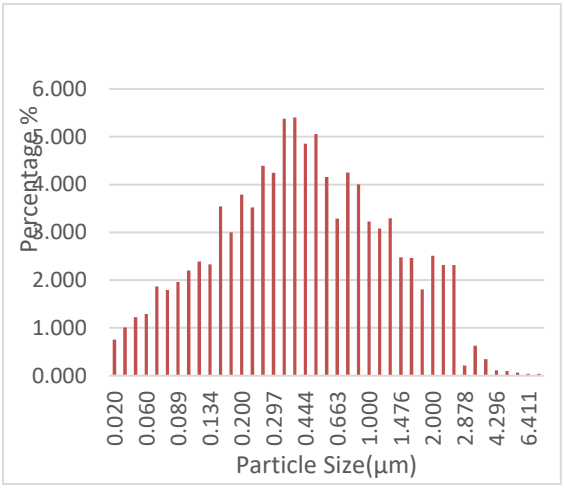

Figure 7. Laser Particle analyzer results for sample 03

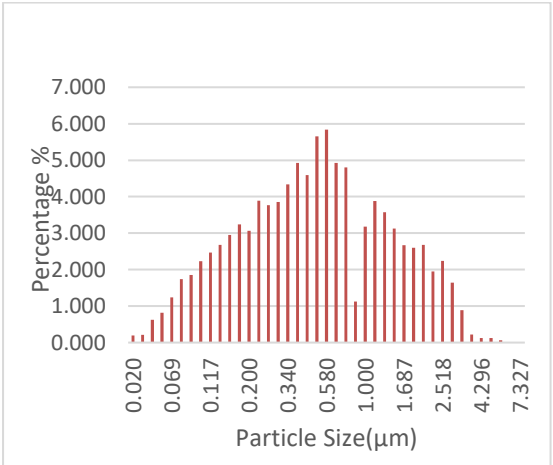

Figure 8. Laser Particle analyzer results for sample 04

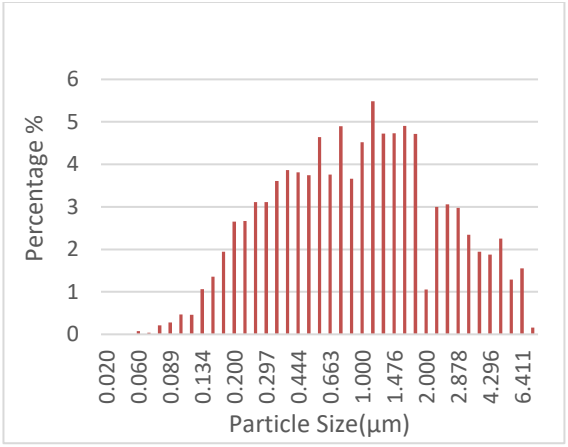

Figure 9. Laser Particle analyzer results for sample 05

Table 2. Parameters for particle size distributions obtained by Laser particle analyser

Sample	Mode particle Size (nm)	Mean particle Size (nm)	Standard Deviation (nm)
1	50	170	267
2	69	286	465
3	389	704	744
4	580	770	769
5	1130	1408	1394

The SEM study reveals the formation of well-dispersed rod-shaped nanoparticles in the samples. Figure 10 clearly shows the formation of nanoparticles in the first sample. They are nearly rod-shaped and have a compromised size with laser particle analyser. The EDS analysis revealed the presence of Ca, P, and O in the sample with Ca/P molar ratio of 1.69.

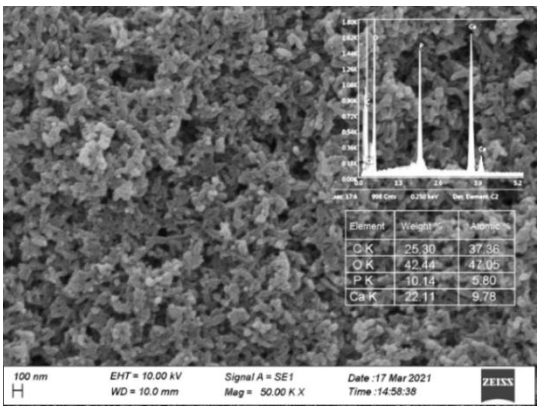

Figure 10. SEM image of hydroxyapatite particles synthesized in first sample

Synthesized nano hydroxyapatite controlled by supersaturation can be particularly used in

preventive, restorative and degenerative dentistry due to its unique properties, such as the re-mineralizing effect on initial enamel lesion, good results on the sensitivity of teeth, ability to bond to the bone chemically, non-toxicity nor inflammation, stimulation of bone growth through the direct action of osteoblasts. Specially the synthesized nano level and purity of hydroxyapatite suit the applications in periodontology, oral and maxillofacial surgery, oral implantology, orthopaedics with the above-mentioned properties in the nano domain and the osteoconductive behaviour which provides the better osteointegration strengthening the bone to implant connection. Synthesized nano powder from other methods does not give higher purity which make it suitable for medical or biological application and micro range particle domain does not provide the significant osteo integrative properties. Simply, the nano range gives the highest surface area so that protein and other fragments bind easily.

IV. CONCLUSION

In summary, the wet chemical precipitation method could fabricate stoichiometric HA nanoparticles with rod shaped morphology. This is very versatile method to synthesize HA nanoparticles in large quantities with reproducibility. The advantage of this method is that it gives water soluble biproducts which can easily be washed to recover high purity nano hydroxyapatite for biological applications. This study basically tailored the particle size to supersaturation of the precursor solution. Because of electrostatic interactions in ionic solutions, the higher precursor concentrations always do not give the higher supersaturation. Therefore, the need of ionic strength consideration for a synthesis was highly noted. The nucleation rate which was mentioned to be inversely proportional to the induction time contributed mainly to the size of the nano particles being synthesized. Higher nucleation rates, in other words lower induction time gave the smaller size and narrow distribution. Although the increased supersaturation is better for the nano particle synthesis, when concentrations are too high, the obtained size distribution, can be broader promoting the growing phase. In this study, it is learnt that supersaturation must be optimum for a narrow particle distribution.

REFERENCES

C. Guzm´an V´azquez, C. Pi˜na Barba, and N. Mungu´ıa, (2005), Stoichiometric hydroxyapatite obtained by precipitation and sol gel processes, revista mexicana de fisica 51 (3), 284–293.

Gross, K.A., Berndt, C.C., Stephens, P. and Dinnebier, R. (1998), “Oxyapatite in hydroxyapatite coatings”, J. Mater. Sci., 33(15), 3985-3991.

Liu, D.M., Troczynski, T. and Tseng, W.J. (2001), “Water-based sol-gel synthesis of hydroxyapatite: process development”, Biomaterial, 22(13), 1721-1730.

Morales, J.G., Burgues, J.J., Boix, T., Fraile, J. and Clemente R.R. (2001), “Precipitation of stoichiometric hydroxyapatite by a continuous method”, Cryst. Res. Technol., 36(1), 15-26.

Mp Ferraz Fj Monteiro C.M. Manuel (2004), Hydroxyapatite nanoparticles: A review of preparation methodologies

Naruporn M, (2008), Nano-size Hydroxyapatite Powders Preparation by Wet-Chemical Precipitation Route, Metals, Materials and Minerals, 18(1),15-20.

Nguyen T. K. Thanh, * N. Maclean, and S. Mahiddine (2014), Mechanisms of Nucleation and Growth of Nanoparticles in Solution, 114,7610-7630.

S. U. Adikary, J. M. N. Jayaweera, and G. A. Sewvandi (2011), Synthesis and Characterization of Hydroxyapatite to be used as a Biomaterial

Sahebali Manafi, Seyyed Hossein Badiee, (2008), Effect of Effect of Ultrasonic on Crystallinity of Nano-Hydroxyapatite via Wet Chemical Method, Pharmaceutical Sciences, 4(2), 163-168.

Sudip Mondal, Apurba Dey, Umapada Pal (2016), Low temperature wet-chemical synthesis of spherical hydroxyapatite nanoparticles and their in-situ cytotoxicity study, 295-307.

Tampieri, A., Celotti, G., Szontagh, F. and Landi, E. (1997), “Sintering and characterization of HA and TCP bio ceramics with control of their strength and phase purity”, J. Mater. Sci. Mater. Med., 8(1), 29-37.

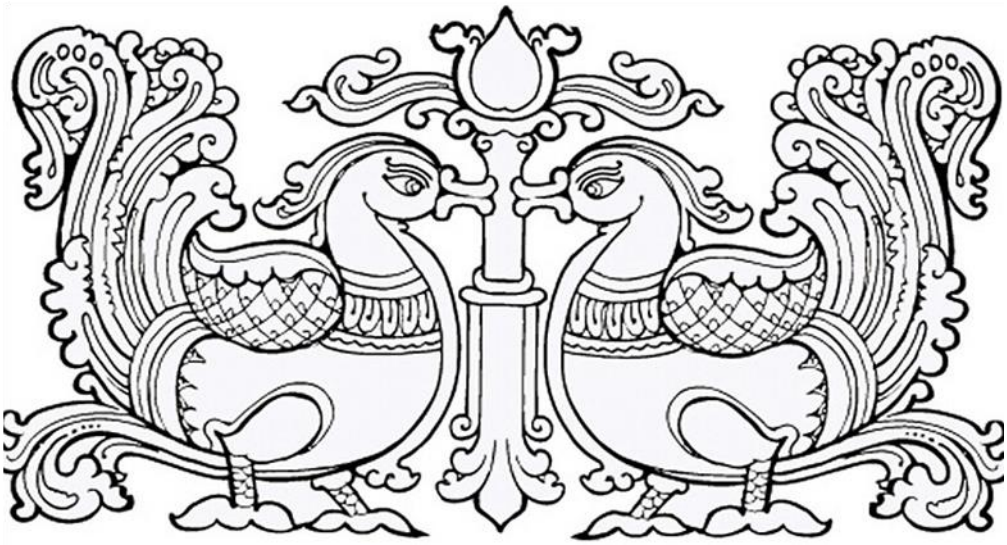

POSTER SESSIONS

Drop Down in Speed of Fast Attack Craft

LDTKD Lokudadalla

Sri Lanka Navy, Sri Lanka

dananjayalokudadalla@gmail.com

Abstract— Sri Lanka Naval fleet consists of 55 Fast Attack Craft (FACs) belonging to the Sri Lanka Navy (SLN) and Coast Guard which are propelled by water jets, conventional V-drive propulsion systems, and Articulated Surface Drive (ASD) powered by twin diesel engines. Recently, the drop in speed of FAC's has been a challenging problem to SLN. The objective of this research is to find out the reasons for the speed drop of FACs, and the effect of hull cleaning/routine underwater maintenance as a solution. The research mainly focused on gathering information related to speed with RPMs and observing changes to the hull, and finally modelling of a similar shaped hull and analysing effects on speed due to the changes in the hull form.

Keywords: ***hull cleaning, fast attack craft, underwater maintenance, Sri Lanka Navy***

I. INTRODUCTION

The fast attack craft is a mono hull planing craft which is also known as "Dvora". These craft are designed for an average of 24m length, 5.5m breadth and 50 Tons of light load displacement. The engines and propulsion system of these craft are as follow;

Table 1. Propulsion systems of FAC series

Craft Series	Engines Used	Propulsion System
P 40, Coast Guard Craft (P 44 Series)	Engines	Conventional V-drive propulsion system
P 41, P 42, P 43, P 47	Engines	LIPS Water Jets
P 45, P 48, P 49	Engines	KAMEWA Water Jets
P 46, P 444	Engines	Articulated Surface Drives (ASDs)

Craft with conventional propulsion systems are designed for a top speed of 36 knots and other craft with ASDs and water jets are designed to achieve 45 knots in full load condition.

A. Planing craft

Planing hulls are designed with more aft sections. A typical 'deep V' bottom hull has the same angle to the 'V' (the same deadrise angle) from amidships to the transom. They are designed to rise completely out of the water at high speed and "hydroplane" on top of the water. At planing stage water is breaking clearly from the transom and the hull is riding on its straight aft sections.

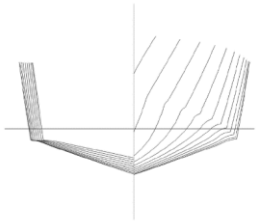

Figure 8. Lines plan of a Mono hull planing craft

A craft can be determined whether it is a planing craft by its Froude number which is defined by the following equation;

$$Fn = \frac{V}{\sqrt{(g.lw)}} \qquad (1)$$

Where; F_n - Froude number
g - Gravitational acceleration
l_w - wetted length

Baird (1998) Defines a high speed vessel as a craft with a maximum operating speed higher than 30 knots, whereas hydrodynamicists tend to use Froude number greater than 0.4 to categorize a fast vessel supported by the submerged hull, such as mono hulls and catamaran hulls.

The pressure carrying the vessel can be divided into hydrostatic and hydrodynamic pressure. The hydrostatic pressure gives the buoyant force which is proportional to the submerged volume (displacement) of the ship. The hydrodynamic pressure depends on the flow around the hull and is approximately proportional to the square of the ship speed. When Froude number > 1.0-1.2 the hydrodynamic force mainly carries the weight and this can be called as a planing craft. [1]

B. Resistance of a ship

Resistance of a ship at a given speed is the force required to tow the ship in the calm water,

assuming no interference from the towing ship. If the hull has no appendages, it is called bear-hull or towing resistance. This is not exactly same as the propulsion resistance due to hull/propeller interaction. A ships resistance is particularly influenced by its speed, displacement and hull form.

The total resistance when not planing can be divided into three main categories as follows;

Viscous resistance/ Frictional resistance (R_f)
Residual resistance (R_r)
Air resistance(R_a)

Viscous resistance (R_f) is also called frictional resistance and is due to the motion of the hull through a viscous fluid which depends on the wetted surface area of the ship(S) and the specific frictional resistance coefficient (C_f). The empirical formula for frictional resistance is as follows;

$$R_f = 0.5\rho C_f S U^2 \quad (2)$$

Where ;
$C_f = \frac{0.075}{(\log_{10} R_n - 2)^2}$; Towing tank conference (ITTC) 1957

$$R_n = \frac{UL}{\nu} \quad (3)$$

$\nu - Kinematic\ viscosity$
$L - Overall\ submerged\ ship\ length$

$$\nu = \frac{\mu}{\rho} \quad (4)$$

$\mu - Dynamic\ viscosity, p - Mass\ density\ of\ fluid$

Residual resistance (R_r) comprises wave resistance (Rw) and eddy resistance (Re). Wave resistance refers to the energy loss caused by waves created by the vessel during its propulsion through the water, while eddy resistance refers to the loss caused by flow separation which creates eddies, particularly at the aft end of the ship.

Air resistance (R_a) in calm weather can be expressed by the following equation;

$$R_a = 0.5\rho_a C_D A U^2 \quad (5)$$

$\rho_a - Mass\ density\ of\ air$
$A - Cross\ sectional\ area\ of\ the\ hull\ form$
$C_D - Wing\ tunnel\ tests\ are\ used\ to\ obtain\ this\ and\ value\ between\ 0.5\ and\ 0.7$

Total resistance can be calculated using the following formula;

$$R_T = R_f + R_r + R_a \quad (6)$$

The drop in speed of FACs is one of the main problems which the Sri Lanka Navy confronts which directly affects the craft's operational capability. This research, is intended to elaborate on identified root causes for the drop in speed of FACs.

II. OBJECTIVE

As a solution to the speed drop of the FACs Sri Lanka Navy adopts hull cleaning of the craft in the periods of six months. Once a year a craft will undergo Routine underwater maintenance and a hull cleaning in the periods of six months. The objective of this research is to identify the reasons for the speed drop of the FACs and provide solutions to minimize the preventable causes of the drop in speed of FACs

III. LITERATURE REVIEW

Researches elaborate on the performance drop of FACs such as drop in designed speed, acceleration delay and poor turn manoeuvring performance of water jet propelled FACs (Pathirana, 2014).

Following root causes were identified in above mentioned research to drop in speed of FACs.

i. Increased skin friction resistance owing to the rough bottom surface due to thick and irregular paint coating, left with protruded weld seams.
ii. Dented shipside and superstructure causing higher wind resistance.
iii. Moderate growth after 4-5 months of routine underwater maintenance that leave a doubt on self-polishing paint scheme (SPC) performance.
iv. Mechanical defects such as higher water jet impeller tip clearance; as per jet manufacturer doubling of tip clearance causes 1 percent speed drop.
v. Overloading of vessels.

Research by Avci and Barlas on the use of trim interceptors shows the gaining of speed by few knots than the bare hull form of the vessel. It is clearly said that the interceptor blade depth has to be adjusted related to the operation speed of the vessel. The study clearly states that the interceptor systems decreases the unwanted trim angles in high speeds and increase the forward speed up to 4 to 5 knots in full scale, and gain approximately 25% fuel savings. The system also decrease the wetted surface area and supplies a clear angle of sight for the boat operators.

A study on the planing behaviour of a fast monohull was investigated with reference to the change in

LCG positions and its effect on the resistance, dynamic trim and sinkage were explored based on dedicated model tests by Danisma. Based on findings in this study a slight aft trim may increase the resistance below the planing speed, but provided with sufficient power it can help the vessel to reach her planing regime as well as reducing the resistance at speeds beyond the planing speed.

A study on increasing frictional resistance of a hull due to surface fouling has to be carried out by Demirel, Uzun, Zhang &Turan. They considered two types (M type and S type) of barnacles and found the change of the percentage of the C_f due to the presence of barnacles. Results are as follows;

Table 2. Effect of resistance due to Barnacles

Sr. No.	Type of Barnacle	Surface Coverage (%)	Change in C_f (%)
a.	M	10	44
		20	71
		40	107
		50	115
b.	S	10	23
		20	43
		40	68
		50	77

IV. METHODOLOGY

i. Collection of data related to the speed of the FACs before and after hull cleaning, tabulate them and analysis of data gathered.
ii. Collection of data related to maximum speed, monthly running hours pattern and the number of patrols carried out by few FACs belongs to SLN over a year and analysis of data gathered.
iii. Gathering data related to the deformation of hull shapes, mechanical defects which can directly affect on reduction of speed of FACs.
iv. Designing a hull form equivalent to a hull shape of FACs and analysis of the hull shape.
v. Calculating planing LCG of the designed hull shape, and planing speed of the designed hull by the software developed by Dingo Tweedie (2004).
vi. CFD representation of flow around the hull form due to movement of the vessel before planing and after planing.
vii. CFD representation of flow pattern around the hull form when the hull is deformed.
viii. Validating of the methods carried out to prevent speed drop of FACs by SLN with the gathered data.

V. DATA REPRESENTATION AND DATA ANALYSIS

Data of the speeds of the FACs before and after hull cleaning has been gathered from the ship's logs/ trial sheets. Speeds of the FACs before and after hull cleaning are as follows;

Table 3. Speeds of FACs before and after hull cleaning

Craft	Speed before slipping	Speed after slipping
P 402	19	23
P 410	40	43
P 423	43.4	36
P 433	32	35
P 435	31.4	40.6
P 439	39	40
CG 403	30.6	34
P 450	23	42
P 451	32	38
P 471	19.9	21.7
P 472	32	40
P 473	16.5	42
P 475	22	42
P 485	36	40
P 497	38.5	42.8
P 4443	44	48.5
P 4444	44	48.5
P 4445	47.5	48
P 4446	44.3	47

The above graph clearly shows that the speed of the craft has been increased in a considerable amount after the hull cleaning. In some craft, the speed gained only a little after the hull cleaning and it was observed that due to the rough sea conditions the speed has not been gained by the craft.

Data of the running hours pattern, patrols carried out during the month and the maximum speed gained by the ship has been collected by using the ship's logs for few FACs and the data tabulated as follows for the convenience of the analysis of the data. The black dot shows the speed after RUWM. (only one FAC is considered here for easy reference)

Table 4. Details of P451 Craft

Month	Number Of Patrols	Running Hrs During Month	Average Speed	
			RPM	KNOTS
Post slipping trials were carried out on 08 March 17 after Hull cleaning and achieved 40 knots when both engines were in maximum RPM (2100 x 2)				
March		9.00	2070 x 2	40.00
April	5	127.00	1850 x 2	30.50
May	7	176.00	1900 x 2	32.00
June	14	295.15	2000 x 2	36.00
July	14	268.10	1800 x 2	30.00
August	10	203.20	1900 x 2	31.00
September	10	99.50	2000 x 2	32.00
Post slipping trials were carried out on 03 October 17 after RUWM and achieved 42 knots				
October		4.30	2070 x 2	38.00
November	4	47.20	1900 x 2	35.00
December	7	72.00	1900 x 2	35.00
January	5	76.00	2000 x 2	36.50

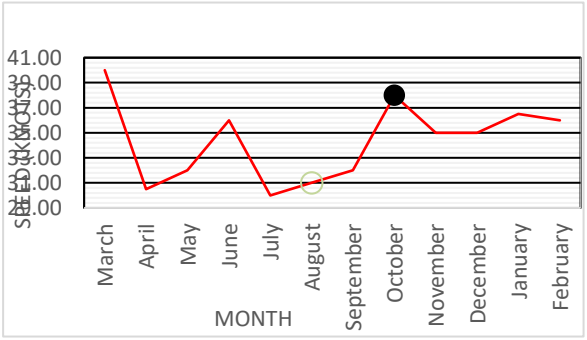

Figure 2. Data tabulation of P451 Craft

A routine under water maintenance (RUWM) is being carried out in each craft per year. In the RUWM a new paint coating is being applied on the hull after cleaning the hull and propellers or in the case of a water jet propelled craft the water jet tunnel, impeller, the nozzle is being cleaned.

A hull cleaning is being carried out every six months for each craft and during this period cleaning of hull fouling, cleaning of propellers/ impellers, water jet tunnel etc. is being carried out. Covering of removed patches of the paint coating is being carried out in this period.

Analysis of the above data validates that hull cleaning or RUWM is an effective method of preventing speed drop of the FACs. By this method it prevents the followings;

i. Added resistance force due to barnacles.
ii. Extra added weight and shifting of LCG of the craft.
iii. Eddy resistance due to fouling of the ship's hull.

Further analysis shows that the running hours pattern of the FACs affects the speed drop of the craft. Months which there is a low running hours during the month has a slight considerable drop of the speed during the month. The reason for this is the rate of fouling of the ship's hull is considerably high when the ship is at rest.

Also, the speed drop occurs when the engines of the craft are not achieving their maximum RPMs due to various reasons. Most of the sea trials show that the same throttle position does not give the same RPM of both engines. Further, calibration errors lead to mismatch of RPMs of both engines installed onboard and it can be directly affects the speed of the craft.

Most of the trim tabs available are locked due to operational defects and locked trim tabs is another reason for craft failing to gain maximum speeds at maximum RPMs. As described previously the interceptor blade/trim tab depth have to be adjusted related to the operation speed of the vessel.

To design an equivalent hull form of a FAC, Delft Ship (Version 10.20) free software is used. The hull form is as follows. The Lines plan is attached herewith as Annex A to this document.

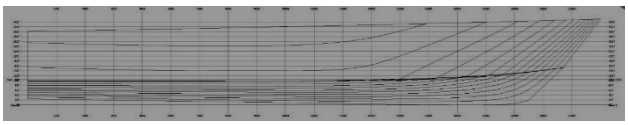

Figure 3. Profile of Hull

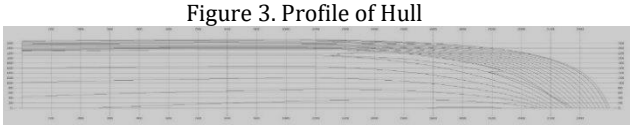

Figure 4. Half Breadth Plan

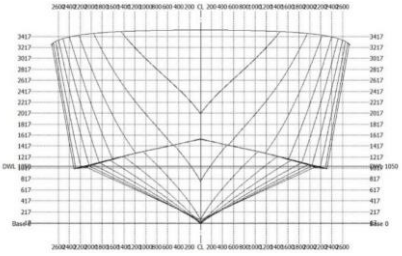

Figure 5. Body Plan FWD

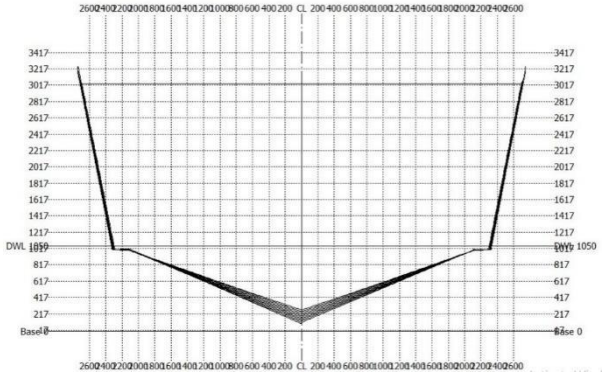

Figure 6. Body Plan AFT

The design hydrostatics of the hull form are as follows

Design length	24.000 (m)	**Midship location**	12.000 (m)
Length over all	24.000 (m)	**Relative water density**	1.0250
Design beam	5.500 (m)	**Mean shell thickness**	0.0000 (m)
Maximum beam	5.492 (m)	**Appendage coefficient**	1.0000
Design draft	1.050 (m)		

Volume properties		**Waterplane properties**	
Moulded volume	38.437 (m³)	Length on waterline	21.899 (m)
Total displaced volume	38.437 (m³)	Beam on waterline	4.661 (m)
Displacement	39.398 (tonnes)	Entrance angle	30.627 (Degr.)
Block coefficient	0.2773	Waterplane area	87.15 (m²)
Prismatic coefficient	0.7563	Waterplane coefficient	0.6602
Vert. prismatic coefficient	0.4200	Waterplane center of floatation	9.534 (m)
Wetted surface area	99.94 (m²)	Transverse moment of inertia	139.63 (m⁴)
Longitudinal center of buoyancy	9.850 (m)	Longitudinal moment of inertia	2775.1 (m⁴)
Longitudinal center of buoyancy	-9.818 %		
Vertical center of buoyancy	0.745 (m)		

Midship properties		**Initial stability**	
Midship section area	2.12 (m²)	Transverse metacentric height	4.377 (m)
Midship coefficient	0.3667	Longitudinal metacentric height	72.942 (m)

Lateral plane	
Lateral area	19.92 (m²)
Longitudinal center of effort	11.178 (m)
Vertical center of effort	0.585 (m)

The following layer properties are calculated for both sides of the ship

Location	Area (m²)	Thickness (m)	Weight (tonnes)	LCG (m)	TCG (m)	VCG (m)
Layer 0	222.96	0.005	3.010	10.790	0.000 (CL)	1.459

Sectional areas

Location (m)	Area (m²)	Location (m)	Area (m²)	Location (m)	Area (m²)	Location (m)	Area (m²)	Location (m)	Area (m²)
1.200	1.84	6.000	1.99	10.800	2.11	15.600	1.91	20.400	0.69
2.400	1.88	7.200	2.02	12.000	2.12	16.800	1.74	21.600	0.05
3.600	1.92	8.400	2.05	13.200	2.09	18.000	1.49	22.800	0.00
4.800	1.95	9.600	2.08	14.400	2.02	19.200	1.17		

Figure 7. Design Hydrostatics

Designed hull particulars have been entered into the software developed by Dingo Tweedie (2004) and the planing speeds at different LCG positions were obtained. The gathered data are as follow for the different LCG positions; (only the data most relevant is mentioned here such as speed where planing of the hull begins)

Table 5. LCG at 10.79m from the transom

V	LCG		$P_{effective}$		Planing/ Not Planing
[kn]	[ft]	[metres]	[ehp]	[ekW]	
10	35.4	10.790	96	71	NP
11	35.4	10.790	140	105	NP
13	35.4	10.790	230	171	NP
15	35.4	10.790	319	238	NP
17	35.4	10.790	409	306	NP
19	35.4	10.790	503	376	NP
21	35.4	10.790	603	450	NP
23	35.4	10.790	710	530	NP
25	35.4	10.790	827	617	NP
27	35.4	10.790	955	713	NP
29	35.4	10.790	1,095	817	NP
31	35.4	10.790	1,249	932	NP
33	35.4	10.790	1,417	1,057	NP
35	35.4	10.790	1,600	1,194	NP
37	35.4	10.790	1,801	1,344	NP

Table 6. LCG at 8.5m from transom

V	**LCG**		**$P_{effective}$**		Planing/ Not Planing
[kn]	[ft]	[metres]	[ehp]	[ekW]	
10	27.89	8.501	96	72	NP
11	27.89	8.501	143	107	NP
13	27.89	8.501	235	175	NP
15	27.89	8.501	325	242	NP
17	27.89	8.501	415	310	NP
19	27.89	8.501	507	378	NP
21	27.89	8.501	603	450	NP
23	27.89	8.501	703	525	NP
25	27.89	8.501	807	603	NP
27	27.89	8.501	917	684	NP
29	27.89	8.501	1,032	771	P
31	27.89	8.501	1,156	863	P
33	27.89	8.501	1,288	961	P
35	27.89	8.501	1,432	1,069	P
37	27.89	8.501	1,589	1,186	P

Table 7. LCG at 7.49m from transom

V	LCG		$P_{effective}$		Planing/ Not Planing
[kn]	[ft]	[metres]	[ehp]	[ekW]	
10	24.6	7.498	107	80	NP
11	24.6	7.498	158	118	NP
13	24.6	7.498	259	193	NP
15	24.6	7.498	358	267	NP
17	24.6	7.498	457	341	NP
19	24.6	7.498	557	416	P
21	24.6	7.498	656	490	P
23	24.6	7.498	755	564	P
25	24.6	7.498	853	637	P
27	24.6	7.498	952	710	P
29	24.6	7.498	1,053	786	P
31	24.6	7.498	1,161	866	P
33	24.6	7.498	1,276	952	P
35	24.6	7.498	1,402	1,046	P
37	24.6	7.498	1,539	1,149	P

Table 8. LCG at 6.5m from transom

V	**LCG**		**$P_{effective}$**		Comments
[kn]	[ft]	[metres]	[ehp]	[ekW]	
10	21.33	6.501	129	96	NP
11	21.33	6.501	191	142	P
13	21.33	6.501	312	233	P
15	21.33	6.501	432	322	P
17	21.33	6.501	549	409	P
19	21.33	6.501	659	492	P
21	21.33	6.501	760	567	P
23	21.33	6.501	850	635	P
25	21.33	6.501	934	697	P
27	21.33	6.501	1,016	758	P
29	21.33	6.501	1,100	821	P
31	21.33	6.501	1,190	888	P
33	21.33	6.501	1,287	960	P
35	21.33	6.501	1,394	1,040	P
37	21.33	6.501	1,512	1,129	P

The above tables show the effect of the LCG position on the planing speed. When the craft's LCG shifts towards transom the speed where craft planes decrease. Also it is obvious that the power required to achieve the planing speed reduces drastically when the LCG shift towards the transom.

Yet there is a limit for the LCG to be shifted in order to maintain the stability, manoeuvrability and habitability of the craft. Furthermore, moving LCG of the craft improves the ability of the craft to plane and further increasing causes power required to maintain the momentum at some point.

CFD analysis has been carried out for a model hull form of a FAC. The hull shape is smooth and fine. The pressure profile, velocity profile and streamlines around the hull are as follows;

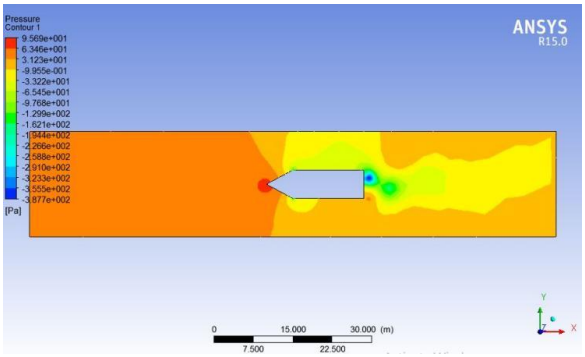

Figure 8. Pressure profile around the model hull

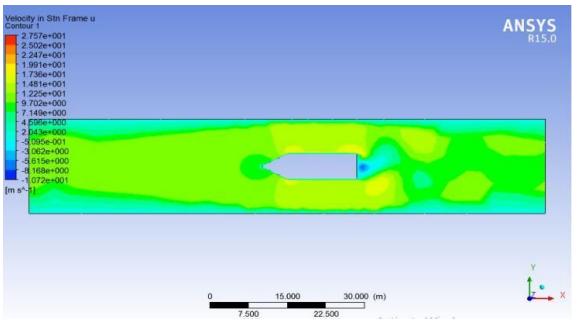

Figure 9. Velocity profile around the model hull

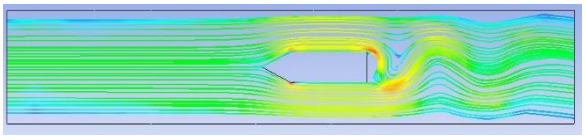

Figure 10. Streamlines around model hull

It is obvious that the pressure profile, streamlines and velocity profile around the hull are fine and smooth due to the smoothness of the hull. In this case, there won't be increased resistance to the hull or eddy resistance generated by the hull. Also, resistance due to wave making might not be added in this situation.

In order to obtain the pressure profile, streamlines and velocity profile around a deformed hull in which fouling is existing a hull form was designed and the CFD analysis was carried out and results are as follows;

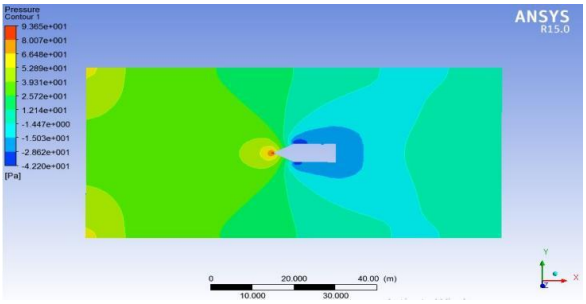

Figure 11. Pressure profile around the deformed hull

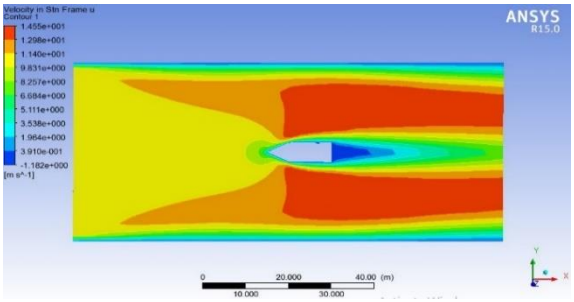

Figure 12. Velocity profile around the deformed hull

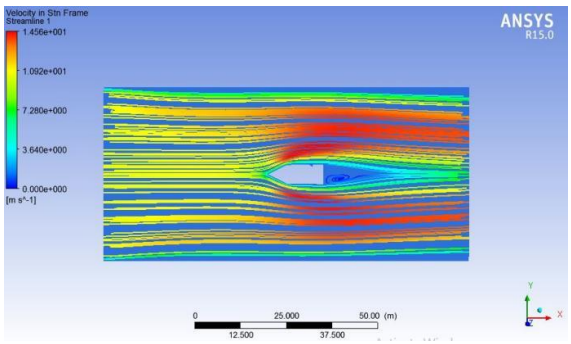

Figure 13. Streamlines around the deformed hull

It can be clearly identified that the maximum velocity of the hull shape has been reduced to 14.5 m/s from 27.5 m/s due to the deformation of the hull. The same effect occurs when fouling occurs in the hull form.

Further, the streamlines create eddies due to the hull shape deformations. This is called as eddy resistance of the hull. It can be clearly identified when the RPM of the engines increases the speed of the craft reduces drastically due to fouling of the hull.

VI. CONCLUSION

As per data gathered it is obvious that the speed of the craft has been drastically increased after a hull cleaning/RUWM. This is mainly due to removing of the fouling/ underwater growth. Furthermore, the following reasons causes the speed drop of the FAC's;

i. Mechanical errors such as defects in trim tabs.
ii. Electrical errors such as RPM differences.
iii. Restrictions in RPMs.
iv. Shifting of LCG of the craft due to heavy loading.

It is true that the main reason for the speed drop due to underwater growth which is named fouling of the hull. Considering all the above facts the RUWM and hull cleaning after six months of RUWM is an effective method to prevent fouling of the hull.

Further, in order to prevent speed drops the FAC's the facts which are mentioned in the above para are to be addressed and rectified.

REFERENCES

D. B. Danisman,(2015) "An Experimental Study of the Effect of Change in LCG on Resistance and Planing Capability of a Fast Vessel," *Researchgate*.

Y. K. Demirel, D. Uzun, Y. Zhang and O. Turan,(2017) "Effect of Barnacle Fouling on Ship Resistance and Powering," *Researchgate*.

O. M. FALTINSEN, (2005) Hydrodynamics of High-Speed Marine Vehicles, *United States of America: Cambridge University Press*.

S. D. Pathirana,(2014) "Drop in Performance of Waterjet Propelled Planing Hull Craft: A case study on FAC in Sri Lanka Navy," *Colombo*.

A. Gultekin Avci, Baris Barlas,(2016) "The Usage of Interceptors in High Speed Craft," *Researchgate*.

"Basic Principles of Ship Propulsion," *MAN Diesel & Turbo.*

ACKNOWLEDGMENT

I am humbly overwhelmed to acknowledge my gratitude to all those who have helped me and guided me to put these ideas, well above the level of simplicity and into something concrete. I would like to express my special thanks to Sri Lanka Navy

for facilitating me with all the practical details related to Fast Attack Crafts.

AUTHOR BIOGRAPHY

A graduate from 28th Intake of General Sir John Kotelawela Defence University in Marine Engineering and presently serving as a Marine Engineer to Sri Lanka Navy at Sri Lanka Naval Dockyard, Trincomalee. Interested in renewable energy, marine engineering and underwater vehicle designing.

A Sustainable Future for Rubber Waste in Sri Lanka

VL Kuruwita Arachchi# and DDTK Kulathunga

Department of Civil Engineering, Faculty of Engineering, General Sir John Kotelawala Defence University, Sri Lanka

#venuka02@gmail.com

Abstract— Innovative construction materials have a high demand in the construction industry with the development of the green building concept and sustainable construction. The use of waste materials is encouraged even with the green rating system, and waste rubber is identified as one of the main waste materials generated in any country. Sri Lanka produces 4.5 billion solid waste materials per year. The management of waste material and implementing them in a productive way is essential for a country to promote sustainability. For rubber waste, solutions such as rubberized concrete have been introduced in developed countries. However, in Sri Lanka, rubberized concrete is not popular in the construction industry. Further, it is not clear whether the quality or the quantity of rubber waste available in Sri Lanka is sufficient to promote such application of rubber waste. Therefore, this study reviews the feasibility of using rubber waste available in Sri Lanka for a commercial application such as rubberized concrete. The wastage of rubber from different sources was identified as 1283.6 tons per month in Sri Lanka. Out of the whole batch of rubber wastage, latex rubber and tire rubber wastage were identified as the main types. The quality of rubber wastage is critical when using rubber waste in application. Literature on rubberized concrete suggests recycled crumb rubber and tire chips of 5mm to 20mm in size as suitable for rubberized concrete. Rubber crumbs of this recommended size can be found in Sri Lanka in sufficient amounts, which implies that there is a future for rubberized concrete in Sri Lanka.

Keywords— waste rubber, rubberized concrete, sustainable, rubber types

I. INTRODUCTION

Among the several issues arise as a result of population growth, waste generation can also be considered as a major problem. Several literatures have studied the effect of population growth on waste generation (Dallas et al. 1996; Lal et al. 2011; Das et al. 2014). From different solid wastes, rubber waste takes an important place as this waste material grows with the rapid development of industries. The critical part on rubber waste is the non-biodegradable character, which cause hazardous impacts on environment (Yamamoto et al. 2001; Yehia 2004).

Sri Lanka experienced 4.5 billion solid waste per year (Gunaruwan et al. 2016) Therefore, it is essential to manage the solid waste properly and generate the solid waste to an asset like most of the developed countries. One such important waste material is rubber waste. Rubber waste is used as an energy source, construction material by reusing, recycling, hydrolysis, mechano-chemical reactions or reclamation (Yehi 2004; Senevirathne et al. 2020). Waste rubber has been identified as useful in many industries. One of the pioneer industry is the construction industry. In recent past decade various research studies were conducted to identify the properties of waste rubber as a construction material. As a result of that rubberized concrete was introduced and implemented on some applications such as, a replacement to lightweight concrete, on highway as a shock absorber, as a sound barrier, road barriers, shooting houses and firing ranges waste rubber used as a construction material. Moreover, implantation of waste rubber in structural elements also under discussion. With such variety of applications, the quality and the quantity of waste rubber is an essential topic to be concerned.

Therefore, the management of rubber waste is timely need area to discuss with the development in industries and population density in Sri Lanka. This study is to identify the rubber waste amount and its sources while conducting an analysis at the end.

II. METHODOLOGY

As the first step of the study, a survey was conducted to identify the sources of rubber waste and the collectors of the rubber waste. Two objectives of this survey are as follows;

i. Identify the sources of waste rubber and nature of the waste from each source

ii. Identify the annually generated quantity of waste rubber

Rubber is a multy function material which is used in many industries for several purposes. As a result of that wastage of rubber is high. Respective to this scenarios several local governing bodies and private institutes act as collecting sources of rubber waste. These sources can be mainly categorized as;

- Local government authorities
- Licensed private collecting institute
- Rubber manufacturing companies

Local government authorities and licensed private collecting institutes collect other solid waste materials too. Therefore, from the collected materials the percentage amount of rubber waste was identified. Importantly, several categories of waste collectors were identified. In addition to the role as merely collectors, some of these institutes collect rubber waste for the purpose of exporting (collectors and exporters), and some act as collectors and recyclers and also as only recyclers. Figure 1 represents the location of various waste collecting centers implemented island wide.

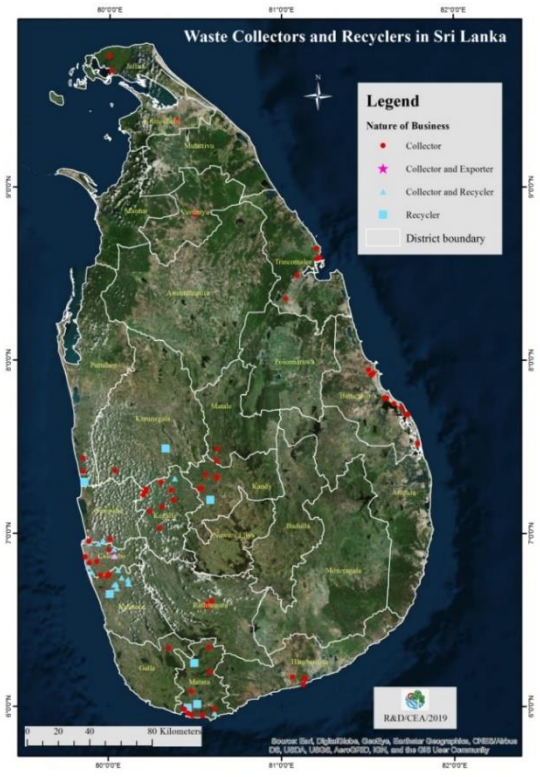

Figure 5. Waste collectors and recyclers in Sri Lanka (CEA 2021b)

Rubber waste from manufacturing process is one source of waste rubber. Therefore, manufacturers who involved in rubber related products, can be identified as collectors of waste rubber who collect the rubber waste from their own manufacturing process. This study extended a survey to identify such manufactures as well.

Study was concluded by doing an analysis on rubber waste collected from each source and finding the percentages. Also, a percentage was obtained for the total rubber waste with respect to total solid waste material collected

III. RESULTS AND DISCUSSION

A. Survey on Local Government Authorities

Central Environmental Authority (CEA) of Sri Lanka is the main governing body on all kinds of waste materials. CEA has organized group of local responsible bodies on waste material. The collecting and managing those waste materials are main two responsibilities of those. The authority appoints the responsible bodies by considering the following factors.

i. Consisting with serious issues of solid waste management.
ii. Daily waste collection amount

By considering above mentioned two factors total of 33 local bodies (Kogyo Co 2016) authorized on collecting waste materials. The details including rubber wastage are tabulated in Table 1.

Table 2. Local government authorities collecting waste material

No	Province	Local authority	Rubber waste %	Waste rubber amount (kg/day)
1	Northern	Karachchi PS	0.2	12
2	Northern	Vadamarachchi PS	0.2	10
3	North-Central	Hingurakgoda PS	0.8	80
4	Uva	Kataragama PS	0.2	16
5	Southern	Hambantota MC	1.0	80
6	Eastern	Kinniya PS	0.6	36
7	Western	Kalutara PS	0.7	56
8	North-Central	Thamankaduwa PS	1.1	110
9	Northern	Jaffna MC	0.2	138
10	North-Central	Anuradhapura MC	0.3	75

11	Eastern	Trincomale e UC	1.0	260
12	Eastern	Batticaloa MC	0.4	240
13	North Western	Chilaw UC	0.2	36
14	North Western	Kurunegala MC	0.3	144
15	Central	Nuwara Eliya MC	0.4	84
16	Sabaraga muwa	Kegalle UC	0.4	60
17	Sabaraga muwa	Rathnapura MC	0.6	192
18	Uva	Badulla MC	0.4	112
19	Western	Gampaha MC	0.7	196
20	Western	Negombo MC	0.5	85
21	Western	Katunayake Seeduwa UC	0.6	140
22	Western	Kotikawatt a Mulleriyaw a PS	0.4	152
23	Western	Moratuwa MC	0.6	510
24	Western	Kesbewa UC	0.6	324
25	Western	Kolonnawa UC	0.4	120
26	Western	Maharagam a UC	0.5	410
27	Western	Kaduwela MC	0.3	255
28	Western	Kalutara UC	0.4	80
29	Western	Beruwala UC	0.5	70
30	Western	Colombo MC	1.1	7750
31	Western	Dehiwela Mt. Lavinia MC	0.6	1020
32	Western	Sri Jayawarden apura Kotte MC	0.4	400
33	Central	Kandy MC	0.8	6240
Total				**19477**

(Kogyo Co 2016)

Analyzing the rubber waste amounts from each authority, three categories can be identified as follows.

Less than 100 kg per day: approximately 43% of all survey candidates
100-1000 kg per day: approximately 48% of all survey candidate
More than 1000 ton per day: approximately 9% of all survey candidate

Total of 19.447 ton of rubber waste collected in island wide from local authorities per day. Even though the percentage is very much low respect to other solid waste, rubber as a non-environmentally friendly material has huge impact on social health, environmental and to economy.. When Analyzing the provincial wise rubber wastage, western province has the highest wastage value of 11.512 ton per day and it is 59% from the overall value.

B. Survey on Private Collecting Institutes

Due to the heap of waste materials produced daily, private collecting institute are established to collect the waste materials all over the country. These institutes are governed by the local authorities and each and every institute should licensed under the CEA (CEA 2021a) Table 2 represents the total number of private collecting centers established in district.

Table 3. Licensed private waste collecting centers

District	Number of collectors
Colombo	79
Gampaha	29
Kalutara	24
Ratnapura	11
Kurunegala	6
Kandy	15
Hambanthota	07
Badulla	05
Puttalam	03
Matale	03
Matara	47
Kegalle	08
Galle	24
Trincomalee	06
Polonnaruwa	05
Vavniya	02
Jaffna	06

Batticaloa	15
Ampara	01
Mulaithivu	01
Nuwara Eliya	01

(CEA 2019)

It is identified that 295 licensed private collectors in island wide, but it is important to mentioned that even though licence is approved to collect all non-hazardous waste materials, these collectors are more or less specified to collect three or four non-hazardous waste material. In that case, every collector does not collect waste rubber. Considering the waste rubber collectors, total of 400.19 ton per month collected in private institutes (CEA 2019).

C. Survey on Rubber Manufacturing Companies

Rubber manufacturing can be divided in several parts, with respect to their industry. However, rubber waste in manufacturing can be basically divided into two categories as tire rubber waste and latex rubber waste as represented in Table 3.

Table 4. Rubber wastage in manufacturing

Categories	**Rubber waste (ton per month)**	**Percentage amount**
Tire rubber waste	200	66.67%
Latex rubber waste	100	33.33%
Total	**300**	**100%**

Approximately, 300 tons of rubber waste generated per month in rubber manufacturing process and majority of that waste falls into tire rubber waste category (i.e. 50% increment compared to latex rubber waste). However, all these values are approximations and impossible to report exact values.

D. Survey on Rubber Manufacturing Companies

Summarizing the total wastage of rubber respect to the sources of collectors, different waste amounts can be observed. This variation in amounts can be explained as result of different number of sources, resources, industry specified on and capacity. The total rubber wastage amounts and respective percentages are summarized in Figure 2.

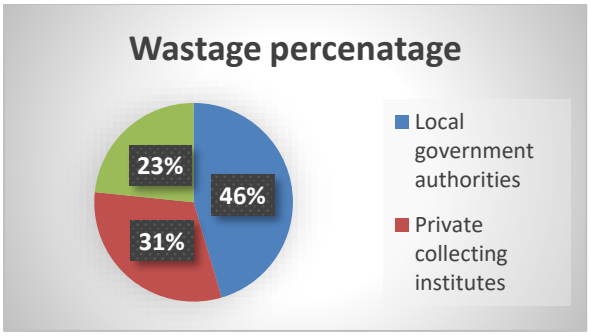

Figure 2. Waste percentages of institutes

Total of 1283.6 ton per month of waste rubber collected from all three sources. Out of the three sources, local government authorities have the highest amount of 583.41 with 45.451% of total. This can be explained by the higher resources and high number of collecting centers. It is worth to mentioned that, total of 63180 ton of solid waste materials are collected by local authorities (Kogyo Co 2016) per month and rubber wastage is 0.923% of the total.

IV. CONCLUSION

Survey on rubber wastage is a critical and timely need. With high environmental effect, to have an idea on rubber wastage collected daily is important. Also, to identify the sources to improve the facilities and to implement necessary actions are the advantages of the study while identifying the feasibility of using rubber crumb for concrete. The conclusion of the study is listed in below.

- The three main groups of rubber wastage collectors of Sri Lanka are local government authorities, Private collecting institutes and manufacturing companies as collectors.
- A total of 1283.6 ton of rubber waste collected per month from all three sources.
- The highest source of collector is the local government authorities with 583.41 ton per month with 45.451% of total.
- The approximate percentage of rubber waste from the total solid waste of the country is 0.34%.
- Sri Lanka available required quality of rubber wastage to use in rubberized concrete.

REFERENCES

CEA (2019) *ANNUAL REPORT - 2019 of Central Environmental Authority*.

CEA (2021a) *Registered Collecters of Non-Hazardous Recyclable Waste*. Available at: 2021/List of Collectors plus Collectors Recyclers updated on 27.04.2021.pdf.

CEA (2021b) *Waste Collectors and Recyclers in Sri Lanka*. Available at: http://www.cea.lk/web/?option=com_content&view=article&layout=edit&id=1407.

Dallas, Michael D and Kerzee, Ruth G and Bing-Canar, John and Mensah, Edward K and Oroke, Kevin G and Swager, R. R. (1996) 'An indicator of solid waste generation potential for Illinois using principal components analysis and geographic information systems', *Journal of the Air \& Waste Management Association*, 46(5), pp. 414–421.

Das, Swapan and Bhattacharyya, B. K. (2014) 'Estimation of municipal solid waste generation and future trends in greater metropolitan regions of Kolkata, India', *Journal of Industrial Engineering and Management Innovation*, 1(1), pp. 31--38.

Gunaruwan, T Lalithasiri and Gunasekara, W. N. (2016) 'Sri Lanka experienced 4.5 billion solid waste per year', *NSBM Journal of Management*, 2(1).

Kogyo Co, K. (2016) *Data Collection Survey on Solid Waste Management in Democratic Socialist Republic of Sri Lanka Final Report Democratic Socialist Republic of Sri Lanka Japan International Cooperation Agency (JICA) Ten (10) Priority Local Authorities*. Available at: http://open_jicareport.jica.go.jp/pdf/12250213.pdf.

Lal, Banwari and Sarma, P. M. and others (2011) *Wealth from waste*. The Energy and Resources Institute (TERI).

Senevirathne, PA and Kulathunga, DDTK and Kuruwitaarachchi, V. (2020) 'Energy Absorption Capacity and Impact Energy of Rubberized Concrete', in *Internation Reseach Coference of Kotelawela Defence University*. Kotelawela Defence University.

Yamamoto, Takashi and Yasuhara, Akio and Shiraishi, Hiroaki and Nakasugi, O. (2001) 'Bisphenol A in hazardous waste landfill leachates', *Chemosphere*, 42(4), pp. 415–418.

Yehia, A. A. (2004) 'Recycling of rubber waste', *Polymer-Plastics technology and engineering*, 43(6), pp. 1735–1754.

KDU IRC INTERNATIONAL RESEARCH CONFERENCE 2021
ID 334

Study of Estimating Greenhouse Gas Emission from Healthcare Solid Waste Management

AID Gamage# and MB Samarakoon

Department of Civil Engineering, Faculty of Engineering,
General Sir John Kotelawala Defence University

#dasungamage97@gmail.com

Abstract— This research focused on the modern-day healthcare waste management and the emission of greenhouse gases from the waste, considering the environmental pollution and the increase of medical problems and the waste due to those increments. This work comprises of the methods and calculations according to the Intergovernmental Panel on Climate Change (IPCC) guidelines and the Institute for Global Environmental Strategies (IGES) Greenhouse Gas emission spreadsheet model. The amounts of waste generated within the facility were studied and information regarding the management was gathered. From the generation, till the disposal of the waste, the required data was gathered. The cycle of generation of the total waste from healthcare facilities from the generation up to the landfill disposal site is discussed. From the processes studied, the emission estimation is found in kilograms of carbon dioxide equivalent per tonne of healthcare waste (kg CO_2e/tonne of waste). Through the data collected, and calculations with the IGES software and IPCC guidelines, it was found that in reaching net emission to zero, healthcare waste management processes in the selected medical facilities should move to more fuel savings, proper recycling, and composting practices.

Keywords: ***solid waste, healthcare, greenhouse gas, emissions***

I. INTRODUCTION

According to recent studies the waste generations and the waste disposal problems are on a rise with the increasing populations (Bundunee & Athapattu, 2015a). In waste considerations, the environmental components are sensitive assessment areas. According to the United Nations and the World Health Organization, waste can be considered as a leading Greenhouse Gas emitting sector in the world (Bereiter et al., 2015). Methane (CH_4), carbon dioxide (CO_2) and nitrous oxide (N_2O) are the main gases which are responsible for the Greenhouse effect. In calculation of the Greenhouse gases, International Panel on Climate Change (IPCC) which is an intergovernmental body of UN implemented guidelines. And with calculated emission factors, the emission from every material and every process can be estimated. In overall waste categorization, the healthcare sector is a leading waste generation area. The increasing of diseases and population undoubtedly increase the waste that is generated in these medical facilities. These wastes are simply categorized by the World Health Organization (WHO) as healthcare non-hazardous (general) waste and healthcare hazardous (clinical) waste. Further is divided into several categories for the ease of waste identification and segregation (World Health Organization, 2007).

II. LITERATURE REVIEW

According to the World Health Organization (WHO) it was estimated around 85% of wastes generated at medical facilities are general waste (Emmanuel et al., 2001). Healthcare waste management in developing countries such as Sri Lanka must be done accordingly because if handled incorrectly it could leave medical staff and the general population in danger (Khan et al., 2019). The solid waste within the healthcare facilities and the emission of greenhouse gases from the processes of those wastes from generation to transporting to the disposal site were studied and analysed. By identifying and gathering data of waste amounts and calculations through the software according to guidelines, the final analysing was completed.

A. Estimation guidelines

In estimating the emission of greenhouse gas from wastes, the IPCC guidelines of 2006 integrated software are being developed in many organizations related to the WHO and UN and can be used.

Waste categorization and Segregation

The World Health Organization (WHO) has categorized healthcare waste into several categories. This depends on the local medical authorities' categorization regarding local situations, wastes, disease types, weather, etc.

- Infectious waste – the waste that contain blood and other bodily fluids, infectious agents from laboratories, and waste from infected patients. (e.g., samples, infected animals, swabs, bandages etc.)

Figure 9. Uncovered storage of segregated healthcare waste

- Sharps – Syringes, needles, disposable scalpels etc.
- Chemical waste – disinfectants, sterilant and heavy metal contained medical devices etc.
- Pharmaceutical waste – waste that are expired, unused drugs or vaccines
- Genotoxic waste – waste that contain vomit, urine from patients that are treated with cytotoxic drugs
- Radioactive waste – such as waste that contain a certain amount of radioactivity diagnostic materials
- General waste

In Colombo - Sri Lanka, a study has been conducted regarding the management of healthcare wastes considering 18 out of 26 government hospitals (Bundunee & Athapattu, 2015b). Studies of landfilling showed an amount of 3.84 metric tonnes of healthcare waste per day is generated.

Table 1. Government healthcare waste generation in the year 2000

	Total health care waste (kg/day)	***Hazardous waste (kg/day)***	
		At 10% of total healthcare waste	*At 25% of total healthcare waste*
Lower estimate	76 623	7 662	19 155
Upper estimate	170 789	17 078	42 697

As per Table 1, a study done for the year 2000 regarding government hospital waste the hazardous waste estimation per year can be percentages of 10% or 25% or in-between (Haniffa, 2004).

B. Waste Management

'Red bag waste' is the general classification done in European countries where the hazardous waste is bagged in red colored bags. While is Sri Lanka it is yellow taped bags or boxes.

In Sri Lanka, separate color-coded system is being followed as per the WHO protocols and the local authorities. The color-coded labels or bins of the color is to be seen in each facility, wards, laboratories, cafeterias, and offices.

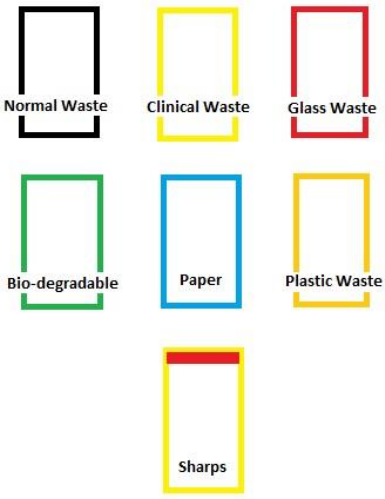

Figure 10 - Color-coded system at Local medical facilities

The yellow bags are sent to incinerator units where they contain both infectious and pathological waste. The yellow boxes which contain sharps waste is also sent to the incinerator units.

The hazardous waste (clinical waste) must be treated or incinerated before being sent to landfill sites while the general waste is generally sent to landfill sites.

C. Emissions

Sources of greenhouse gas emission are from burning of fossil fuels and mix waste landfilling. The emission of greenhouse gases can be classified as direct and indirect (Khan et al., 2019).

- Direct emissions – emissions from the respective locations and the entity owned sources.
- Indirect emissions - use of electricity and other functions and the emission from those sources.

The emissions, savings and net emissions must be considered when conducting an estimation regarding greenhouse gas emissions.

III. METHODOLOGY

A. Scenario description

Step 01 included site visits to the selected medical facilities, studying the waste management practices, having interviews with staff, and my personal observations. Waste generation data was gathered in step 01.

Step 02 included data regarding after the waste were generated and data when the waste was transported up to the landfill or treatment sites.

Step 03 included the data analyzing part using an estimation software which was developed by Institute for Global Environmental Strategies according to the World Health Organization's IPCC guidelines.

B. Facility Selection

The selected medical facilities have modern technology and has highest amounts of patient populations.

- The National Hospital of Sri Lanka (NHSL)
- The Colombo South Teaching Hospital
- The University Hospital of Kotelawala Defence University (UHKDU)
- The Navy General Hospital

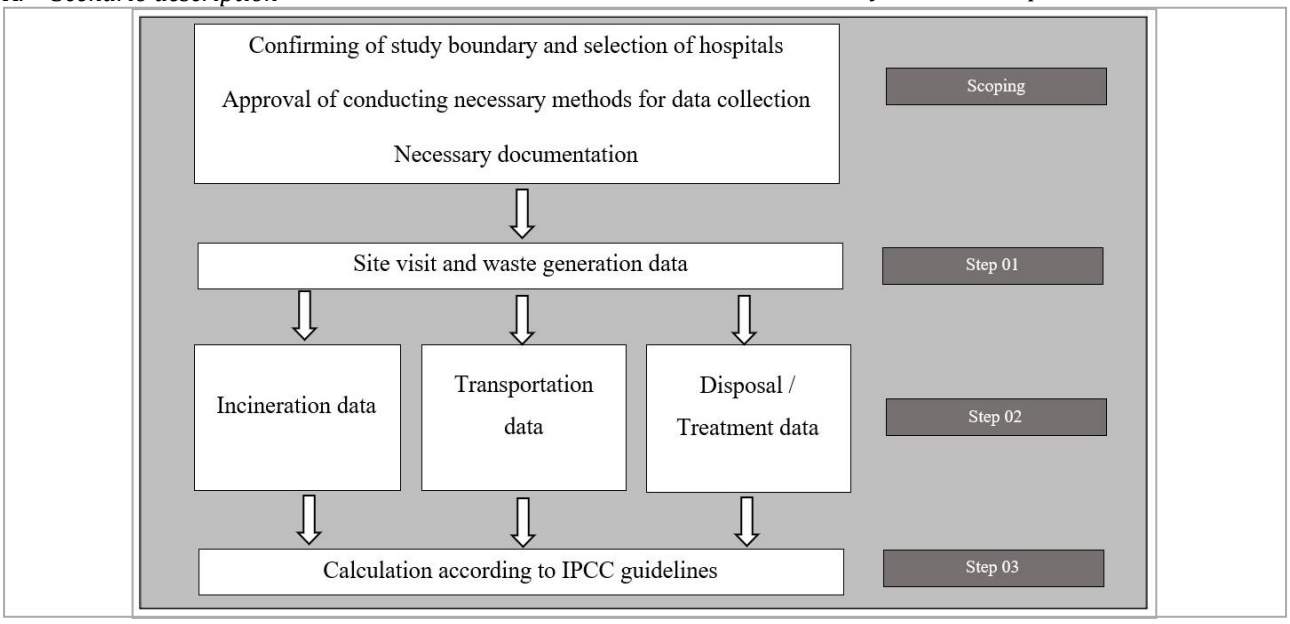

Figure 11. Scenario description

Figure 3 shows the overall study that was conducted in three steps. Figure 5 shows the study boundary of the research. A separate documentation were used for step 01 and step 02 studies only considering solid waste of the healthcare facilities.

Figure 4 shows the most common waste segregation categories that can be seen at medical facilities. The selected medical facilities are situated in the Colombo area and its outskirts. All the selected medical facilities are government-based hospitals, while 2 are military administered. The

National Hospital of Sri Lanka (NHSL) being the country's central medical facility, and the Colombo South Teaching Hospital which specializes in emergency situations use a semi-government treatment unit for incineration of hazardous waste. Other two facilities have on-site incineration units.

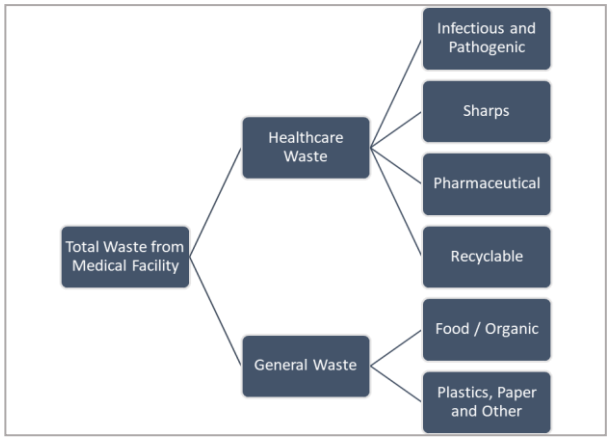

Figure 12. Local facility waste segregation

C. Data Collection

The data regarding step 01 and 02 were collected with site visits. Site visits were conducted two to four visits per each medical facility. Each visit consisted of data collection from record books, interviews with expertise personnel, working staff, and personal observation.

Main locations within the facility for data collections were the infection control units, the on-site Public Health Inspector (PHI), local ward record books and the temporary waste storage record books.

The collected data were fed to the software which finally outputs the estimation amounts of greenhouse gas per ton of waste.

D. Estimation Software

The estimation software follows the tier 3 calculations for greenhouse gas emission for wastes, which demonstrates that global emission factors are used rather than country specific data. Since Sri Lanka's emission factors were not calculated the tier 3 approach is the most suitable in estimating greenhouse gas emissions. Figure 4 demonstrates the study boundary of data collection. The software is developed at Institute for Global Environmental Strategies (IGES). The IPCC guidelines of the year 2006 were followed in the software and is specifically developed for South Asian countries (Menikpura, 2013).

E. Emission from sectors

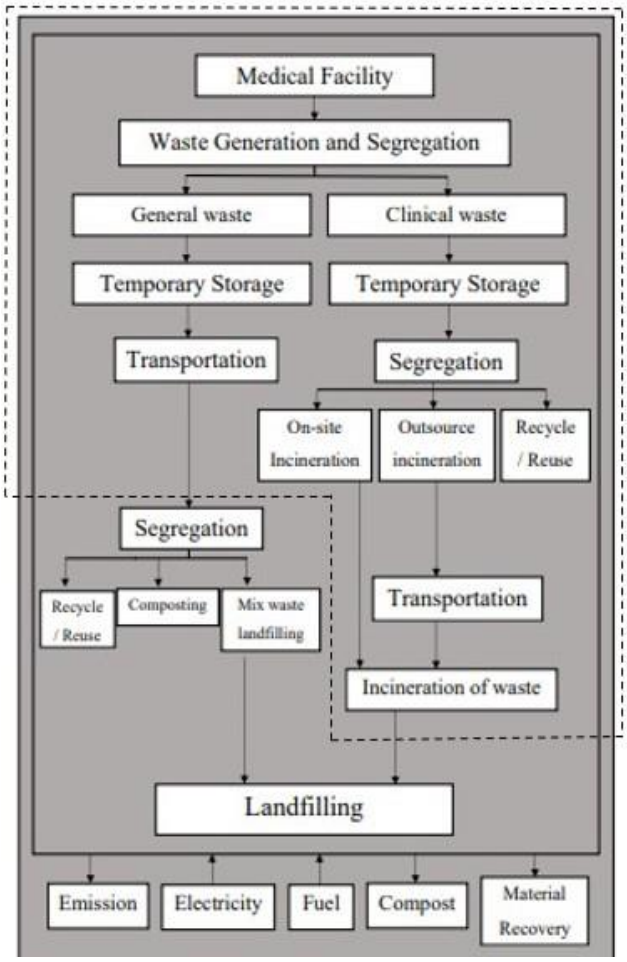

Figure 13. Study boundary (Cradle to gate analysis)

The wastes generated were put to processes from the management of the wastes where the emission of greenhouse gases occur due to those processes. The equations for each of the processes are integrated within the software.

The studied processes of these healthcare wastes are transportation, incineration, composting, and recycling.

1. Transportation – In Sri Lanka transportation is done with either waste-trucks or tractors. Either Petrol or diesel is used. Depending on the route, fuel consumption and routine of the emissions depend.

2. Incineration - The main objective of incineration is to reduce the volume of waste. However, when it comes to hazardous healthcare waste, it is necessary to

Table 2 - Monthly waste generation in kilograms (Step 01)

Hospital Name	Pathological & Infectious waste	Sharps waste	Radioactive waste	Recyclable waste	General waste	Total waste generated
National Hospital of Sri Lanka	46205.6	7469.36	1	637	147000	**201312.96**
Colombo South Teaching Hospital	15586	899.2	0	183	36000	**52668.2**
University Hospital of KDU	3600	268	0	54	19200	**23122**
Navy General Hospital	740	96	0	21	3900	**4757**

incinerate the waste within 24 hours after generation. Incineration is the highest greenhouse gas emitting process as the fuel consumption and electricity consumption is high. Incineration directly eliminates the emission of methane (CH_4) and replaces it with carbon dioxide (CO_2) which is considerably lower impacting than methane.

3. Composting - There is an emitting of greenhouse gas in composting, but it is replacing a higher emission possibility by landfilling the wastes. The food waste and the garden waste is used in composting. In most steps there is a possibility of using machinery for composting but the non-machinery involving processes are recommended. Even though healthcare waste contains organic waste in hazardous waste, they are not used for composting considering health factors and other situations.

4. Recycling - Recycling is a massive GHG avoidance as the material recovery helps a lot to avoid material dumping at landfill sites. In healthcare waste only selected materials are being used for recycling. That too is to be sent to the closest treatment unit, which is on-site, and then used back. The theory in greenhouse gas regarding recycling as follows. Through recycling materials the emissions due to producing new material is avoided/ reduced.

IV. RESULTS AND DISCUSSION

Inventory – Step 01 and 02

The inventory analysis of this study which is generated waste within the facility was done through step 01.

Through collected data, it showed the waste generation and amounts were of both the healthcare hazardous and healthcare nonhazardous wastes. The Table II shows the monthly waste generation data.

While the general wastes were the only input for non-hazardous waste all other wastes were of hazardous healthcare waste. The hazardous waste composition has increased over the last decade. To which the representation shows the percentage is 27%.

The general waste composition of different materials was also gathered and each of the facility generates a similar amount of general waste material composition. Even though the percentages were similar the waste amounts were different since, NHSL has high patient attendance and the highest of the waste generating facility. The lowest being the Navy general hospital which has low patient attendance and low bed strengths.

The waste data regarding transportation, incineration, composting, and recycling were

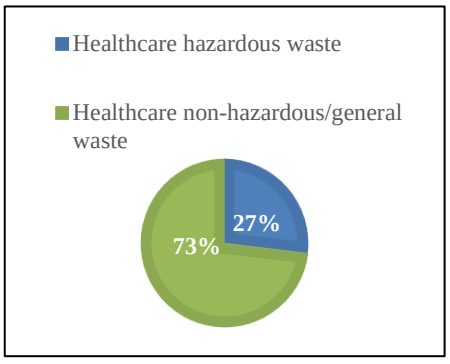

Figure 14 - Resulted healthcare waste composition

gathered through the documentation and book records.

Wastes from NHSL and Colombo South Teaching hospital were shown together as the clinical waste is both transported to relevant locations together.

The NHSL, UHKDU and the Navy General medical facilities have zero generation of wastes of metal and other. The metal wastes from the Colombo South hospital resulted because of small constructions were taken in place.

Table 3. General waste composition (NHSL and Colombo South)

Monthly General waste amounts	NHSL	%	Colombo South	%
Food waste	67500	**45.92**	16500	**45.83**
Garden waste	45000	**30.61**	10800	**30.00**
Plastic, Polythene & PVC	23400	**15.92**	5100	**14.17**
Paper	1500	**1.02**	300	**0.83**
Textile	4800	**3.27**	1800	**5.00**
Leather, rubber, foam	3000	**2.04**	900	**2.50**
Glass	1800	**1.22**	450	**1.25**
Metal	0	**0.00**	120	**0.33**
Other	0	**0.00**	30	**0.08**

Table 4. General waste composition (UHKDU and Navy General)

Monthly General waste amounts	UHKDU	%	Navy General	%
Food waste	10500	**54.69**	1800	**46.15**
Garden waste	4200	**21.88**	1350	**34.62**
Plastic, Polythene & PVC	3300	**17.19**	600	**15.38**
Paper	450	**2.34**	0	**0.00**
Textile	0	**0.00**	0	**0.00**
Leather, rubber, foam	450	**2.34**	60	**1.54**
Glass	300	**1.56**	90	**2.31**

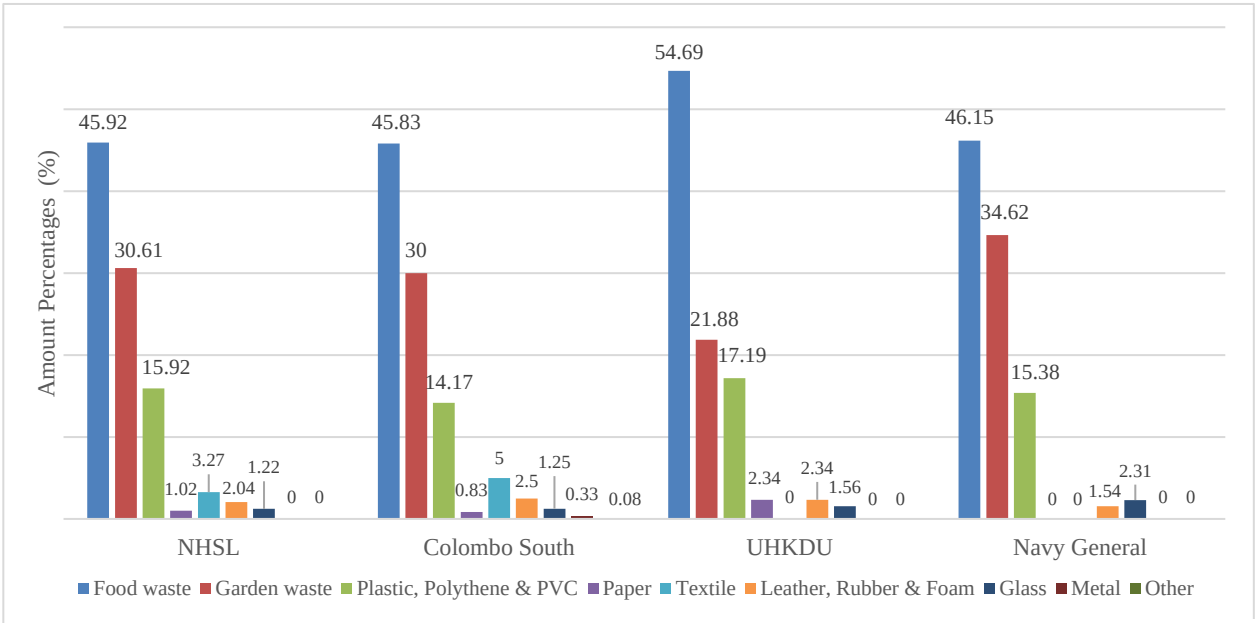

Figure 15. Waste Percentages of Each Facility (Inventory Analysis – Step 01)

Transportation data for the healthcare waste data are shown in Tables 5 and 6 The University hospital of KDU and the Navy General hospitals have onsite incinerator units and because of that the transportation emission of hazardous waste for those two medical facilities are zero.

The waste transported through carts which require no fuels. Colombo South composts 900kg of food waste while Navy General composts the whole of garden waste which is 1100kg per month. Approximately 800 kg of food waste is sent to the piggery.

Table 5. Healthcare hazardous waste transportation data

	Healthcare hazardous waste	**Distance (km)**	**Fuel usage (litres per month)**
National Hospital of Sri Lanka	Sent to treatment facility	One route starting from Colombo South hospital to treatment facility: 22.4	48.69
Colombo South Teaching Hospital			
University Hospital of KDU	On-site incineration	-	-
Navy General Hospital			

The medical facilities in the study are segregating the whole collected wastes into hazardous and non-hazardous wastes.
As per the data collected and observations, UHKDU and the Navy General Hospital have on-site incineration units therefore has no transportation fuel usages regarding hazardous wastes.

Table 6. Non-hazardous waste Transportation data

	Healthcare non-hazardous waste	**Distance (km)**	**Fuel usage (litres per month)**
National Hospital of Sri Lanka	Muthurajawela waste dump	15.1	197
Colombo South Teaching Hospital	Karadiyana waste dump	9.1	119
University Hospital of KDU	Karadiyana waste dump	4.2	63.6
Navy General Hospital	Muthurajawela waste dump	1.8	19

Table 7. Recycling material data (kg)

Monthly Recyclable	**NHSL**	**Colombo South**	**UHKDU**	**Navy General**
Paper/car-dboard	202	48	12	0
Plastics	110	55	8	0
Glasses	325	80	34	21

Computation and analysis of data through software - Step 03

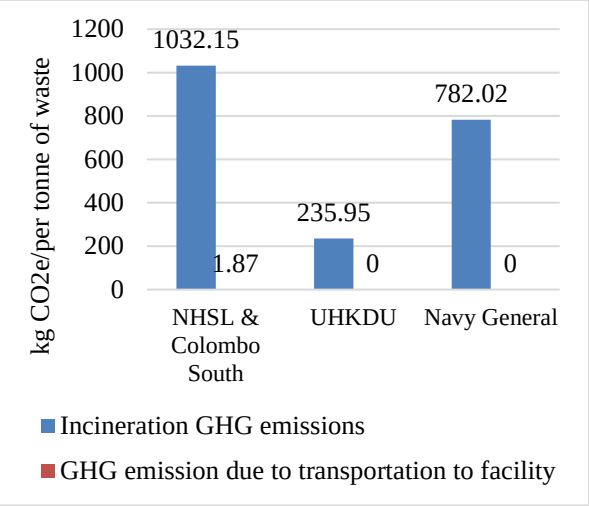

Figure 8. Hazardous waste transportation and incineration emissions

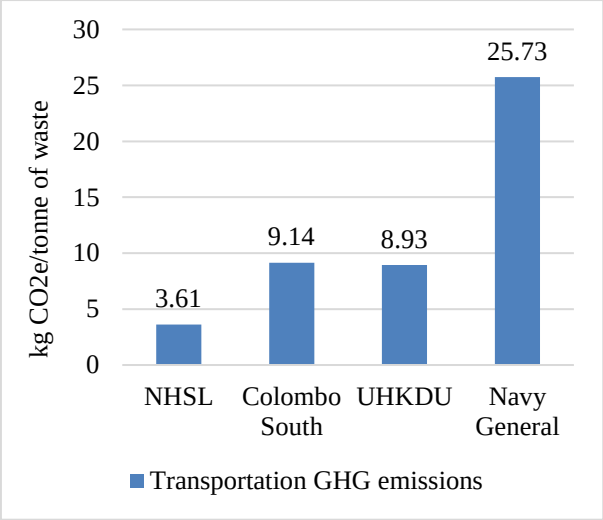

Figure 9. Non-hazardous waste transportation emissions

Emission due to transportation depends on the route the waste truck takes and the monthly fuel consumption. The national Hospital of Sri Lanka's final disposal site is Muthurajawela which is the highest distance in all hospitals. Hence the maximum distance and highest fuel consumption occurs in that process. The emission of greenhouse gases can be reduced if the distance to the landfill is reduced.

The emissions and savings related to composting showed a high value of minus (-) values in the net emissions. A ton of waste degradation will give a value of 177 kg CO_2e. This shows that the process is avoiding greenhouse gas emissions and savings the possible emissions. The avoided savings is defining that the number of emissions that is avoided, by terminating the waste to go and degrade at the landfill and emit methane (CH_4) emissions.

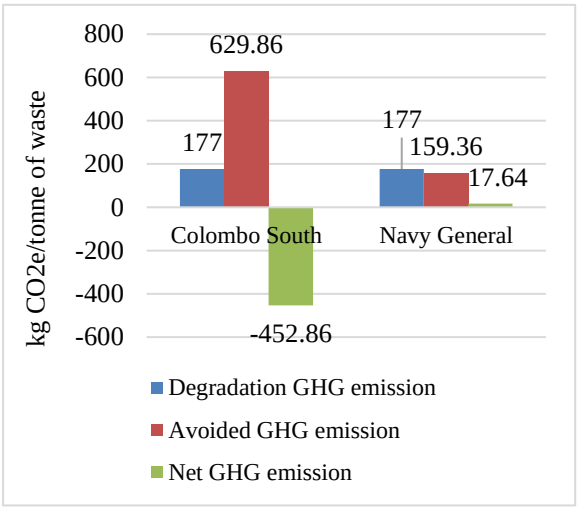

Figure 10. Non-hazardous waste composting emissions

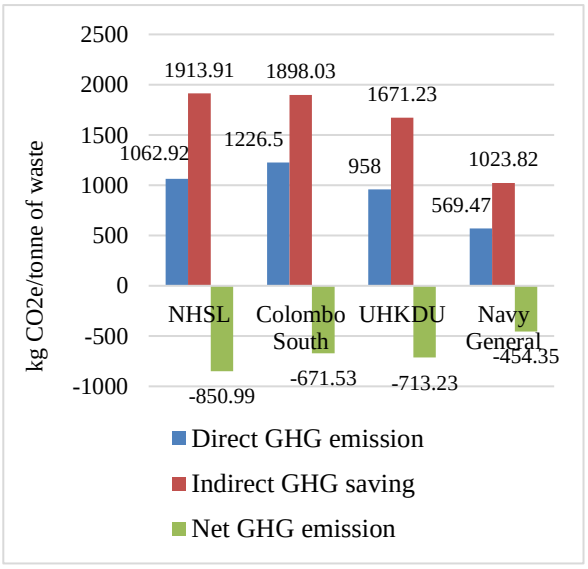

Figure 11. Waste recycling emissions and savings

If considering the composting process alone, the Colombo South Teaching hospital has achieved net zero emissions and saving the possible emissions that is expected at landfills.

Final Estimation

The final estimation with all the wastes and all the emissions studied in the research is as follows in Table VIII. Due to the 4 hospitals in the study, an estimated value of 263.163 kg of CO_2e per tonne of waste will be emitted to atmosphere due to processes in waste management with a waste amount of 281860.16 kg (281.86 tonnes) of average monthly total waste. The net emittance of greenhouse gas carbon dioxide equivalence (kg CO_2e) were 74 176.85 kg CO_2e.

Table 8. Final emissions per month and per tonne of waste

	Direct Emissions	Indirect Savings	Net Emissions
Total monthly	75145.77	-968.92	74176.85
Per tonne of waste	266.60	-3.437	263.163

The direct emission per tonne of healthcare waste studied in the research emits 266.6 kg CO_2e. However, with the emission saving processes such as composting and recycling reduces the total emission by 3.437 kg CO_2e. This gives the final net emission value of 263.163 kg CO_2e per tonne of waste from the studied 4 medical facilities.

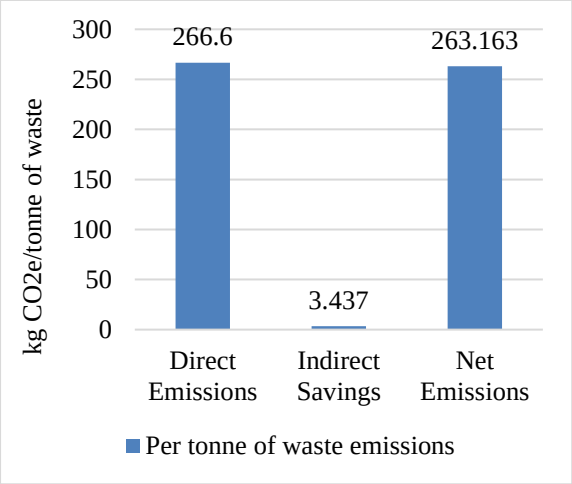

Figure 12 - Per tonne waste emissions

- Total waste data collected = 2810860.16 kg (281.86 tonne)
- Total net emissions per tonne = 263.163 kg of CO_2e per tonne of waste

As for simplification of the research, from the cradle to gate analysis of healthcare waste a single tonne of waste will emit a net amount of 263.163 kilograms of carbon dioxide equilants of greenhouse gases in the entire disposal route.

V. CONCLUSION

The study consists of present-day healthcare waste management and the greenhouse gas emissions from the processes that the waste goes through.

The direct emissions, indirect emissions and emission savings from healthcare wastes were estimated in the study. The study was divided in to 3 different steps and conducted through site visits and data gathering. And the final results of emissions due to a tonne of healthcare waste were estimated.

The minus (-) values show the significant saving is higher than the emission in the whole process. Considering the air quality and pollutant emissions in the study authorities should enforce more emission standards for the healthcare waste managements and its processes. Modern technology could be equipped with the current high fuel consuming and electricity consuming machinery, more focus towards composting and recycling of materials and such actions could avoid and prevent higher emissions of greenhouse gases.

The amounts in results are at the stable situation when considering studies from other countries regarding healthcare waste and greenhouse emissions (Khan et al., 2019) as in Sri Lanka's waste management is more focusing in achieving higher values in energy saving and material recovery.

Through possible steps and actions, a more functional management system could prevent further emissions of greenhouse gases to the atmosphere by healthcare wastes.

REFERENCES

Bereiter, B. et al. (2015) 'Revision of the EPICA Dome C CO_2 record from 800 to 600-kyr before present', Geophysical Research Letters, pp. 542–549. doi: 10.1002/2014GL061957.

Bundunee, L. and Athapattu, C. (2015) 'Waste Management Practices of Government Hospitals in Figure 11 - Waste recycling emissions and savings Figure 10 - Per tonne waste emissions Colombo, Sri Lanka', International Journal of Waste Resources, 05(02). doi: 10.4172/2252-5211.1000178.

Emmanuel, J. et al. (2001) 'Safe management of wastes from health care activities.', Bulletin of the World Health Organization, 79(2), pp. 171–171. doi: 10.1590/S0042-96862001000200013.

Khan, B. A. et al. (2019) 'Greenhouse gas emission from small clinics solid waste management scenarios in an urban area of an underdeveloping country: A life cycle perspective', Journal of the Air and Waste Management Association. Taylor & Francis, 69(7), pp. 823–833. doi: 10.1080/10962247.2019.1578297.

Haniffa, R. (2004). Management of healthcare waste in Sri Lanka. The Ceylon Medical Journal, 49(3), 93-95. https://doi.org/10.4038/cmj.v49i3.3250

Menikpura, N. (2013) 'User Manual Estimation Tool for Greenhouse Gas (GHG) Emissions from Municipal Solid Waste (MSW) Management in a Life Cycle Perspective', Institute for Global Environmental, p. 44. Available at: https://www.researchgate.net/profile/Nirmala_Menikpura/publication/236900694_GHG_calculator_for_solid_waste/links/57ed6c3208ae03fa0e829631.pdf.

World Health Organization (2007) 'Health-care waste', Health topics, p. 127. Available at: https://www.who.int/topics/medical_waste/en/.

ACKNOWLEDGMENT

The author would like to express gratitude to everyone who supported and for the guidance delivered throughout this study.

ID 469

Design of a Plastic Waste Clean-up Array System for Bolgoda Lake

N Azmy#, PGRW Premaratne, WAAR Wanasekara and MCP Dissanayake

Department of Mechanical Engineering, Faculty of Engineering, General Sir John Kotelawala Defence University, Sri Lanka

#34-eng-116@kdu.ac.lk

Abstract— The harmful effects of plastic in waterbodies are well established. Its effects extend to animals in higher trophic levels. This paper presents a reliable and cost-effective waste clean-up device capable of removing floating and partially buoyant waste from freshwater bodies. The device described is a passive clean up system which consists of three main phases, namely, catching, concentration, and collection phase. The catching phase traps the waste and directs it towards a collection cage. The collection cage retains the captured waste, and a conveyor belt extracts it. Finally, the waste trapped is transferred to an exit tray which slides the waste into a bin on the riverbank. A prototype of the device was fabricated and tested in Weras Ganga. The majority of the waste extracted was plastic packaging. However, small quantities of organic substances were extracted as well.

Keywords: ***plastic pollution, trash collector, conveyor belt, rivers***

I. INTRODUCTION

Plastic is a synthetic substance made from hydrocarbons which can be moulded into solid items of nearly all shapes and sizes (Azmy, 2002). It has become the biggest contributor to the degradation of water quality due to its buoyancy, resilience, and toxicant sorption properties (Ericksen et al. 2014). The factors driving the amount of plastics entering rivers include, population growth, urbanization and industrialization patterns within catchment areas, rainfall rates and the presence of structural barriers such as weirs and dams (Ericksen et al. 2014).

Natural degradation of plastic occurs due to photo-degradation followed by thermo-oxidative degradation (Webb et al. 2013). UV rays provide activation energy to initiate the introduction of oxygen atoms into the polymer. This allows the plastics to become porous and split into smaller fragments before the polymer chains achieve a sufficiently low molecular weight for the microorganisms to metabolize them (Webb et al. 2013). These microbes either transform carbon into carbon dioxide in the polymer chains or integrate it into biomolecules (Webb et al. 2013). This process takes 50 or more years to completely degrade the plastics (Webb et al. 2013).

The fragmentation of plastic results in a high surface to volume ratio and they continue to accumulate in the form of environmental contaminants such as Persistent Organic Pollutants (POPs). The adsorption of POPs onto plastic can be transferred into tissues and organs of animals through ingestion and magnified through the food web as shown in Fig. 1. By bioaccumulation and bio-concentration, they impact higher trophic levels.

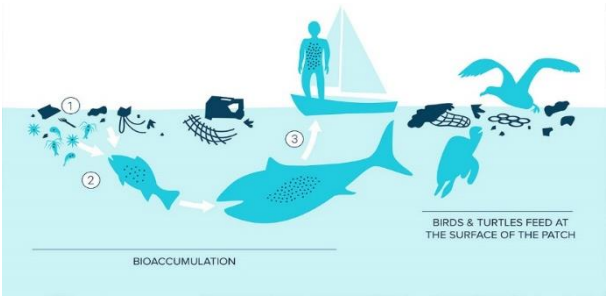

Figure 1. Impact of plastic debris

The global resin and fibre production has increased by 99% from 1950 to 2015, surpassing most other man made materials (Geyer, Jambeck and Law, 2017). In 2015, the volume of plastic entering the ocean annually was 4.8 to 12.7 million metric tons from 192 coastal countries. This approximately accounts for 1.7 to 4.6% of the total plastic waste produced (Jambeck et al. 2015). In 2014 a study revealed that 5 trillion plastic pieces weighing over 250,000 tons were afloat at the sea (Ericksen et al. 2014). If the current consumption patterns continues, the pieces of plastic in the ocean will surpass the number of fish by 2050 (United Nations Environment Programme, 2018).

A. Classification of plastic in the water column

As shown in Table 1 plastic can be classified into three main types based on size, namely macro plastics, meso plastics and micro plastics. The detection and removal methods for each type needs to be addressed separately as they differ in shape, size, material, composition, and abundance. The device described in this paper is designed to extract macro plastics from freshwater bodies, thus, preventing it from entering the ocean.

Table 1. Categories of marine plastic litter in terms of size

Diameter	Source	Example
Micro (≤ 5mm)	Primary and secondary microplastics	Primary: industrial and domestic products; Secondary: textile, fibres, tyre dust
Meso (5 - 20 mm)	Fragmentation of larger plastic items	Bottle caps, fragments
Macro (> 20mm)	Lost items from maritime activities or from rivers	Plastic bags, food and other packaging, fishing floats, buoys, balloons

Source : Andrady, 2015

Technologies addressing plastic pollution: In Sri Lanka, waste in freshwater bodies is most often removed using excavators or by scooping it out manually. Some water ways contain Bamboo shafts across them to trap waste. In 2020, the ocean strainer, a boom made of polyurethane foam blocks covered in water resistant material was placed across the Dehiwala canal to act as a barrier and prevent plastic waste from entering the ocean (Hoole, 2019). This is similar to placing a bamboo shaft across the river. However, research suggests that foam blocks are more efficient in trapping waste and preventing it from overtopping than bamboo shafts (Ho, 2015).

"Mr. Trash Wheel" and the "The interceptor" are river waste collection devices that are currently implemented. "Mr. Trash Wheel" is implemented in the Baltimore Harbour and "The Interceptor" has been implemented in Indonesia, Malaysia, and the Dominican Republic (Lindquist, 2017). Both systems use renewable power sources. "Mr. Trash Wheel" uses a water wheel as the main power source and solar panels as a backup power source (Lindquist, 2017). "The interceptor" solely runs on solar power.

"The Interceptor" uses a fixed barrier to divert waste towards the collection system while "Mr Trash Wheel" uses a flexible boom to divert waste to the collection system (Lindquist, 2017; How it works - The Interceptor, no date). However, they are both costly to be implemented (Goodwin et al. no date).

The novel features of the device described in this paper are that it is much more economical, the waste collected is transferred to land hence less manpower is required, the device requires very little power as the conveyor belt does not run throughout the day and the size of plastic collected is only limited by the mesh size of the skirt.

This paper consists of three main sections, the methodology which consists of design details of the system and the methods used to test the device. The results contain key insights observed during testing. The next two sections contain the advantages, limitations, and further improvements that can be done.

II. METHODOLOGY

The first step in the deign process was to select a suitable location. The system was designed based on the flow rate and dimensions of the selected waterway. Finally, a prototype of the device was fabricated and tested to ensure it works as required.

A. Site selection

Tides, wind, flow velocity, previous waste clean-up measures taken, and the rate of pollution were the factors considered in this regard.

Based on the rate of pollution, locations short listed include the Dehiwala Canal, Lunawa Canal and Weras Ganga (Fig. 2). After careful consideration of factors such as accessibility, ease of installation and previous clean-up measures taken, Weras Ganga, a tributary of Bolgoda Lake was selected. A prototype of the device was tested at Meda Ela, which is a tributary of Weras Ganga (Fig. 2).

Figure 2. Locations considered and selected testing location

Meda Ela was selected because its easily accessible, the flood walls and bridge eases installation, has an average flow rate and floating plastic waste was observed.

The flow rate of Meda Ela was experimentally found by measuring the time taken for a floater to reach a known distance. The experiment was conducted multiple times and an average value of 0.44 ms^{-1} was obtained.

B. Tides

The water level of Meda Ela was measured on two consecutive days to assess the rise and fall of it during high and low tides. The high tide and low tide times were obtained from tide tables (Fig. 3). The depth obtained was 1 m. A significant variation was not observed during high and low tides.

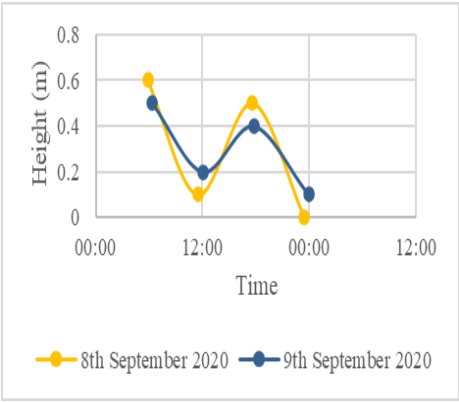

Figure 3. Tide tables for the 8th and 9th of September

C. Designing the device

This concept consists of a floating barrier (boom), where buoyant plastic particles can be caught, while neutrally buoyant aquatic animals can swim underneath (Fig. 4).

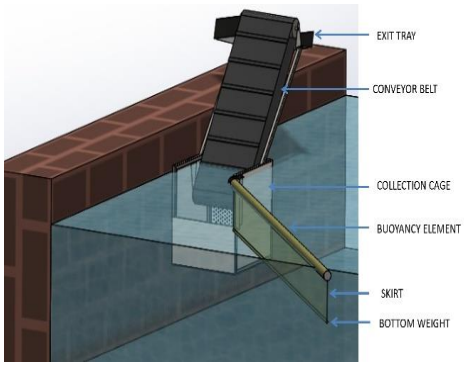

Figure 4. Initial draft of the device

The system removes plastic waste in three phases. Initially, waste is caught in front of the floating boom, the boom acts as a barrier and prevents waste from flowing downstream. Next, the accumulated particles slowly progress along the boom towards the collection cage and new particles are continuously added to this stream. Finally, the stream of waste enters the collection cage and forms a point of high concentration, from which waste is extracted using a conveyor belt. The waste extracted is transferred to an exit tray which slides it into a bin located on the riverbank. The relevant local authorities can empty the bin as and when required.

The Catching Phase: The boom consists of three main parts, namely, a buoyancy element, skirt, and a bottom weight (Fig. 4). The design requirements of the boom are buoyancy, its ability to transport plastic, bending stiffness, skirt orientation and axial stiffness.

The buoyancy element keeps the boom afloat while preventing trapped waste from overtopping. In addition, it compensates for the deadweight of the structure as well as the external forces acting on it. Moreover, it aids in guiding plastic towards the collection cage. For the prototype, a 3 m PVC pipe with an outer diameter of 90 mm and wall thickness of 5 mm was sealed at both ends and was used as the floater (Fig. 5).

Figure 5. Boom used in the prototype

The buoyancy element was fixed to the collection cage using a specially designed hinge capable of moving up, down, in and out (Fig. 6). The hinge was designed to be able to withstand the changes in water level and flow direction.

Figure 6. Boom Hinge

The skirt captures partially submerged debris and directs it towards the collection cage. It spans the entire length of the buoyancy element. For the prototype, a 2.54 mm x 2.54 mm diamond polyester mesh with a thickness of 0.78 mm and a width of 420 mm was used (Fig. 5).

To maximize the skirts efficiency, vertical orientation must be maintained (Sivasubramanian et al. 2014). Hence, a bottom weight was needed. As per the calculations, the bottom weight required was 2 kg.

1) The Concentration Phase: The boom was placed at an angle with respect to the riverbank, with the opening against the flow. This angle allows the current to transport the debris towards the collection cage and form a high concentration area, from which debris can be easily removed. The maximum deployment angle of the boom at a speed of 0.5 ms^{-1} should be 45 degrees (Shahryar, 2017). This angle should decrease as the flow rate increases.

2) The Collection Phase: Plastics that get accumulated in the collection cage is removed by a mesh conveyor belt. The conveyor belt system was designed to remove 30 kg of waste per day. The linear and rotational speed (rpm) of the conveyor to remove this quantity of waste in 15 min, 30 min and 60 min were considered. The roller rpm and belt speed were found using Equation 1.

$$M = \rho_{belt} \times K \times (0.9B - 0.05)^2 \times V_{belt} \quad (1)$$

After careful consideration, the conveyor operation time was selected as 60 minutes. The calculated speed and rpm were 0.263 ms^{-1} and 83.71 respectively. Purchasing a stainless-steel mesh conveyor with cleats for the prototype was not economically feasible. Therefore, a conveyor belt was fabricated. The materials used were lashing belts, a plastic mesh for the conveyor, and pieces of Galvanized Iron mesh for the cleats.

To minimize the energy requirement, the belt was designed to run for one hour daily. The conveyor belt transferred the waste to an exit tray which slides the waste into a bin located on the riverbank (Fig. 4). A bin made of wire mesh was used to remove any trapped water within the trash.

D. Material selection

The materials selected for the system and prototype are included in Table 2.

Table 2. Materials selected for the device and materials used for the prototype.

Component	**Selected Materials**	**Materials used for the Prototype**
Frame	Stainless Steel Box Bar	Mild Steel Box Bar
Shafts	Stainless Steel	Mild Steel
Bearing Support	Stainless Steel Plate	Mild Steel Plate
Floater	PVC pipe	PVC pipe
Conveyor	Stainless steel mesh conveyor	Lashing belts, Plastic Mesh, GI Mesh
Skirt	Wire Mesh	Plastic Mesh
Side Panels - Conveyor Belt	Aluminium Sheet	Alloy Coated Steel Sheets
Side panels - Collection Cage		
Exit Tray		
Power transfer mechanism	Gear Drive	Chain Drive

E. Testing

To ensure that the device functions as required a prototype of it was fabricated and tested for a period of three days. The prototype designed was scaled down by 0.8. On day one, the device was installed and observed for around 5 hours. The drawbacks were noted, the system was removed, and modifications were made and re-installed on the next day.

Three cases were observed during testing:

- The flow of waste along the boom
- The retention of waste in the collection cage
- The ability of the conveyor belt to extract the retained waste.

The results obtained for each of these cases are discussed in the following section.

III. RESULTS AND DISCUSSION

A. Types of waste collected

Majority of waste collected was plastic. Plastic packaging items such as PET bottles, beverage packets, cigarette packets were prevalent (Fig. 7). This shows that plastic packaging is one of the largest aquatic plastic polluters. Moreover, the device removed organic materials such as small aquatic-plants and wood as well.

Small aquatic plants did not affect the system. They flowed along the boom, got retained in the collection cage, and got extracted by the conveyor belt. In contrast, larger plants obstructed the boom and prevented waste from flowing towards the collection cage. Extraction of plastic entangled with these plants was not possible.

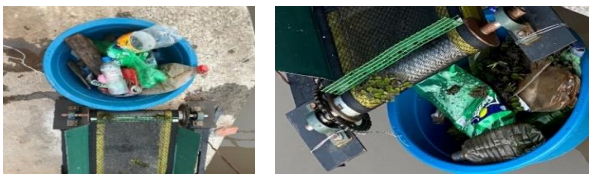

Figure 7. Waste collected by the prototype

During testing, large aquatic plants were removed ~~by~~ manually by increasing the angle of the boom. This was not an efficient way to manage the plants. It resulted in a certain amount of waste entrapped by the boom to escape along with the plants. Placing a barrier on the opposite end of the bridge to trap large plants without affecting the flow solved this issue.

B. Boom

1) Angle of the Boom: The flow of waste along the boom was monitored by adjusting the angle of the boom with respect to the collection cage. Initially, the angle of the boom was set at approximately 170 degrees. At this angle, some waste moved along the boom towards the collection cage, but some did not. Next, the angle of the boom was adjusted to approximately 150 degrees. Here, the amount of waste that moved along the boom increased.

The minimum deployment angle of the boom during testing was only 60 degrees. This was less than the recommended angle. However, decreasing the angle further would have increased the space between the retention wall and the end of the boom. This change would have caused waste to escape from that gap.

2) Skirt Material: The entanglement of waste with the skirt material and the formation of a barrier decreased the amount of waste that reached the collection cage. In Fig. 8, waste inside the yellow rectangle was stuck due to the piece of wood not moving into the collection cage. Waste is encircled in red to show the two different aspects.

There were no environmental impacts of using a mesh as the skirt material. When the skirt was removed there were no fish, aquatic plants, or other animals caught on it. However, since the testing period was short, the long-term impact of using a mesh is unknown.

Figure 8. Waste Getting Stuck on the Boom

3) The orientation of the skirt: The skirt retaining its vertical orientation was one of the main requirements of the system. Initially, due to the bottom weight being insufficient (0.6 kg) the skirt did not retain its position. As a solution to this, the bottom weight was increased by removing the end caps of the GI pipe that was used as the bottom

weight (1.03 kg). This solution worked to a certain extent but did not retain its vertical orientation fully. However, as per calculations, the bottom weight has to be 2 kg for the skirt to retain its vertical position.

C. Environmental conditions

The effects on the system due to tides and an increase in flow velocity were observed.

During testing, the flow velocity did not significantly increase therefore overtopping of waste was not observed. Also, large fluctuations in the water level during high and low tides were not observed.

Environmental conditions during testing were relatively constant. Therefore, the durability of the device in extreme weather conditions is unknown.

D. Collection Mechanism

1) Effectiveness of the Collection Cage in Retaining Waste: As shown in Fig. 9, the collection cage was able to effectively retain waste. However, the capacity of waste it was capable of retaining was limited to its size. Since the prototype was a scaled-down (1:0.8) version of the device

the amount of waste that the collection cage is capable of retaining is much higher.

Figure 9. Waste Entrapped in the Collection Cage

2) Efficiency of the Conveyor Belt: The conveyor belt was able to extract all waste retained by the collection cage including large PET bottles. However, during the initial testing period, flat waste particles got trapped between the cleats and the belt. This waste got dislodged at locations where it was not been collected. Therefore, such waste entered back into the water.

Fig. 10 shows a plastic bottle (which is circled in red) getting trapped between the conveyor belt and a cleat. It results in the overthrowing of the beverage packet shown inside the yellow rectangle. The trapped bottle got dislodged when it was under the conveyor and entered back into the water stream. This trapped bottle destabilized the bucket used to collect waste and caused some of the waste to enter back into the water stream (the waste in the yellow rectangle). This was caused by the cleats being fastened at the two ends only. As a solution to this, the cleats were fastened to the conveyor from the centre as well. This prevented waste from sliding between the cleats and conveyor.

The length of the conveyor belt did not reach the top of the retention wall therefore, as the design description states an exit tray that transfers the waste into a bin on the riverbank could not be fixed. As a solution, an easily removable bucket with holes drilled, was attached to the end of the conveyor to extract waste falling from it. However, this limited the amount of waste that could be removed by the conveyor belt in a single cycle. The bucket had to be removed, emptied, and replaced a few times during extraction.

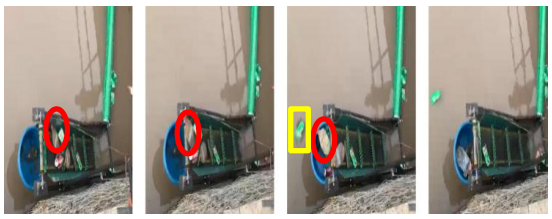

Figure 10. Waste Getting Trapped Between the Conveyor Belt and a Cleat

Due to the complexity in obtaining grid electricity for the device, a vehicle battery was used to power the motor. The motor used for the prototype was a 12 V brushed DC motor. Drawbacks of the motor were, when the tension of the belt increased the motor overheated, and the load-carrying capacity of the belt was limited by the power of the motor. However, large quantities of waste were not extracted by the conveyor belt at once, hence the motor performed as expected during testing.

E. Financial feasibility of the system

The cost incurred to design, fabricate, and implement the prototype was approximately Rs. 30,000. Despite the low cost of fabrication and testing of the prototype the actual cost of the final device would approximately be around Rs.72,000 ($ 373.35). This is due to the use of materials that would increase the durability of the device.

The bar chart in Fig 11 compares the cost to implement this device when compared with devices such as “The Interceptor” and “Inner Harbour Water Wheel”. However, these devices have been

tested and optimized for many years. Therefore, the cost is justifiable.

"The interceptor" can remove 50,000 kg per day. The operational cost of the proposed device is not known as it is still in the pilot stage. "The inner harbour water wheel" was designed to remove 22,500 kg of waste per day. The operational cost of the device has not been published. The device proposed in this paper can extract 300 kg of waste per hour. The operational cost of the device would increase if it were allowed to run throughout the day as the motor is powered by grid electricity. If solar panels were used instead, the operational cost would reduce but the manufacturing cost would increase.

The cost was converted to USD using the exchange rate given by the central bank ($ 1= Rs. 192.85).

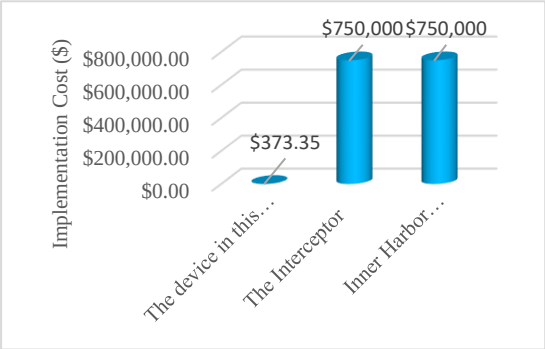

Figure 11. Cost comparison of existing devices with the device introduced in the paper

Further testing is needed in order to establish the total amount of waste that can be extracted by the system, maximum load that can be carried by the plastic mesh conveyor belt used in the prototype, durability of the device in extreme weather conditions, movement of partially submerged waste along the collection cage, effects of biofouling on the system. The system must be tested for a long period in order to obtain reliable results.

IV. CONCLUSION

Manually removing waste from rivers is a tedious process. The device introduced in this paper can trap and extract debris efficiently with little to no human involvement.

There are several novel features of this device in comparison to other commercial devices. The waste collection system is adjacent to the riverbank. Therefore, overhauling it for repairs and maintenance is straightforward. Moreover, collecting the extracted waste is a simple process of emptying a bin.

Systems such as "Inner Harbour Water Wheel" and "The Interceptor" are advanced commercially available products. They can remove large quantities of waste efficiently. However, they are expensive to implement in a developing country like Sri Lanka. In comparison, the cost of fabrication and implementation of this device is much lower.

In order to optimize the amount of waste collected, this device can be operated in locations with low backflow of water, that will increase its waste trapping efficiency.

The results clearly illustrate the device's capability to trap and extract waste in average weather conditions. However, its durability in extreme conditions is unknown. Testing the device for an extended period would validate the results.

To maximize its efficiency in wide rivers, two devices can be placed on either end of the riverbank with a clearance between them for vessels to navigate through. This would increase its capture efficiency. However, implementing two devices would increase the cost by two-fold.

The device can be modified to become more cost-effective and eco-friendlier. The suggested improvements are as follows.

A. Further Improvements

- Using a renewable power source such as solar power or hydropower (water wheel). The use of solar power is easier as Sri Lanka has sunlight throughout the year.
- Fully automating the system by using a timer circuit.
- Fixing a garbage level detection system to the collection bin to remotely monitor the waste collection.
- Adding a tension adjusting system and an auto-cleaning system.
- Exposure of the moving parts of the device could result in waste getting entangled with them. This has to be addressed appropriately.
- To reduce the material cost of the device, recycled materials or anodic protection can be used.

REFERENCES

Andrady, A. L. (2015) 'Persistence of Plastic Litter in the Oceans', in Bergmann, M., Gutow, L., and Klages, M. (eds)

Marine Anthropogenic Litter. Cham: Springer International Publishing, pp. 57–72. doi: 10.1007/978-3-319-16510-3_3.

Azmy, S. A. M. (2002) Study on plastic accumulation in the sea. National Aquatic Resources Research and Development Agency, p. 24.

Ericksen, M. et al. (2014) 'Plastic Pollution in the World's Oceans: More than 5 Trillion Plastic Pieces Weighing over 250,000 Tons Afloat at Sea', Plos one, p. 15. doi: http://dx.doi.org/10.6084/m9.figshare.1015289.

Geyer, R., Jambeck, J. R. and Law, K. L. (2017) 'Production, use, and fate of all plastics ever made', Science Advances, 3(7), p. e1700782. doi: 10.1126/sciadv.1700782.

Goodwin, A. et al. (no date) 'Intellectual property, Standards, Benchmarking and Userneeds Review', p. 28.

Ho, J. (2015) Floating Debris Boom Design Recommendations - Based on physical model study & literature review at UNM. Modeling Report. The University of New Mexico, p. 22. Available at: http://www.unm.edu/~hydlab/Assets/pdf/FloatingBoom.pdf.

Hoole, E. (2019) Caring For Canals: Colombo's Waterways And What To Do With Them, roar media. Available at: https://roar.media/english/life/in-the-know/caring-for-canals-colombos-waterways-and-what-to-do-with-them (Accessed: 11 November 2020).

How it works - The Interceptor (no date) The Ocean Cleanup. Available at: https://theoceancleanup.com/rivers/ (Accessed: 28 October 2020).

Jambeck, J. R. et al. (2015) 'Plastic waste inputs from land into the ocean', Science, 347(6223), pp. 768–771. doi: 10.1126/science.1260352.

Lindquist, A. (2017) Dirty Jobs: How Baltimore's 'Mr. Trash Wheel' Collected 1 Million Pounds of Trash From A Harbor | GE News, General Elecctric. Available at: https://www.ge.com/news/reports/dirty-jobs-baltimores-mr-trash-wheel-collected-1-million-pounds-trash-inner-harbor (Accessed: 9 September 2020).

Royer, S.-J. and Deheyn, D. D. (2019) 'The Technological Challenges of Dealing With Plastics in the Environment', Marine Technology Society Journal, 53(September/ October 2019), pp. 13–20.

Shahryar, J. (2017) Petroleum Waste Treatment and Pollution Control.

Sivasubramanian, N. et al. (2014) How the oceans can clean themselves -a feasibility study. Available at: https://www.researchgate.net/publication/336940737_How_the_oceans_can_clean_themselves_--_a_feasibility_study (Accessed: 2 October 2020).

United Nations Environment Programme (2018) Single-use plastics, a roadmap for sustainability.

Webb, H. K. et al. (2013) 'Plastic Degradation and Its Environmental Implications with Special Reference to Poly(ethylene terephthalate)', Polymers, 5(1), pp. 1–18. doi: 10.3390/polym5010001.

ACKNOWLEDGMENT

Our utmost appreciation goes towards the Department of Mechanical Engineering of General Sir John Kotelawala Defence University for giving us their support throughout the project. We would like to thank our supervisor, Captain (E) M.C.P. Dissanayake, whose expertise was invaluable. His insightful feedback pushed us to sharpen our thinking and brought our work to a higher level.

AUTHOR BIOGRAPHIES

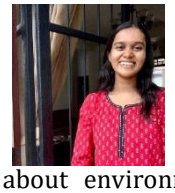

[1]N Azmy graduated from General Sir John Kotelawala Defence University in 2021, with a bachelor's degree in Mechanical Engineering. She is passionate about environmental conservation and believes that finding sustainable engineering solutions is the way forward. Currently, she works as a design engineer at Future Fibers which is a leading supplier of composite rigging to the marine industry.

[2]P.G.R.W. Premaratne currently performs as the Facility Maintenance Engineer at Hayleys Advantis 3PL Plus. He recently completed his bachelor's degree in mechanical engineering at General Sir John Kotelawala Defence University and currently reading for his master's in project management at University of Bedfordshire. He has completed his internship at Piramal Glass Ceylon PLC as a trainee Mechanical Engineer.

[3]WAAR Wanasekara graduated in mechanical engineering from General Sir John Kotelawala Defence University. Gained the first industrial exposure at Colombo dockyard plc. Currently working as an Assistant Engineer at Ceylon Steel Corporation. Involved in quality assurance of rolled and drawn steel products.

[4]Cmde (E) MCP Dissanayake, CEng (India) is currently performing as the Head of Department (Marine Engineering) and hold 2 No's patents for his research papers published so far. He is an inventor and published 06 No's publications on Brackish Water Reverse Osmosis application, Fan Boat Building and Oscillation Water Column, Ocean Wave Eenrg Converter. He was the Director in Research & Development at Sri Lanka Navy and has received commendations in number of occasions from Commander of the Navy, HE the President of Sri Lanka for his innovation. Further, he was awarded with prestigious, Japanese, Sri Lanka Technical Award for his own developed low-cost Reverse Osmosis Plant, to eliminate chronic kidney disease from Sri Lanka. Moreover, he has a vast exposure on marine diesel engines and possesses a master's degree in Marine Engineering from Australian Maritime College, University of Tasmania, Australia.

Advancements of Electronic Stethoscope: A review

HSH Perera

Deparment of Electrical,Electronic and Telecommunication Engineering, Faculty of Engineering, General Sir John Kotelawala Defence University, Sri Lanka

hshperera99@gmail.com

Abstract— Auscultation is one of the most popular methods of disease diagnosis and stethoscope has been an integral device of medical examination as it is used to listen to internal body sounds. But it inherits many limitations in traditional conventional stethoscope. Hence, an electronic stethoscope provides a much more advanced and modern solution for those limitations, and it increases the accuracy of different internal body sound recognition, assisting medical professionals to make a proper disease diagnosis. Despite the conventional stethoscope, electronic stethoscope amplifies the auscultation sound captured at the chest piece and converts it to an electrical signal which is then transmitted through an advanced designed circuitry to apply further signal processing techniques. The main objective of this review is to analyse the evaluation of medical stethoscope and the advancements that have been done using modern technology to improve electronic stethoscope by adding various features including noise reduction techniques and real time visualization techniques. Further, the paper discusses how wireless data transmission techniques have been included in electronic stethoscope, making it is possible to provide graphical analysis of the sound signal and the advanced mathematical techniques applied to make denoising and feature extraction process in an accurate way. It further reviews the alternations and modifications that have been possible due to electronic stethoscope enhancing the quality of healthcare sector.

Keywords: ***auscultation, electronic stethoscope, real time visualization techniques, feature extraction***

I. INTRODUCTION

In a rapidly developing world, technology has affected almost all the fields in the world over the years. In the field of medicine, there has been many advancements with the arrival of new technologies. Electronic stethoscope is one such improved medical device which make auscultation process easier and more accurate. Stethoscope plays a vital role in the field of medicine to hear internal sounds of the body mainly cardiac and respiratory sounds. Internal body sound auscultation is one of the basic ways to assess the diseases diagnosis. Modern technology has introduced many newer methods such as ultrasound imaging and doppler techniques for diseases diagnosis. But despite other methods of detecting most of the diseases including cardiac diseases, auscultation method is widely practiced in the world using conventional stethoscope due to its easiness to detect health problems.

In 1816, French physician René Laennec invented the medical stethoscope by placing a wooden hollow cylinder between patient's chest and physician's ear to detect auscultation of heart and lungs (Swarup and Makaryus, 2018). After adding many improvements for Laennec's stethoscope, conventional stethoscope which is also known as traditional acoustic stethoscope was introduced as a noninvasive acoustic diagnostic tool which is simple, light weight, easily available, affordable. Hence, it is widely used by doctors, and it has become the sign of the medical professionals today. Conventional stethoscope mainly includes a chest piece which is connected by a split "Y" hollow flexible tube to the earpieces (Figure 1). The flexible PVC ear tubes basically isolate the auscultation sound and transfer it to the physician's ears with a minimum quality loss (www.linkedin.com, n.d.). Chest piece which is known as the head of the stethoscope consists of a diaphragm - to transmit higher frequency components and bell-for lower frequency sounds transmission (Landge, Kidambi, Singhal and Basha, 2018). But it further got many difficulties since most of the internal body sounds including cardiac sounds contain low frequency components between 10-200 Hz (Swarup and Makaryus, 2018). Moreover, the sound quality of the conventional stethoscope is very low specially when there is a thick chest wall. And due to

variations of hearing sensitivity and disturbances in the measuring environment, sometimes physicians may not be able to recognize low frequency features of cardiac and pulmonary sounds. Artifacts and background noises, leakages in tubing can also disturb in feature recognition of cardiac sounds. Since there is no technique for noise reduction and further analysis in conventional stethoscope, it can lead doctors for wrong diseases diagnosis due to low accuracy.

Electronic stethoscope has been developed with many more advancements to overcome most of those difficulties and limitations of conventional stethoscope and it can be used for auscultation process for disease diagnosis with high accuracy. Electronic stethoscopes can be used in most of the clinical scenarios including listening to internal cardiac and pulmonary sounds, to detect abnorma changes in breathing sounds, to detect air or fluid around lungs etc. Further, it increases the accuracy of heart mummer recognition and cardiac disease diagnosis as well. The key component of the electronic stethoscope over conventional stethoscope is it converts the acoustic sounds into electrical signal and an advanced analysis can be done. Electronic stethoscope combined with sound amplification, filters and other noise reduction techniques improves the sound quality making auscultation process more accurate. A wireless data transmission can be done by using Bluetooth connection module in the recorder. Thus, the recorded data can be transmitted to wireless mobile terminal such as mobile phone or any kind of a computer for further analysis. This can be used to for remote patient monitoring and can obtain a real time graphical analysis of cardiac sounds captured at chest piece. Moreover, enhancements can be added for digitally record the captured data and play back options with different speeds. Hence, due to its high efficiency and accuracy, electronic stethoscope can be developed as a main medical device to detect cardiac sounds.

There are different variety of electronic stethoscopes commercially available with different technical advancements and specifications. Many researches have been done to improve the further efficiency and accuracy adding more features to electronic stethoscope (Figure2). Thus, the review paper mainly focuses on how electronic stethoscopes are developed as a sophisticated medical device for the auscultation process in disease diagnosis with a higher efficiency.

Figure 6 . Components of Conventional stethoscope
Source: (www.linkedin.com, n.d.)

II. METHODOLOGY

Literature review plays an integral role in academic field which study and analyse the knowledge on different areas. It is also a better source of a general summary of an interested topic. The Research topic was initialized, and further reading was done to obtain broader knowledge on area of study. First, by searching key words in different data bases like Google scholar, ResearchGate etc., journals, review papers and research articles published recently related to topic were collected. Abstract of sources were checked in order to omit duplicates and to obtain only the relevant articles. Due to limitations of the conventional stethoscope, many studies have been conducted to overcome those difficulties providing innovative solutions through modern technology, resulting advanced cost effective electronic stethoscopes with higher accuracy. Hence, the sources were studied in depth to provide an efficient literature review on advancements of an electronic stethoscope.

III. LITERATURE REVIEW

A. Key Modules in Electronic Stethoscope

Electronic stethoscope mainly consists of three modules: data acquisition; pre-processing; signal processing.

1) Data Acquisition: Since internal body sounds contain low frequency component, amplification of the auscultated sound below the threshold is required. In the first module, it includes sensor or a microphone on chest piece to capture the acoustic sounds and amplifiers to amplify acoustic sound into audible level along with transducers to identify cardiac sounds. Since the sound signal can contain noise and artifacts, external filters are added to exclude unwanted frequency components beyond the required range. By adding a loudspeaker, it overcomes the difficulties if there are issues with variations of sensitivity of hearing enabling doctors to listen to internal body sounds clearly in real time, but further analysis and graphical visualization is absent.

Hence, a microcontroller or an analog to digital converter is included to convert amplified and filtered acoustic sound signal into a digital signal. It is essential to determine the correct bit resolution and sampling frequency for a better signal analysis. For a higher accuracy to be obtained, an analog to digital converter with a high bit resolution and high sampling frequency should be obtained. Moreover, the air gap between the diaphragm and microphone open up the possibility to generate unwanted ambient noise between two diaphragm surfaces which in turn can results a false electrical signal. To overcome such difficulties, a piezoelectric transducer can be added which removes ambient noise of the signal. In a piezoelectric transducer, piezoelectric crystals are combined to diaphragm of the chest piece which generates the electrical signal due to its deformation. Hence, electrical charges releases when a pressure is applied due to cardiac sounds including heartbeat or any other pulmonary sounds. Therefore, the ambient noise present in captured sound at chest piece is filtered out before the amplification, enabling an optimal listening of the actual auscultation sound for medical professionals. 3M® Littmann electronic stethoscopes include piezoelectric sensor which further amplify the sound signal up to 24 times (Landge, Kidambi, Singhal and Basha, 2018). Micro-electromechanical system (MEMS) piezoresistive electronic sensors also generate electrical signals with higher sensitivity and accuracy (Zhang et al, 2016). Electronic stethoscopes with those sensors show significant role is cardiac disease diagnosis with a higher performance.

Another alternative for the purpose of transducer is a capacitive MEMS. Despite other methods of transducers, this system detects the change in the capacitance, which is created due to acoustic pressure occurred by cardiac sounds. Hence, the resultant electrical signal generated at this system is directly proportional to the acoustic pressure (Bassiachvili et al, 2008). Thus, in capacitive MEMS, the capacitance change is converted into an electrical signal. Compared to other types of sensors, MEMS sensor is smaller in size and contains a higher temperature stability. Thinklabs® One Digital stethoscope is a one good commercially available example for an electronic stethoscope where capacitive MEMS is included *(Swarup and Makaryus, 2018)*. Thus, the electronic stethoscopes containing capacitive MEMS include an adaptive noise canceller and can amplify the acoustic sound up to 100 times resulting a better amplification (Leng, San Tan, Chai and Wang, 2015). In addition to that, Thinklabs® One Digital stethoscopes contains advanced techniques for specific cardiac sound extraction and for further analysis of cardiac and pulmonary frequencies.

2) Pre-Processing : Pre-processing module includes denoising techniques and signal normalization techniques along with segmentation to enhance the electrical signal with more accuracy. This module is used to filter out artifacts and other noises using digital filters which have not been filtered by external filters used in data acquisition module. This in turn removes undesired features and sounds in the cardiac sounds detected in data acquisition module and increases the accuracy of the obtained acoustic signal. Different bandpass filters, High pass and low pass filters have been used for linear filtering depending on different situations according to the requirement. It helps in extracting the desired signal within the interested frequency band eliminating noise. Thus, the techniques used in pre-processing module in turn increases the signal-noise ratio (SNR) of the final output signal. The obtained signal is then normalized to a certain range and segmented into cycles localizing the sound peaks which make possible to detect specific components of cardiac sounds clearly and to conduct further feature extraction techniques. Specially, since stethoscope is an integral medical device in cardiac disease diagnosis, advanced techniques for segmentation

and feature extraction procedures make it possible for doctors to perform auscultation and diagnosis with ease. Hidden Markov Model (HMM) is a statistical Markov model which is widely used for segmentation where both the specificity and Sensitivity are above 95% (Ghosh, Nagarajan and Tripathy, 2020). Short Time Fourier Transform, Continuous Wavelet Transform (CWT), Discrete Wavelet Transform etc are some more advanced techniques that can be used in pre-processing module (Ghosh, Nagarajan and Tripathy, 2020).

Figure 2. Commercially available Electronic stethoscopes Source : (Pinto et al., 2017)

3) Signal Processing: The last module of the electronic stethoscope is used for signal processing. In this module, feature extraction and a higher order classification of the cardiac sounds can be obtained using advanced mathematical techniques. Hence it enables to extract required features converting raw data into a parametric representation of interested sections for better cardiac sound classification. Feature classification provides a better interface for medical professionals to conduct an accurate diagnostic decision making. Based on the performance of different heart sound classifiers, Support Vector Machine (SVM) with kernel function and Artificial Neural Networks (ANN) can be considered as good heart sound classifiers due to the high sensitivity and accuracy of above 98% (Ghosh, Nagarajan and Tripathy, 2020). Support Vector Machine (SVM) is a linear data-based model which can be used to detect smaller murmurs where a higher accuracy can be obtained with a reduced amount of computing power (Ghosh, Nagarajan and Tripathy, 2020). To detect heart sound abnormalities in real-time, Artificial Neural Networks (ANN) shows significant sensitivity and accuracy but when comparing with SVM, ANN requires higher computational power and time (Ghosh, Nagarajan and Tripathy, 2020). Since almost all the physiological signals are non-stationary signals, feature extraction procedure is quite challenging, and it requires analysis in both time and frequency domains to conduct a better analysis.Short-Time Fourier transform (STFT), Discrete Wavelet Transform (DWT), Discrete Cosine Transform (DCT), Linear Frequency Band Cepstral (LFBC), the Mel-Frequency Cepstrum Coefficients (MFCC) and linear predictive coding (LPC) provides advanced and accurate feature extraction procedures used for cardiac sound analysis (Ghosh, Nagarajan and Tripathy, 2020). These advanced mathematical techniques make it possible to conduct an effective analysis of non-stationary biological signals captured at diaphragm becoming aid for doctors to conduct advanced auscultation procedure. Thinklabs® One Digital stethoscope is one such good example available in the industry which contains specific cardiac sound extraction techniques and advanced mathematical algorithms for pulmonary disease detection.

Figure 3. Smartphone Sthethoscope apps : a. SensiCardiac,b.StethoCloud

Source : (Leng, San Tan, Chai and Wang, 2015)

4) Modifications Can be Added in Designing

The electrical signal created by conversion of the audio signal can be recorded by adding a recorder along with a wireless data transmission module based on Bluetooth connection. In addition, small digital display can be added in the electronic stethoscope for data visualization. But, since it is not practical to include a large display, a clear analysed graphical content and more information may not be available on the display.

Due to variations in advanced technologies and techniques used, a wide variety of high quality electronic stethoscopes are available today. L`ittmann 3M model, the Thinklabs One Digital, Welch Allyn Elite electronic stethoscope, Cardionics E-scope II, EcoScope, and ViScope etc are few of the electronic stethoscopes that are commercially available today (Pinto et al., 2017). Among them, L`ittmann 3M model, the Thinklabs One Digital are widely used electronic stethoscopes which contains bell mode and diaphragm mode with higher order amplification and ambient noise reduction techniques. Welch-Allyn® Elite is another advanced Electronic Stethoscope which contains a bell mode with a varying frequency range. When a cardiac sound is to be detected, 20 - 420 Hz frequency range is used and 350 - 1900 Hz range in diaphragm mode is used to detect pulmonary diseases and abnormalities *(Swarup and Makaryus, 2018)*. Cardionics E-scope II is another type which uses a microphone and amplify the sound signal up to 30 times, but feature extraction techniques are absent. Bluetooth based wireless data transmission modules are widely used in most of the commercially available electronic stethoscopes. Some advanced digital stethoscopes have the ability to connect with remote signal processing units in devices by transmitting the signal wirelessly. A smartphone, handheld PC or any type of a computer can be connected as the wireless mobile terminal to capture the data via Bluetooth through wireless data transmission modules for real-time graphical visualization of the signal.

For the analysis of sound data obtained from electronic stethoscope, some advanced software have been developed which make diagnosis process easier and accurate for doctors. Smartphone stethoscope apps have been developed for real time graphical visualization of auscultation sounds by connecting with electronic stethoscopes. SensiCardiac, StethoCloud, Thinklabs, Thinklabs and Mobile Stethoscope are some mobile phone apps that are already used in the field (Leng, San Tan, Chai and Wang, 2015) (Figure 3). According to surveys and researches, SensiCardiac app is considered as the best and accurate software to detect heart murmurs (Leng, San Tan, Chai and Wang, 2015). It contains advance cardiac sound classification and feature extraction techniques, hence it has a higher sensitivity to detect both pathological murmurs and normal ones accurately. The Littmann Steth assist software included in Littmann M3200 model also analyses and converts the data and display a phonocardiogram or spectral graph as the output *(Landge, Kidambi, Singhal and Basha, 2018)* (Figure 4). Thinklabs app also gives the ability to record the signal and real time visualisation of PCG signal and contains screen signal editing techniques as well. The software can be modified by adding various denoising techniques to remove artifacts, play back options with different speeds and to store and record data. Moreover, there are ongoing researches to develop software by adding more complex mathematical algorithms and machine learning approaches for cardiac feature recognition.

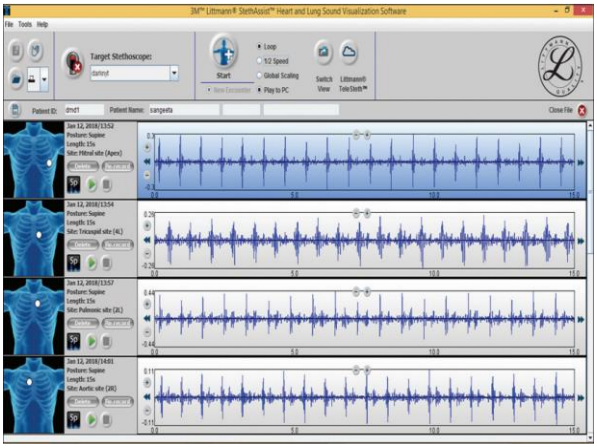

Figure 4.Graphical representation of phonocardiogram using Littman Steth assist software

Source : (Landge, Kidambi, Singhal and Basha, 2018)

5) Impact on Medical Sector

When using traditional stethoscope for covid-19 patients in wards, doctors have to face many difficulties. But to prevent intensive care conditions of covid-19 patients, it is essential to perform auscultation procedure for accurate disease diagnosis. These types of electronic stethoscopes can be very beneficial compared to Conventional stethoscope because doctors have the opportunity to analyse cardiac and respiratory sounds of the

patient through real-time wireless mobile terminals easily *(Jain et al., 2021)*. Hence, medical professionals can listen to auscultation sound of covid-19 patients using a headset or quality earphones and can obtain a visualization of cardiac sounds using smartphone. Moreover, since the advanced electronic stethoscope are capable of transmitting captured data wirelessly, it can be further developed for the use of remote patient monitoring in telemedicine allowing specialized physicians to exam patients and analysis cardiac and pulmonary sounds in real time *(Landge, Kidambi, Singhal and Basha, 2018).* Thus, this can in turn become a highlighted even in the field of telemedicine as well.

Moreover, when giving cancer treatments like Iodine131, patients are isolated due to penetrating radiation. Thus, auscultation procedure cannot be conduct by conventional stethoscope though it is required to monitor cancer patients frequently. To overcome this, digital stethoscopes can be used. By giving instructions about the placement of diaphragm for the patients, doctors can listen and analyse internal body sounds in multiple times with advanced play back and speed changing options.

When there are limited resources are available for disease diagnosis procedure, and an ECG machines cannot be accessed in emergency situations, electronic stethoscope makes possible for doctor to detect cardiac murmurs and supports to recognize cardiopulmonary pathological features for accurate disease diagnosis compared to conventional stethoscope.

Since conventional stethoscope is a single purpose device, it is difficult to use when teaching junior medical students. To overcome those practical issues electronic stethoscopes are used because the added loudspeaker enables multiple listeners to hear internal body sounds multiple times and the graphical representations of the signal can be used by senior doctors to teach about even the very low frequency components of cardiac sounds (Legget et al., 2018).

IV. DISCUSSION

The paper reviews about the limitations of the conventional stethoscope and how electronic stethoscope has overcome the drawbacks by using advanced modern technology. It shows that the electronic stethoscope has become an accurate, effective medical device that can be used to conduct auscultation procedure for disease diagnosis. Thus, conventional stethoscope is already outdated to conduct auscultation process due to the high efficiency and accuracy of the electronic stethoscope (Landge, Kidambi, Singhal and Basha, 2018). But, still, most of the doctors are lack of modern and sophisticated medical devices like electronic stethoscopes which make easier for doctors to conduct an accurate clinical decision making. Hence, it may cause auscultation procedure to be more complex, resulting wrong disease diagnosis due to low accuracy. Since real-time visualization, graphical analysis and feature extraction can be done using electronic stethoscopes incorporated with wireless data transmission techniques like Bluetooth technology, it makes easier for doctors to conduct remote patient monitoring marking a revolutionized point in telemedicine. It further makes it possible to detect even very low frequency components which cannot be detect by conventional stethoscope. Moreover, electronic stethoscope enables advanced noise reduction techniques over conventional stethoscope and most of the researches approaches to enhance the feature extractions and noise reduction techniques in pre-processing and signal processing modules providing modern solutions and advancements in clinical disease diagnosis procedure through auscultation.

V. CONCLUSION

The review paper addresses the key advancements and features that can be included in electronic stethoscope to increase the efficiency of auscultation procedure for accurate disease diagnosis. The paper discusses about the designing process and the main modules of the electronic stethoscope. Already existing electronic stethoscopes are not deeply analysed and compared among others due to shortage of literature based on comparison of electronic stethoscopes. Further improvements on amplification, denoising, feature extraction and real-time visualization techniques depicts that the modern technology has made the auscultation process with revolutionary advancements compared to traditional conventional stethoscope. In conclusion, the literature review paper reveals how innovative advancements in modern technology that can be included in stethoscopes to improve the accuracy of auscultation and in turn to enhance the overall quality of the healthcare sector.

REFERENCES

Bank, I., Vliegen, H.W. and Bruschke, A.V.G. (2016). The 200th anniversary of the stethoscope: Can this low-tech device survive in the high-tech 21st century? European Heart Journal, 37(47), pp.3536–3543.

Chorba, J.S., Shapiro, A.M., Le, L., Maidens, J., Prince, J., Pham, S., Kanzawa, M.M., Barbosa, D.N., Currie, C., Brooks, C., White,

B.E., Huskin, A., Paek, J., Geocaris, J., Elnathan, D., Ronquillo, R., Kim, R., Alam, Z.H., Mahadevan, V.S. and Fuller, S.G. (2021).

Deep Learning Algorithm for Automated Cardiac Murmur Detection via a Digital Stethoscope Platform. Journal of the American Heart Association.

Ghosh, S., Nagarajan, P. and Tripathy, R., 2020. Heart Sound Data Acquisition and Preprocessing Techniques: A Review. [online] ResearchGate. Available at:

<https://www.researchgate.net/publication/339351484_Heart_Sound_Data_Acquisition_and_Preprocessing_Techniques_A_Review> [Accessed 17 June 2021].

Høyte, H., Jensen, T. and Gjesdal, K. (2005). Cardiac auscultation training of medical students: a comparison of electronic sensor-based and acoustic stethoscopes. BMC Medical Education, 5(1).

Jain, A., Sahu, R., Jain, A., Gaumnitz, T., Sethi, P. and Lodha, R. (2021). Development and validation of a low-cost electronic stethoscope: DIY digital stethoscope. *BMJ Innovations*, [online] p.bmjinnov. Available at: <https://innovations.bmj.com/content/early/2021/06/29/bmjinnov-2021-000715 >[Accessed 17 June 2021].

Landge, K. et al. (2018) "Electronic stethoscopes: Brief review of clinical utility, evidence, and future implications," Journal of the practice of cardiovascular sciences, 4(2), p. 65.

Legget, M.E., Toh, M., Meintjes, A., Fitzsimons, S., Gamble, G. and Doughty, R.N. (2018). Digital devices for teaching cardiac

auscultation - a randomized pilot study. Medical Education Online, 23(1), p.1524688.

Leng, S., Tan, R., Chai, K., Wang, C., Ghista, D. and Zhong, L., 2015. The electronic stethoscope. [online] ResearchGate. Available at: <https://www.researchgate.net/publication/279966845_The_electronic_stethoscope> [Accessed 17 June 2021].

Malik, B., Eya, N., Migdadi, H., Ngala, M.J., Abd-Alhameed, R.A. and Noras, J.M. (2017). Design and development of an electronic stethoscope. [online] IEEE Xplore. Available at: <https://ieeexplore.ieee.org/document/8101963> [Accessed 18 Jun. 2021].

Patents.google.com. n.d. *Piezo element stethoscope*. [online] Available at: <https://patents.google.com/patent/US8447043> [Accessed 17 June 2021].

Patil D. D., K. and R. K., S., 2012. *DESIGN OF WIRELESS ELECTRONIC STETHOSCOPE BASED ON ZIGBEE*. [online] researchgate. Available at: <https://www.researchgate.net/publication/220489493_Design_of_Wireless_Electronic_Stethoscope_Based_on_Zigbee>

Pinto, C., Pereira, D., Coimbra, J., Português, J., Gama, V. and Coimbra, M., 2017. (PDF) A comparative study of electronic

stethoscopes for cardiac auscultation. [online] ResearchGate. Available at:

<https://www.researchgate.net/publication/320118417_A_comparative_study_of_electronic_stethoscopes_for_cardiac_auscultation>[Accessed 12 June 2021].

Swarup, S. and Makaryus, A. (2018). Digital stethoscope: technology update. Medical Devices: Evidence and Research, [online] Volume 11, pp.29–36. Available at: <https://www.ncbi.nlm.nih.gov/pmc/articles/PMC5757962/.>

www.linkedin.com. (n.d.). *A General Study on Stethoscopes.....* [online] Available at: <https://www.linkedin.com/pulse/general-study-stethoscopes-gaston-ravin-dias> [Accessed 9 Aug. 2021].

ACKNOWLEDGMENT

The author would like to thank Ms V Jayawardana for the extended support.

AUTHOR BIOGRAPHY

Sithumini Perera is currently a BSc (Hons) Biomedical Engineering undergraduate in the Department of Electrical, Electronic and Telecommunication Engineering of the Faculty of Engineering at General Sir John Kotelawala Defence University.

Analysis of the Potential Use of the Anaerobic Digester to Treat the Food Waste at KDU Cadets' Mess

SAAAK Athukorala#, RMPS Bandara and MSR De Soyza

Department of Mechanical Engineering, Faculty of Engineering, General Sir John Kotelawala Defence University, Sri Lanka

#athukorala.saaak@kdu.ac.lk

Abstract— The global energy demand is on the rise while the resources are depleting in an equally high rate. Hence, it is of paramount importance to take measures to ensure that future generations have access to affordable and sustainable energy sources. "Biogas" is a clean and renewable source of energy that has the potential to reduce (especially in the rural sector) the use of fossil fuels that are depleting at a rapid rate, causing serious environmental problems. Furthermore, it provides a feasible option to reduce dumping of garbage without making any use of the same. Being a developing country, Sri Lanka could save foreign exchange outflow due to importation of petroleum products promoting renewable energy sources such as biogas. In this study, the biogas potential from different substrates found in the daily food waste from the Officer Cadets' Mess of General Sir John Kotelawala Defence University (KDU) was investigated. The total waste generated has been found to be 351.9 kg per day, and the average biogas yield was estimated as 33,518.13 l/day. The average energy potential from biogas was identified as 724.032 MJ/day that would save the consumption of 16.84 kg of LPG on daily basis. Furthermore, it has also been identified that 40,000 kg of liquid bio fertilizer can be obtained from the existing 40 m^3 digester installed at the University. It is estimated that the total potential savings per annum from the biogas plant for KDU is LKR 1,223,881.90 as per present economic status.

***Keywords**: waste, anaerobic digester, biogas, LPG, savings*

I. INTRODUCTION

The fossil fuels have largely catered for the global primary energy demand with 84% contribution in 2019 (*BP's Annual Review*, 2020) and it is estimated that fossil fuel resources will deplete by 2060 (Jackson Howarth, 2019). The potential for biogas production on a global basis is considerable and with biogas being considered as a renewable fuel, it will have a major role to play in the future energy mix, not only as a fuel for transportation but also as a fuel for domestic cooking. Being a CO_2-neutral and renewable source, biogas can address the GHG emission issues in a better way. Also, bio-manure generated after decomposition can be used successfully as fertilizer. A sustainable circle of nutrients and energy is thus created between consumers and producers (Anders Mathiasson, 2015).

Sri Lanka as a developing country, has always made attempts to mitigate emissions and adverse impacts due to climate change. Being a biodiversity hotspot on earth, it has many natural resources to be utilized for renewable energy production. Sri Lanka possesses experience with biogas systems for a long period of time. The potential of biogas as a feasible option in the energy sector was identified a long time back. This is a highly feasible and a desirable option for Sri Lanka, as a significant segment of the population are struggling for energy. This resulted in a program of the United Nations that adopted a resolution as Colombo Declaration back in April 1974 after holding a convention in Colombo, which emphasized that one of the urgent priorities in the region is Energy from renewable sources. (Barnett et al. 1978)

The main component of a biogas plant is the digester, which is an airtight container in which bacteria break-down organic waste through a process of anaerobic fermentation and generates a gas (biogas) that is mostly comprised of Methane and Carbon Dioxide (CO_2), which can be used for cooking and heating, or it can be used to generate electricity. As more waste material is added to the digester, a liquid waste (slurry) is also produced, which can be used as a fertilizer (Heezen et al. 2016). Biogas can be mixed with other fuels such as natural gas, which is a fossil fuel, and used as a source of energy for domestic purposes. Given that the Carbon Dioxide in air is

absorbed by plants in the process of photosynthesis, biogas gives no net increase in Carbon Dioxide emissions compared to fossil fuels.

Biogas is produced as a result of anaerobic digestion of organic substances by a consortium of microorganisms through a serious of metabolic stages such as hydrolysis, acidogenesis, acetogenesis and methanogens. The methane-producing bacteria operate best under neutral to slightly alkaline conditions. Once the process of fermentation has stabilized under anaerobic conditions, the pH value will normally take a figure between 7 and 8.5. If the pH value drops below 6.2, the medium will have a toxic effect (Schwarz, 2007). Combustible biogas content includes about 50-70% of Methane, 30-40% of Carbon Dioxide, Hydrogen Sulfide, water vapour, Nitrogen and other impurities. The energy content of biogas will mostly depend on the Methane content of biogas and the average calorific value of biogas is about 21.6 MJ/m^3 (Minde, Magdum and Kalyanraman, 2013).

As a whole, anaerobic digestion provides a proper way of utilizing food waste to avoid contamining the environment, and-also will help to reduce GHG emission by reducing the usage of liquified petroleum gas (LPG). Utilization of biodegradable food waste to produce bio methane in an anaerobic digester reduces the environmental impacts, which could occur from emission of Methane due to open garbage dumping.

KDU presently has a biogas plant of 40 cubic meter capacity, which was constructed in 2012. The plant provides biogas for the cadets' mess kitchen for cooking and heating purposes.

The KDU Cadets' mess kitchen is providing meals for nearly 600 cadets daily, where considerable amount of food waste is generated on daily basis. This wastage is treated in an anaerobic digester to produce biogas and utilized in the Cadets' Mess kitchen as an alternative energy source for cooking where it can save substantial amount of energy. The effluent output of the plant is used as fertilizer for flowerbeds and trees in the KDU premises that contribute to monetary savings for the KDU. Furthermore, the effluent fertilizer promotes the proper growth of plants who do not need any additional chemical fertilizer. The main objective of this project is to estimate the potential of the biogas plant in order to cater for the energy requirement of the KDU Cadets' mess.

II. METHODOLOGY

Data related to the daily food waste were collected for few weeks in order to obtain an average value of the same. However, it was observed that the same food menu is repeated on a weekly basis and hence the analysis was done for an average value recorded per day. Mass of the leftover meals of the previous day was measured in the cadets' mess. Values obtained were used to calculate potential biogas yield of food waste per day separately. The average daily biogas potential was calculated by using reference data (Dilhani, Alwis and Sugathapala, 2012) of food wastes. It was assumed that cadets' appetite stayed the same for each menu and the menus were not changed during the period of data collection.

The potential of biogas was compared with that of LPG and was analyzed critically on the basis of economic and environmental aspects. The possible GHG emission reduction per annum was also calculated. It was assumed that the food waste and water were added with a 1:3 ratio in order to achive optimal thermophilic digestion conditions in the biogas digester at KDU.

III. ANALYSIS

Food waste data on daily basis in the cadets' mess were collected as shown in Table 1.

Table 5. Mass of daily food waste in kilogrammes

	Mon	**Tue**	**Wed**	**Thu**	**Fri**	**Sat**	**Sun**
Mixed Waste	180.9	224.6	196.4	194.5	184.6	193.2	207.6
Beans	12.5	-	14.6	-	11.8	-	-
Fish	-	32.4	28.4		29.3	-	33.6
Chicken	34.6	-	-	30.7	-	28.4	-
Leaks	-	-	14.6	-	-	12.4	-
Tomato	15.1	15.9	14.6	13.4	12.6	11.7	15.4
Onion	10.2	12.4	11.8	10.7	9.6	12.1	11.3
Banana	25.8	-	-	28.4	-	22.5	32.7
Banana Peel	46.4	-	-	44.3	-	46.8	49.6
Lady's Fingers	32.4	-	-	-	24.6	-	-
Orange Peel	-	26.4	-	-	-	28.4	-
Beets	-	24	-	-	-	-	-
Carrot	-	-	12.5	-	-	-	18

Potatoes	18.6	22.4	21.7	19.5	20.3	24.7	-
Total	376.5	358.1	314.6	341.5	324.3	380.2	368.2

Table 6: Methane yield from different substrates

Sample	Total solid %	Volatile Solids (%)	Ultimate methane yield (l/kg of Vs)
Carrot	9.5	91.3	309
Potato	19.0	91.9	267
Tomato	7.5	98.1	384
Ladies fingers	12.3	91.9	350
Onions	82.4	88.2	400
Beet	22.5	81.4	231
Brinjals	8.39	91.1	396
Banana Peels	18.3	91.7	314
Banana	12.8	94.3	274
v. Orange Peels	22.6	94.7	455
vi. Beans	18.0	92.8	383
vii. Meat	17.0	93.1	241
viii. Mixed	13.7	86.0	472

Source: Dilhani, Alwis and Sugathapala (2012)

Average quantity of daily waste was found to be 351.9 kg. Mass of volatile solids and the respective yield of biogas for different substrates were also calculated. Table 2 provides the ultimate Metane yield for different substrates as presented by Dilhani et al. (2012). Table 3 shows the calculated values of average volatile solid mass and average biogas yield on Mondays. Similarly, the same was calculated for other days of the week as presented in Table 4.

Table 7: Total volatile solid mass & Average methane yield on Mondays

	Total Volatile Solid Mass (kg)	Average Methane Yield
Mixed Food Remains	21.17	9995.07
Beans	2.08	799.70
Meat/Fish	5.47	1318.27
Banana	3.11	853.23
Banana Peel	7.78	2444.81
Potatoes	3.24	866.94
Brinjals	1.32	522.72
Onion	7.41	2965.21
Tomato	1.11	426.24
Ladies' Fingers	3.66	1279.61
TOTAL	56.35	21471.80

Table 8: Daily average total volatile solid mass & daily average methane yield on weekly basis

	Daily Average of Volatile Solid Mass (kg)	Daily Average of Methane Yield (l)
Monday	56.35	21471.80
Tuesday	52.51	21842.54
Wednesday	44.54	18581.21
Thursday	50.74	19639.01
Friday	49.35	18942.04
Saturday	51.67	20031.24
Sunday	51.75	20268.32

According to the data, the daily average mass of volatile solid waste was calculated.

Average total volatile solid mass per day

$$= \frac{\sum \text{Daily Average of volatile solid mass}}{7} = 50.98 \text{ kg}$$

Average methane yield per day:

$$= \frac{\sum \text{Daily Average of yield of methane}}{7}$$

$$= 20110.88 \text{ litres/day}$$

Average Biogas yield per day assuming methane content in biogas as 60%

$$= \frac{20110.88}{0.6}$$

$$= 33{,}518.13 \text{ litres/day}$$

Calculation of potential energy yield from biogas was calculated subsequently. The average calorific value of biogas was assumed to be 21.6 MJ/m^3 (Minde, Magdum and Kalyanraman, 2013)

Hence, average energy yield from biogas produced per day = 33.52 x 21.6 = 724.032 MJ/day

Continuous feeding of the digester is proposed and it is suggested to have an alternative feed during the vacation. It can be fulfilled by garden waste from KDU premises. Since the cadets are not at KDU during the vacation, biogas requirement also will be less. Hence, the full quantity of feed will not be required and only the minimum feed required to keep the continuity of biogas production in the digester will be needed.

A. Comparison between LPG and Biogas

Liquefied Petroleum Gas (LPG) is used for cooking purposes in the KDU cadets' mess kitchen. Cooking process consumes up to 5–6 Cylinders of LPG per day. As per calculations above, daily average energy yield of biogas is estimated as follows:

Daily average energy yield of biogas = 724.032 MJ

Calorific value of LPG = 43 MJ/kg

Total mass of LPG that can be saved per day

= 724.032/43

= 16.84 kg

A medium size LPG cylinder contains 12.5 kg of LPG. Hence, it is evident that the daily supply of biogas saves almost 1.3 gas cylinders per day. Given that the current price of a LPG cylinder in the market is Rs. 1495.00, the monetary saving can be calculated as:

Monetary saving per day

$$= \frac{16.84 \text{ x } 1495.00}{12.5}$$

= Rs. 2014.06

Annual Saving = 2014.06 x 365 days

= Rs. 735,131.90

B. Saving from bio-fertilizer (digestate)

Anaerobic digester can provide 1000 kg of liquid bio-fertilizer per m^3 of a biogas plant per year. According to the present market price, liquid bio-fertilizer can be valued for Rs 5 per kg.

Hence, bio-fertilizer yield from a 40 m^3 plant=40000 kg

Annual income =Rs.200,000

C.Potential saving by the utilizing of garbage

The government allocates Rs. 2500.00 per ton of garbage for dumping. By assuming 330 days per annum (excluding vacations, during which the cadets' mess does not function):

Degradable waste generated per day = 0.35 tons

Degradable waste generated per year = 115.5 tons

Savings from disposing degradable waste in the digestor

= Rs. 115.5 x 2500

= Rs. 288,750

D. Monetary saving potential of the biogas plant

Total potential savings per annum from the biogas plant

= 288,750.00+200,000.00+735,131.90

= Rs 1,223,881.90

Total expenditure on LPG per year

= 6 x 1495 x 330

= Rs 2,960,100.00

Annual Percentage Saving of Biogas plant

$$= \frac{1{,}223{,}881.90 \times 100\%}{2{,}960{,}100.00}$$

= 41.35%

E. Reduction in GHG Emissions

Possible saving in LPG consumption annually

$= 16.84 \times 330 = 5557.2$ kg/yr

Annual possible GHG emission reduction Since the GHG emission per LPG kilo grams is 2.9kgCO (IPCC, 1996).

$= 2.9 \times 3333 = 16.116$ tons/yr

IV. DISCUSSION

Based on calculations 16.84 kg of LPG could be saved daily and 41.35% of an annual monetary saving could be achieved by direct and indirect savings. Proper utilization of the biogas plant will enable generation of energy from bio-degradable food waste, which could have dumped without any use. The effluent, which contains higher nutritious level,

could be used to reduce the consumption of commercial fertilizer.

It is important to note that, in order to achieve the above objectives, the plant must be continuously fed. If the feeding process continues without any issue, the biogas yield will be maintained at a constant level with only negligible fluctuations. It is required to add waste and water in a ratio of 3:1 in order to facilitate the growth of bacteria and to ensure the generation of biogas is maintained at an acceptable rate. Usage of a chopping machine to chop the food waste in to small pieces could be helpful to accelerate the biogas production and to optimize the yield of biogas.

The temperature within the digester has to be sustained in a range between 30^0 – 35 ^{0}C by incorporating a proper insulation in order to avoid overheating during dry periods and overcooling during rainy periods so that the mesophilic digestion can be made optimal. Removal of Hydrogen Sulfide (H_2S) and water vapour to be done in order to have a cleaner biogas yield.

V. CONCLUSION

Biogas is considered as a cleaner energy source that can be produced by using biodegradable food waste. Production of biogas is more preferable in order to reduce the dependency on fossil fuels.

Kitchen of the Officer Cadets' mess at the General Sir John Kotelawala Defence University generates 351.9 kg of food waste per day. The waste can be pre-treated and used as bio-manure in the biogas digester in order to produce biogas by anaerobic digestion in controlled conditions, to be used for cooking purposes. Potential biogas yield is 33,518.13 litres per day which can replace 16.84 kg of LPG on a daily basis. The total monetary saving potential of the plant is estimated to be Rs 1,223,881.90 per annum.

REFERENCES

Anders Mathiasson (2015) 'International Gas Union Biogas - from refuse to energy News , views and knowledge on gas – worldwide', p. 13. Available at: website: www.igu.org.

Dilhani, J. A. T., Alwis, P. A. De and Sugathapala, D. T. (2012) 'Biogas Production Using Market Garbage', (Cmc), pp. 1–13.

Fossil Fuels Still Supply 84 Percent Of World Energy — And Other Eye Openers From BP's Annual Review (no date). Available at: https://www.forbes.com/sites/rrapier/2020/06/20/bp-review-new-highs-in-global-energy-consumption-and-carbon-emissions-in-2019/?sh=428c71e266a1 (Accessed: 16 June 2021).

Heezen, P. A. M. et al. (2016) Measuring small-scale biogas capacity and production, Chemical Engineering Transactions. Available at: www.irena.org.

IPCC (1996) EFDB - Basic Search. Available at: https://www.ipcc-nggip.iges.or.jp/EFDB/find_ef.php.

Jackson Howarth (2019) When will fossil fuels run out? | Octopus Energy. Available at: https://octopus.energy/blog/when-will-fossil-fuels-run-out/ (Accessed: 17 June 2021).

Minde, G., Magdum, S. and Kalyanraman, V. (2013) 'Biogas as a Sustainable Alternative for Current Energy Need of India', Journal of Sustainable Energy and Environment, 4(3), pp. 121–132.

Schwarz, D. (2007) 'Environment and Infrastructure Biogas Technology Eschborn 07.12.2007'.

ජාතික ලොතරැයි මණ්ඩලය
தேசிய லொத்தர் சபை
National Lotteries Board
Taylor & Francis
Taylor & Francis Group
BANK OF CEYLON
BOC
Bankers to the Nation
PEOPLE'S BANK
HUAWEI

ISBN 978-624-5574-51-3